Role of Extracellular Vesicles from *Fusarium graminearum* and *Fusarium oxysporum* f. sp. *vasinfectum* in Fungal-Plant Interactions

---

Submitted by

Donovan Garcia-Ceron BSc, MSc

A thesis submitted in total fulfilment of the requirements for the degree of

Doctor of Philosophy

Department of Biochemistry and Genetics

School of Molecular Sciences

College of Science, Health and Engineering

La Trobe University

Victoria

Australia

December 2021

Table of Contents

List of Publications

- Extracellular vesicles from *Fusarium graminearum* contain protein effectors expressed during infection of corn

Garcia-Ceron D., Lowe R. G. T., McKenna J. A., Brain L. M., Dawson C. S., Clark B., Berkowitz O., Faou P., Whelan J., Bleackley M. R., Anderson M. A. Journal of Fungi. **2021**; 7(11):977. doi.org/10.3390/jof7110977

- Fungal Extracellular Vesicles in Pathophysiology

Garcia-Ceron D., Bleackley M. R., Anderson M. A. Fungal Extracellular Vesicles in Pathophysiology. In: Mathivanan S., Fonseka P., Nedeva C., Atukorala I. (eds) New Frontiers: Extracellular Vesicles. Subcellular Biochemistry, vol 97. Springer, Cham. **2021.** doi.org/10.1007/978-3-030-67171-6_7

- Size-Exclusion Chromatography Allows the Isolation of EVs From the Filamentous Fungal Plant Pathogen *Fusarium oxysporum* f. sp. *vasinfectum* (*Fov*)

Garcia-Ceron D., Dawson C. S., Faou P., Bleackley M. R., Anderson M. A. Proteomics. **2021** Feb 20:e2000240. doi: 10.1002/pmic.202000240.

- Protein Markers for *Candida albicans* EVs Include Claudin-Like Sur7 Family Proteins

Dawson C. S., Garcia-Ceron D., Rajapaksha H., Faou P., Bleackley M. R., Anderson M. A. Journal of Extracellular Vesicles. **2020** Apr 16;9(1):1750810. doi: 10.1080/20013078.2020.1750810.

- Extracellular Vesicles from The Cotton Pathogen *Fusarium oxysporum* f. sp. *vasinfectum* Induce a Phytotoxic Response in Plants

Bleackley M. R., Samuel M., Garcia-Ceron D., McKenna J. A., Lowe R. G. T., Pathan M., Zhao K., Ang C. S., Mathivanan S., Anderson M. A. Frontiers in Plant Science. **2020** Jan 10;10:1610. doi: 10.3389/fpls.2019.01610.

List of Figures

List of Tables

Abbreviations

½ PDB	Half-strength potato dextrose broth
CAZy	Carbohydrate-active enzymes
CD	Czapek Dox medium
CWDE	Cell wall-degrading enzymes
DPBS	Dulbecco's phosphate buffered saline
f. sp.	Forma specialis
ff. ssp.	Formae speciales
Fgr	*Fusarium graminearum* PH-1
Fov	*Fusarium oxysporum* f. sp. *vasinfectum*
LFQ	Label-free quantitation
Log_2(FC)	Log_2(fold-change)
NTA	Nanoparticle tracking analysis
SDB	Saboraud's dextrose broth
SOD1	Superoxide dismutase
SP	Signal peptide
TEM	Transmission electron microscopy
UA	Uranyl acetate
UC	Differential ultracentrifugation
WT	Wild type
YNB	Yeast nitrogen base
YNB+	Yeast nitrogen base w/o CHOs, supplemented with amino acids
Δ	Gene knockout

Statement of Authorship

This thesis includes work by the author that has been published or accepted for publication as described in the text. Except where reference is made in the text of the thesis, this thesis contains no other material published elsewhere or extracted in whole or in part from a thesis accepted for the award of any other degree or diploma. No other person's work has been used without due acknowledgement in the main text of the thesis. This thesis has not been submitted for the award of any degree or diploma in any other tertiary institution.

Donovan Garcia-Ceron

Signed _____ Date: 01/12/2021

Acknowledgements

Thank-you to my family. Your love gets me going and has enabled me to do what I want in life. Thank-you to my supervisors, Marilyn Anderson, Mark Bleackley and Maria Liaskos, and my mentor Suresh Mathivanan. You showed me the real meaning of leadership, empathy, and resilience. Thank you to all the Anderson lab members, past and present, for being always helpful and supportive. Thank-you to La Trobe university for awarding me a Postgraduate Research Scholarship (LTUPRS), and a Full Fee Research Scholarship (LTUFFRS). Thank-you to Consejo Nacional de Ciencia y Tecnologia (CONACYT) for awarding me a Foreign Scholarship. Thank-you to the School of Molecular Science and the La Trobe Research Centre for Extracellular Vesicles (RCEV) for awarding me travel and write-up grants. Thank-you to the Australian Plant Pathology Society and the Australian Society for Biochemistry and Molecular Biology for conferring me different awards. Thank-you to the amazing people at the School of MolSci admin office; your job is vital for what happens inside the lab. Thank-you to everyone along the way that decided to help me without expecting something in return. You all made this PhD possible.

Abstract

Fungi are among the most devastating microbial pathogens in agriculture. There are numerous species that cause diseases in specific hosts, and the genus *Fusarium* includes many species that infect plants [1]. Among them, *Fusarium graminearum* (*Fgr*) and *Fusarium oxysporum* f. sp. *vasinfectum* (*Fov*), which infect cereals and cotton, respectively, are major pathogens globally, and have key impacts on yield and quality of products [2-4]. There is low efficiency in managing *Fgr* and *Fov* and increasing reports of pesticide resistance and fungal persistence are emerging [5,6].

The impacts on global food and fiber production presented by *Fgr* and *Fov* justify a deeper understanding of the fundamental biology of their host-pathogen interactions, such as cell-cell communication, to identify new antifungal targets and improve crop protection.

Recently, the regulation of processes such as macromolecule transport, activation of host immune cells, and drug resistance have been attributed to the extracellular vesicles (EVs) produced by human-pathogenic yeast [7-9]. EVs are membrane-bound particles of 30-1000 nm released from the plasma membrane of cells from different kingdoms and have various cargoes [10]. EVs from fungal pathogens have only been described recently and relatively little is known about their function and biosynthesis.

EVs from mammalian organisms have a variety of functions such as tissue repair [11], transmission of prions [12], roles in tumor growth and metastasis [13], cardioprotective effects against myocardial infarction [14], and are a potential platform for liquid biopsies and improved drug delivery [12,15,16].

Most of the research on fungal EVs has focused on yeast pathogens and when this thesis started, very little was known about the role of EVs from plant fungal pathogens. This was caused by difficulties in isolating EVs in the quantity and quality needed for biochemical analysis. This thesis addresses fungal culture conditions and optimization of EV isolation techniques to improve the yield and quality EVs from *Fgr* and *Fov* cultures. This was followed by a comprehensive proteomic analysis on EVs from *Fgr* and *Fov* to identify the protein cargo and potential roles in the infection process. Finally, *Fgr* EVs were examined for the presence of the putative fungal EV protein marker Sur7, first reported in *C. albicans* [17]. The fungal version of Sur7 has similarity to the mammalian tetraspanins, which are protein markers exploited to study EVs via a myriad of techniques, many of which cannot be used to study fungal EVs. If Sur7 becomes a confirmed marker of fungal EVs, the characterization of fungal EVs could be significantly expanded.

Preface

Chapter One of this thesis provides an overview of the importance of *Fusarium graminearum* (*Fgr*) and *Fusarium oxysporum* f. sp. *vasinfectum* (*Fov*) in molecular plant pathology, as well as the function of fungal extracellular vesicles (EVs) in human disease.

Chapter 2 is composed of two published research articles. The first, *Extracellular vesicles from the cotton pathogen* Fusarium oxysporum *f. sp.* vasinfectum *(*Fov*) induce a hypersensitive response in plants* describes the first isolation of EVs from *Fov* and their proteome, and reveals that EVs carry components that cause a hypersensitive response in cotton plants. While this was a breakthrough observation, challenges in the recovery of EVs from *Fov* led to the subsequent work to improve the yield and quality of *Fov* EVs. This was published in the second research article; *Size-exclusion chromatography allows the isolation of EVs from the filamentous fungal pathogen* Fusarium oxysporum f. sp. vasinfectum *(*Fov*).* This article describes the optimization of an EV isolation protocol for filamentous fungi by using size-exclusion chromatography and provides a description of the changes in the EV proteome that occur when *Fov* is grown on different culture media.

Chapter 3 includes the publication *Extracellular vesicles from* Fusarium graminearum *contain protein effectors expressed during infection of corn.* This work presents the isolation and proteomic analysis of EVs isolated from *Fusarium graminearum* (*Fgr*), a major pathogen of cereals, with a focus on protein effectors, which are important components of plant-fungal interactions. Also, a transcriptomic analysis of corn plants infected by *Fgr* revealed genes that increase in expression as the infection progresses, some of which encode proteins detected in EV samples. This chapter provides a list of potential protein effectors that had typical effector characteristics such as small size and signal peptide, plus another set of proteins that may belong to an undescribed class of effectors.

Chapter 4 describes collaborative work with other members of the laboratory to identify potential markers for fungal EVs which would be valuable tools to assist in purification and to track the EVs in biological systems. This work was conducted with EVs from *Candida albicans* and has been published in *Protein markers for Candida albicans EVs include claudin-like Sur7 family proteins*. The protein Sur7 was identified as a good candidate for a fungal EV marker due to its similarity to the human tetraspanins, some of which are markers for mammalian EVs. This chapter moves on to describe how a polyclonal antibody was raised to the *Fgr* homolog of Sur7 and tested for the detection of *Fgr* EVs. A Western blot analysis confirmed the presence of Sur7 in EV samples, indicating that Sur7 may indeed be a protein marker for fungal EVs.

Finally, the contributions of this thesis to the research field are presented, as well as the future directions needed to reach a better understanding of the function of EVs in plant-fungal interactions.

1. Chapter One: Introduction

Fungi are some of the most destructive pathogens in agriculture. Some can infect a broad range of plants, evolve rapid resistance to fungicides, and remain in contaminated soils for years. Cotton and cereals are globally important for fibre and food supplies, but these crops suffer fungal infections that require intensive management. Descriptions of a cotton and cereal pathogen, respectively, are provided next, finishing with an introduction to the research field of fungal extracellular vesicles (EVs) which may provide useful information in the search for new antifungals.

1.1 *Fusarium oxysporum* forma specialis *vasinfectum* (*Fov*)

The genus *Fusarium* has a plethora of strains with host specificities that are indicated by the term 'forma specialis' (f. sp.) [18]. For *Fov*, the f. sp. reveals that it infects mainly cotton (*Gossypium hirsutum*) causing a disease known as Fusarium wilt. *Fov* has been detected in all cotton-producing countries worldwide, thriving in soil where it invades the root of the plant and then colonizes the plant's vascular system [19]. As the disease progresses, *Fov* causes discoloration of the leaves from green to yellow and browning of the fibrous component of the stem, leading to necrosis of the entire plant [20]. *Fov*, similar to other *Fusarium* pathogens, is extremely persistent in the right soil conditions even in the absence of its host, being able to remain in the soil indefinitely [21]. The generation of resistant

cultivated varieties is the most effective measure to control *Fov*, but practices such as soil solarization, seed thermotherapy, and fungicide application are also common [6].

Some *Fusarium* pathogens achieve entrance to the plant by secreting cell wall-degrading enzymes (CWDE). For instance, *Fov* produces polygalacturonase and glucanases to access the root of the cotton plant [19,22]. Similarly, *F. oxysporum* f. sp. *cubense* secretes cellulase and pectinase that degrade tissues in the banana plant [23], and *F. solani* f. sp. *pisi* produces cutinase when invading pea stems [24]. Once the pathogen has entered its host, the infection is supported by the production of pathogenicity-related molecules. For example, a mitogen-activated protein (MAP) kinase encoded by the gene *fmk1* was essential for *F. oxysporum* f. sp. *lycopersici* infection of tomato, and strains lacking *fmk1* were not infectious [25]. Complementation of *fmk1* mutants with *pmk1*, an orthologous gene from the rice pathogen *Magnaporthe oryzae*, restored pathogenicity and invasive growth in *F. oxysporum* f. sp. *lycopersici*, indicating that *fmk1* is conserved in other soil-borne pathogens and has implications on virulence [25]. Similarly, *F. oxysporum* strains lacking the protein kinase FoSNF1 had altered production of CWDE, and their virulence was reduced [26,27]. A correlation between the production of CWDE and the pathogenicity of other fungal pathogens has also been established [28].

Fov continues to spread into new countries [2], and there are no varieties of cotton that are resistant to Fusarium wilt. Thus, efforts are urgently required to improve

management of *Fov*. Secretion processes, such as those as those presented above, are crucial for the pathogenicity of *Fov* and other *Fusarium* fungi, making them attractive targets for development of new antifungal interventions.

1.2 *Fusarium graminearum* (*Fgr*)

Fgr, also known as *Gibberella zeae*, is a filamentous fungus that infects corn, wheat, oats, rice, and barley, causing a disease known as Fusarium head blight (FHB). The disease is present in every continent, with estimated global losses of up to 50% of production [29] and USD 3.5 billion dollars losses in the US in the decade of 1990 [29]. China had losses of up to 2.5 million tons of grain during epidemic years, with up to 7 million hectares infected by *Fgr* [29,30]. FHB has a devastating effect on food security [31], causing cereals to become light colored and necrotic. *Fgr* colonizes the plant by depositing spores on aerial parts of the plant where it develops mycelia that reach the stomata and other vulnerable areas. Next, it proceeds to invade the vascular system until necrosis occurs, leading to plant death [32]. The accumulation of pink conidiospores and the occurrence of several types of mycotoxins are typical indications of FHB [33,34]. *Fgr* infections remain difficult to manage due to a combination of poor fungicide effectiveness and the lack of resistant cultivated varieties. Hence, removing contaminated plant material and reducing the number of cereal crops consecutively planted are the best techniques available to control *Fgr* [1].

The production of mycotoxins is a critical feature of *Fgr*. Mycotoxins are toxic to humans and animals and are the main limiting factor for wheat production in the world [30]. The trichothecene deoxynivalenol (DON) is the most relevant mycotoxin found in grain, causing diarrhea, contact dermatitis and hemorrhages in animals [35]. In humans, DON causes nausea, vomiting and convulsions, as well as neurological disorders and immunosuppression [35]. Zearalenone (ZEA), an important polyketide mycotoxin also produced by *Fgr*, has estrogenic effects and reduces animal fertility [35]. It is estimated that 50% of food samples in the European Union contain DON, and 80% contain ZEA [36], while in China DON and ZEA occur in 96% of tested foods [37]. A better understanding of the fungal export of DON and ZEA from the cell is necessary to address the alarming incidence of mycotoxins in food crops, and their impact on human and animal health.

Fgr uses other compounds to support its infection. For instance, *Fgr* strains lacking the gene *mgv1*, which encodes a MAP kinase involved in plant penetration [38], had changes in their morphology and a weaker fungal cell wall [39]. Similarly, disruption of the MAP kinase GPMK1, involved in extracellular CWDE production, caused morphological changes and abolition of pathogenicity of *Fgr* [40]. These studies revealed that transduction pathways regulated by MAP kinases have main roles in this fungus [41,42]. These observations suggest that the secretion of mycotoxins and virulence factors in *Fgr* is important for pathogenesis, however

the vehicles that allow the secretion of some of these compounds are unknown [43,44]. While the characterization of virulence factors secreted via conventional signals is required, evidence points to the existence of different classes of virulence factors that are unconventionally secreted [45-48], and may be attractive candidates as targets for new antifungals. Extracellular vesicles are a newly described mechanism of unconventional secretion that is described next.

1.3 Fungal Extracellular vesicles (EVs)

EVs are a non-canonical secretion mechanism for macromolecules [49], metabolites [50], pigments [51], and even prions [12]. EVs are best described in mammals, but are also produced by bacteria, fungi, plants, and parasites [51-59]. In mammalian cells, EVs are produced via three main mechanisms: from fusion of the plasma membrane with multivesicular bodies (MVBs) aided by the endosomal sorting complexes required for transport (ESCRT) proteins; by direct outward budding of the plasma membrane; or by the formation of apoptotic bodies [10]. EVs are typically between 30-1000 nm in size depending on the biosynthetic pathway [10]. Although the biogenesis of fungal EVs has not been elucidated, strains lacking ESCRT proteins had alterations in the production of EVs [60], hence it is hypothesized that ESCRT proteins probably have a role in the formation of fungal EVs (Figure 1).

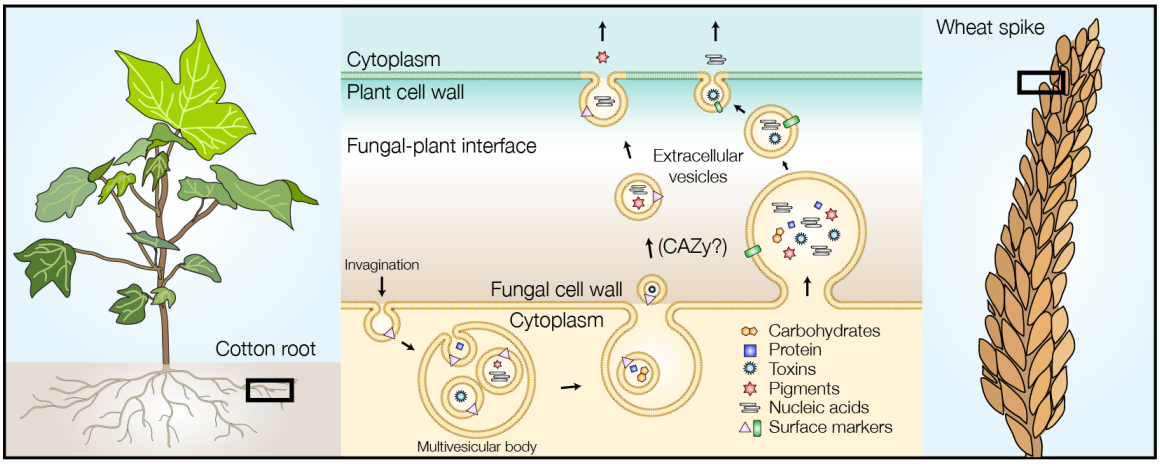

Figure 1 Possible mechanisms for fungal extracellular vesicle (EV) biogenesis. Fungal EVs may originate from the fusion of multivesicular bodies with the plasma membrane, or by direct outward budding. Fungal EVs transport carbohydrate-active enzymes (CAZy) to potentially assist in movement through the fungal cell wall and/or degrade the plant cell wall and deliver their cargo. These processes are likely to occur at the fungal-plant interface, such as the cotton root for *Fusarium oxysporum* f. sp. *vasinfectum* (*Fov*) and the wheat spike for *Fusarium graminearum* (*Fgr*).

The observation that EVs from the human yeast pathogen *Cryptococcus neoformans* transport polysaccharides to build its immunogenic capsule [7] has led to the hypothesis that other fungi rely on EVs for transporting virulence-related cargo. The different functions of fungal EVs and their role in pathophysiology are presented in section 1.4.

1.4 Fungal Extracellular Vesicles in Pathophysiology

This section of Chapter 1 has been published as a book chapter:

Garcia-Ceron D., Bleackley M.R., Anderson M.A. (2021) **Fungal Extracellular Vesicles in Pathophysiology.** In: Mathivanan S., Fonseka P., Nedeva C., Atukorala I. (eds) New Frontiers: Extracellular Vesicles. Subcellular Biochemistry, vol 97. Springer, Cham. **https://doi.org/10.1007/978-3-030-67171-6_7**

Statement of Contribution

Donovan Garcia-Ceron:
- Prepared the contents and figures for the manuscript
- Drafted and provided revisions for the draft prior to submission

Other authors have made the following contributions:
- Bleackley MR and Anderson MA contributed to the concepts for the content and edited the manuscript

Chapter 7
Fungal Extracellular Vesicles in Pathophysiology

Donovan Garcia-Ceron, Mark R. Bleackley, and Marilyn A. Anderson

Abstract Fungal pathogens are a concern in medicine and agriculture that has been exacerbated by the emergence of antifungal-resistant varieties that severely threaten human and animal health, as well as food security. This had led to the search for new and sustainable treatments for fungal diseases. Innovative solutions require a deeper understanding of the interactions between fungal pathogens and their hosts, and the key determinants of fungal virulence. Recently, a link has emerged between the release of extracellular vesicles (EVs) and fungal virulence that may contribute to finding new methods for fungal control. Fungal EVs carry pigments, carbohydrates, protein, nucleic acids and other macromolecules with similar functions as those found in EVs from other organisms, however certain fungal features, such as the fungal cell wall, impact EV release and cargo. Fungal EVs modulate immune responses in the host, have a role in cell-cell communication and transport molecules that function in virulence. Understanding the function of fungal EVs will expand our knowledge of host-pathogen interactions and may provide new and specific targets for antifungal drugs and agrichemicals.

Keywords Fungi · Extracellular vesicles · Yeast · Plant pathogens · Filamentous fungi

D. Garcia-Ceron · M. A. Anderson (✉)
La Trobe University, Melbourne, Australia
e-mail: 18538197@students.latrobe.edu.au; m.anderson@latrobe.edu.au

M. R. Bleackley
Incannex, Melbourne, Australia
e-mail: m.bleackley@latrobe.edu.au

S. Mathivanan et al. (eds.), *New Frontiers: Extracellular Vesicles*, Subcellular Biochemistry 97, https://doi.org/10.1007/978-3-030-67171-6_7

The Impact of Fungi on Human Health

Of the estimated 1.5 million total fungal species (Hawksworth 2001), there are 300 severe human pathogens, most of which are members of the genera *Candida, Aspergillus*, and *Cryptococcus* (LIFE 2017). Almost a billion people have fungal infections of skin, nails and hair that are non-life-threatening. However, 150 million people suffer severe fungal diseases, and 1.5 million die each year as a consequence of fungal infections (Bongomin et al. 2017; Brown et al. 2012).

Invasive fungal diseases also impose a huge burden on healthcare systems since they have mortalities of 30 to 90% (Fisher et al. 2020). The estimated cost of hospital care for patients with fungal infections was USD 7.2 billion in 2017 in the US alone (Benedict et al. 2019).

Candida spp. cause infections of mouth, vagina and skin, as well as life-threatening systemic blood infections. Drug-resistant *Candida* strains have a reported mortality of around 25% (CDC 2019) and the cost of hospitalizations due to *Candida spp.* is estimated to be USD 1.4 billion (Benedict et al. 2019). The ability of fungi to infect different tissues and the similarities in the biochemistry of fungal and host cells have created challenges for the generation of new antifungal treatments (Rodrigues and Nosanchuk 2020; Fisher et al. 2020). Right now, a potential crisis is developing due to the spread of drug-resistant *Candida auris.* This species is often resistant to all three main classes of available antifungal treatments (CDC 2019). With an increase of 318% in infection rates in the US from 2015 to 2018, ease of transmission, and challenges in elimination by disinfection, *C. auris* is rapidly becoming a global threat (CDC 2019).

Aspergillus spp. typically cause respiratory diseases such as allergic bronchopulmonary aspergillosis (ABPA) and severe asthma with fungal sensitization (SAFS). The main pathogenic species are *A. fumigatus*, *A. flavus*, *A. niger*, and *A. terreus* (Lockhart et al. 2020). There are 4.8 million estimated cases of ABPA around the world, and 1.2 million patients develop chronic pulmonary aspergillosis after suffering from tuberculosis (Denning et al. 2011, 2013). The healthcare cost of patients affected by *Aspergillus spp.* is estimated around USD 1.2 billion in 2017, placing a huge load on health infrastructure (Benedict et al. 2019), and although current antifungal therapy is usually effective against these pathogens, there are emerging reports of antifungal resistance (Lockhart et al. 2020). Approximately one third of drug-resistant isolates have no identifiable resistance mechanism, although it is hypothesized that efflux pumps aid in this process (Snelders et al. 2008; da Silva Ferreira et al. 2004).

Cryptococcus spp. cause lung infections in immunocompromised patients, and the disease can evolve into meningoencephalitis particularly in HIV-infected individuals (Rodrigues et al. 1999). It is estimated that almost a quarter of a million of new cases of cryptococcal meningitis occur each year causing 180,000 deaths (Rajasingham et al. 2017).

The Impact of Fungi on Agriculture

There are 8000 estimated species of fungal plant pathogens in the world (Hawksworth 2001). From these, the top 5 most devastating pathogens are *Magnaporthe oryzae, Botrytis cinerea, Puccinia spp., Fusarium graminearum* and *Fusarium oxysporum* (Dean et al. 2012).

M. oryzae causes rice blast disease. The fungus is responsible for global losses of 30% per year, which would have fed 60 million people (Nalley et al. 2016). The disease is present in 85 countries and there is no comprehensive access to resistant varieties of rice (Ryan 2016; Nalley et al. 2016). Reports indicate that if rice blast is not managed, demand for this crop will not be met in future years (Ray et al. 2013).

B. cinerea, also known as gray mold, can infect more than 200 plant species. This broad host spectrum leads to crop losses of about USD10 billion each year (Williamson et al. 2007; Dean et al. 2012). Pesticides are employed extensively to control *B. cinerea* and represent 10% of the world's pesticide market (Dean et al. 2012).

Puccinia spp. cause rust on a variety of crops. The most important members of this genus are those that infect wheat, such as *Puccinia graminis* f. sp. *tritici* (stem rust), *P. graminis* f. sp. *striiformis* (stripe rust), and *P. triticina* (leaf rust) (Dracatos et al. 2018). In 1998 a highly virulent race of *P. graminis* f. sp. *tritici*, named Ug99, emerged in Uganda and migrated into east and southern Africa and the middle east (Saunders et al. 2019). Since then, stem rust epidemics have occurred in Germany, Sweden, the UK, Italy, and western Siberia with losses of 30–40% (Saunders et al. 2019; Bhattacharya 2017; Shamanin et al. 2016). Ug99 can affect 80% of the world's wheat varieties, making this fungus a serious threat to global food security (Singh et al. 2011).

Fusarium graminearum is a pathogen of cereals, such as wheat, barley and corn. It causes a disease named head blight that is characterized by loss of grain quality and a potential accumulation of mycotoxins (Goswami and Kistler 2004). Mycotoxins, such as zearalenone (ZEA) and deoxynivalenol (DON) are secondary metabolites that are particularly toxic for animals and humans (Sobrova et al. 2010). In the US, epidemics of *Fusarium* head blight of wheat caused losses of almost USD 2.4 billion between 1993 and 2001 (Nganje et al. 2004).

The *Fusarium oxysporum* species complex includes more than 100 plant pathogens that each show strong affinity to specific host plants, as well as human and animal hosts. The term *forma specialis* (f. sp.) is used to indicate this host specificity (DeIulio et al. 2018). *F. oxysporum* f. sp. *cubense* (Foc) causes Panama disease of banana. Race 1 of Foc infections almost eradicated *Gros Michel* bananas in the mid-1950s causing losses of USD 2.3 billion (Altendorf 2019). Now, race 4 of Foc is one of the biggest threats to the USD 400 billion banana industry worldwide, with presence in Australia, China, south east Asia, the middle east and Africa (O'Neill et al. 2016; Zheng et al. 2018; Ordoñez et al. 2015).

Characteristics Unique to Fungal EVs

EVs have been isolated from yeast and filamentous fungi (Table 7.1). They are similar in morphology and cargo to EVs from other species (Bleackley et al. 2019a; Rizzo et al. 2020a). Studies on fungal extracellular vesicles lagged remarkably behind studies on human EVs, until a role was proposed in pathogenesis for fungal EVs and in facilitating the colonization of a host (Fig. 7.1) (Freitas et al. 2019; Rodrigues et al. 2007). This hypothesis is based on observations that fungal EVs are loaded with virulence-associated proteins, pigments, cell wall degrading enzymes, immunogenic carbohydrates, and nucleic acids and different types of lipids (Rodrigues et al. 2007, 2008; Alves et al. 2019; Vallejo et al. 2011, 2012b; Albuquerque et al. 2008; Rizzo et al. 2020a). EVs from filamentous fungi are understudied compared to yeast, and there is a gap in the knowledge surrounding the role of EVs in host-pathogen interactions.

Similar to mammalian EVs, the cargo of fungal EVs consists of proteins, nucleic acids and lipids involved in metabolism or basic cytoplasmic processes (Fig. 7.2). Most research on fungal EV cargo has focused on proteins (Bleackley et al. 2019a). Like EVs from other kingdoms, many of the proteins that are packaged into fungal EVs work in basic physiological processes. However, there are proteins in fungal EVs that are specific to fungi, such as those involved with the synthesis and maintenance of the fungal cell wall (Bleackley et al. 2019a; Dawson et al. 2020).

The Fungal Cell Wall Impacts EV Content

The fungal cell wall distinguishes fungi from other eukaryotic cells as it contains polysaccharides that are unique to fungi and hence ideal targets for specific antifungal drugs. Fungal EVs carry proteins involved in cell wall architecture, synthesis and integrity (Bleackley et al. 2019a; Zhao et al. 2019; Brown et al. 2015; Rodrigues et al. 2008). Several synthases of cell wall polysaccharides such as glucan and chitin have been detected in EVs from *C. neoformans*, *H. capsulatum*, *C. albicans*, *P. brasiliensis*, *S. cerevisiae* and *F. oxysporum* f. sp. *vasinfectum*, among others (Rodrigues et al. 2008; Gil-Bona et al. 2015; de Paula et al. 2019; Zhao et al. 2019; Bleackley et al. 2019b). EVs from yeast-form *C. albicans* transport 1,3 beta-glucanosyltransferase and interestingly, EVs from biofilm-form *C. albicans* also carry cell wall-degrading enzymes with exo-1,3-beta-glucosidase activity. This supports the observation that the spectrum of EV proteins that affect cell wall architecture changes depending on fungal morphology (Dawson et al. 2020). Other cell wall degrading enzymes found in EVs include chitinases and glucanases (Bleackley et al. 2019b; Oliveira et al. 2010b). These enzymes may be involved in providing cell wall elasticity to allow EV release (Brown et al. 2015) and in stress-triggered cell wall remodeling (Hopke et al. 2018). This cell wall remodeling allows

Table 7.1 All fungal EV studies reported to date with a focus on pathophysiology.

Organism	Studied Morphology	Host	EV Isolation Method	Characterization	Pathophysiological Role of EVs	Main Sources
Candida albicans	Yeast, biofilm	Humans	UC, SEC	Proteomics, RNA analysis	Macrophages and dendritic cells: Increased production of cytokines. *G. mellonella*: Reduction of fungal burden after EV exposure. Biofilm EVs: Role in drug resistance.	Vargas et al. (2015, 2020) Zarnowski et al. (2018), Dawson et al. (2020)
Pichia fermentans	Yeast, biofilm	–	UC	RNA analysis	Not yet reported	Leone et al. (2018)
Cryptococcus gattii	Yeast	Humans	UC	–	Macrophages: Phagocytosis of *C. gattii* EVs	Bielska et al. (2018)
Cryptococcus neoformans	Yeast	Humans	UC	Proteomics, lipidomics, RNA analysis	Macrophages: Increased production of cytokines. Brain endothelial cells: Membrane fuses with EVs from *C. neoformans.*	Huang et al. (2012), Oliveira et al. (2010a), Peres da Silva et al. (2015a), Rodrigues et al. (2007, 2008)
Exophalia dermatitidis	Yeast	Humans	UC, sucrose gradient	–	Neuroblastoma cells: Increased cytotoxicity of melanized EVs	Lavrin et al. (2020)
Histoplasma capsulatum	Yeast	Humans	UC	Proteomics, lipidomics, metabolomics	Macrophages: Reduced phagocytosis	Albuquerque et al. (2008), Baltazar et al. (2016, 2018); Cleare et al. (2020)
Malassezia sympodialis	Yeast	Humans	UC	Proteomics, RNA analysis	PBM cells: Increased cytokine production. Keratinocytes and monocytes: Internalization of *M. sympodialis* EVs	Gehrmann et al. (2011), Johansson et al. (2018)
Paracoccidioides brasiliensis	Yeast	Humans	UC	Proteomics, lipidomics, glycomics, RNA analysis	Macrophages: M1 polarization	da Silva et al. (2016), Peres da Silva et al. (2015a, b), Vallejo et al. (2011)

(continued)

Table 7.1 (continued)

Organism	Studied Morphology	Host	EV Isolation Method	Characterization	Pathophysiological Role of EVs	Main Sources
Paracoccidioides lutzii	Yeast	Humans	UC	Proteomics, glycomics	Not yet reported	Peres da Silva et al. (2015b)
Saccharomyces cerevisiae	Yeast	–	UC	Proteomics, RNA analysis	Prion Sup35: Transported via EVs.	Kabani and Melki (2015), Oliveira et al. (2010b), Zhao et al. (2019)
Sporothrix brasiliensis	Yeast	Humans	UC	Proteomics	Dendritic cells: Increased phagocytic index; higher CFU of EV-exposed cells; increased cytokine production. Mice: Increased skin lesion; higher fungal load in organs	Ikeda et al. (2018)
Sporothrix schenckii	Yeast	Humans	UC	–	Not yet reported	Albuquerque et al. (2008)
Alternaria infectoria	Filamentous	Plants	UC	Proteomics	Not yet reported	Silva et al. (2014)
Aspergillus flavus	Filamentous	Humans	UC	–	Macrophages: Increased production of cytokines; M1 polarization. *G. mellonella*: Reduction of fungal burden after EV exposure.	Brauer et al. (2020)
Aspergillus fumigatus	Filamentous	Humans	UC	Proteomics	Macrophages: Increased EV phagocytosis; increased cytokine production. Neutrophils: Increased EV phagocytosis.	Souza et al. (2019)
Fusarium oxysporum f. sp. vasinfectum	Filamentous	Plants	UC, sucrose gradient	Proteomics	Not yet reported	Bleackley et al. (2019b)
Rhizopus delemar	Filamentous	Humans	Total exosome isolation reagent	RNA analysis	Not yet reported	Liu et al. (2018)

Trichoderma reesei	Filamentous	Humans	Modified UC	Proteomics	Not yet reported	de Paula et al. (2019)
Trichophyton interdigitale	Filamentous	Humans	UC	-	Macrophages: Increased production of cytokines; M1 polarization. Keratinocytes: Increased production of cytokines	Bitencourt et al. (2018)

Production of fungal EVs has been reported for 20 species, and 12 studies have shown that EVs have the ability to modulate immune responses in the host. For recent reviews refer to (Freitas et al. 2019; Rizzo et al. 2020a)

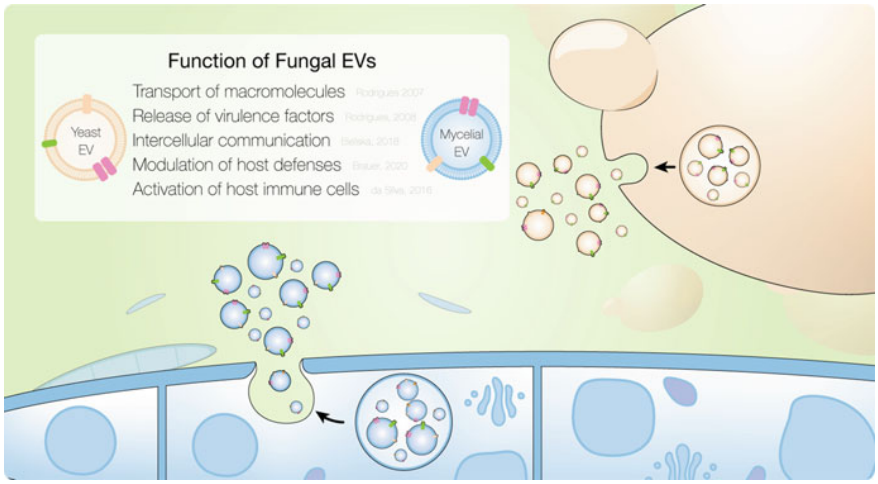

Fig. 7.1 Functions of fungal EVs. Yeast and filamentous fungi secrete EVs that work by transporting macromolecules (Rodrigues et al. 2007), releasing virulence factors (Rodrigues et al. 2008), in intercellular communication (Bielska et al. 2018), by modulating the host defenses and activating immune cells (da Silva et al. 2016; Brauer et al. 2020)

fungi to escape the host immune surveillance and resist biotic and abiotic stresses (Hopke et al. 2018).

Fungal EVs Must Traverse the Cell Wall to Reach the Host

The fungal cell wall represents a significant barrier for EV release. It is often considered a rigid, protective barrier that shields the fungal cell from biotic and abiotic stresses. However, the fungal cell wall is a dynamic organelle that interacts with the extracellular environment and the cell.

There are three main mechanisms thought to be involved in EV release through the cell wall (Wolf et al. 2014). The first is that EVs are discharged by simple turgor pressure after they are released from the plasma membrane. Fungal cell walls have pores that allow molecules of up to 5.8 nm, or 400,000 Da, to diffuse across freely (De Nobel et al. 1989, 1990). This process would not allow free diffusion of EVs. However, Walker and colleagues described fungal cell walls as viscoelastic after observing the transit of liposomes of 60–80 nm, carrying the antifungal amphotericin B across the cell walls of *C. albicans* and *C. neoformans* (Walker et al. 2018). EVs may cross the cell wall in a similar manner.

The second mechanism for fungal EV release uses cell wall-degrading enzymes contained in EVs, such as glucanases, chitinases and mannosidases, to loosen the cell wall and enable passage of the EVs (Albuquerque et al. 2008; Gil-Bona et al. 2015; Zhao et al. 2019; Bleackley et al. 2019b). These proteins have been detected in

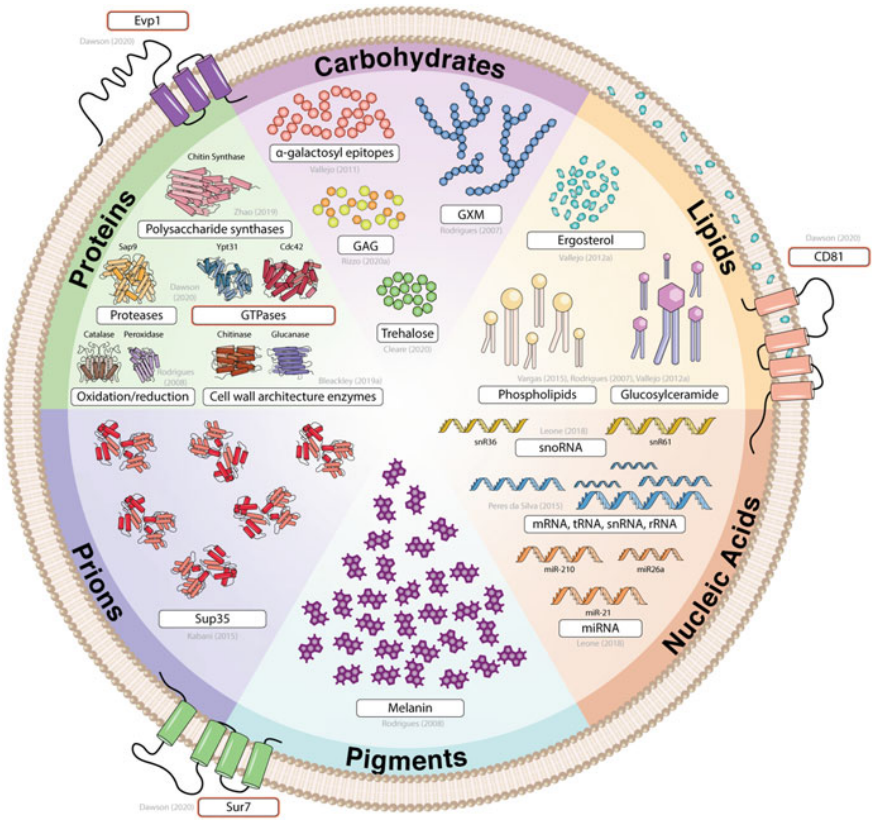

Fig. 7.2 Typical contents of fungal EVs. Carbohydrates include immunogenic molecules such as glucuronoxylomannan (GXM) (Rodrigues et al. 2007), galactosaminogalactan (GAG) (Rizzo et al. 2020b), and α-galactosyl epitopes (Vallejo et al. 2011); trehalose was associated to fungal adaptation (Cleare et al. 2020). Several proteins associated with virulence, such as catalase/peroxidase (Rodrigues et al. 2008), and with cell wall remodeling (Bleackley et al. 2019b), like glucanases and chitin synthase (Zhao et al. 2019), have been reported for different fungi. Potential protein markers from *C. albicans* (highlighted with red) include GTPases and eisosomal membrane proteins like Sur7, CD81 and Evp1 (Dawson et al. 2020). Lipid content includes glucosylceramide (Vargas et al. 2015; Rodrigues et al. 2007) ergosterol and general phospholipids (Vallejo et al. 2012b). Small RNAs have been described in EVs from several fungi. snR36 and snR61 have roles in rRNA synthesis and O-methylation of RNA, respectively (Peres da Silva et al. 2015b; Leone et al. 2018). miRNAs like miR-210, miR26a and miR21, function in cell differentiation and proliferation (Leone et al. 2018; Asangani et al. 2008). Melanin, a pigment used by *C. neoformans*, has been detected in EVs from this pathogen (Rodrigues et al. 2008). Transport of the prion Sup35 was characterized in EVs from *S. cerevisiae* (Kabani and Melki 2015)

most fungal species studied to date, supporting an important role in EV release depending on their location in the vesicle. Interestingly, since *C. neoformans* forms complexes of chitin and glucuronoxylomannan (GXM) that induce the production of IL-10, IL-17 an TNF-α in macrophages (Ramos et al. 2012), some authors have

suggested that cell wall-degrading enzymes transported by EVs generate smaller polysaccharides from the cell wall that elicit immune responses (Nimrichter et al. 2016).

The third proposed mechanism for EV release is through cell wall channels, suggested after observations of tubulin and actin were detected in EV preparations (Wolf et al. 2014; Rodrigues et al. 2008). Microscopy evidence does not support the presence of channels for EV release in *C. neoformans*, but rather a free transit through the cell wall (Wolf et al. 2014).

The importance of the cell wall in EV function is gaining traction. EV trafficking is an opportunity for the exchange of macromolecules within the cell wall and with the extracellular compartment (Zhao et al. 2019; Champer et al. 2016; Vallejo et al. 2012b), suggesting a facilitating role of EVs for adaptation of fungal cells to the environment. *S. cerevisiae* strains lacking genes associated with cell wall biosynthesis produced more EVs than wildtype, showing that the cell wall also works as a partial barrier to EV release. EVs may also function in cell wall strengthening under conditions that affect cell wall integrity (Zhao et al. 2019).

The reports discussed above have built a better understanding of the role of the fungal cell wall during EV production. Still, other points remain unanswered such as the effect of cell walls with different polysaccharide composition and thickness on EV release and content, and the role of the cell wall on EV release from filamentous and plant pathogenic fungi.

Emergence of Protein Markers for Fungal EVs

Mammalian and fungal EVs display different EV-specific protein markers. Typical mammalian EV markers such as tetraspanins and ESCRT proteins are not present in fungal EVs (Fig. 7.3) (Bleackley et al. 2019a) which has hampered the identification and isolation of fungal EVs. A recent study on EVs from *C. albicans* has provided a list of 47 proteins that could be employed as markers (Dawson et al. 2020). Some of these are eisosome-related proteins Sur7, Nce101 and Evp1. The fungal eisosome is a site of endocytosis located at the plasma membrane (Walther et al. 2006), which supports the hypothesis of EV formation via multivesicular bodies (Raposo and Stoorvogel 2013; Wolf et al. 2014). Other potential fungal EV markers include Rab GTPases Sec4 and Ypt31, and Rho GTPases Cdc42, Rac1, Rho1 and Rho3. It remains to be determined whether these markers are present in EVs from other fungal species.

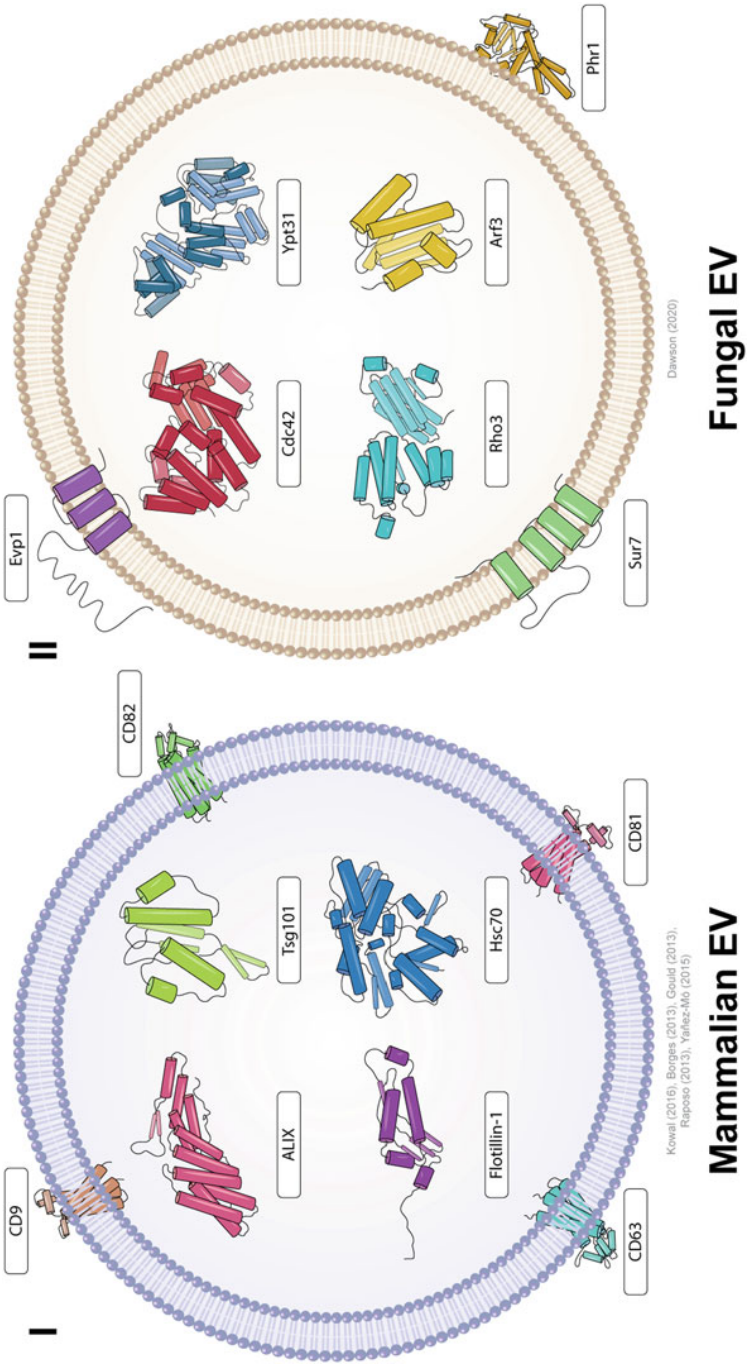

Fig. 7.3 Protein markers for mammalian and fungal EVs. I. Some of the most employed markers for mammalian EVs in isolation and characterization include ALIX, and tetraspanins such as CD63 and CD82 (Kowal et al. 2016; Borges et al. 2013; Gould and Raposo 2013; Raposo and Stoorvogel 2013; Yáñez-Mó et al. 2015). Such proteins have not been detected as markers in fungal EVs. II. Protein markers for fungal EVs have been proposed for *C. albicans*. These include eisosomal proteins EVp1, Sur7 and Nce101; GTPases such as Rho3, Arf3 and Ypt31 (Dawson et al. 2020)

Role of Fungal EVs in Pathophysiology

The role of fungal EVs in host-pathogen interactions has been reviewed widely (Joffe et al. 2016; Rodrigues and Casadevall 2018; Samuel et al. 2015). There are several reports showing direct links between EV production by human pathogens and changes in immune responses from the host (Fig. 7.4). These reports are discussed below.

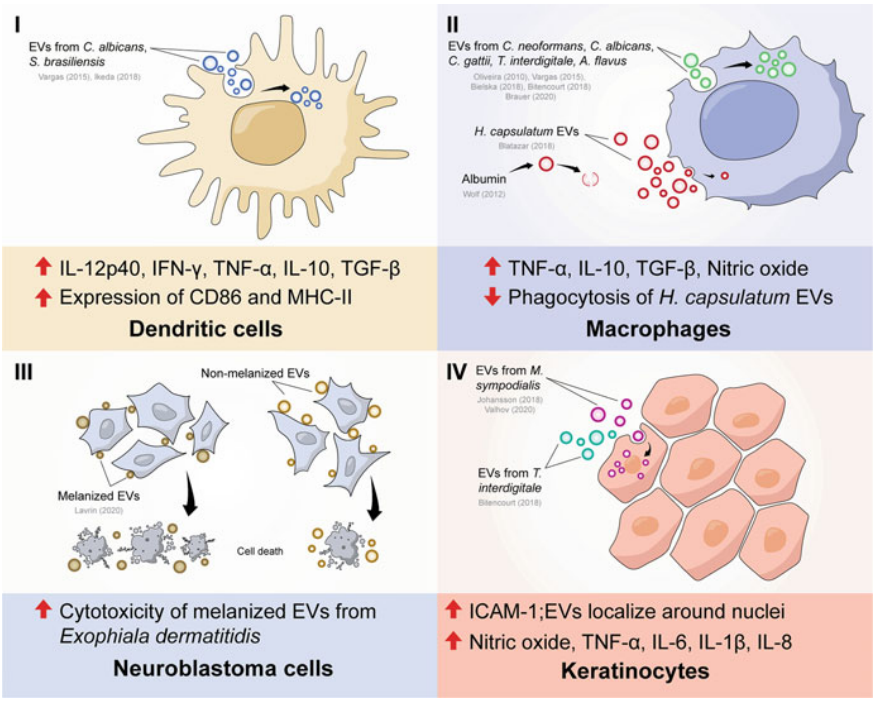

Fig. 7.4 Fungal EVs modulate the immune response of host cells. I. EVs from *C. albicans* and *S. brasiliensis* activate dendritic cells and increase the production of cytokines such as IL-12p40, IFN-γ, TNF-α, IL-10 and TGF-β. Other proteins upregulated in response to the presence of EVs were CD86 and MHC-II (Vargas et al. 2015; Ikeda et al. 2018). II. EVs from pathogenic fungi increase the production of TNF-α, TGF-β and nitric oxide by macrophages (Bielska et al. 2018; Bitencourt et al. 2018; Brauer et al. 2020; Oliveira et al. 2010a; Vargas et al. 2015). Incubation of macrophages with EVs from *H. capsulatum* reduced the ability of macrophages to phagocytize *H. capsulatum* (Baltazar et al. 2018). These studies revealed that albumin disrupts EVs (Wolf et al. 2012). III. EVs from the yeast *E. dermatitidis* were more cytotoxic than non-melanized EVs and had a greater ability to cause cell death (Lavrin et al. 2020). IV. Expression of the intracellular adhesion molecule 1 (ICAM-1), involved in immune defense of skin cells, was increased in keratinocytes after incubation with *M. sympodialis* EVs, which localized around the nuclei (Johansson et al. 2018; Vallhov et al. 2020). Similarly, keratinocytes increased production of cytokines after exposure to *T. interdigitale* EVs (Bitencourt et al. 2018)

Interactions of Yeast EVs with the Host Immune System

Fungal EVs have the ability to modify the immune response from the host (Zamith-Miranda et al. 2018). EVs from *C. neoformans* were internalized by murine macrophages, resulting in the production of TNF-α, a fungicidal cytokine, IL-10 and TGF-β (Fig. 7.4, II) (Oliveira et al. 2010a). Importantly, *C. neoformans* EVs appear to cross the blood-brain barrier. This observation is relevant since the infection mechanism that leads to cryptococcal meningoencephalitis is largely unknown and it may be mediated by *C. neoformans* EVs (Huang et al. 2012). Finally, EVs from *C. neoformans* (and from the bacterium *Bacillus anthracis*) are destabilized by human albumin and may have a short life *in vivo*, suggesting that content might be discharged shortly after EV release (Fig. 7.4, II) (Wolf et al. 2012).

Fungal EVs also protect *Histoplasma capsulatum* from the host defense arsenal by inhibiting phagocytosis by human bone marrow macrophages (Fig. 7.4, II) (Baltazar et al. 2018). The interaction between *H. capsulatum* and host cells also caused changes to EV content, suggesting that the composition of EVs is actively regulated (Baltazar et al. 2016, 2018).

C. albicans EVs modulate the immune response of murine macrophages and dendritic cells (Fig. 7.4, I and II), where they cause production of nitric oxide and several cytokines. EVs from *C. albicans* also conferred a protective effect in the infection model *Galleria mellonella.* Inoculating *G. mellonella* larvae with EVs from *C. albicans* prior to a yeast challenge reduced the survival of viable yeast compared to larvae that had not been pre-exposed to EVs, confirming the ability of EVs to modify immune responses (Vargas et al. 2015). A similar protective effect from *C. albicans* EVs was reported for mice, suggesting that fungal EVs may be used as a vaccination (Vargas et al. 2020).

Host cells also produce EVs in the presence of fungi. For instance, macrophages produce EVs with a different proteome after interaction with *C. albicans*. They have more proteins involved in immune responses, signaling and cytoskeleton reorganization, showing a role for EVs in cell communication (Reales-Calderon et al. 2017).

An important example of the involvement of EVs in cell-cell communications and in pathophysiology has come from a study with *Cryptococcus gattii*, the causative agent of respiratory infections (Bielska et al. 2018). This fungus uses a "division of labor" mechanism whereby cells with higher virulence due to mitochondrial changes facilitate the proliferation of cells without the mitochondrial modification, creating a pool of pathogenic fungi inside macrophages (Voelz et al. 2014). This process is mediated by EVs from *C. gattii* (Bielska et al. 2018). Similarly, *C. neoformans* can transition to the more virulent lineage VNIa-5, through a process that involves secreted proteins from the more virulent strain that are enriched in EVs (Hai et al. 2020).

Further evidence for the role of EVs in communication between fungi and host are the observations that dendritic cells increase phagocytosis rates of the yeast *Sporothrix brasiliensis* after they have been exposed to EVs from this pathogen (Fig. 7.4, I) (Ikeda et al. 2018). The same study reported that subcutaneous lesions in mice

were more severe, and the fungal load was higher at the time of euthanization, for mice that were administered EVs from *S. brasiliensis* prior to infection with the fungus (Ikeda et al. 2018). These findings are contrary to reports of a protective role of fungal EVs in *G. mellonella* (Vargas et al. 2015).

Fungal pigments carried by EVs can also enhance the virulence of fungal pathogens. For example, melanized EVs from the black yeast *E. dermatitidis* reduced the viability of neuroblastoma cells significantly more than non-melanized EVs (Fig. 7.4, III) (Lavrin et al. 2020). The authors suggest that these type of fungal infections might be involved in triggering neurodegenerative diseases such as Parkinson's disease (Lavrin et al. 2020).

EVs from fungi associated with non-life-threatening diseases have also been studied. *Malassezia sympodialis* is a yeast that causes atopic eczema (Bieber and Novak 2009). EVs from this fungus carry allergens and antigens with the capacity to activate human keratinocytes and monocytes (Fig. 7.4, IV) (Gehrmann et al. 2011; Johansson et al. 2018; Vallhov et al. 2020).

Interactions of Mycelial EVs with the Host Immune System

EVs from filamentous fungal pathogens are understudied compared to EVs from yeast. As mentioned above, *Aspergillus spp.* are a severe threat to human health and the role of EVs during infection of these pathogens is mostly unknown. However, EVs from *A. fumigatus* accelerate phagocytosis by neutrophils and macrophages, and macrophages increase production of cytokines TNF-α and CCL2, showing that EVs from filamentous fungi also modulate immune responses in the host (Souza et al. 2019).

Human granulocytes also produce EVs in response to *A. fumigatus* (Shopova et al. 2020). These mammalian EVs are enriched with antifungal molecules and were able to limit fungal growth, showing that the exchange of EVs modulates immune responses from the host and the pathogen (Shopova et al. 2020).

Similar to *C. albicans*, EVs from *Aspergillus flavus* increased the production of cytokines in bone marrow macrophages, which also increased phagocytic rates and developed the M1 phenotype (Brauer et al. 2020). Prior exposure to *C. albicans* EVs also protects *G. mellonella* larvae from a lethal fungal infection (Brauer et al. 2020), showing that both mycelial and yeast EVs can enhance the antifungal response from the host.

Human keratinocytes increase production of nitric oxide and cytokines after incubation with EVs from the dermatophyte *Trichophyton interdigitale*. Bone marrow macrophages responded in the same way as the keratinocytes after exposure to EVs from this fungus, and an M1 phenotype was also observed (Bitencourt et al. 2018). Preconditioning of bone marrow macrophages with EVs from *T. interdigitale* conidia also increased the fungicidal activity of the macrophages when they were incubated with the fungus (Bitencourt et al. 2018). Similar findings have been reported for *Paracoccidioides brasiliensis* (da Silva et al. 2016).

EV Content from Human Fungal Pathogens Suggests a Role in Virulence

Protein

Fungal EVs from human pathogens contain proteins that modulate the immune responses of host cells and that facilitate infection (Rodrigues et al. 2008; Peres da Silva et al. 2015a; da Silva et al. 2016; Rizzo et al. 2020a). For instance, proteins involved in protection against oxidative stress have been reported in EVs from plant and human pathogens (Vallejo et al. 2012a; Rodrigues et al. 2008; Bleackley et al. 2019b; Dawson et al. 2020). It is known that redox proteins, such as catalase and peroxidase, are used by fungi during colonization of the host (Warris and Ballou 2019). Another example of transport of virulence-associated proteins found in fungal EVs is phospholipase b, which disrupts phospholipids of the host and is essential for *C. albicans* virulence (Ghannoum 2000).

Fungal EVs carry a variety of proteases that function by enhancing fungal virulence (Yike 2011). For instance, the *C. albicans* protease Sap9 facilitates biofilm formation (Dutton et al. 2016; Dawson et al. 2020) and the peptidase YscII from *S. cerevisiae* is used to obtain leucine from environmental sources (Hirsch et al. 1988; Oliveira et al. 2010b).

Fungal EVs also transport enzymes involved in the production of pigments such as melanin, which can act as virulence factors. Melanin reduces phagocytosis by immune cells, alters cytokine production and reduces the toxicity of antifungal compounds (Taborda et al. 2008; Liu and Nizet 2009; Nosanchuk and Casadevall 2003; Panepinto et al. 2009; Nosanchuk et al. 2015). Laccase, involved in melanin production, was detected in EVs from *C. neoformans* (Rodrigues et al. 2008) and Eisenman and colleagues proposed melanization of *C. neoformans* occurs via synthesis inside EVs (Eisenman et al. 2009). Melanized EVs isolated from the black yeast *Exophiala dermatitidis* had a more potent cytotoxic effect on neuroblastoma cells than non-melanized EVs, showing that melanin is an important component for cytotoxicity (Lavrin et al. 2020).

RNA

EVs from *C. neoformans*, *P. brasiliensis*, *C. albicans* and *S. cerevisiae* carry RNA sequences of less than 250 nt. composed of mRNA, tRNA, rRNA, snRNA, snoRNA and miRNA (Peres da Silva et al. 2015a). Some of these sequences are involved in splicing control and RNA degradation (Peres da Silva et al. 2015a; Leone et al. 2018). EVs from *P. fermentans*, *C. neoformans*, *C. albicans*, *S. cerevisiae* and *P. brasiliensis* contain snR36 and snR61, snoRNAs involved in rRNA synthesis and O-methylation of RNA, respectively (Peres da Silva et al. 2015a; Leone et al. 2018). Other RNAs detected in EVs from *Pichia fermentans* with human orthologues, miR-210 and miR-26a, are induced during cell differentiation and hypoxia, and have a

potential role in pseudohyphal cell formation (Leone et al. 2018; Ramteke et al. 2015; Lee et al. 2015; Leeper et al. 2011). miR-21, also found in *P. fermentans* EVs, has a role in cell proliferation and apoptosis in human cells (Asangani et al. 2008).

The RNA content of EVs from the pathogen *Rhizopus delemar* included around 400 sequences of 18–30 bases, with roles in regulation of carbohydrate metabolism and biosynthesis of secondary metabolites, which in some fungal species is tightly related to virulence (Liu et al. 2018; Pusztahelyi et al. 2015). Analysis of RNA from *Paracoccidioides spp.* EVs revealed sRNA sequences that map to genes encoding fungal proteins such as α-amylase and β-glucanase, with a proposed role of regulating virulence genes (Peres da Silva et al. 2019).

The Golgi reassembly and stacking protein (GRASP) has a role in RNA export via EVs in *C. neoformans*, which may involve a tightly regulated mechanism (Peres da Silva et al. 2018). GRASP also functions in polysaccharide secretion in *C. neoformans* (Kmetzsch et al. 2011) suggesting an important role in vesicle loading.

Carbohydrates

There has been limited work on the carbohydrate content of EVs, partly due to the relatively large amount of material needed for glycomic analysis.

C. neoformans has an extracellular capsule made of glucuronoxylomannan (GXM) which decreases the phagocytic ability of immune cells and is associated with virulence (Vecchiarelli 2000). EVs have a fundamental role in the transport of GXM from the cytosol to the cell surface (Rodrigues et al. 2007, 2008).

A comparative analysis of the cargo of *H. capsulatum* EVs produced in different growth media revealed macromolecules associated with virulence, such as the glycolipid ergosterylglucoside. Trehalose, also detected in *H. capsulatum* EVs, is a carbohydrate associated to thermotolerance and growth under limited carbon sources (Cleare et al. 2020; François and Parrou 2001; Thammahong et al. 2017; Hare et al. 1998).

EVs from *A. fumigatus* also transport polysaccharides. Carbohydrate analysis revealed the presence of glucans, galactomannan and galactosaminogalactan (GAG) in EVs (Rizzo et al. 2020b). GAG is a cell wall polysaccharide that has potent immunomodulatory effects in mice (Fontaine et al. 2011; Gresnigt et al. 2014), supporting the role of fungal EVs in altering immune responses in the host.

Further glycomic studies on EVs from *Paracoccidioides* revealed α-galactosyl epitopes, which have the ability of activating immune cells (Vallejo et al. 2011). Also found in EVs were different types of cell wall oligosaccharides like 4,6-α-glucan and galactofuranosylmannan (da Silva et al. 2015; Peres da Silva et al. 2015b).

Lipids

Similar to the carbohydrate analysis, high amounts of EV material are needed to perform lipid analyses and hence there are few reports on the lipid composition of fungal EVs, since lipids may have a relatively low abundance based on EV size (Bleackley et al. 2019a).

EVs from *C. neoformans* contain sterol derivatives that, in other fungi, are involved in resistance to different types of stress and hence are targets of antifungal molecules (Lv et al. 2016; Rodrigues et al. 2007). Glucosylceramide, with a well-described role in fungal virulence, has also been detected in EVs from *C. neoformans* and from *C. albicans* (Rodrigues et al. 2007; Vargas et al. 2015; Rittershaus et al. 2006).

A lipidomic analysis of EVs from *P. brasiliensis*, revealed the presence of a plethora of phospholipids, fatty acids and sterols, with the most abundant being brassicasterol (Vallejo et al. 2012b). Brassicasterol has been linked to resistance to azole antifugal drugs (Camacho and Niño-Vega 2017), suggesting a potential link between EV production and drug resistance.

Prions

The transmission of prion Sup35 via EVs from *S. cerevisiae* has been reported recently (Liu et al. 2016; Kabani and Melki 2015). Although prions are best spread by direct contact between cells, EVs transport Sup35 into the extracellular space, creating a new mechanism of prion transmission in fungi. The transport of prions via EVs and their role in disease is well characterized in mammalian systems (Quek and Hill 2017).

Fungal EVs in Drug Resistance

Recent research has shed light on the role of EVs in drug resistance and in the morphological changes between yeast and biofilms. A *C. albicans* study revealed that EVs from planktonic cells are morphologically different and have a different proteome compared to biofilm-derived EVs. Also, WT EVs are able to confer resistance to antifungal-susceptible *C. albicans* strains. These data show that EVs have a role in biofilm matrix biogenesis and that there is a direct link between EV production and drug resistance (Zarnowski et al. 2018; Dawson et al. 2020). A role for morphological shifts was also reported for the industrial fungus *Pichia fermentans*, in a process that my mediated by EVs (Leone et al. 2018). Similarly, EVs were able protect *S. cerevisiae* from the antifungal caspofungin and the plant defensin NaD1 (Zhao et al. 2019). The authors proposed two mechanisms for EV-mediated drug resistance: the first is that EVs act as decoys and interact with these lipid-binding antifungals, effectively sequestering them. The second mechanism relies on EV internalization by host cells that derives in reinforcement of the fungal cell wall and in protection against the antifungal agents (Zhao et al. 2019).

EVs from Fungal Plant Pathogens Contain Molecules Related to Virulence

Little is known about the content and function of EVs from fungal plant pathogens compared to human fungal pathogens. Proteomic data is available only for EVs from *Alternaria infectoria* (Silva et al. 2014), and *Fusarium oxysporum* f. sp. *vasinfectum* (Fov) (Silva et al. 2014; Bleackley et al. 2019b). However, some proteins indicate a potential role for fungal EVs during infection. For instance, Fov EVs contain a Hsp70-like protein. Hsp70 is involved in conidiation and plant infection in *Fusarium pseudograminearum*, an emerging plant pathogen (Chen et al. 2019).

Fov EVs are enriched with two types of polyketide synthases that might be involved in the production of the pigment bikaverin. EVs and/or this pigment are thought to be responsible for causing a hypersensitive response on cotton cotyledons (Bleackley et al. 2019b). Polyketide synthases are used extensively in toxin production from plant pathogens and have a clear role in virulence (Choquer et al. 2005; Yang et al. 1996; Noar et al. 2019; Ruocco et al. 2018; Woo et al. 2012).

Proteases from plant pathogenic fungi can also increase the severity of plant diseases (Podder et al. 2019). Fov EVs were enriched with various proteases such as carboxypeptidases D and F, glutamate carboxypeptidase II, Pep1, vacuolar protease a, and aspartic-type signal peptidase a (Bleackley et al. 2019b). The role of these proteases in the context of a plant infection still needs to be addressed.

A. infectoria EVs contain proteins involved in polysaccharide metabolism, pigment synthesis, and trafficking of vesicles (Silva et al. 2014).

Conclusion

The production of fungal extracellular vesicles has been reported for pathogenic and non-pathogenic fungal species. Fungal EVs are similar in morphology and content to EVs from other organisms, and multi omic analyses have revealed that EVs supports a role in cell wall remodeling, infection, and interactions between yeast and filamentous fungi with their animal or plant host.

The field of fungal EVs has consistently advanced towards a better understanding of EV function. The absence of universal fungal markers to assist in isolation and tracking in biological systems, the lack of knowledge on EV heterogeneity from a single fungal species, as well as little information on specific pathways represent exciting challenges. The diversity of fungi provides the opportunity to investigate new pathogens and interactions with their hosts, which in time will lead to elicit a more complete role of fungal EVs in the context of infection.

A better understanding of EV cargo and how they enhance virulence of fungal pathogens or prime the immune response of the host for protection against pathogens is highly likely to lead to the development of new drugs for treatment of fungal diseases.

References

Albuquerque PC, Nakayasu ES, Rodrigues ML, Frases S, Casadevall A, Zancope-Oliveira RM, Almeida IC, Nosanchuk JD (2008) Vesicular transport in *Histoplasma capsulatum*: an effective mechanism for trans-cell wall transfer of proteins and lipids in ascomycetes. Cell Microbiol 10 (8):1695–1710. https://doi.org/10.1111/j.1462-5822.2008.01160.x

Altendorf S (2019) Banana *Fusarium* wilt tropical race 4: a mounting threat to global banana markets? FAO Food Outlook, FAO

Alves LR, da Silva RP, Sanchez DA, Zamith-Miranda D, Rodrigues ML, Goldenberg S, Puccia R, Nosanchuk JD (2019) Extracellular vesicle-mediated RNA release in *Histoplasma capsulatum*. bioRxiv:570291. doi:https://doi.org/10.1101/570291

Asangani IA, Rasheed SA, Nikolova DA, Leupold JH, Colburn NH, Post S, Allgayer H (2008) MicroRNA-21 (miR-21) post-transcriptionally downregulates tumor suppressor Pdcd4 and stimulates invasion, intravasation and metastasis in colorectal cancer. Oncogene 27(15):2128–2136. https://doi.org/10.1038/sj.onc.1210856

Baltazar L, Nakayasu ES, Sobreira TJ, Choi H, Casadevall A, Nimrichter L, Nosanchuk JD (2016) Antibody binding alters the characteristics and contents of extracellular vesicles released by *Histoplasma capsulatum*. mSphere 1(2). https://doi.org/10.1128/mSphere.00085-15

Baltazar LM, Zamith-Miranda D, Burnet MC, Choi H, Nimrichter L, Nakayasu ES, Nosanchuk JD (2018) Concentration-dependent protein loading of extracellular vesicles released by *Histoplasma capsulatum* after antibody treatment and its modulatory action upon macrophages. Sci Rep 8(1):8065. https://doi.org/10.1038/s41598-018-25665-5

Benedict K, Jackson BR, Chiller T, Beer KD (2019) Estimation of direct healthcare costs of fungal diseases in the United States. Clin Infect Dis 68(11):1791–1797. https://doi.org/10.1093/cid/ciy776

Bhattacharya S (2017) Deadly new wheat disease threatens Europe's crops. Nature 542(7640):145–146. https://doi.org/10.1038/nature.2017.21424

Bieber T, Novak N (2009) Pathogenesis of atopic dermatitis: new developments. Curr Allergy Asthma Rep 9(4):291–294. https://doi.org/10.1007/s11882-009-0041-2

Bielska E, Sisquella MA, Aldeieg M, Birch C, O'Donoghue EJ, May RC (2018) Pathogen-derived extracellular vesicles mediate virulence in the fatal human pathogen *Cryptococcus gattii*. Nat Commun 9(1):1556. https://doi.org/10.1038/s41467-018-03991-6

Bitencourt TA, Rezende CP, Quaresemin NR, Moreno P, Hatanaka O, Rossi A, Martinez-Rossi NM, Almeida F (2018) Extracellular vesicles from the Dermatophyte *Trichophyton interdigitale* modulate macrophage and keratinocyte functions. Front Immunol 9(2343). https://doi.org/10.3389/fimmu.2018.02343

Bleackley MR, Dawson CS, Anderson MA (2019a) Fungal extracellular vesicles with a focus on proteomic analysis. Proteomics 19(8):1800232. https://doi.org/10.1002/pmic.201800232

Bleackley M, Samuel M, Garcia-Ceron D, Mckenna J, Lowe R, Pathan M, Zhao K, Ang C, Mathivanan S, Anderson M (2019b) Extracellular vesicles from the cotton pathogen *Fusarium oxysporum* f. sp. *vasinfectum* induce a phytotoxic response in plants. Front Plant Sci 10:1610. https://doi.org/10.3389/fpls.2019.01610

Bongomin F, Gago S, Oladele RO, Denning DW (2017) Global and multi-National Prevalence of fungal diseases-estimate precision. J Fungi (Basel, Switzerland) 3(4):57. https://doi.org/10.3390/jof3040057

Borges FT, Reis LA, Schor N (2013) Extracellular vesicles: structure, function, and potential clinical uses in renal diseases. Braz J Med Biol Res 46(10):824–830. https://doi.org/10.1590/1414-431X20132964

Brauer VS, Pessoni AM, Bitencourt TA, de Paula RG, de Oliveira Rocha L, Goldman GH, Almeida F (2020) Extracellular vesicles from *Aspergillus flavus* induce M1 polarization in vitro. mSphere 5(3):e00190–e00120. https://doi.org/10.1128/mSphere.00190-20

Brown GD, Denning DW, Gow NA, Levitz SM, Netea MG, White TC (2012) Hidden killers: human fungal infections. Sci Transl Med 4(165). https://doi.org/10.1126/scitranslmed.3004404

Brown L, Wolf JM, Prados-Rosales R, Casadevall A (2015) Through the wall: extracellular vesicles in gram-positive bacteria, mycobacteria and fungi. Nat Rev Microbiol 13(10):620–630. https://doi.org/10.1038/nrmicro3480

Camacho E, Niño-Vega GA (2017) *Paracoccidioides Spp.*: virulence factors and immune-evasion strategies. Mediat Inflamm 2017:5313691. https://doi.org/10.1155/2017/5313691

CDC (2019) Antibiotic resistance threats in the United States. U.S. Department of Health and Human Services, Atlanta, GA

Champer J, Ito JI, Clemons KV, Stevens DA, Kalkum M (2016) Proteomic analysis of pathogenic fungi reveals highly expressed conserved Cell Wall proteins. J Fungi (Basel, Switzerland) 2 (1):6. https://doi.org/10.3390/jof2010006

Chen L, Geng X, Ma Y, Zhao J, Chen W, Xing X, Shi Y, Sun B, Li H (2019) The ER Lumenal Hsp70 protein FpLhs1 is important for Conidiation and plant infection in *Fusarium pseudograminearum*. Front Microbiol 10(1401). https://doi.org/10.3389/fmicb.2019.01401

Choquer M, Dekkers KL, Chen HQ, Cao L, Ueng PP, Daub ME, Chung KR (2005) The CTB1 gene encoding a fungal polyketide synthase is required for cercosporin biosynthesis and fungal virulence of *Cercospora nicotianae*. Molecular plant-microbe interactions: MPMI 18(5):468–476. https://doi.org/10.1094/mpmi-18-0468

Cleare LG, Zamith D, Heyman HM, Couvillion SP, Nimrichter L, Rodrigues ML, Nakayasu ES, Nosanchuk JD (2020) Media matters! Alterations in the loading and release of *Histoplasma capsulatum* extracellular vesicles in response to different nutritional milieus. Cell Microbiol: e13217. https://doi.org/10.1111/cmi.13217

da Silva RP, Heiss C, Black I, Azadi P, Gerlach JQ, Travassos LR, Joshi L, Kilcoyne M, Puccia R (2015) Extracellular vesicles from *Paracoccidioides pathogenic* species transport polysaccharide and expose ligands for DC-SIGN receptors. Sci Rep 5:14213. https://doi.org/10.1038/srep14213. https://www.nature.com/articles/srep14213#supplementary-information

da Silva TA, Roque-Barreira MC, Casadevall A, Almeida F (2016) Extracellular vesicles from *Paracoccidioides brasiliensis* induced M1 polarization in vitro. Sci Rep 6:35867. https://doi.org/10.1038/srep35867

da Silva Ferreira ME, Capellaro JL, dos Reis Marques E, Malavazi I, Perlin D, Park S, Anderson JB, Colombo AL, Arthington-Skaggs BA, Goldman MHS, Goldman GH (2004) *In Vitro* evolution of Itraconazole resistance in *Aspergillus fumigatus* involves multiple mechanisms of resistance. Antimicrob Agents Chemother 48(11):4405. https://doi.org/10.1128/AAC.48.11.4405-4413.2004

Dawson CS, Garcia-Ceron D, Rajapaksha H, Faou P, Bleackley MR, Anderson MA (2020) Protein markers for *Candida albicans* EVs include claudin-like Sur7 family proteins. J Extracell Vesicles 9(1):1750810. https://doi.org/10.1080/20013078.2020.1750810

De Nobel JG, Dijkers C, Hooijberg E, Klis FM (1989) Increased Cell Wall porosity in *Saccharomyces cerevisiae* after treatment with Dithiothreitol or EDTA. Microbiology 135(7):2077–2084. https://doi.org/10.1099/00221287-135-7-2077

De Nobel JG, Klis FM, Munnik T, Priem J, van den Ende H (1990) An assay of relative cell wall porosity in *Saccharomyces cerevisiae*, *Kluyveromyces lactis* and *Schizosaccharomyces pombe*. Yeast 6(6):483–490. https://doi.org/10.1002/yea.320060605

de Paula RG, Antoniêto ACC, Nogueira KMV, Ribeiro LFC, Rocha MC, Malavazi I, Almeida F, Silva RN (2019) Extracellular vesicles carry cellulases in the industrial fungus *Trichoderma reesei*. Biotechnol Biofuels 12(1):146. https://doi.org/10.1186/s13068-019-1487-7

Dean R, Van Kan JAL, Pretorius ZA, Hammond-Kosak KE, Di Pietro A, Spanu PD, Rudd JJ, Dickman M, Kahmann R, Ellis J, Foster GD (2012) The top 10 fungal pathogens in molecular plant pathology. Mol Plant Pathol 13(4):414–430. https://doi.org/10.1111/j.1364-3703.2011.00783.x

DeIulio GA, Guo L, Zhang Y, Goldberg JM, Kistler HC, Ma L-J (2018) Kinome expansion in the *Fusarium oxysporum* species complex driven by accessory chromosomes. mSphere 3(3): e00231–e00218. https://doi.org/10.1128/mSphere.00231-18

Denning DW, Pleuvry A, Cole DC (2011) Global burden of chronic pulmonary aspergillosis as a sequel to pulmonary tuberculosis. Bull World Health Organ 89(12):864–872. https://doi.org/10.2471/BLT.11.089441

Denning DW, Pleuvry A, Cole DC (2013) Global burden of allergic bronchopulmonary aspergillosis with asthma and its complication chronic pulmonary aspergillosis in adults. Med Mycol 51 (4):361–370. https://doi.org/10.3109/13693786.2012.738312

Dracatos PM, Haghdoust R, Singh D, Park RF (2018) Exploring and exploiting the boundaries of host specificity using the cereal rust and mildew models. New Phytol 218(2):453–462. https://doi.org/10.1111/nph.15044

Dutton LC, Jenkinson HF, Lamont RJ, Nobbs AH (2016) Role of *Candida albicans* secreted aspartyl protease Sap9 in interkingdom biofilm formation. Pathog Dis 74(3). https://doi.org/10.1093/femspd/ftw005

Eisenman HC, Frases S, Nicola AM, Rodrigues ML, Casadevall A (2009) Vesicle-associated melanization in *Cryptococcus neoformans*. Microbiology 155 (Pt 12):3860–3867. doi:https://doi.org/10.1099/mic.0.032854-0

Fisher MC, Gurr SJ, Cuomo CA, Blehert DS, Jin H, Stukenbrock EH, Stajich JE, Kahmann R, Boone C, Denning DW, Gow NAR, Klein BS, Kronstad JW, Sheppard DC, Taylor JW, Wright GD, Heitman J, Casadevall A, Cowen LE (2020) Threats posed by the fungal kingdom to humans, wildlife, and agriculture. MBio 11(3):e00449–e00420. https://doi.org/10.1128/mBio.00449-20

Fontaine T, Delangle A, Simenel C, Coddeville B, van Vliet SJ, van Kooyk Y, Bozza S, Moretti S, Schwarz F, Trichot C, Aebi M, Delepierre M, Elbim C, Romani L, Latgé J-P (2011) Galactosaminogalactan, a new immunosuppressive polysaccharide of *Aspergillus fumigatus*. PLoS Pathog 7 (11):e1002372-e1002372. doi:https://doi.org/10.1371/journal.ppat.1002372

François J, Parrou JL (2001) Reserve carbohydrates metabolism in the yeast *Saccharomyces cerevisiae*. FEMS Microbiol Rev 25(1):125–145. https://doi.org/10.1111/j.1574-6976.2001.tb00574.x

Freitas MS, Bonato VLD, Pessoni AM, Rodrigues ML, Casadevall A, Almeida F (2019) Fungal extracellular vesicles as potential targets for immune interventions. mSphere 4(6):e00747–e00719. https://doi.org/10.1128/mSphere.00747-19

Gehrmann U, Qazi KR, Johansson C, Hultenby K, Karlsson M, Lundeberg L, Gabrielsson S, Scheynius A (2011) Nanovesicles from *Malassezia sympodialis* and host Exosomes induce cytokine responses–novel mechanisms for host-microbe interactions in atopic eczema. PLoS One 6(7):e21480. https://doi.org/10.1371/journal.pone.0021480

Ghannoum MA (2000) Potential role of phospholipases in virulence and fungal pathogenesis. Clin Microbiol Rev 13(1):122–143. https://doi.org/10.1128/cmr.13.1.122-143.2000

Gil-Bona A, Llama-Palacios A, Parra CM, Vivanco F, Nombela C, Monteoliva L, Gil C (2015) Proteomics unravels extracellular vesicles as carriers of classical cytoplasmic proteins in *Candida albicans*. J Proteome Res 14(1):142–153. https://doi.org/10.1021/pr5007944

Goswami RS, Kistler HC (2004) Heading for disaster: *Fusarium graminearum* on cereal crops. Mol Plant Pathol 5(6):515–525. https://doi.org/10.1111/j.1364-3703.2004.00252.x

Gould SJ, Raposo G (2013) As we wait: coping with an imperfect nomenclature for extracellular vesicles. J Extracell Vesicles 2:. doi:https://doi.org/10.3402/jev.v2i0.20389

Gresnigt MS, Bozza S, Becker KL, Joosten LA, Abdollahi-Roodsaz S, van der Berg WB, Dinarello CA, Netea MG, Fontaine T, De Luca A, Moretti S, Romani L, Latge JP, van de Veerdonk FL (2014) A polysaccharide virulence factor from *Aspergillus fumigatus* elicits anti-inflammatory effects through induction of Interleukin-1 receptor antagonist. PLoS Pathog 10(3):e1003936. https://doi.org/10.1371/journal.ppat.1003936

Hai TP, Tuan TL, Van Anh D, Mai TN, Phu Huong LN, Thwaites GE, Johnson E, Van Vinh Chau N, Baker S, Ashton PM, Day JN (2020) The virulence of the *Cryptococcus neoformans* VNIa-5 lineage is highly plastic and associated with isolate background. bioRxiv:2020.2002.2024.962134. doi:https://doi.org/10.1101/2020.02.24.962134

Hare PD, Cress WA, Van Staden J (1998) Dissecting the roles of osmolyte accumulation during stress. Plant Cell Environ 21(6):535–553. https://doi.org/10.1046/j.1365-3040.1998.00309.x

Hawksworth DL (2001) The magnitude of fungal diversity: the 1.5 million species estimate revisited. Mycol Res 105(12):1422–1432. https://doi.org/10.1017/S0953756201004725

Hirsch HH, Suarez Rendueles P, Achstetter T, Wolf DH (1988) Aminopeptidase yscII of yeast. Isolation of mutants and their biochemical and genetic analysis. Eur J Biochem 173(3):589–598. https://doi.org/10.1111/j.1432-1033.1988.tb14040.x

Hopke A, Brown AJP, Hall RA, Wheeler RT (2018) Dynamic fungal Cell Wall architecture in stress adaptation and immune evasion. Trends Microbiol 26(4):284–295. https://doi.org/10.1016/j.tim.2018.01.007

Huang S-H, Wu C-H, Chang YC, Kwon-Chung KJ, Brown RJ, Jong A (2012) Cryptococcus neoformans-derived microvesicles enhance the pathogenesis of fungal brain infection. PLoS One 7(11):e48570. https://doi.org/10.1371/journal.pone.0048570

Ikeda MAK, de Almeida JRF, Jannuzzi GP, Cronemberger-Andrade A, Torrecilhas ACT, Moretti NS, da Cunha JPC, de Almeida SR, Ferreira KS (2018) Extracellular vesicles from *Sporothrix brasiliensis* are an important virulence factor that induce an increase in fungal burden in experimental Sporotrichosis. Front Microbiol 9:2286–2286. https://doi.org/10.3389/fmicb.2018.02286

Joffe LS, Nimrichter L, Rodrigues ML, Del Poeta M (2016) Potential roles of fungal extracellular vesicles during infection. mSphere 1(4):e00099–e00016. https://doi.org/10.1128/mSphere.00099-16

Johansson HJ, Vallhov H, Holm T, Gehrmann U, Andersson A, Johansson C, Blom H, Carroni M, Lehtiö J, Scheynius A (2018) Extracellular nanovesicles released from the commensal yeast *Malassezia sympodialis* are enriched in allergens and interact with cells in human skin. Sci Rep 8(1):9182. https://doi.org/10.1038/s41598-018-27451-9

Kabani M, Melki R (2015) Sup35p in its soluble and prion states is packaged inside extracellular vesicles. MBio 6(4):e01017–e01015. https://doi.org/10.1128/mBio.01017-15

Kmetzsch L, Joffe LS, Staats CC, de Oliveira DL, Fonseca FL, Cordero RJ, Casadevall A, Nimrichter L, Schrank A, Vainstein MH, Rodrigues ML (2011) Role for Golgi reassembly and stacking protein (GRASP) in polysaccharide secretion and fungal virulence. Mol Microbiol 81(1):206–218. https://doi.org/10.1111/j.1365-2958.2011.07686.x

Kowal J, Arras G, Colombo M, Jouve M, Morath JP, Primdal-Bengtson B, Dingli F, Loew D, Tkach M, Théry C (2016) Proteomic comparison defines novel markers to characterize heterogeneous populations of extracellular vesicle subtypes. Proc Natl Acad Sci 113(8):E968. https://doi.org/10.1073/pnas.1521230113

Lavrin T, Konte T, Kostanjsek R, Sitar S, Sepcic K, Prpar Mihevc S, Zagar E, Zupunski V, Lenassi M, Rogelj B, Gunde Cimerman N (2020) The neurotropic Black yeast *Exophiala dermatitidis* induces Neurocytotoxicity in Neuroblastoma cells and progressive cell death. Cell 9(4). https://doi.org/10.3390/cells9040963

Lee S-W, Yang J, Kim S-Y, Jeong H-K, Lee J, Kim WJ, Lee EJ, Kim H-S (2015) MicroRNA-26a induced by hypoxia targets HDAC6 in myogenic differentiation of embryonic stem cells. Nucleic Acids Res 43(4):2057–2073. https://doi.org/10.1093/nar/gkv088

Leeper NJ, Raiesdana A, Kojima Y, Chun HJ, Azuma J, Maegdefessel L, Kundu RK, Quertermous T, Tsao PS, Spin JM (2011) MicroRNA-26a is a novel regulator of vascular smooth muscle cell function. J Cell Physiol 226(4):1035–1043. https://doi.org/10.1002/jcp.22422

Leone F, Bellani L, Muccifora S, Giorgetti L, Bongioanni P, Simili M, Maserti B, Del Carratore R (2018) Analysis of extracellular vesicles produced in the biofilm by the dimorphic yeast *Pichia fermentans*. J Cell Physiol 233(4):2759–2767. https://doi.org/10.1002/jcp.25885

LIFE (2017) The burden of fungal disease: new evidence to show the scale of the problem across the globe. https://www.gaffi.org/the-burden-of-fungal-disease-new-evidence-to-show-the-scale-of-the-problem-across-the-globe/. Accessed 30-04-2020

Liu GY, Nizet V (2009) Color me bad: microbial pigments as virulence factors. Trends Microbiol 17(9):406–413. https://doi.org/10.1016/j.tim.2009.06.006

Liu S, Hossinger A, Hofmann JP, Denner P, Vorberg IM (2016) Horizontal transmission of cytosolic Sup35 prions by extracellular vesicles. MBio 7(4):e00915–e00916. https://doi.org/10.1128/mBio.00915-16

Liu M, Bruni GO, Taylor CM, Zhang Z, Wang P (2018) Comparative genome-wide analysis of extracellular small RNAs from the mucormycosis pathogen *Rhizopus delemar*. Sci Rep 8 (1):5243. https://doi.org/10.1038/s41598-018-23611-z

Lockhart SR, Beer K, Toda M (2020) Azole-resistant *Aspergillus fumigatus*: what you need to know. Clin Microbiol Newsl 42(1):1–6. https://doi.org/10.1016/j.clinmicnews.2019.12.003

Lv Q-Z, Yan L, Jiang Y-Y (2016) The synthesis, regulation, and functions of sterols in *Candida albicans*: well-known but still lots to learn. Virulence 7(6):649–659. https://doi.org/10.1080/21505594.2016.1188236

Nalley L, Tsiboe F, Durand-Morat A, Shew A, Thoma G (2016) Economic and environmental impact of Rice blast pathogen (*Magnaporthe oryzae*) alleviation in the United States. PLoS One 11(12):e0167295. https://doi.org/10.1371/journal.pone.0167295

Nganje WE, Kaitibie S, Wilson W, Leistritz L, Bangsund D (2004) Economic impact of *Fusarium* head blight in wheat and barley: 1993–2001 (trans: station AE), vol 538. North Dakota State University, Fargo, ND

Nimrichter L, de Souza MM, Del Poeta M, Nosanchuk JD, Joffe L, Tavares Pde M, Rodrigues ML (2016) Extracellular vesicle-associated transitory Cell Wall components and their impact on the interaction of fungi with host cells. Front Microbiol 7:1034. https://doi.org/10.3389/fmicb.2016.01034

Noar RD, Thomas E, Daub ME (2019) A novel polyketide synthase gene cluster in the plant pathogenic fungus *Pseudocercospora fijiensis*. PLoS One 14(2):e0212229. https://doi.org/10.1371/journal.pone.0212229

Nosanchuk JD, Casadevall A (2003) The contribution of melanin to microbial pathogenesis. Cell Microbiol 5(4):203–223. https://doi.org/10.1046/j.1462-5814.2003.00268.x

Nosanchuk JD, Stark RE, Casadevall A (2015) Fungal melanin: what do we know about structure? Front Microbiol 6(1463). https://doi.org/10.3389/fmicb.2015.01463

O'Neill WT, Henderson J, Pattemore JA, O'Dwyer C, Perry S, Beasley DR, Tan YP, Smyth AL, Goosem CH, Thomson KM, Hobbs RL, Grice KRE, Trevorrow P, Vawdrey LL, Pathania N, Shivas RG (2016) Detection of *Fusarium oxysporum* f. sp. *cubense* tropical race 4 strain in northern Queensland. Aust Plant Dis Notes 11(1):33. https://doi.org/10.1007/s13314-016-0218-1

Oliveira DL, Freire-de-Lima CG, Nosanchuk JD, Casadevall A, Rodrigues ML, Nimrichter L (2010a) Extracellular vesicles from *Cryptococcus neoformans* modulate macrophage functions. Infect Immun 78(4):1601–1609. https://doi.org/10.1128/iai.01171-09

Oliveira DL, Nakayasu ES, Joffe LS, Guimarães AJ, Sobreira TJP, Nosanchuk JD, Cordero RJB, Frases S, Casadevall A, Almeida IC, Nimrichter L, Rodrigues ML (2010b) Characterization of yeast extracellular vesicles: evidence for the participation of different pathways of cellular traffic in vesicle biogenesis. PLoS One 5(6):e11113. https://doi.org/10.1371/journal.pone.0011113

Ordoñez N, García-Bastidas F, Laghari HB, Akkary MY, Harfouche EN, al Awar BN, Kema GHJ (2015) First report of *Fusarium oxysporum* f. sp. *cubense* tropical race 4 causing Panama disease in Cavendish bananas in Pakistan and Lebanon. Plant Dis 100(1):209. https://doi.org/10.1094/PDIS-12-14-1356-PDN

Panepinto J, Komperda K, Frases S, Park YD, Djordjevic JT, Casadevall A, Williamson PR (2009) Sec6-dependent sorting of fungal extracellular exosomes and laccase of *Cryptococcus neoformans*. Mol Microbiol 71(5):1165–1176. https://doi.org/10.1111/j.1365-2958.2008.06588.x

Peres da Silva R, Heiss C, Black I, Azadi P, Gerlach JQ, Travassos LR, Joshi L, Kilcoyne M, Puccia R (2015a) Extracellular vesicles from Paracoccidioides pathogenic species transport polysaccharide and expose ligands for DC-SIGN receptors. Sci Rep 5:14213. https://doi.org/10.1038/srep14213

Peres da Silva R, Puccia R, Rodrigues ML, Oliveira DL, Joffe LS, César GV, Nimrichter L, Goldenberg S, Alves LR (2015b) Extracellular vesicle-mediated export of fungal RNA. Sci Rep 5:7763. https://doi.org/10.1038/srep07763. https://www.nature.com/articles/srep07763#supplementary-information

Peres da Silva R, Martins ST, Rizzo J, Dos Reis FCG, Joffe LS, Vainstein M, Kmetzsch L, Oliveira DL, Puccia R, Goldenberg S, Rodrigues ML, Alves LR (2018) Golgi reassembly and stacking protein (GRASP) participates in vesicle-mediated RNA export in *Cryptococcus neoformans*. Genes 9(8):400. https://doi.org/10.3390/genes9080400

Peres da Silva R, Longo LGV, Cunha J, Sobreira TJP, Rodrigues ML, Faoro H, Goldenberg S, Alves LR, Puccia R (2019) Comparison of the RNA content of extracellular vesicles derived from *Paracoccidioides brasiliensis* and *Paracoccidioides lutzii*. Cell 8(7). https://doi.org/10.3390/cells8070765

Podder S, Saha D, Ghosh TC (2019) Deciphering the intrinsic properties of fungal proteases in optimizing phytopathogenic interaction. Gene 711:143934. https://doi.org/10.1016/j.gene.2019.06.024

Pusztahelyi T, Holb I, Pócsi I (2015) Secondary metabolites in fungus-plant interactions. Front Plant Sci 6(573). https://doi.org/10.3389/fpls.2015.00573

Quek C, Hill AF (2017) The role of extracellular vesicles in neurodegenerative diseases. Biochem Biophys Res Commun 483(4):1178–1186. https://doi.org/10.1016/j.bbrc.2016.09.090

Rajasingham R, Smith RM, Park BJ, Jarvis JN, Govender NP, Chiller TM, Denning DW, Loyse A, Boulware DR (2017) Global burden of disease of HIV-associated cryptococcal meningitis: an updated analysis. Lancet Infect Dis 17(8):873–881. https://doi.org/10.1016/S1473-3099(17)30243-8

Ramos CL, Fonseca FL, Rodrigues J, Guimarães AJ, Cinelli LP, Miranda K, Nimrichter L, Casadevall A, Travassos LR, Rodrigues ML (2012) Chitin-like molecules associate with *Cryptococcus neoformans* glucuronoxylomannan to form a glycan complex with previously unknown properties. Eukaryot Cell 11(9):1086–1094. https://doi.org/10.1128/EC.00001-12

Ramteke A, Ting H, Agarwal C, Mateen S, Somasagara R, Hussain A, Graner M, Frederick B, Agarwal R, Deep G (2015) Exosomes secreted under hypoxia enhance invasiveness and stemness of prostate cancer cells by targeting adherens junction molecules. Mol Carcinog 54(7):554–565. https://doi.org/10.1002/mc.22124

Raposo G, Stoorvogel W (2013) Extracellular vesicles: exosomes, microvesicles, and friends. J Cell Biol 200(4):373–383. https://doi.org/10.1083/jcb.201211138

Ray DK, Mueller ND, West PC, Foley JA (2013) Yield trends are insufficient to double global crop production by 2050. PLoS One 8(6):e66428. https://doi.org/10.1371/journal.pone.0066428

Reales-Calderon JA, Vaz C, Monteoliva L, Molero G, Gil C (2017) Candida albicans modifies the protein composition and size distribution of THP-1 macrophage-derived extracellular vesicles. J Proteome Res 16(1):87–105. https://doi.org/10.1021/acs.jproteome.6b00605

Rittershaus PC, Kechichian TB, Allegood JC, Merrill AH, Jr., Hennig M, Luberto C, Del Poeta M (2006) Glucosylceramide synthase is an essential regulator of pathogenicity of *Cryptococcus neoformans*. J Clin Invest 116 (6):1651–1659. doi:https://doi.org/10.1172/jci27890

Rizzo J, Chaze T, Miranda K, Roberson R, Gorgette O, Nimrichter L, Matondo M, Latgé J, Beauvais A, Rodrigues M (2020a) Characterization of extracellular vesicles produced by *Aspergillus fumigatus* protoplasts. mSphere In press

Rizzo J, Rodrigues ML, Janbon G (2020b) Extracellular vesicles in fungi: past, present, and future perspectives. Front Cell Infect Microbiol 10(346). https://doi.org/10.3389/fcimb.2020.00346

Rodrigues ML, Casadevall A (2018) A two-way road: novel roles for fungal extracellular vesicles. Mol Microbiol 110(1):11–15. https://doi.org/10.1111/mmi.14095

Rodrigues ML, Nosanchuk JD (2020) Fungal diseases as neglected pathogens: a wake-up call to public health officials. PLoS Negl Trop Dis 14(2):e0007964. https://doi.org/10.1371/journal.pntd.0007964

Rodrigues ML, Alviano CS, Travassos LR (1999) Pathogenicity of *Cryptococcus neoformans*: virulence factors and immunological mechanisms. Microbes Infect 1(4):293–301. https://doi.org/10.1016/s1286-4579(99)80025-2

Rodrigues ML, Nimrichter L, Oliveira DL, Frases S, Miranda K, Zaragoza O, Alvarez M, Nakouzi A, Feldmesser M, Casadevall A (2007) Vesicular polysaccharide export in *Cryptococcus neoformans* is a eukaryotic solution to the problem of fungal trans-cell wall transport. Eukaryot Cell 6(1):48–59. https://doi.org/10.1128/EC.00318-06

Rodrigues ML, Nakayasu ES, Oliveira DL, Nimrichter L, Nosanchuk JD, Almeida IC, Casadevall A (2008) Extracellular vesicles produced by *Cryptococcus neoformans* contain protein components associated with virulence. Eukaryot Cell 7(1):58–67. https://doi.org/10.1128/EC.00370-07

Ruocco M, Baroncelli R, Cacciola SO, Pane C, Monti MM, Firrao G, Vergara M, Magnano di San Lio G, Vannacci G, Scala F (2018) Polyketide synthases of *Diaporthe helianthi* and involvement of DhPKS1 in virulence on sunflower. BMC Genomics 19(1):27. https://doi.org/10.1186/s12864-017-4405-z

Ryan JR (2016) Chapter 8 - Biological Threat to Agriculture. In: Ryan JR (ed) Biosecurity and Bioterrorism (Second Edition). Butterworth-Heinemann, pp 185–216. doi:https://doi.org/10.1016/B978-0-12-802029-6.00008-6

Samuel M, Bleackley M, Anderson M, Mathivanan S (2015) Extracellular vesicles including exosomes in cross kingdom regulation: a viewpoint from plant-fungal interactions. Front Plant Sci 6:766–766. https://doi.org/10.3389/fpls.2015.00766

Saunders DGO, Pretorius ZA, Hovmøller MS (2019) Tackling the re-emergence of wheat stem rust in Western Europe. Commun Biol 2(1):51. https://doi.org/10.1038/s42003-019-0294-9

Shamanin V, Salina E, Wanyera R, Zelenskiy Y, Olivera P, Morgounov A (2016) Genetic diversity of spring wheat from Kazakhstan and Russia for resistance to stem rust Ug99. Euphytica 212 (2):287–296. https://doi.org/10.1007/s10681-016-1769-0

Shopova IA, Belyaev I, Dasari P, Jahreis S, Stroe MC, Cseresnyés Z, Zimmermann A-K, Medyukhina A, Svensson C-M, Krüger T, Szeifert V, Nietzsche S, Conrad T, Blango MG, Kniemeyer O, von Lilienfeld-Toal M, Zipfel PF, Ligeti E, Figge MT, Brakhage AA (2020) Human neutrophils produce antifungal extracellular vesicles against *Aspergillus fumigatus*. MBio 11(2):e00596–e00520. https://doi.org/10.1128/mBio.00596-20

Silva BMA, Prados-Rosales R, Espadas-Moreno J, Wolf JM, Luque-Garcia JL, Gonçalves T, Casadevall A (2014) Characterization of *Alternaria infectoria* extracellular vesicles. Med Mycol 52(2):202–210. https://doi.org/10.1093/mmy/myt003

Singh RP, Hodson DP, Huerta-Espino J, Jin Y, Bhavani S, Njau P, Herrera-Foessel S, Singh PK, Singh S, Govindan V (2011) The emergence of Ug99 races of the stem rust fungus is a threat to world wheat production. Annu Rev Phytopathol 49(1):465–481. https://doi.org/10.1146/annurev-phyto-072910-095423

Snelders E, van der Lee HAL, Kuijpers J, Rijs AJMM, Varga J, Samson RA, Mellado E, Donders ART, Melchers WJG, Verweij PE (2008) Emergence of azole resistance in *Aspergillus fumigatus* and spread of a single resistance mechanism. PLoS Med 5(11):e219–e219. https://doi.org/10.1371/journal.pmed.0050219

Sobrova P, Adam V, Vasatkova A, Beklova M, Zeman L, Kizek R (2010) Deoxynivalenol and its toxicity. Interdiscip Toxicol 3(3):94–99. https://doi.org/10.2478/v10102-010-0019-x

Souza JAM, Baltazar LM, Carregal VM, Gouveia-Eufrasio L, de Oliveira AG, Dias WG, Campos Rocha M, Rocha de Miranda K, Malavazi I, Santos DA, FJG F, de Souza DG, Teixeira MM, Soriani FM (2019, 2008) Characterization of *Aspergillus fumigatus* extracellular vesicles and their effects on macrophages and neutrophils functions. Front Microbiol:10. https://doi.org/10.3389/fmicb.2019.02008

Taborda CP, da Silva MB, Nosanchuk JD, Travassos LR (2008) Melanin as a virulence factor of *Paracoccidioides brasiliensis* and other dimorphic pathogenic fungi: a minireview. Mycopathologia 165(4–5):331–339. https://doi.org/10.1007/s11046-007-9061-4

Thammahong A, Puttikamonkul S, Perfect JR, Brennan RG, Cramer RA (2017) Central role of the Trehalose biosynthesis pathway in the pathogenesis of human fungal infections: opportunities and challenges for therapeutic development. Microbiol Mol Biol Rev 81(2). https://doi.org/10.1128/mmbr.00053-16

Vallejo MC, Matsuo AL, Ganiko L, Medeiros LC, Miranda K, Silva LS, Freymuller-Haapalainen E, Sinigaglia-Coimbra R, Almeida IC, Puccia R (2011) The pathogenic fungus *Paracoccidioides brasiliensis* exports extracellular vesicles containing highly immunogenic alpha-Galactosyl epitopes. Eukaryot Cell 10(3):343–351. https://doi.org/10.1128/ec.00227-10

Vallejo MC, Nakayasu ES, Longo LVG, Ganiko L, Lopes FG, Matsuo AL, Almeida IC, Puccia R (2012a) Lipidomic analysis of extracellular vesicles from the pathogenic phase of *Paracoccidioides brasiliensis*. PLoS One 7(6):e39463. https://doi.org/10.1371/journal.pone.0039463

Vallejo MC, Nakayasu ES, Matsuo AL, Sobreira TJP, Longo LVG, Ganiko L, Almeida IC, Puccia R (2012b) Vesicle and vesicle-free extracellular proteome of *Paracoccidioides brasiliensis*: comparative analysis with other pathogenic fungi. J Proteome Res 11(3):1676–1685. https://doi.org/10.1021/pr200872s

Vallhov H, Johansson C, Veerman RE, Scheynius A (2020) Extracellular vesicles released from the skin commensal yeast *Malassezia sympodialis* activate human primary keratinocytes. Front Cell Infect Microbiol 10(6). https://doi.org/10.3389/fcimb.2020.00006

Vargas G, Rocha JD, Oliveira DL, Albuquerque PC, Frases S, Santos SS, Nosanchuk JD, Gomes AM, Medeiros LC, Miranda K, Sobreira TJ, Nakayasu ES, Arigi EA, Casadevall A, Guimaraes AJ, Rodrigues ML, Freire-de-Lima CG, Almeida IC, Nimrichter L (2015) Compositional and immunobiological analyses of extracellular vesicles released by *Candida albicans*. Cell Microbiol 17(3):389–407. https://doi.org/10.1111/cmi.12374

Vargas G, Honorato L, Guimarães AJ, Rodrigues ML, Reis FCG, Vale AM, Ray A, Nosanchuk JD, Nimrichter L (2020) Protective effect of fungal extracellular vesicles against murine candidiasis. Cell Microbiol n/a (n/a):e13238. doi:https://doi.org/10.1111/cmi.13238

Vecchiarelli A (2000) Immunoregulation by capsular components of *Cryptococcus neoformans*. Med Mycol 38(6):407–417. https://doi.org/10.1080/mmy.38.6.407.417

Voelz K, Johnston SA, Smith LM, Hall RA, Idnurm A, May RC (2014) 'Division of labour' in response to host oxidative burst drives a fatal *Cryptococcus gattii* outbreak. Nat Commun 5 (1):5194. https://doi.org/10.1038/ncomms6194

Walker L, Sood P, Lenardon MD, Milne G, Olson J, Jensen G, Wolf J, Casadevall A, Adler-Moore J, Gow NAR (2018) The viscoelastic properties of the fungal Cell Wall allow traffic of AmBisome as intact liposome vesicles. MBio 9(1):e02383–e02317. https://doi.org/10.1128/mBio.02383-17

Walther TC, Brickner JH, Aguilar PS, Bernales S, Pantoja C, Walter P (2006) Eisosomes mark static sites of endocytosis. Nature 439(7079):998–1003. https://doi.org/10.1038/nature04472

Warris A, Ballou ER (2019) Oxidative responses and fungal infection biology. Semin Cell Dev Biol 89:34–46. https://doi.org/10.1016/j.semcdb.2018.03.004

Williamson B, Tudzynski B, Tudzynski P, van Kan JA (2007) *Botrytis cinerea*: the cause of grey mould disease. Mol Plant Pathol 8(5):561–580. https://doi.org/10.1111/j.1364-3703.2007.00417.x

Wolf JM, Rivera J, Casadevall A (2012) Serum albumin disrupts *Cryptococcus neoformans* and *Bacillus anthracis* extracellular vesicles. Cell Microbiol 14(5):762–773. https://doi.org/10.1111/j.1462-5822.2012.01757.x

Wolf JM, Espadas-Moreno J, Luque-Garcia JL, Casadevall A (2014) Interaction of *Cryptococcus neoformans* extracellular vesicles with the cell wall. Eukaryot Cell 13(12):1484–1493. https://doi.org/10.1128/EC.00111-14

Woo PCY, Lam C-W, Tam EWT, Leung CKF, Wong SSY, Lau SKP, Yuen K-Y (2012) First discovery of two Polyketide synthase genes for Mitorubrinic acid and Mitorubrinol yellow pigment biosynthesis and implications in virulence of *Penicillium marneffei*. PLoS Negl Trop Dis 6(10):e1871. https://doi.org/10.1371/journal.pntd.0001871

Yáñez-Mó M, Siljander PRM, Andreu Z, Zavec AB, Borràs FE, Buzas EI, Buzas K, Casal E, Cappello F, Carvalho J, Colás E, Silva AC-d, Fais S, Falcon-Perez JM, Ghobrial IM, Giebel B, Gimona M, Graner M, Gursel I, Gursel M, Heegaard NHH, Hendrix A, Kierulf P, Kokubun K, Kosanovic M, Kralj-Iglic V, Krämer-Albers E-M, Laitinen S, Lässer C, Lener T, Ligeti E, Linē A, Lipps G, Llorente A, Lötvall J, Manček-Keber M, Marcilla A, Mittelbrunn M, Nazarenko I, Hoen ENMN-t, Nyman TA, O'Driscoll L, Olivan M, Oliveira C, Pállinger É, del Portillo HA, Reventós J, Rigau M, Rohde E, Sammar M, Sánchez-Madrid F, Santarém N, Schallmoser K, Ostenfeld MS, Stoorvogel W, Stukelj R, Van der Grein SG, Vasconcelos MH, Wauben MHM, De Wever O (2015) Biological properties of extracellular vesicles and their physiological functions. J Extracell Vesicles 4: doi:https://doi.org/10.3402/jev.v4.27066

Yang G, Rose MS, Turgeon BG, Yoder OC (1996) A polyketide synthase is required for fungal virulence and production of the polyketide T-toxin. Plant Cell 8(11):2139–2150. https://doi.org/10.1105/tpc.8.11.2139

Yike I (2011) Fungal proteases and their pathophysiological effects. Mycopathologia 171(5):299–323. https://doi.org/10.1007/s11046-010-9386-2

Zamith-Miranda D, Nimrichter L, Rodrigues ML, Nosanchuk JD (2018) Fungal extracellular vesicles: modulating host–pathogen interactions by both the fungus and the host. Microbes Infect 20(9):501–504. https://doi.org/10.1016/j.micinf.2018.01.011

Zarnowski R, Sanchez H, Covelli AS, Dominguez E, Jaromin A, Bernhardt J, Mitchell KF, Heiss C, Azadi P, Mitchell A, Andes DR (2018) Candida albicans biofilm-induced vesicles confer drug resistance through matrix biogenesis. PLoS Biol 16(10):e2006872–e2006872. https://doi.org/10.1371/journal.pbio.2006872

Zhao K, Bleackley M, Chisanga D, Gangoda L, Fonseka P, Liem M, Kalra H, Al Saffar H, Keerthikumar S, Ang C-S, Adda CG, Jiang L, Yap K, Poon IK, Lock P, Bulone V, Anderson M, Mathivanan S (2019) Extracellular vesicles secreted by *Saccharomyces cerevisiae* are involved in cell wall remodelling. Commun Biol 2(1):305. https://doi.org/10.1038/s42003-019-0538-8

Zheng S-J, García-Bastidas FA, Li X, Zeng L, Bai T, Xu S, Yin K, Li H, Fu G, Yu Y, Yang L, Nguyen HC, Douangboupha B, Khaing AA, Drenth A, Seidl MF, Meijer HJG, Kema GHJ (2018) New geographical insights of the latest expansion of *Fusarium oxysporum* f.sp. *cubense* tropical race 4 into the greater Mekong subregion. Front Plant Sci 9(457). https://doi.org/10.3389/fpls.2018.00457

2. Chapter Two

When this thesis was started there were few research articles on fungal EVs in the literature and there was still debate about whether fungi produced EVs, largely because there was doubt that EVs would be able to traverse the fungal cell wall. A handful of research articles [7,51,56] described EVs from the yeast pathogens *Cryptococcus neoformans* and *Histoplasma capsulatum* and preliminary proteomic studies. Only one article had been published describing EVs from the filamentous fungus *Alternaria infectoria,* but there were no studies on EVs from filamentous fungi in the context of plant pathogenesis. The two articles presented in this chapter describe the isolation and proteome of EVs produced by the cotton pathogen *Fusarium oxysporum f. sp. vasinfectum*.

2.1 Extracellular vesicles from the cotton pathogen *Fusarium oxysporum* f. sp. *vasinfectum* (*Fov*) induce a hypersensitive response in plants

The findings from this study have been published in a peer-reviewed journal, Frontiers in Plant Science, January 2020.

Bleackley MR, Samuel M, Garcia-Ceron D, McKenna JA, Lowe RGT, Pathan M, Zhao K, Ang CS, Mathivanan S, Anderson MA. **Extracellular Vesicles From the Cotton Pathogen *Fusarium oxysporum* f. sp. *vasinfectum* Induce a Phytotoxic Response in Plants.** Front Plant Sci. 2020 Jan 10;10:1610. doi: 10.3389/fpls.2019.01610.

Statement of Contribution

Donovan Garcia-Ceron has:

- Isolated EVs
- Prepared samples for mass spectrometry
- Performed the gene ontology analysis

frontiers in Plant Science

ORIGINAL RESEARCH
published: 10 January 2020
doi: 10.3389/fpls.2019.01610

Extracellular Vesicles From the Cotton Pathogen *Fusarium oxysporum* f. sp. *vasinfectum* Induce a Phytotoxic Response in Plants

Mark R. Bleackley[1‡], Monisha Samuel[1†‡], Donovan Garcia-Ceron[1], James A. McKenna[1], Rohan G. T. Lowe[1], Mohashin Pathan[1], Kening Zhao[1], Ching-Seng Ang[2], Suresh Mathivanan[1] and Marilyn A. Anderson[1]*

[1] Department of Biochemistry and Genetics, La Trobe Institute for Molecular Science, La Trobe University, Bundoora, VIC, Australia, [2] Bio21 Institute, University of Melbourne, Parkville, VIC, Australia

Extracellular vesicles (EVs) represent a system for the coordinated secretion of a variety of molecular cargo including proteins, lipids, nucleic acids, and metabolites. They have an essential role in intercellular communication in multicellular organisms and have more recently been implicated in host-pathogen interactions. Study of the role for EVs in fungal biology has focused on pathogenic yeasts that are major pathogens in humans. In this study we have expanded the investigation of fungal EVs to plant pathogens, specifically the major cotton pathogen *Fusarium oxysporum* f. sp. *vasinfectum*. EVs isolated from *F. oxysporum* f. sp. *vasinfectum* culture medium have a morphology and size distribution similar to EVs from yeasts such as *Candida albicans* and *Cryptococcus neoformans.* A unique feature of the EVs from *F. oxysporum* f. sp. *vasinfectum* is their purple color, which is predicted to arise from a napthoquinone pigment being packaged into the EVs. Proteomic analysis of *F. oxysporum* f. sp. *vasinfectum* EVs revealed that they are enriched in proteins that function in synthesis of polyketides as well as proteases and proteins that function in basic cellular processes. Infiltration of *F. oxysporum* f. sp. *vasinfectum* EVs into the leaves of cotton or *N. benthamiana* plants led to a phytotoxic response. These observations lead to the hypothesis that *F. oxysporum* f. sp. *vasinfectum* EVs are likely to play a crucial role in the infection process.

Keywords: fungi, extracellular vesicle (EV), host-pathogen interaction, polyketide, pigment

OPEN ACCESS

Edited by:
Jan Schirawski,
Friedrich Schiller University Jena, Germany

Reviewed by:
Wei-Hua Tang,
Shanghai Institutes for Biological Sciences (CAS), China
Laurence Veronique Bindschedler, University of London, United Kingdom

****Correspondence:***
Marilyn A. Anderson
m.anderson@latrobe.edu.au

[†]Present address:
Monisha Samuel
Division of Immunology and Allergy, Department of Medicine Solna, Karolinska University Hospital, Karolinska Institutet, Stockholm, Sweden

[‡]These authors have contributed equally to this work

Specialty section:
This article was submitted to Plant Microbe Interactions, a section of the journal Frontiers in Plant Science

Received: *31 July 2019*
Accepted: *15 November 2019*
Published: *10 January 2020*

Citation:
Bleackley MR, Samuel M, Garcia-Ceron D, McKenna JA, Lowe RGT, Pathan M, Zhao K, Ang C-S, Mathivanan S and Anderson MA (2020) Extracellular Vesicles From the Cotton Pathogen Fusarium oxysporum f. sp. vasinfectum Induce a Phytotoxic Response in Plants. Front. Plant Sci. 10:1610. doi: 10.3389/fpls.2019.01610

INTRODUCTION

Extracellular vesicles (EVs) are involved in intercellular communications in all kingdoms of life (Pathirana and Kaparakis-Liaskos, 2016; Maas et al., 2017; Bielska et al., 2018; Rybak and Robatzek, 2019). These small, lipid bilayer encapsulated particles provide a mechanism for the coordinated transport of heterogeneous cargo. This is not limited to transport between cells within an organism but also extends to cross kingdom interactions such as those between microbial pathogens and their hosts (Schorey et al., 2015; Rutter and Innes, 2018). The best characterized EVs are from

mammalian cells; their cargo includes nucleic acids, proteins, lipids, and metabolites (Kalra et al., 2012; Maas et al., 2017). Uptake of EVs by target cells induces changes in gene/protein expression that consequently lead to altered physiology and other phenotypes (Greening and Simpson, 2018). Our understanding of EVs at the host-pathogen interface comes largely from the study of outer membrane vesicles (OMVs) produced by Gram negative bacteria that infect humans (Pathirana and Kaparakis-Liaskos, 2016). OMVs contribute to the host–pathogen interaction through their cargo, which can induce immune responses (Ellis et al., 2010), contribute to adhesion to mucosal surfaces (Olofsson et al., 2010), act as virulence factors (Bomberger et al., 2009) or toxins (Horstman and Kuehn, 2000), degrade antibiotics (Kim et al., 2018), acquire trace nutrients (Prados-Rosales et al., 2014), and function in inter-microbe competition (Vasilyeva et al., 2008).

Investigation of fungal EVs is in its relative infancy compared to mammalian EVs or bacterial OMVs with most studies on pathogenic yeasts that infect humans (reviewed in Bleackley et al., 2019). Like mammalian EVs and bacterial OMVs, fungal EV cargo consists of proteins, lipids, and nucleic acids. Polysaccharides are also transported by fungal EVs (Griffith et al., 2004; da Silva et al., 2015). Proteomic characterization of the cargo in EVs from pathogenic yeast has led to predicted roles in stress responses, and metabolism of various cellular building blocks including proteins, lipids, and carbohydrates. Functional analysis of EVs *in vitro* supports several roles for these vesicles in host–pathogen interactions. For example, EVs from a number of pathogenic yeast induce responses when applied to cultured innate immune cells, indicating EVs are probably sensed by the host during infection (Oliveira et al., 2010; Wolf et al., 2015; da Silva et al., 2016). Antifungal drug resistance is also linked to EV production; EVs from biofilms produced by the major human fungal pathogen *Candida albicans* contribute to resistance to antifungal azoles (Zarnowski et al., 2018) and *S. cerevisiae* EVs have a protective function against both caspofungin and antifungal peptides(Zhao et al., 2019). Virulence has also been linked to EV production. Hypervirulence of a *Cryptococcus gattii* strain is facilitated by intra-cellular communication between fungal cells mediated by EVs (Bielska et al., 2018).

Little is known about the role of EVs in plant–fungal interactions, although there has been speculation based on the study of mammalian yeast pathogens (Samuel et al., 2015; Boevink, 2017). Experimental investigation into the role for EVs in the plant–fungal interaction has focused on EVs produced by the plant, defense related cargo, and the effect they have on fungi (Rutter and Innes, 2018). Multivesicular bodies, which are the site of biogenesis for many EVs, accumulate at plasmodesmata during fungal infections leading to a potential role for vesicles in the callose deposition that isolates dying cells from living cells (An et al., 2006; Bohlenius et al., 2010; Li et al., 2018). Plant EVs may also deliver antifungal molecules to the pathogen. For example, EVs from sunflower seedlings inhibit the growth of *Sclerotinia sclerotiorum* spores (Regente et al., 2017). Plant EVs are also proposed to transport antimicrobial glucosinylates (Rutter and Innes, 2017). Very little is known about EVs produced by filamentous fungi, with data limited to a handful of studies on *Alternaria infectoria* (Silva et al., 2013), *Trichophyton rubrum* (Bitencourt et al., 2018), and *Rhizopus delemar* (Liu et al., 2018). The EVs from the filamentous fungi in these studies are similar to those produced by yeast with respect to morphology, cargo, and recognition by innate immune cells.

To address the lack of knowledge on how EVs contribute to fungal pathogenesis in plants, we have isolated and characterized EVs from the cotton pathogen *Fusarium oxysporum* f. sp. *vasinfectum*. The *F. oxysporum* species complex causes vascular wilt disease in many economically relevant crops and are considered hemibiotrophic pathogens because the infection consists of both a biotrophic and necrotrophic phase (Gordon 2017). The EVs had a similar morphology to those from yeasts and contained protein cargo that was functionally related to those described for human pathogens. EVs from *F. oxysporum* were deep purple in color and were phytotoxic when applied to plant leaves. This supports a role for fungal EVs in the host–pathogen interaction with plants.

MATERIALS AND METHODS

Strains and Growth Conditions

F. oxysporum f. sp. *vasinfectum*, Australian isolate VCG01111 isolated from cotton, (gift from Wayne O'Neill, Farming Systems Institute, Department of Primary Industries (DPI), Queensland, Australia), was maintained on half strength potato dextrose agar (1/2 PDA) at 25°C. Liquid cultures were grown in half-strength potato dextrose broth (1/2 PDB) at room temperature with shaking at 90 rpm. *S. cerevisiae* BY4741 were maintained on 1% yeast extract, 2% peptone, 2% dextrose, 2% agar (YPD-agar) at 30°C. Liquid cultures were grown in YPD at 30°C with shaking at 125 rpm.

Isolation of EVs

EVs were isolated using a procedure modified from Rodrigues et al. (2007). Briefly, *F. oxysporum* f. sp. *vasinfectum* mycelium was cultured in ½ PDB for 72 h at room temperature. Mycelium was removed from the culture medium by filtration through sterile Miracloth. Spores and cell debris were removed from the culture medium by centrifugation at 4,000 x *g* for 15 min in a Heraeus Multifuge X3 centrifuge (Thermo Fisher) followed by 15,000 x *g* for 30 min in an Avanti J-E centrifuge (Beckman Coulter). Supernatant was further centrifuged at 100,000 x *g* using an SW32 rotor in an Optima L-100 XP ultracentrifuge (Beckman Coulter). EV pellets were resuspended in sterile phosphate-buffered saline (PBS). Protein content of EVs was initially assessed using a Qubit fluorimeter (Thermo Fisher) and then separated on SDS-PAGE gels and stained with SYPRO-Ruby (Invitrogen), and protein content was determined according to the manufacturer's instructions. When needed, EVs were concentrated by pelleting using a TL-

100 ultracentrifuge with a TLA100.3 rotor (Beckman Coulter); the supernatant was removed and the pellet resuspended in an appropriate volume to yield the desired concentration.

Transmission Electron Microscopy

EV samples (5 µl at 0.05 µg/ml protein) were deposited onto carbon-coated 400-mesh copper grids (ProSciTech) that had been glow discharged for 1 min in a K950X turbo evaporator coupled to a K350 glow discharge unit (Quorum Technologies Ltd), incubated for 1 min then washed with ultrapure water. Grids were then stained three times with 4 µl of 2% (v/v) uranyl acetate (Agar Scientific). Excess solution was blotted off and the grids were dried overnight. Images were captured using a JEM 2100 electron microscope (JEOL Ltd) operated at 200 kV.

Nanoparticle Tracking Analysis

Particle size and number of purified EVs were determined using a Nanosight NS300 with a 405 nm (blue) laser (Malvern Instruments). Samples (0.1 µg/ml) were diluted 1:1,000 with sterile PBS and injected using a syringe pump with a flow rate of 50. Three technical replicates were performed per sample with 1 min videos recorded for analysis. All samples were measured in triplicate and data were analyzed using NTA 3.2 Dev Build 3.2.16 with the auto-analysis settings.

Proteomic Analysis

Three separate pools of EVs (each pooled from two or three independent biological replicates) with 15 µg of total protein in each, were loaded onto precast NuPAGE® 4–12% Bis-Tris gels in 1x MES SDS running buffer. *Gels* were run at 150 V followed by visualization of proteins with Coomassie stain (Bio-Rad). Gel bands (10) were excised and subjected to in-gel reduction, alkylation, and trypsinization as described in Mathivanan et al. (2012). Briefly, gel bands were reduced with 10 mM DTT (Bio-Rad), alkylated with 25 mM iodoacetamide (Sigma) and digested overnight at 37°C with 150 ng of sequencing grade trypsin (Promega). Tryptic peptides were extracted by 0.1% trifluoroacetic acid in 50% (w/v) acetonitrile and analyzed by LC-MS/MS using LTQ Orbitrap Elite (Thermo Scientific), fitted with nanoflow reversed-phase-HPLC (Ultimate 3000 RSLC, Dionex). The nano-HPLC system was equipped with an Acclaim Pepmap nano-trap column (Dionex—C18, 100 Å, 75 µm × 2 cm) and an Acclaim Pepmap RSLC analytical column (Dionex—C18, 100 Å, 75 µm × 50cm). Typically, for each LC-MS/MS experiment, 3 µl of the peptide mix was loaded onto the enrichment (trap) column at an isocratic flow of 5 µl/min of 3% CH_3CN containing 0.1% formic acid for 5 min before the enrichment column is switched in-line with the analytical column. The eluents used for the LC were 0.1% v/v formic acid (solvent A) and 100% CH_3CN/0.1% formic acid v/v. The gradient used was 3% B to 25% B for 23 min, 25% B to 40% B in 2 min, 40% B to 85% B in 2 min, and maintained at 85% B for 2 min before equilibration for 10 min at 3% B prior to the next injection. The Orbitrap Elite MS was operated in the data-dependent mode with a capillary temperature of 250°C, nano ESI spray voltage of +1.9 kv, and S-lens RF value of 60%. All spectra were acquired in positive mode with full scan MS spectra scanning from m/z 300–1,650 in the FT mode at 240,000 resolution after accumulating to a target value of 1.00e6 and maximum accumulation time of 200 ms. Lockmass of 445.12003 m/z was used. For MS/MS, the 20 most intense peptide ions with minimum target value of 2,000 and charge states ≥2 were isolated with isolation window of 1.6 m/z and fragmented by low energy CID with normalized collision energy of 30 and activation Q of 0.25. A whole cell lysate (WCL) sample, prepared by lysing *F. oxysporum* f. sp. *vasinfectum* mycelia using glass beads in a Tissue lyser (Qiagen) and clarifying *via* centrifugation, was also analyzed using the same method for comparison.

Bioinformatic Analysis of Proteomic Data Set

Mascot Generic File Format (MGF) files were generated using MSConvert with the parameter of peak picking set. X!Tandem VENGEANCE (2015.12.15) was then used to search the MGF files against a target and decoy databases. A predicted protein set for *F. oxysporum* f. sp. *vasinfectum* was downloaded from Ensembl Fungi (FO_Cotton_V1, GCA_000260175) and used to generate the target database. Search parameters used were: fixed modification (carboamidomethylation of cysteine; +57 Da), variable modifications (oxidation of methionine; +16 Da and N-terminal acetylation; +42 Da), three missed tryptic cleavages, 20 ppm peptide mass tolerance, and 0.6 Da fragment ion mass tolerance. Protein identifications were shortlisted to obtain a master list with less than 1% false discovery rate. Proteins that were identified by at least two unique peptides in two of three samples were classified as EV proteins.

Predicted functions of *F. oxysporum* f. sp. *vasinfectum* ORFs were assigned by homology searching using Blast2Go v4.19 with default parameters (Conesa et al., 2005). Functional enrichment analysis was also performed using Blast2Go with Fisher's exact test. Statistically significant GO terms that were enriched in EV proteins were condensed further to minimize overlap using the reduced GO terms function in Blast2Go.

Absorbance Spectroscopy of EVs

Absorbance spectroscopy was performed using a SpectraMax m2 spectrophotometer. EVs fractions were loaded into 1 cm pathlength 70 µl UV-Cuvette micro (BRAND, Germany) cuvettes and the absorbance spectra were measured in 10 nm intervals. Data were analyzed using Microsoft Excel.

Leaf Infiltration Assays

Coker 315 cotton seeds were germinated at 25°C in an Adaptis (Conviron) growth cabinet with 16 h light and 8 h dark for 10 days with 5 seeds per squat pot in standard pine park potting mix. *Nicotiana benthamiana* were grown in an Adaptis (Conviron) growth cabinet with 16 h light and 8 h dark for 4–6 weeks. Infiltrations were performed on the cotton cotyledons or *N. benthamiana* leaves using a protocol modified from Poon et al. (2018) used for infiltration of *Agrobacterium* into the leaves

of *N. benthamiana* for transient protein expression. EVs were prepared to a protein concentration of 0.1 μg/ml in 1 ml PBS and infiltrated into the undersides of the cotyledons using a non-luer lock 1 ml syringe (Terumo). Four infiltrations were performed on each leaf. All infiltrations were paired with a PBS control on the second cotyledon of the plant for cotton or on the other half of the leaf for *N. benthamiana*. Cotton cotyledons were also infiltrated with a solution of hyphae and spores that had been removed from the culture supernatant during EV isolation. Hyphae and spores were washed, resuspended in PBS, and diluted until the solution was slightly turbid (OD 600 nm ~ 0.5) and still flowed easily to facilitate infiltration. After infiltration plants were returned to the growth cabinet for 5 days. After 5 days the cotyledons/leaves were removed from the plants and images of lesions on cotyledons were taken using a Nex-7 camera (Sony).

Optiprep Density Gradient Analysis of EVs

Density gradient ultracentrifugation was performed as described previously with modifications (Kalra et al., 2013). A discontinuous iodixanol gradient consisting of 40% w/v, 20% w/v, 10% w/v, and 5% w/v solutions of iodixanol was prepared by diluting a stock solution of OptiPrep [60% w/v aqueous iodixanol (Sigma)] in 0.25 M sucrose/10 mM Tris, pH 7.5. The crude EVs isolated from the *F. oxysporum* f. sp. *vasinfectum* culture by differential centrifugation coupled with ultracentrifugation, were resuspended in the OptiPrep solution, and overlaid onto the top layer. A control tube consisting 3 ml of each 40%, 20%, 10%, and 5% solutions was also prepared. Both tubes were simultaneously subjected to ultracentrifugation at 100,000 × *g* for 18 h at 4°C (Beckman Coulter: SW-28 rotor). The 12 fractions were collected separately for further analysis. EVs were pelleted by ultracentrifugation at 100,000 × *g* for 1 h at 4°C (Beckman Coulter: TLA-55 rotor). Pellets were then washed with 1 ml of PBS and the supernatant was removed with two successive ultracentrifugations at 100,000 × *g* for 1 h at 4°C (Beckman Coulter: TLA-55 rotor) and resuspended in 30 μl before being stored at -80°C.

RESULTS

F. oxysporum f. sp. *vasinfectum* Produces EVs

EVs were isolated from the supernatant from *F. oxysporum* f. sp. *vasinfectum* suspension cultures grown in ½ PDB using differential centrifugation and ultracentrifugation. Unexpectedly the EV fraction had a deep purple color and dual absorbance maximum at 550 and 590 nm (**Figure 1A**). Nanoparticle tracking analysis was used to determine the number of particles and the distribution of particle diameters (**Figure 1B**). *F. oxysporum* f. sp. *vasinfectum* produced 1.0 x 10^{12} (st dev 2.8 x 10^{11}) EVs per mL of culture medium with an average mean particle diameter of 155.1 nm (st dev 3.5 nm) and an average mode of 150.0 nm (st dev 5.1 nm). The average protein concentration of the EV fraction measured by Qubit was 0.05 μg/μl. TEM revealed that the particles had the characteristic cup-like morphology of EVs (**Figure 1C**). In addition to the cup-shaped particles, there were an equivalent number of multi-lobed, rosette-shaped particles observed in the sample.

F. oxysporum f. sp. *vasinfectum* EVs Contain Proteins That Function in a Variety of Cellular Processes

The protein cargo of *F. oxysporum* f. sp. *vasinfectum* EVs was characterized by tryptic digest followed by LC-MS/MS using an LTQ Orbitrap Elite mass spectrometer. The criteria for positive identification of a protein from the mass spectrometry data set were the detection of at least two unique peptides in at least two of three samples. As a result, we identified list of 482 proteins (**Table S1**). The most abundant proteins (**Table 1**) in the EVs included three proteases (FOTG_10608, FOTG_12971, FOTG_06834), two frequency/period clock proteins (FOTG_02405, FOTG_15292), an HSP70 like protein (FOTG_06291), and a polyketide synthase (FOTG_13424) (**Table 1**). An additional polyketide synthase (FOTG_01390)

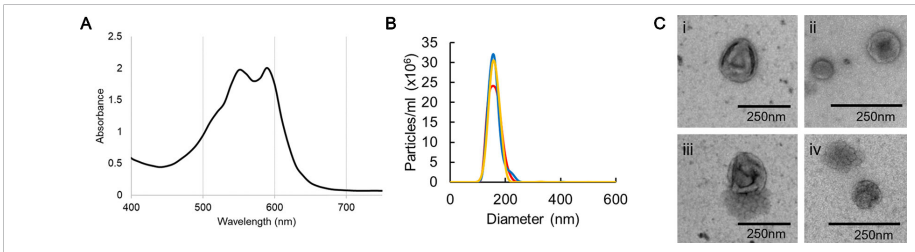

FIGURE 1 | Characterization of EVs isolated from *F. oxysporum* f. sp. *vasinfectum*. EVs were isolated using differential centrifugation followed by ultracentrifugation. **(A)** Absorption spectrum of the *F. oxysporum* f. sp. *vasinfectum* EV preparation had dual maxima at 550 and 590 nm. Data are representative of three independent replicates. **(B)** The number and size distribution of the isolated EVs were determined using nanoparticle tracking analysis. The data from the three technical replicates from one biological sample are representative of all samples used in this study. The average quantity and size of EVs from three independent isolations of EVs from *F. oxysporum* f. sp. *vasinfectum* were 1.0 x 10^{12} ± 2.8 x 10^{11} particles/ml of culture, mean diameter 155.1 nm ± 3.5 nm, mode diameter 150.0 nm ± 5.1 nm. Values are presented ± standard deviation of three biological replicates. **(C)** TEM confirmed that most particles had the characteristic cup like morphology of EVs (i–iii); some particles had a multi-lobed rosette morphology as seen in (iv).

TABLE 1 | The 30 most abundant proteins identified in *F. oxysporum* f. sp. *vasinfectum* EVs.

Protein	Locus	Function	Associated GO terms
FOTG_08633	EXM24125	Uncharacterized protein	
FOTG_10608	EXM21679	Related to tripeptidyl-peptidase i	F: serine-type endopeptidase activity; P: proteolysis
FOTG_02405	EXM33907	Frequency clock protein	C: nucleus; C: cytoplasm; P: regulation of transcription, DNA-templated; P: circadian rhythm
FOTG_03632	EXM32021	Glucose-regulated protein	C: Golgi apparatus; C: nuclear membrane; C: luminal surveillance complex; F: ATP binding; F: ATPase activity; F: unfolded protein binding; P: karyogamy involved in conjugation with cellular fusion; P: SRP-dependent cotranslational protein targeting to membrane, translocation; P: response to unfolded protein; P: ER-associated ubiquitin-dependent protein catabolic process; P: posttranslational protein targeting to membrane, translocation; P: *de novo* posttranslational protein folding
FOTG_15292	EXM16413	Related to period clock protein frq	C: nucleus; C: cytoplasm; P: regulation of transcription, DNA-templated; P: circadian rhythm
FOTG_07604	EXM25889	Uncharacterized protein	
FOTG_05803	EXM28573	Protein disulfide-isomerase	C: endoplasmic reticulum; F: protein disulfide isomerase activity; F: FMN binding; F: oxidoreductase activity; P: cell redox homeostasis; P: oxidation–reduction process
FOTG_06653	EXM27334	Uncharacterized protein	
FOTG_03515	EXM31837	Related to csf1 protein	C: integral component of membrane; P: fermentation
FOTG_12971	EXM18981	Cerevisin	F: serine-type endopeptidase activity; P: proteolysis
FOTG_02417	EXM33929	Transcription initiation factor tfiid subunit 12	C: SAGA complex; C: transcription factor TFIID complex; C: SLIK (SAGA-like) complex; F: RNA polymerase II activating transcription factor binding; F: chromatin binding; F: translation initiation factor activity; F: TBP-class protein binding; F: protein complex scaffold; F: identical protein binding; F: protein heterodimerization activity; P: regulation of transcription from RNA polymerase II promoter; P: histone acetylation; P: RNA polymerase II transcriptional preinitiation complex assembly; C: chromatin; C: ribosome; P: regulation of translational initiation
FOTG_15593	EXM16120	Related to cell wall protein	-
FOTG_06397	EXM26950	Related to glu asp-trna amidotransferase subunit a	F: transferase activity; F: carbon–nitrogen ligase activity, with glutamine as amido-N-donor
FOTG_11173	EXM21071	Related to oxidoreductase	-
FOTG_10869	EXM21345	qi74 protein	F: oxidoreductase activity, acting on CH-OH group of donors; F: flavin adenine dinucleotide binding; P: oxidation–reduction process
FOTG_08528	EXM24551	Acetyl- carboxylase	F: acetyl-CoA carboxylase activity; F: biotin carboxylase activity; F: ATP binding; F: metal ion binding; P: fatty acid biosynthetic process; P: pyruvate metabolic process; C: biotin carboxylase complex
FOTG_13424	EXM18486	Polyketide synthase	F: oxidoreductase activity; F: transferase activity; F: phosphopantetheine binding; P: oxidation–reduction process
FOTG_03629	EXM32018	Probable endonuclease exonuclease phosphatase family protein	F: endonuclease activity; F: exonuclease activity; P: nucleic acid phosphodiester bond hydrolysis
FOTG_16641	EXM14982	Probable isoamyl alcohol oxidase	F: oxidoreductase activity, acting on CH-OH group of donors; F: flavin adenine dinucleotide binding; P: oxidation–reduction process
FOTG_06610	EXM27272	Elongation factor 3	F: translation elongation factor activity; F: ATP binding; F: ATPase activity; C: ribosome; P: regulation of translational elongation
FOTG_06834	EXM26538	Vacuolar protease a	F: aspartic-type endopeptidase activity; P: cellular response to starvation; P: lysosomal microautophagy; P: proteolysis involved in cellular protein catabolic process
FOTG_03516	EXM31838	Elongation factor 2	C: integral component of membrane; F: translation elongation factor activity; F: GTPase activity; F: GTP binding; C: ribosome; P: regulation of translational elongation
FOTG_02422	EXM33936	atp-citrate synthase subunit 1	C: nucleus; C: cytosol; C: large ribosomal subunit; F: structural constituent of ribosome; F: lyase activity; F: transferase activity, transferring acyl groups, acyl groups converted into alkyl on transfer; F: cofactor binding; P: translation; P: ribosome biogenesis
FOTG_07981	EXM24972	Protein mms22	C: nucleus; P: DNA repair; P: replication fork processing
FOTG_06022	EXM27593	Calnexin	C: integral component of endoplasmic reticulum membrane; F: calcium ion binding; F: unfolded protein binding; P: protein folding; P: ER-associated ubiquitin-dependent protein catabolic process
FOTG_03469	EXM31757	Starch phosphorylase	F: glycogen phosphorylase activity; F: pyridoxal phosphate binding; P: carbohydrate metabolic process
FOTG_14342	EXM17503	Related to rf2 protein	F: chitinase activity; F: chitin binding; P: carbohydrate metabolic process; P: chitin catabolic process; P: cell wall macromolecule catabolic process
FOTG_06291	EXM28051	hsp70-like protein	C: nucleus; C: cytoplasm; C: integral component of membrane; F: ATP binding; F: unfolded protein binding; P: protein folding; P: SRP-dependent cotranslational protein targeting to membrane, translocation

and a fusarubin cluster-esterase (encoded by FOTG_16162) were also identified but at lower abundance.

Functional enrichment analysis of the EV proteins identified 287 GO terms that were enriched with an adjusted p-value cut-off of 0.05 (**Table S2**). The enriched GO terms were condensed to remove overlapping terms and give a broader picture of the annotated functions, cellular locations, and biological processes that were overrepresented in the *F. oxysporum* EVs (**Figure 2**). A similar enrichment analysis was performed using a proteomic data set from WCL. Basic cellular processes including protein and nucleotide metabolism, lipid biosynthesis, and cell structure were overrepresented EVs. Both the EVs and

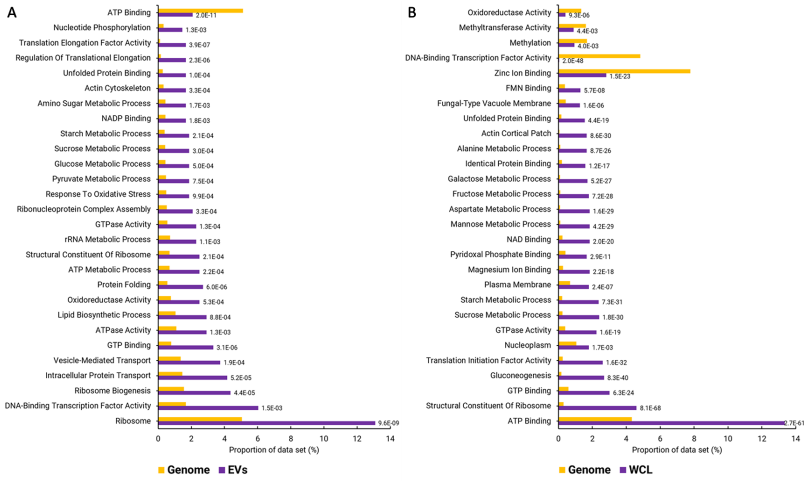

FIGURE 2 | GO terms over- and underrepresented in *F. oxysporum* f. sp. *vasinfectum* EV proteins. **(A)** GO terms that are over- or underrepresented in the set of EV proteins. EV proteins were identified by LC-MS/MS with the peptides aligned to the predicted *F. oxysporum* f. sp. *vasinfectum* proteome. A protein was listed as an EV protein if there were at least two unique peptides from the protein identified in at least two of three EV pools. **(B)** Under- and overrepresented GO terms identified in the list of proteins identified in *F. oxysporum* f. sp. *vasinfectum* whole cell lysate. These lists are the top 30 terms; full lists can be found in **Tables S2** and **S3**. GO terms were assigned to transcripts based on homology searches using Blast2Go. GO term enrichment was also performed using Blast2GO. The number next to each bar is the p-value for the GO term.

WCL were enriched for proteins that function in carbohydrate metabolism, the unfolded protein binding, GTP binding, GTPase activity, and ribosomes. Functions such as oxidoreductase activity, oxidative stress response, and vesicle mediated transport were only enriched in EVs. ATP binding was underrepresented in EVs but overrepresented in WCL, whereas DNA-binding transcription factor activity was overrepresented in EVs and underrepresented in WCL.

F. oxysporum f. sp. *vasinfectum* EVs Are Phytotoxic to Plant Leaves

To determine whether EVs produced by *F. oxysporum* f. sp. *vasinfectum* had any effect on plant tissue, EVs were infiltrated into the underside of the cotyledons of cotton seedlings or young leaves of *N. benthamiana*. After 5 days the *F. oxysporum* f. sp. *vasinfectum* EVs induced the formation of a discolored area on the cotyledon or leaf corresponding to the infiltration area, which is indicative of phytotoxicity (**Figure 3A**). In contrast, there was no discoloration in the infiltration areas of any of the cotyledons or leaves that were infiltrated with sterile PBS demonstrating that the infiltration procedure itself was not responsible for the discolored region. Infiltration of resuspended spores and hyphae led to the formation of discolored spots that were much smaller than those observed for the EVs. To determine whether the toxicity observed in the cotyledon was merely a response to foreign material or if it was specific to components of the *F. oxysporum* f. sp. *vasinfectum* EVs, the infiltration experiment was repeated with EVs isolated from the non-pathogenic fungus *S. cerevisiae*. No discoloration was observed in the regions infiltrated with *S. cerevisiae* EVs; indeed it was difficult to discern between the *S. cerevisiae* EV infiltrated and the paired PBS infiltrated cotyledons (**Figure 3B**). As *F. oxysporum* f. sp. *vasinfectum* is a specific pathogen of cotton, the infiltration experiment was repeated on *N. benthamiana* to determine if the phytotoxic effect was host specific. Infiltration of EVs from *F. oxysporum* f. sp. *vasinfectum* was also phytotoxic on *N. benthamiana* leaves (**Figure 3C**), indicating that the phytotoxic effect is not host specific. Consistent with observations in cotton, *S. cerevisiae* EVs did not elicit a response in *N. benthamiana* leaves (**Figure 3D**). Infiltration of cotton cotyledons with resuspended spores and hyphae led to a much-subdued phytotoxic effect (**Figure 3E**), indicating that it is not just a response to fungal material that causes the phytotoxic response in plants but something specific to EVs.

As there are several different molecules produced by fungi that can induce a cell death response in plants further purification of the *F. oxysporum* f. sp. *vasinfectum* EVs by Optiprep density gradient centrifugation was performed. The purple pigment separated into two sections of the Optiprep gradient. The first section spanned fractions 4–7 and a second more condensed section in fraction 10 (**Figure 4A**). After removal of the iodixanol, a selection of these fractions were infiltrated into cotton cotyledons. Fractions 5, 6, and 7 induced the strongest response and also contained an enrichment of EVs

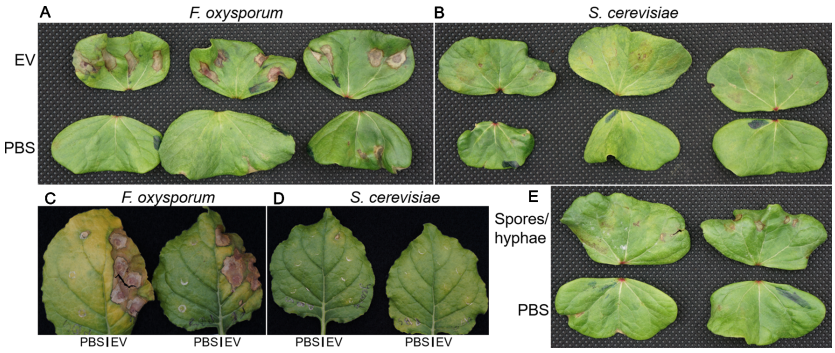

FIGURE 3 | The effect of fungal EVs on cotton cotyledons. EVs were purified from *F. oxysporum* f. sp. *vasinfectum* and *S. cerevisiae* and diluted to a protein concentration of 0.1 μg/ml in PBS. **(A**, **B)** Paired cotyledons were infiltrated at four points with the EV solution and PBS control. After 5 days incubation, the cotyledons were removed from the plants and imaged. Cotyledons infiltrated with EVs from *F. oxysporum* f. sp. *vasinfectum* **(A)** had discolored/brown spots around the sites of infiltration, whereas the cotyledons infiltrated with EVs from *S. cerevisiae* **(B)** only had mild discoloration or no response. Cotyledons infiltrated with PBS had no observable effect (the brown spot on the third cotyledon in the *F. oxysporum* panel **(A)** is due to a pinch point as a result of a fold in the leaf and not infiltration). **(C**, **D)** *N. benthamiana* leaves were infiltrated with EVs at multiple points on the right half and PBS on the left. After 5 days the leaves were removed from the plants and imaged. Leaf halves infiltrated with EVs from *F. oxysporum* f. sp. *vasinfectum* **(C)** showed substantial discoloration around the sites of infiltration, whereas the half infiltrated with PBS had no discoloration. Leaf halves infiltrated with EVs from *S. cerevisiae* **(D)** appeared similar to the corresponding PBS infiltrated leave halves. Infiltration of cotton cotyledons with resuspended *F. oxysporum* f. sp. *vasinfectum* spores and hyphae **(E)** led to the formation of very small discolored spots at the sites of infiltration, but they were much smaller than those observed with EVs. Images are representative of three independent experiments.

(**Figures 4B–D**). Co-purification of the pigment with the EVs on the optiprep gradient supports the notion that the pigment is packaged in the EVs. The phytotoxicity of these fractions on cotton plants indicated that EVs and/or the pigment are responsible for initiating the response.

DISCUSSION

We have isolated EVs from the plant pathogen *F. oxysporum* f. sp. *vasinfectum*, characterized their protein cargo, and discovered that they have a phytotoxic effect when applied to the leaves of cotton and *N. benthamiana*. A unique feature of the EVs isolated from *F. oxysporum* f. sp. *vasinfectum* was their deep purple color, which has not been reported for EVs from any other species.

There are no marker proteins for fungal EVs so confirmation that the particles we had isolated *via* ultracentrifugation were indeed EVs depended on physical characterization. TEM confirmed that the EVs isolated from *F. oxysporum* f. sp. *vasinfectum* had the characteristic morphology of EVs from other organisms. NTA confirmed that the population of EVs had a similar size distribution to those reported for *C. albicans* and *C. neoformans* that also used NTA for size analysis (Bielska and May, 2019). Larger vesicles (diameter greater than 450 nm) have been detected in *C. neoformans, C. albicans*, and *Malassezia sympodialis* EV preparations (Bielska and May, 2019) but were not detected in this analysis. The rosette-shaped particles have been described previously in an isolation of EVs from *S. cerevisiae*, but their origin and identity remain unknown (Giardina et al., 2014).

Proteomic characterization of EVs from *F. oxysporum* f. sp. *vasinfectum* was conducted to elucidate potential functions of these particles in the host–pathogen interaction. Proteomic analysis *F. oxysporum* f. sp. *vasinfectum* EVs identified 482 proteins, which is greater than the 205 (or fewer) proteins identified in the early studies on yeast EVs (Rodrigues et al., 2008; Vallejo et al., 2012; Gil-Bona et al., 2014; Wolf et al., 2014; Vargas et al., 2015; Wolf et al., 2015) and lower than the 600 (or greater) reported from *S. cerevisiae* and *C. albicans* EVs obtained using similar methods of isolation and proteomic analysis (Zhao et al., 2019; unpublished data from the Anderson lab). This may have arisen from the lower yield of EVs from *F. oxysporum* f. sp. *vasinfectum* compared to yeast cultures. Functional enrichment analysis of the *F. oxysporum* f. sp. *vasinfectum* EV cargo proteins mostly identified basic cellular metabolic and biosynthetic processes. In addition, there were many proteins with unknown function. Yeast EVs are also enriched for proteins that function in these basal cellular processes as well as proteins that function in pathogenesis, stress responses, and cell wall dynamics (Bleackley et al., 2019). The latter protein groups were not identified in the *F. oxysporum* f. sp. *vasinfectum* EVs but this is probably due to the relatively poor annotation of the genome of *F. oxysporum* f. sp. *vasinfectum*. It is likely that a subset of the uncharacterized proteins, as well as proteins that have been incorrectly annotated based on sequence homology, have a function in *F. oxysporum* f. sp. *vasinfectum* pathogenesis.

An Hsp70 like protein was also found in *F. oxysporum* f. sp. *vasinfectum* EVs. Hsp70 was one of the few identified in all previously published proteomic data sets for *C. albicans* and *C. neoformans* EVs (reviewed in Bleackley et al., 2019) and is also

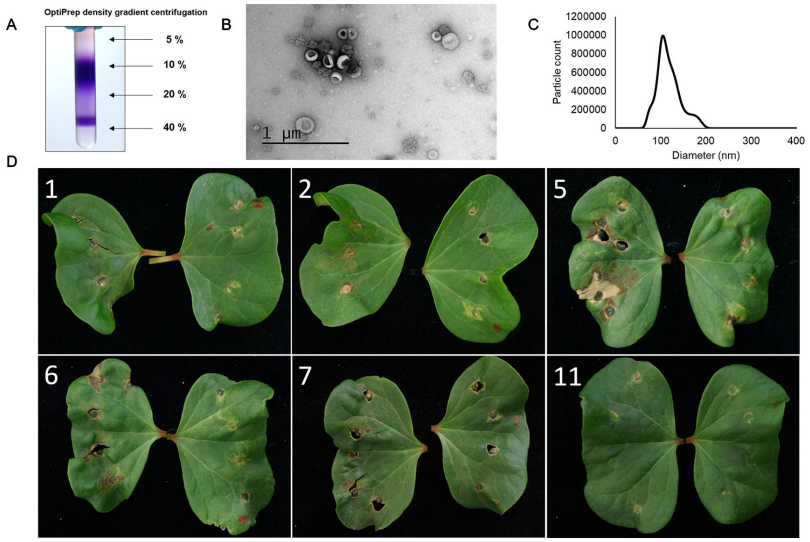

FIGURE 4 | The optiprep fractions containing both EVs and the purple pigment are responsible for the hypersensitive response induced by the crude EV fraction in plants. **(A)** Optiprep gradient centrifugation of the crude EV fraction revealed that the purple pigment concentrates in two regions, one centered at 10% and a second close to 40% iodixanol. The purple pigment was concentrated in fractions 5–7. **(B)** Representative TEM of fractions 5–7. Particles with characteristic cup-like morphology of EVs were detected in these fractions as well as some rosette-shaped particles. **(C)** Representative NTA of fractions 5–7. The mode particle diameter was 104.5 nm; no particles were detected below 46.5 nm or above 226.5 nm. **(D)** Application of select fractions (numbered in white) to the cotyledons of a cotton plant. Fractions (left cotyledon) were all paired with a PBS control (right cotyledon). Fraction 5 induced the strongest response with fractions 6 and 7 inducing a lesser response. Fractions 1, 2, and 11 did not induce a response beyond that observed for the PBS control. The brown spots and holes on the control cotyledons are due to wounding of the leaf during infiltration.

found in mammalian exosomes (Lancaster and Febbraio, 2005). Hsp70 proteins are molecular chaperones that assist in protein folding and stability (Mayer and Bukau, 2005) that have been proposed as molecules that communicate intercellular stresses through packaging into EVs (De Maio, 2011). HSP70 may prove to be a valuable marker for fungal EVs. Marker proteins in mammalian EVs facilitate analysis of EV purity, that is, from potential contamination from organelle fragments (Lötvall et al., 2014), and the lack of markers for fungal EVs means that this is not currently possible.

One of the most striking observations in this study was the deep purple color of the EVs isolated from *F. oxysporum* f. sp. *vasinfectum*. The pigment not only co-purified with the EVs during ultracentrifugation but also co-purified with the EVs during the Optiprep gradient analysis. Packaging of pigments into EVs could represent a conserved secretion mechanism across fungi because melanin, a pigment that has a role in the virulence of *C. neoformans*, is also packaged into a subset of EVs (Rodrigues et al., 2008). Proteomic analysis of EVs isolated from *A. infectoria,* which also contain melanin, identified a polyketide synthase involved in biosynthesis of melanin and other pigments as EV cargo (Silva et al., 2013). *Fusarium* spp., like most fungi, produce a wide variety of secondary metabolites, which include mycotoxins that negatively impact agricultural production as well as molecules that have served as a starting point for development of pharmaceuticals (Brown et al., 2012). The source of the purple color was initially suspected to be a polyketide secondary metabolite similar to purpurfusarin, which was identified from a *F. graminearum* strain over expressing *PGL1* (Frandsen et al., 2016). Purple pigments have since been isolated from *F. oxysporum* cultures grown on defined minimal dextrose broth (Lebeau et al., 2019). The absorbance spectra of an ethanol extract of lyophilized culture medium was consistent with the dual maxima at 550 and 590 nm of the EVs. These purple pigments were further refined and had typical UV-Vis absorbance profiles for napthoquinones, but specific peaks in the UV spectra indicated that they are not purpurfusarin (Frandsen et al., 2016) or 8-*O*-methyl anhydrofusarubin (Studt et al., 2012), which are known purple pigments from *Fusarium*. Bikaverin, a polyketide with antibiotic properties (Limón et al., 2010), was also detected in the extracts containing the pigments (Lebeau et al., 2019); it follows that perhaps bikaverin is also packaged into EVs. Analysis of the small molecule content of EVs is required to further enhance understanding of potential role of EVs in the secretion of polyketides and other fungal metabolites. Identification of the two polyketide synthases and

one fusarubin cluster-esterase as EV cargo in this study could point towards EVs as a site of biosynthesis for pigments and/or toxins.

We speculated that *F. oxysporum* f. sp. *vasinfectum* EVs had a role in the fungal–plant interaction because the role of EVs in bacterial infections is well described in mammalian systems (Pathirana and Kaparakis-Liaskos, 2016). Furthermore, pathogenic yeasts such as *C. albicans, C. neoformans*, and *Paracoccidioides brasiliensis* are able to activate innate immune cells such as macrophages (Oliveira et al., 2010) and dendritic cells (Vargas et al., 2015; Wolf et al., 2015). EVs are also a contributing factor to the hypervirulence phenotype of a strain of *C. gattii* (Bielska et al., 2018). This led to the hypothesis that EVs would play a role in fungal pathogenesis in plants. EVs from *F. oxysporum* f. sp. *vasinfectum* that were infiltrated into cotyledons of cotton or leaves of *N. benthamiana* were phytotoxic. This toxicity was not merely a response to fungal cell wall polysaccharides or lipids as there was no phytotoxic response to EVs from *S. cerevisiae* or to intact fungal spores and hyphae from *F. oxysporum* f. sp. *vasinfectum*. EVs as the source of the phytotoxicity was further supported by the observation that after further fractionation of the initial EV prep using Optiprep gradient centrifugation, the EV enriched fractions retained phytotoxic activity whereas fractions that did not contain EVs did not. Although the leaf is not the normal route of infection for *F. oxysporum* f. sp. *vasinfectum*, the effect of EVs on leaf tissue demonstrates that the EVs do carry phytotoxic compounds. Furthermore, a similar phytotoxic effect was observed the *F. oxysporum* f. sp. *vasinfectum* EVs were infiltrated into *N. benthamiana*, a plant that is not a host for *F. oxysporum* f. sp. *vasinfectum,* demonstrates that the EVs contain a phytotoxic compound and it is not a host specific virulence factor that is eliciting this response. This could be related to the pigments and/or other polyketides that are associated with the EVs as these molecules can have a range of detrimental effects on plant cells (Möbius and Hertweck, 2009). Alternatively, EV proteins could be the cause of the phytotoxicity. Several proteases, a family of proteins that contribute to pathogenesis of various plant pathogens (Olivieri et al., 2002; Yike, 2011; Lowe et al., 2015), were packaged into EVs and could play a key role in contributing to the damage caused by the EVs. The phytotoxic effect of EVs during an infection is likely to be less extreme that the one observed here due to the amount of EVs used in these experiments compared to what would be present during an infection. EVs were isolated from a 1 L culture and resuspended in approximately 2 ml of PBS prior to infiltration and exceeds what would be expected to be produced by the fungus at any one point during an infection. However, a fungus would continuously be producing EVs during an infection so the cumulative exposure to EVs would increase over time. The high concentration, single dose of EVs was used to ensure that an effect was observed upon infiltration. Future investigation on the role of EVs in an infection will need to investigate physiologically relevant EV concentrations and use more sensitive techniques to measure the response in the plant.

In summary, *F. oxysporum* f. sp. *vasinfectum* produces EVs similar in morphology and size to EVs from other fungal species. These EVs carry protein cargo and pigments that may have a role in pathogenesis. Preliminary data demonstrated that EVs from *F. oxysporum* f. sp. *vasinfectum* are phytotoxic to leaves of both its host plant cotton and the unrelated plant *N. benthamiana*. This may be a response turned on by the plant in recognition of the fungal EVs to limit the spread of infection and may explain why *F. oxysporum* f. sp. *vasinfectum* enters the plant through the roots instead of the leaves. Alternatively, EV release could be downregulated during the biotrophic phase of the infection and then turned on when the fungus switches to necrotrophy. Further characterization of EVs from *F. oxysporum* f. sp. *vasinfectum* and other agricultural fungal pathogens will improve our understanding of the plant–pathogen interaction and may ultimately lead to identification of new targets to enhance disease protection in crop plants.

DATA AVAILABILITY STATEMENT

All datasets for this study are included in the article/**Supplementary Material**.

AUTHOR CONTRIBUTIONS

MB performed infiltration assays, analyzed proteomic data, and wrote the manuscript. MS performed EV isolations and characterization, prepared samples for mass spec, and performed infiltration assays. DG-C performed EV isolations and characterization, prepared samples for mass spec. JM aided in design of infiltration assays and collected images from infiltration assays. RL annotated the proteome and analyzed proteomic data. MP analyzed proteomic data. KZ isolated yeast EVs. C-SA performed proteomic data collection. SM conceived the project, oversaw the experimental work and data analysis. MA conceived the project, oversaw the experimental work and data analysis, and revised the manuscript.

FUNDING

This work was funded by Australian Research Council grants to MA (DP160100309) and SM (DP170102312 and DE150101777). JM is a Commonwealth Scientific and Industrial Research Organisation Science and Industry Endowment Fund STEM Fellow.

SUPPLEMENTARY MATERIAL

The Supplementary Material for this article can be found online at: https://www.frontiersin.org/articles/10.3389/fpls.2019.01610/full#supplementary-material

TABLE S1 | Full list of proteins in EVs.

TABLE S2 | EV enriched GO terms.

TABLE S3 | WCL enriched GO terms.

REFERENCES

An, Q., Ehlers, K., Kogel, K. H., Van Bel, A. J., and Hückelhoven, R. (2006). Multivesicular compartments proliferate in susceptible and resistant MLA12-barley leaves in response to infection by the biotrophic powdery mildew fungus. *New Phytol.* 172 (3), 563–576. doi: 10.1111/j.1469-8137.2006.01844.x

Bielska, E., and May, R. C. (2019). Extracellular vesicles of human pathogenic fungi. *Curr. Opin. Microbiol.* 52, 90–99. doi: 10.1016/j.mib.2019.05.007

Bielska, E., Sisquella, M. A., Aldeieg, M., Birch, C., O'Donoghue, E. J., and May, R. C. (2018). Pathogen-derived extracellular vesicles mediate virulence in the fatal human pathogen Cryptococcus gattii. *Nat. Commun.* 9 (1), 1556. doi: 10.1038/s41467-018-03991-6

Bitencourt, T. A., Rezende, C. P., Quaresemin, N. R., Moreno, P., Hatanaka, O., Rossi, A., et al. (2018). Extracellular vesicles from the dermatophyte trichophyton interdigitale modulate macrophage and keratinocyte functions. *Front. Immunol.* 9, 2343. doi: 10.3389/fimmu.2018.02343

Bleackley, M. R., Dawson, C. S., and Anderson, M. A. (2019). Fungal extracellular vesicles with a focus on proteomic analysis. *Proteomics* 19 (8), 1800232. doi: 10.1002/pmic.201800232

Boevink, P. C. (2017). Exchanging missives and missiles: the roles of extracellular vesicles in plant–pathogen interactions. *J. Exp. Bot.* 68 (20), 5411. doi: 10.1093/jxb/erx369

Bohlenius, H., Morch, S. M., Godfrey, D., Nielsen, M. E., and Thordal-Christensen, H. (2010). The multivesicular body-localized GTPase ARFA1b/1c is important for callose deposition and ROR2 syntaxin-dependent preinvasive basal defense in barley. *Plant Cell* 22 (11), 3831–3844. doi: 10.1105/tpc.110.078063

Bomberger, J. M., Maceachran, D. P., Coutermarsh, B. A., Ye, S., O'Toole, G. A., and Stanton, B. A. (2009). Long-distance delivery of bacterial virulence factors by Pseudomonas aeruginosa outer membrane vesicles. *PLoS Pathog.* 5 (4), e1000382. doi: 10.1371/journal.ppat.1000382

Brown, D. W., Butchko, R. A., Baker, S. E., and Proctor, R. H. (2012). Phylogenomic and functional domain analysis of polyketide synthases in Fusarium. *Fungal Biol.* 116 (2), 318–331. doi: 10.1016/j.funbio.2011.12.005

Conesa, A., Götz, S., García-Gómez, J. M., Terol, J., Talón, M., and Robles, M. (2005). Blast2GO: a universal tool for annotation, visualization and analysis in functional genomics research. *Bioinformatics* 21 (18), 3674–3676. doi: 10.1093/bioinformatics/bti610

da Silva, R. P., Heiss, C., Black, I., Azadi, P., Gerlach, J. Q., Travassos, L. R., et al. (2015). Extracellular vesicles from Paracoccidioides pathogenic species transport polysaccharide and expose ligands for DC-SIGN receptors. *Sci. Rep.* 5, 14213. doi: 10.1038/srep14213

da Silva, T. A., Roque-Barreira, M. C., Casadevall, A., and Almeida, F. (2016). Extracellular vesicles from Paracoccidioides brasiliensis induced M1 polarization *in vitro*. *Sci. Rep.* 6, 35867. doi: 10.1038/srep35867

De Maio, A. (2011). Extracellular heat shock proteins, cellular export vesicles, and the Stress Observation System: a form of communication during injury, infection, and cell damage. It is never known how far a controversial finding will go! Dedicated to Ferruccio Ritossa. *Cell Stress Chaperones* 16 (3), 235–249. doi: 10.1007/s12192-010-0236-4

Ellis, T. N., Leiman, S. A., and Kuehn, M. J. (2010). Naturally produced outer membrane vesicles from Pseudomonas aeruginosa Elicit a potent innate immune response via combined sensing of both Lipopolysaccharide and protein components. *Infect. Immun.* 78 (9), 3822–3831. doi: 10.1128/Iai.00433-10

Frandsen, R. J., Rasmussen, S. A., Knudsen, P. B., Uhlig, S., Petersen, D., Lysøe, E., et al. (2016). Black perithecial pigmentation in Fusarium species is due to the accumulation of 5-deoxybostrycoidin-based melanin. *Sci. Rep.* 6, 26206. doi: 10.1038/srep26206

Giardina, B. J., Stein, K., and Chiang, H.-L. (2014). The endocytosis gene END3 is essential for the glucose-induced rapid decline of small vesicles in the extracellular fraction in Saccharomyces cerevisiae. *J Extracell. Vesicles* 3 (1), 23497. doi: 10.3402/jev.v3.23497

Gil-Bona, A., Llama-Palacios, A., Parra, C. M., Vivanco, F., Nombela, C., Monteoliva, L., et al. (2014). Proteomics unravels extracellular vesicles as carriers of classical cytoplasmic proteins in Candida albicans. *J. Proteome Res.* 14 (1), 142–153. doi: 10.1021/pr5007944

Gordon, T. R. (2017). Fusarium oxysporum and the Fusarium wilt syndrome. *Ann. Rev. Phytopathol.* 55, 23–39. doi: 10.1146/annurev-phyto-080615-095919

Greening, D. W., and Simpson, R. J. (2018). Understanding extracellular vesicle diversity–current status. *Expert Rev. Proteomic.* 15 (11), 887–910. doi: 10.1080/14789450.2018

Griffith, C. L., Klutts, J. S., Zhang, L., Levery, S. B., and Doering, T. L. (2004). UDP-glucose dehydrogenase plays multiple roles in the biology of the pathogenic fungus Cryptococcus neoformans. *J Biol. Chem.* 279 (49), 51669–51676. doi: 10.1074/jbc.M408889200

Horstman, A. L., and Kuehn, M. J. (2000). Enterotoxigenic Escherichia coli secretes active heat-labile enterotoxin via outer membrane vesicles. *J. Biol. Chem.* 275 (17), 12489–12496. doi: 10.1074/jbc.275.17.12489

Kalra, H., Simpson, R. J., Ji, H., Aikawa, E., Altevogt, P., Askenase, P., et al. (2012). Vesiclepedia: a compendium for extracellular vesicles with continuous community annotation. *PLoS Biol.* 10 (12), e1001450. doi: 10.1371/journal.pbio.1001450

Kalra, H., Adda, C. G., Liem, M., Ang, C. S., Mechler, A., Simpson, R. J., et al. (2013). Comparative proteomics evaluation of plasma exosome isolation techniques and assessment of the stability of exosomes in normal human blood plasma. *Proteomics* 13 (22), 3354–3364. doi: 10.1002/pmic.201300282

Kim, S. W., Park, S. B., Im, S. P., Lee, J. S., Jung, J. W., Gong, T. W., et al. (2018). Outer membrane vesicles from beta-lactam-resistant Escherichia coli enable the survival of beta-lactam-susceptible E. coli in the presence of beta-lactam antibiotics. *Sci. Rep.* 8 (1), 5402. doi: 10.1038/s41598-018-23656-0

Lancaster, G. I., and Febbraio, M. A. (2005). Exosome-dependent trafficking of HSP70 A novel secretory pathway for cellular stress proteins. *J Biol. Chem.* 280 (24), 23349–23355. doi: 10.1074/jbc.M502017200

Lebeau, J., Petit, T., Clerc, P., Dufossé, L., and Caro, Y. (2019). Isolation of two novel purple naphthoquinone pigments concomitant with the bioactive red bikaverin and derivates thereof produced by Fusarium oxysporum. *Biotechnol. Prog.* 35 (1), e2738. doi: 10.1002/btpr2738

Li, X., Bao, H., Wang, Z., Wang, M., Fan, B., Zhu, C., et al. (2018). Biogenesis and function of multivesicular bodies in plant immunity. *Front. Plant Sci.* 9, 979. doi: 10.3389/fpls.2018.00979

Limón, M. C., Rodríguez-Ortiz, R., and Avalos, J. (2010). Bikaverin production and applications. *Appl. Microbiol. Biotechnol.* 87 (1), 21–29. doi: 10.1007/s00253-010-2551-1

Liu, M., Bruni, G. O., Taylor, C. M., Zhang, Z., and Wang, P. (2018). Comparative genome-wide analysis of extracellular small RNAs from the mucormycosis pathogen Rhizopus delemar. *Sci. Rep.* 8 (1), 5243. doi: 10.1038/s41598-018-23611-z

Lötvall, J., Hill, A. F., Hochberg, F., Buzás, E. I., Di Vizio, D., Gardiner, C., et al. (2014). Minimal experimental requirements for definition of extracellular vesicles and their functions: a position statement from the International Society for Extracellular Vesicles, Taylor & Francis.

Lowe, R. G. T., McCorkelle, O., Bleackley, M., Collins, C., Faou, P., Mathivanan, S., et al. (2015). Extracellular peptidases of the cereal pathogen Fusarium graminearum. *Front. Plant Sci.* 6, 962. doi: 10.3389/fpls.2015.00962

Maas, S. L., Breakefield, X. O., and Weaver, A. M. (2017). Extracellular vesicles: unique intercellular delivery vehicles. *Trends Cell Biol.* 27 (3), 172–188. doi: 10.1016/j.tcb.2016.11.003

Mathivanan, S., Ji, H., Tauro, B. J., Chen, Y.-S., and Simpson, R. J. (2012). Identifying mutated proteins secreted by colon cancer cell lines using mass spectrometry. *J. Proteomics* 76, 141–149. doi: 10.1016/j.jprot.2012.06.031

Mayer, M., and Bukau, B. (2005). Hsp70 chaperones: cellular functions and molecular mechanism. *Cell. Mol. Life Sci.* 62 (6), 670. doi: 10.1007/s00018-004-4464-6

Möbius, N., and Hertweck, C. (2009). Fungal phytotoxins as mediators of virulence. *Curr. Opin. Plant Biol.* 12 (4), 390–398. doi: 10.1016/j.pbi.2009.06.004

Oliveira, D. L., Freire-de-Lima, C. G., Nosanchuk, J. D., Casadevall, A., Rodrigues, M. L., and Nimrichter, L. (2010). Extracellular vesicles from Cryptococcus neoformans modulate macrophage functions. *Infect. Immun.* 78 (4), 1601–1609. doi: 10.1128/IAI.01171-09

Olivieri, F., Zanetti, M. E., Oliva, C. R., Covarrubias, A. A., and Casalongué, C. A. (2002). Characterization of an extracellular serine protease of Fusarium eumartii and its action on pathogenesis related proteins. *Eur. J. Plant Pathol.* 108 (1), 63–72. doi: 10.1023/A:1013920929965

Olofsson, A., Vallstrom, A., Petzold, K., Tegtmeyer, N., Schleucher, J., Carlsson, S., et al. (2010). Biochemical and functional characterization of Helicobacter

pylori vesicles. *Mol. Microbiol.* 77 (6), 1539–1555. doi: 10.1111/j.1365-2958.2010.07307.x

Pathirana, R. D., and Kaparakis-Liaskos, M. (2016). Bacterial membrane vesicles: biogenesis, immune regulation and pathogenesis. *Cell. Microbiol.* 18 (11), 1518–1524. doi: 10.1111/cmi.12658

Poon, S., Harris, K. S., Jackson, M. A., McCorkelle, O. C., Gilding, E. K., Durek, T., et al. (2018). Co-expression of a cyclizing asparaginyl endopeptidase enables efficient production of cyclic peptides in planta. *J. Exp. Bot.* 69 (3), 633–641. doi: 10.1093/jxb/erx422

Prados-Rosales, R., Weinrick, B. C., Pique, D. G., Jacobs, W. R. Jr., Casadevall, A., and Rodriguez, G. M. (2014). Role for Mycobacterium tuberculosis membrane vesicles in iron acquisition. *J. Bacteriol.* 196 (6), 1250–1256. doi: 10.1128/JB.01090-13

Regente, M., Pinedo, M., San Clemente, H., Balliau, T., Jamet, E., and de la Canal, L. (2017). Plant extracellular vesicles are incorporated by a fungal pathogen and inhibit its growth. *J. Exp. Bot.* 68 (20), 5485–5495. doi: 10.1093/jxb/erx355

Rodrigues, M. L., Nimrichter, L., Oliveira, D. L., Frases, S., Miranda, K., Zaragoza, O., et al. (2007). Vesicular polysaccharide export in Cryptococcus neoformans is a eukaryotic solution to the problem of fungal trans-cell wall transport. *Eukaryotic Cell* 6 (1), 48–59. doi: 10.1128/Ec.00318-06

Rodrigues, M. L., Nakayasu, E. S., Oliveira, D. L., Nimrichter, L., Nosanchuk, J. D., Almeida, I. C., et al. (2008). Extracellular vesicles produced by Cryptococcus neoformans contain protein components associated with virulence. *Eukaryotic Cell* 7 (1), 58–67. doi: 10.1128/EC.00370-07

Rutter, B. D., and Innes, R. W. (2017). Extracellular vesicles isolated from the leaf apoplast carry stress-response proteins. *Plant Physiol.* 173 (1), 728–741. doi: 10.1104/pp.16.01253

Rutter, B. D., and Innes, R. W. (2018). Extracellular vesicles as key mediators of plant–microbe interactions. *Curr. Opin. Plant Biol.* 44, 16–22. doi: 10.1016/j.pbi.2018.01.008

Rybak, K., and Robatzek, S. (2019). Functions of extracellular vesicles in immunity and virulence. *Plant Physiol.* 179 (4), 1236–1247. doi: 10.1104/pp.18.01557

Samuel, M., Bleackley, M., Anderson, M., and Mathivanan, S. (2015). Extracellular vesicles including exosomes in cross kingdom regulation: a viewpoint from plant-fungal interactions. *Front. Plant Sci.* 6, 766. doi: 10.3389/fpls.2015.00766

Schorey, J. S., Cheng, Y., Singh, P. P., and Smith, V. L. (2015). Exosomes and other extracellular vesicles in host–pathogen interactions. *EMBO Rep.* 16 (1), 24–43.

Silva, B. M., Prados-Rosales, R., Espadas-Moreno, J., Wolf, J. M., Luque-Garcia, J. L., Gonçalves, T., et al. (2013). Characterization of Alternaria infectoria extracellular vesicles. *Sabouraudia* 52 (2), 202–210. doi: 10.1093/mmy/myt003

Studt, L., Wiemann, P., Kleigrewe, K., Humpf, H.-U., and Tudzynski, B. (2012). Biosynthesis of fusarubins accounts for pigmentation of Fusarium fujikuroi perithecia. *Appl. Environ. Microbiol.* 78 (12), 4468–4480. doi: 10.1128/AEM.00823-12

Vallejo, M. C., Nakayasu, E. S., Matsuo, A. L., Sobreira, T. J., Longo, L. V., Ganiko, L., et al. (2012). Vesicle and vesicle-free extracellular proteome of Paracoccidioides brasiliensis: comparative analysis with other pathogenic fungi. *J. Proteome Res.* 11 (3), 1676–1685. doi: 10.1021/pr200872s

Vargas, G., Rocha, J. D., Oliveira, D. L., Albuquerque, P. C., Frases, S., Santos, S. S., et al. (2015). Compositional and immunobiological analyses of extracellular vesicles released by Candida albicans. *Cell. Microbiol.* 17 (3), 389–407. doi: 10.1111/cmi.12374

Vasilyeva, N. V., Tsfasman, I. M., Suzina, N. E., Stepnaya, O. A., and Kulaev, I. S. (2008). Secretion of bacteriolytic endopeptidase L5 of Lysobacter sp XL1 into the medium by means of outer membrane vesicles. *Febs J.* 275 (15), 3827–3835. doi: 10.1111/j.1742-4658.2008.06530.x

Wolf, J. M., Espadas-Moreno, J., Luque-Garcia, J. L., and Casadevall, A. (2014). Interaction of Cryptococcus neoformans extracellular vesicles with the cell wall. *Eukaryotic cell* 13 (12), 1484–1493. doi: 10.1128/EC.00111-14

Wolf, J. M., Espadas, J., Luque-Garcia, J., Reynolds, T., and Casadevall, A. (2015). Lipid biosynthetic genes affect Candida albicans extracellular vesicle morphology, cargo, and immunostimulatory properties. *Eukaryotic Cell* 14 (8), 745–754. doi: 10.1128/EC.00054-15

Yike, I. (2011). Fungal proteases and their pathophysiological effects. *Mycopathologia* 171 (5), 299–323. doi: 10.1007/s11046-010-9386-2

Zarnowski, R., Sanchez, H., Covelli, A. S., Dominguez, E., Jaromin, A., Berhardt, J., et al. (2018). Candida albicans biofilm–induced vesicles confer drug resistance through matrix biogenesis. *PLoS Biol.* 16 (10), e2006872. doi: 10.1371/journal.pbio.2006872

Zhao, K., Bleackley, M., Chisanga, D., Gangoda, L., Fonseka, P., Liem, M., et al. (2019). Extracellular vesicles secreted by Saccharomyces cerevisiae are involved in cell wall remodelling. *Commun. Biol.* 2, 305. doi: 10.1038/s42003-019-0538-8

Conflict of Interest: The authors declare that the research was conducted in the absence of any commercial or financial relationships that could be construed as a potential conflict of interest.

2.2 Development of an improved isolation method for recovery of EVs from *Fov*

Study 1 was the first report that *Fov* produces EVs, and that they potentially have a role in fungal-plant interactions. Sufficient material was obtained for a proteomics analysis, but the yield of EVs from the fungal cultures was low. EVs from several cultures had to be pooled to achieve the concentrations used in the bioassay on the cotton plants. Furthermore, variations between different batches of the commercial powder used to prepare the half-strength potato dextrose broth (½ PDB) growth medium resulted in differences in fungal growth and hence differences in EV yield. Finally, growing *Fov* at room temperature contributed to biomass variability across biological replicates at the end of the incubation period.

For these reasons, it was essential to generate a more reproducible cultivation and isolation protocol tailored for *Fov*, that would increase EV yield and allow reproducible downstream analyses. A refrigerated incubator (Incu-shaker 10 L, Benchmark) was obtained to prevent any fluctuations in temperature during the culture period, and a defined growth medium was used to avoid batch to batch variation. Finally, EVs prepared from *Fov* grown on different media were compared to determine whether the medium affected the cargo incorporated into the EVs. The isolation of EVs from *Fov* and the effect on the medium on EV cargo are presented in Section 2.3.

2.3 Size-exclusion chromatography allows the isolation of EVs from the filamentous fungal pathogen *Fusarium oxysporum* f. sp. *vasinfectum* (*Fov*)

The findings from this study have been published in a peer-reviewed journal, Proteomics, February 2021.

Garcia-Ceron D, Dawson CS, Faou P, Bleackley MR, Anderson MA (2020). **Size-Exclusion Chromatography Allows the Isolation of EVs From the Filamentous Fungal Plant Pathogen *Fusarium oxysporum* f. sp. *vasinfectum* (*Fov*)**. Proteomics 20:e2000240. doi: 10.1002/pmic.202000240.

Statement of Contribution

Donovan Garcia-Ceron:
- Designed and performed the experiments
- Analyzed and interpreted the data
- Prepared figures and wrote the manuscript
- Provided revisions during the peer-review of the manuscript

Other authors have made the following contributions:
- Bleackley MR and Anderson MA conceived the project, contributed to the experimental design, and edited the manuscript; Dawson CS performed part of the statistical analysis; Faou P processed the mass spectrometry samples.

Received: 17 September 2020 | Revised: 1 February 2021 | Accepted: 3 February 2021 | Accepted article online: 20 February 2021

DOI: 10.1002/pmic.202000240

Proteomics
Proteomics and Systems Biology

RESEARCH ARTICLE

Size-exclusion chromatography allows the isolation of EVs from the filamentous fungal plant pathogen *Fusarium oxysporum* f. sp. *vasinfectum* (Fov)

Donovan Garcia-Ceron[1] | **Charlotte S. Dawson**[2] | **Pierre Faou**[3] | **Mark R. Bleackley**[1] | **Marilyn A. Anderson**[1]

[1] Department of Biochemistry and Genetics, La Trobe Institute for Molecular Science, La Trobe University, Bundoora, Victoria, Australia

[2] Cambridge Centre for Proteomics, Department of Biochemistry, Jeffrey Cheah Biomedical Centre, University of Cambridge, Cambridge, United Kingdom

[3] La Trobe Comprehensive Proteomics Platform, La Trobe Institute for Molecular Science, La Trobe University, Bundoora, Victoria, Australia

Correspondence
Prof. Marilyn A. Anderson, Department of Biochemistry and Genetics, La Trobe Institute for Molecular Science, La Trobe University, LIMS 2 - Kingsbury Drive Bundoora, Victoria 3086, Australia.
Email: m.anderson@latrobe.edu.au

Funding information
Australian Research Council, Grant/Award Numbers: DP160100309, DP200103393

Abstract

Extracellular vesicles (EVs) are nano-sized compartments involved in cell communication and macromolecule transport that are well characterized in mammalian organisms. Fungal EVs transport virulence-related cargo and modulate the host immune response, but most work has been focused on human yeast pathogens. Additionally, the study of EVs from filamentous fungi has been hindered by the lack of protein markers and efficient isolation methods. In this study we performed the isolation and proteomic characterization of EVs from the filamentous cotton pathogen *Fusarium oxysporum* f. sp. *vasinfectum* (Fov). EVs were recovered from two different growth media, Czapek Dox and Saboraud's dextrose broth, and purified by size-exclusion chromatography. Our results show that the EV proteome changes depending on the growth medium but EV production remains constant. EVs contained proteins involved in polyketide synthesis, cell wall modifications, proteases and potential effectors. These results support a role in modulation of host-pathogen interactions for Fov EVs.

KEYWORDS
cotton, extracellular vesicles (EVs), fungi, Fusarium, host-pathogen interactions

1 | INTRODUCTION

Extracellular vesicles (EVs) are produced by human, animal, plant and microbial organisms [1]. EVs are particles of up to a micrometer, delimitated by a lipidic membrane, with roles in transporting macromolecules, cell communication, neurodegenerative diseases, cancer and other pathologies [2, 3].

Fungi also secrete EVs, but these have been severely understudied compared to EVs from mammalian systems [4]. Fungal EVs carry proteins, nucleic acids, pigments, polysaccharides, and molecules associated with virulence [5, 6].

Fungal EVs have a role in disease progression [7], unconventional secretion [8], transport of virulence factors that support fungal survival [8], and in cell wall remodeling [9]. EVs are also involved in antimicrobial resistance and biofilm formation in the human pathogen *Candida albicans* [10]. EVs from yeast have already gained recognition as key components of human-fungal interactions.

One of the world's most severe plant pathogens is the filamentous fungus *Fusarium oxysporum* [11]. The term "forma specialis" was adopted to indicate host-specificity among strains of *F. oxysporum* [12], and so far over 100 formae speciales have been reported [13]. *F. oxysporum* f. sp. *vasinfectum* (Fov) causes cotton wilt and is present in all major cotton-producing regions of the world [14, 15]. Studying the

Abbreviations: ½ PDB, half-strength potato dextrose broth; CD, Czapek Dox medium; DPBS, Dulbecco's phosphate buffered saline; Fov, *Fusarium oxysporum* f. sp. *vasinfectum*; LFQ, label-free quantitation; Log2(FC), log2(fold-change); NTA, nanoparticle tracking analysis; PCA, Principal component analysis; SDB, Saboraud's dextrose broth; TEM, transmission electron microscopy; UA, Uranyl acetate; UC, Differential ultracentrifugation

production of EVs from Fov will lead to a clearer view of host-pathogen interactions in fungi.

Although most techniques for the analysis of fungal EVs have been adapted from mammalian EV research, optimization is required to ensure an efficient isolation of fungal EVs. The most common methods for EV isolation involve separation by particle size, density, immunoaffinity, or precipitation with polymers [16, 17]. The study of fungal EVs has been limited by availability of appropriate isolation methods, since some of the best protocols for isolation, characterization and quality control of mammalian EVs rely on protein markers for their detection, and these have only recently been proposed for fungi [18]. Hence, methods such as immunoaffinity or flow cytometry have not been used to investigate fungal EVs.

Ultracentrifugation (UC) continues to be the most common isolation method for fungal EVs [4, 8]. Despite this, UC has major drawbacks such as loss of EV integrity, the requirement for expensive and specialized equipment, and time-consuming procedures [19, 20]. Other isolation methods, such as polymer-based precipitation of EVs also present disadvantages such as co-precipitation of contaminants and polymer interference in mass spectrometry analysis [21].

Size-exclusion chromatography (SEC) is effective for isolation of EVs from human plasma [22], urine [23], and cell culture-conditioned medium [24]. EVs from the human yeast pathogen *C. albicans* have been isolated by combining UC and SEC [10]. EVs purified only by SEC are suitable for proteomic characterization and other downstream analyses [25]. Therefore, SEC offers attractive advantages for isolation of EVs from fungi.

EV literature is only available for a few species of filamentous fungi. *Aspergillus fumigatus* produces EVs that can alter immune responses from the host [26] and *Aspergillus flavus* EVs induce M1 polarization of macrophages and may favor fungal clearance in larval models [27]. The only proteomic characterizations of EVs from plant pathogens are from *Alternaria infectoria* [28], *Zymoseptoria tritici* [29] and a previous Fov analysis [30]. EVs from *A. infectoria* contain proteins involved in cell wall remodeling, synthesis of polyketides and metabolism [28], while *Z. tritici* EVs transport the putative fungal EV marker Sur7 [16, 29]. Fov EVs contained substantially more proteins than EVs from other filamentous fungi [30]. Fov EVs are phytotoxic, co-purify with a purple pigment and contain proteins involved in polyketide biosynthesis, proteases, and basic cellular processes [30]. Limitations in EV yield impacted the proteomic analysis of this study [30]; therefore, a more robust isolation method is required to better understand the function of EVs from Fov.

In this study we sought to adapt SEC for the isolation of EVs from Fov and perform a proteomic analysis of EVs recovered from two culture media that are different in nutrient composition: Czapek Dox (CD) and Saboraud's dextrose broth (SDB). CD is a defined medium that is not as abundant in nutrients as SDB, which is an animal tissue lysate. We discovered that EVs were produced in similar number and with consistent morphology in the two media tested but there were significant differences in protein content. We also found that SEC is an inexpensive method for EV isolation, making it easier for laboratories to begin research on fungal EVs.

Statement of significance

We characterized the proteome of Fov EVs recovered from two different growth media. The size-exclusion chromatography isolation protocol adapted in this study allowed an inexpensive and efficient isolation of EVs, which may benefit their study from other filamentous fungi and may be attractive for research groups that do not rely on sophisticated equipment for EV isolation. Furthermore, our results revealed that there is a different enrichment of EV proteins depending on the growth medium used, and those proteins associated with virulence, cell wall modifications, and potential effectors were identified in EV samples. This proteomic description suggests a role for fungal EVs in modulating host-pathogen interactions and expands the knowledge about the function of EVs from plant pathogens.

2 | MATERIALS AND METHODS

2.1 | Culture conditions and processing

Fusarium oxysporum f. sp. *vasinfectum* (Fov, Australian isolate VCG01111 from cotton; gift from Wayne O'Neil, Farming System Institute, DPI, Queensland, Australia) was maintained in half-strength Potato Dextrose Broth (½ PDB) agar plates at 25°C. In liquid culture, Fov was grown in Czapek Dox (CD) (Becton Dickinson) for 72 h at 25°C, and 100 rpm of agitation. Mycelia were removed by filtering with Miracloth (Calbiochem), and the filtrate was centrifuged at 4000 x *g* to pellet the spores. The supernatant was discarded, and the spores were washed three times with Dulbecco's phosphate buffered saline (DPBS, Gibco). An aliquot containing 1.9×10^7 spores/mL was resuspended in 1 mL of 20% glycerol and stored at −80°C.

2.2 | Isolation of vesicles

Fov was grown in 500 mL of CD or Saboraud's Dextrose Broth (SDB) (Becton Dickinson) with 3.8×10^4 spores/mL for 72 h at 25°C, with 100 rpm of agitation. Mycelia were separated from culture supernatants with sterile Miracloth. Fov growth was monitored by measuring the OD_{600} of the culture supernatant in a SpectraMax M2 plate reader (Molecular Devices) and weighing the removed mycelia. Culture supernatants were then passed through 0.45 µm membrane filters (HV type, Millipore) and concentrated approximately 1000 times using centrifugal filter units (30 kDa MWCO, Millipore).

Vesicles were isolated by size-exclusion chromatography (SEC) using an adapted protocol [19]. Briefly, 500 µL of concentrated supernatant were mixed with 5 µL of a 0.1 mg/mL solution of the fluorescent lipophilic dye FM5-95 (Thermo Fisher) to achieve a final concentration of 1.75 µM. The sample was incubated for 15 min at room temperature and protected from light, and then applied to a CellThru plastic column with a 1 cm diameter (Takara) containing 10 mL of Sepharose CL-2B (Sigma-Aldrich), equilibrated with DPBS. New resin was used for every isolation. Samples were eluted with DPBS to collect 300 µL fractions in black microtiter plates (Greiner) protected from light. Fraction fluorescence (Ex. 560 nm, Em. 734 nm) was measured immediately in a SpectraMax M2 plate reader and the protein concentration of each fraction was determined by micro BCA assay (Thermo Fisher). Fractions with fluorescence levels above 3.5 RFU were pooled and named "EV signal". Secretomes, which include secreted soluble proteins and EVs, were prepared by concentrating 50 mL of 0.45 µm-filtered culture supernatants with 3 kDa MWCO centrifugal filter units (Millipore) down to 1 mL. Cell lysates were prepared by grinding mycelia in 1 mL of DPBS with glass beads (710–1180 µm, Sigma) using a TissueLyser (Qiagen), and clarifying by centrifugation at 21,130 x *g* for 5 min at 4°C, retaining the supernatant.

2.3 | Nanoparticle tracking analysis (NTA)

Particle size and concentration of EV signals were measured with a NanoSight NS3000 (Malvern Panalytical). Samples were diluted in DPBS and immediately loaded using 1 mL syringes, with automated injection at an infusion rate of 50. The dilution of the sample was adjusted to achieve a particle count per frame of 30–200. Captures were set to 60 s with three technical replicates each. Capture settings were set to a screen gain of 2, and camera level of 13. Process settings were set to screen gain of 5, and threshold of 3. DPBS was used as blank. Analysis was performed at 25°C. EV signals were analyzed in triplicates using the same settings, with NanoSight software version 3.2. Individual SEC fractions were analyzed in a ZetaView (Particle Metrix). Samples were diluted in DPBS to visualize 50–200 particles per frame, using the scatter mode with an intensity of 80. Eleven technical replicates were used for statistical analyses. All measurements were performed at 25°C.

2.4 | Transmission electron microscopy (TEM)

Samples were prepared as described previously [18]. Briefly, a K950X turbo evaporator coupled to a K350 glow discharge unit (Quorum Technologies) was used to discharge carbon-coated 400-mes copper grids (ProSciTech) for 60 s. EV samples were centrifuged for 5 min at 21,130 x *g* and 4°C prior to preparation. EV samples (5 µL) were placed on the grid and incubated for 5 min at room temperature. Excess sample was absorbed with filter paper before the grid was washed with 5 µL of ultrapure water, and excess water was absorbed with filter paper. Samples were stained with three consecutive washes of 4 µL of 2% uranyl acetate (UA) (Agar Scientific). Excess UA was blotted with filter paper. Grids were dried overnight at room temperature before imaging. Imaging was performed on a Jeol JEM-2100 electron microscope operating at 200 kV.

2.5 | Mass spectrometry (MS)

Sets of three samples (EVs, secretome, cell lysate) were obtained from an individual culture. Three biological replicates were analyzed for CD and SDB respectively. The protein content of EV signals, secretomes and cell lysates was determined using a Qubit4 fluorometer (Thermo Fisher). In total, 18 samples were prepared for LC-MS/MS as described previously [18]. Briefly, 15 µg of protein from the samples were separated by short-range SDS-PAGE. Proteins were fixed to the gel with 50% methanol and 7% acetic acid for 30 min before bands were excised. Proteins were then reduced with 2 mM TCEP (Thermo Fisher) and alkylated with 40 mM iodoacetamide, followed by incubation with 1 µg of sequence-grade trypsin (Promega) for 18 h at 37°C. One µg of peptides per sample was analyzed by mass spectrometry by injection on an Ultimate 3000 RSLnano UPLC instrument (Thermo Fisher) coupled to a Q-Exactive HF Orbitrap mass spectrometer (Thermo Fisher). The peptide search was performed with MaxQuant 1.6.3.3, using the label-free quantitation (LFQ) function and matched against the Fov proteome from Uniprot (UP000030701, downloaded 12th of June 2019). The output MaxQuant protein list was processed in R studio running the R version 3.6.0. The generated protein list was filtered by removing contaminant proteins, proteins with only one matching peptide or those that were present in only one biological replicate, LFQ intensities were quantile-normalized, and missing LFQ intensities were imputed using the "candidaev" package [18] which is based on the DEP package [31]. Proteins with a Benjamini-Hochberg adjusted *p*-value above 0.05 and Log_2-(fold change) (Log_2-FC) above 1 were considered significantly enriched.

2.6 | Gene ontology (GO) and principal component analysis (PCA)

The reference genome of Fov (UP000030701, downloaded 12th of June 2019) was loaded into Blast2GO [32] and proteins were blasted, mapped and annotated according to Blast2GO's default settings. The resulting list was used as the genome reference to perform gene ontology (GO) analyses. Lists of proteins detected in EVs, secretomes and cell lysates were loaded into Blast2GO and the GO analysis was obtained with Fisher's exact test. The "reduced to most specific" function was applied for all GO lists. GO terms with a *p*-value below 0.05 were considered overrepresented.

A principal component analysis (PCA) was performed to visualize the variance between the proteomes of CD and SBD samples. The LFQ intensities of significantly enriched proteins in EVs, secretomes and cell lysates were processed in ClustVis [33] to generate a score plot. Prior to the analysis, the data were not transformed, unit variance was

TABLE 1 Biomass and OD600 monitoring of Fov cultures

Growth medium	OD_{600}	Biomass (mg)
Czapek Dox	0.46 ± 0.06	590 ± 0.11
Saboraud's Dextrose Broth	1.05 ± 0.09	2080 ± 0.08

Fov was grown for 72 h at 25°C in 50 mL of medium. Mycelia were separated with Miracloth, air-dried and weighted. The OD_{600} of supernatants were measured in an SpectraMax M2 plate reader. Values are the average of three replicates and the standard error of the mean.

selected for row scaling, and the PCA method selected was SVD with imputation.

2.7 | Data availability

The mass spectrometry proteomics data have been deposited to the ProteomeXchange Consortium via the PRIDE [34] partner repository with the dataset identifier PXD023907 at https://doi.org/10.6019/PXD023907. These include the RAW files, mzTab file, the MaxQuant search parameters and MaxQuant .txt output file, and the Fov Uniprot reference genome FASTA file. The source code used to perform the differential enrichment was adapted from a previous study [18]. The source code for this study is available at github.com/csdaw/fovev.

3 | RESULTS

3.1 | Size-exclusion chromatography (SEC) allows the isolation of EVs from Fov

EVs were purified from culture supernatants of Fov grown in Czapek Dox (CD) or Saboraud's Dextrose Broth (SDB), using SEC. Fov growth was monitored in 50 mL cultures. After 72 h, the CD and SDB culture supernatants (without mycelia) had an average OD_{600} of 0.46 ± 0.06 and 1.05 ± 0.09, respectively (n = 3). The average net weight biomass of the CD and SDB mycelia were 590 ± 0.11 mg and 2083 ± 0.08 mg, respectively (Table 1, n = 3).

The fluorescence signal used to track the lipid in the EVs typically peaked in fractions 10 to 15. This peak, named "EV signal" was normally above 5 relative fluorescence units (RFU) (n = 6), and the fractions comprising the peak were pooled for downstream analyses (Figure 1A,C). Two negative controls were performed to confirm that this fluorescence signal was not an artifact. For the first control, 500 mL of CD or SDB medium without fungal inoculum were concentrated (30 kDa MWCO) and mixed with FM5-95 before SEC purification. The second control was prepared by inoculating 500 mL of CD or SDB medium with Fov, concentrating the culture supernatant and mixing with 5 µL of DPBS instead of FM5-95, and subjecting it to SEC. These two controls did not produce a fluorescence signal (Figure S1). Soluble protein eluted around fractions 20 to 35, as determined by micro BCA assay (n = 4) (Figure 1A,C). Particles eluted mostly in the fractions that comprise the EV signal (Figure 1B,C).

3.2 | Fov produces similar levels of EVs in different culture media

Nanoparticle tracking analysis (NTA) was used to determine particle size and concentration of the EVs. The EV signals (pooled fractions) from CD and SDB cultures had an average concentration of 7.6 × 10^{10} particles/mL and 6.0 × 10^{10} particles/mL, respectively, with sizes ranging from 100–300 nm and an average diameter of about 120 nm (n = 3 each, Table S1). The differences in particle production between CD and SDB cultures were not statistically significant (*p*-value: 0.8, Table S1). The total protein in the CD and SDB EV signals, calculated with a Qubit4 fluorometer, was 0.093 and 0.0826 µg/µL, respectively (n = 3, each). Using these data, CD EVs had a protein-per-particle ratio of 1.2 × 10^{-12} µg/particle, while the ratio for the SDB EVs was 1.3 × 10^{-12} µg/particle. NTA confirmed that EVs from Fov elute mostly separated from soluble protein (Figure S2). EVs eluted in 1800 µL (six fractions of 300 µL). Adjusted to biomass, CD cultures produced 2.3 × 10^{11} particles/g of biomass, while SDB cultures produced 5.3 × 10^{10} particles/g of biomass. Additional NTA controls (Figure S3) showed that particles in uninoculated media or after the 72 h-incubation are in the 10^{8} particles/mL range, while the particles in the EV signals purified by SEC are around 10^{11} total particles per isolation.

Transmission-electron microscopy revealed sphere and cup-like structures typical of EVs (Figure 2A-D) which were dehydrated as a result of UA treatment [2]. EV-like structures were not identified when imaging fractions 20–35 (Figure 2E,F).

3.3 | Gene ontology reveals differential enrichment of EV proteins based on the growth medium

A comparative proteomic study was performed to determine whether the protein cargo in the Fov EVs changed with growth conditions in vitro.

3.3.1 | Comparison of EV proteome

After validating protein sequences, 465 proteins were detected in CD EV samples. SDB EVs returned 658 sequences. Both EV types shared 311 proteins (Figure 3A). For each protein list, a gene ontology (GO) analysis was performed to better understand protein function. The reported GO terms represent the three classifications: biological process (P), cellular compartment (C) and molecular function (F). Venn diagrams indicating the protein similarity between all the studied samples are included in Figure 3A, II and III.

For the 465 CD EV proteins, 150 GO terms were upregulated compared to Fov's Uniprot genome (UP000030701, downloaded 12th of June 2019). Overrepresented GO terms in CD EVs were related to ATP binding, mitochondria, ribosomes, and others (Figure 3B). Zinc ion binding and component of membrane terms were both underrepresented in CD EV proteins compared to Fov's Uniprot genome. For the

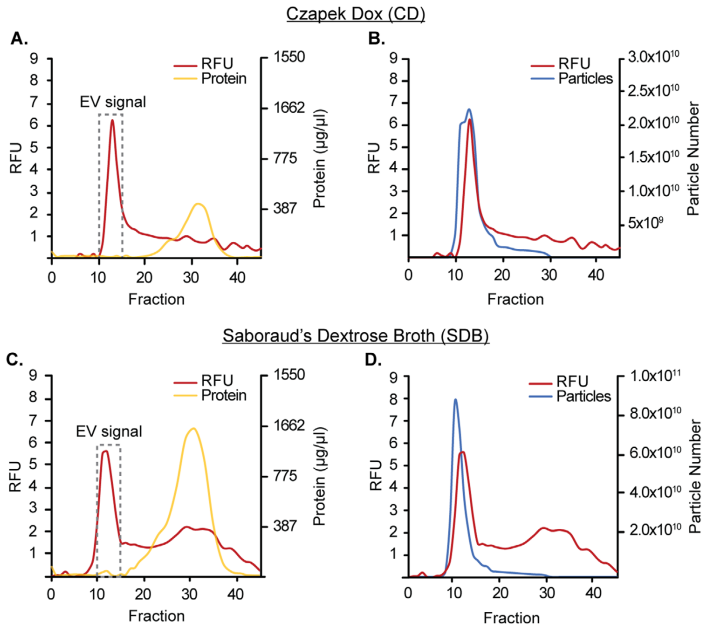

FIGURE 1 Size-exclusion chromatography efficiently separates Fov EVs from soluble protein. EVs from Fov were labelled with FM5-95 and purified by SEC. Fov EVs from both Czapek Dox (CD) and Saboraud's Dextrose Broth (SDB) had fluorescence maxima around six RFU and eluted in fractions 10 to 15 (red series). Soluble protein eluted around fractions 20 to 40 (yellow series) (A and C). CD and SDB EV signals had an average concentration of 7.6×10^{10} particles/mL and 6×10^{10} particles/mL, respectively, (n = 3). Additional NTA controls showed that particles elute mostly on the EV signal (B and D, blue series, n = 1)

658 proteins detected in SDB EVs, 206 GO terms were differentially represented. These were involved with ribosomes, drug binding, O-glycosyl hydrolysis, and others. "Component of membrane" was a GO term underrepresented in proteins from SDB EVs (Figure 3C).

The analysis of the 311 common EV proteins returned 117 significantly different GO terms compared to Fov's Uniprot genome. Proteins with putative functions in ribosomes, peptidases, GTPases and carbohydrate binding proteins were identified in both types of EV samples. These proteins are mainly components of ribosomes, the fungal cell wall and proteasomes (Figure 3D).

3.3.2 | Comparison of the secretome

Comparing all secretome proteins in CD (312) and SDB samples (264) (Figure 4A) revealed that more of the secreted proteins in the CD samples were involved in oxidation-reduction, metabolism of sulfur compounds and amides, and were bound to intracellular organelles (Figure 4B), compared to SDB secreted proteins which were overrepresented in aspartic-type endopeptidase activity, glycerolipid metabolism, and cellulase activity (Figure 4B).

Compared to Fov's Uniprot genome, secretome proteins common to both CD and SDB were overrepresented in cytoplasmic functions, serine and aspartic endopeptidase activities and 1,3-β-glucanosyltransferase activity. In this comparison, Fov's Uniprot genome had a higher number of proteins involved in DNA binding, membrane transport, and membrane components (Figure 4C).

3.3.3 | Comparison of cell lysates

A similar GO analysis was performed for cell lysates proteins as described above for the secretome. The comparison of all CD and SDB cell lysate proteins (Figure 5A) revealed that more CD proteins were involved in cell wall organization, threonine endopeptidase activity and glycolytic processes (Figure 5B), compared to SDB cell lysate proteins. The latter were overrepresented in protein binding, ribonucleotide metabolism, and metabolism of benzene-containing compounds, compared to CD cell lysate proteins (Figure 5B).

Common cell lysate proteins were overrepresented in proteasome and ribosome-related functions, threonine endopeptidase activity, and gluconeogenesis, compared to Fov's Uniprot genome (Figure 5C).

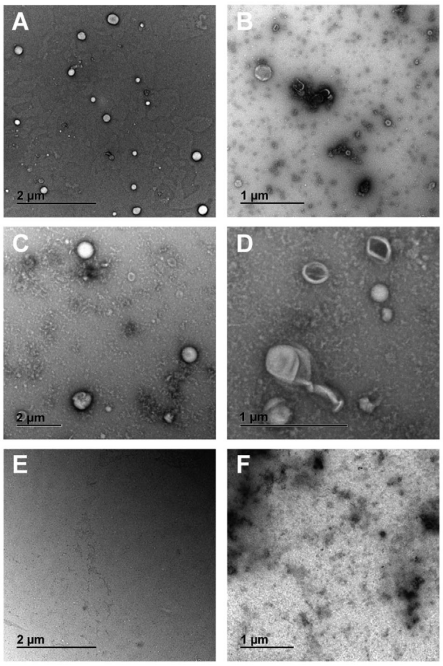

FIGURE 2 TEM characterization of EVs from Fov. TEM images of particles from CD EVs (A and B), SDB EVs (C and D), and pooled fractions 20–35 (E and F)

Principal component analysis (PCA) showed clustering of EV, secretome and cell lysate samples (Figure S4). For CD samples, principal components (PC) 1 and 2 explained 32.3% and 21.1% of the total variance respectively, while PC 2 and 3 explain a total of 37.2%. In SDB samples PC 1 and 2 explain 25.9% and 23.2% of the variance, respectively, while PC 2 and 3 explain a total of 37.6% of the variance.

3.4 | Proteomic analysis suggests a role for Fov EVs in virulence and cell wall remodeling

After filtering protein lists, LFQ data was used to determine significant differences in protein abundance between EVs, secretomes and cell lysates.

3.4.1 | EV proteins from CD cultures

From the 465 proteins detected, 28 proteins were significantly more abundant in CD EVs compared to the CD cell lysate (Table 2). Six proteins have annotated roles in oxidation/reduction, four in cell wall remodeling, and three as proteases. These proteins also included an AltA1 domain-containing protein (X0LMZ6) with 49.5% identity to a small-secreted cysteine-rich protein (SSCRP) from *Fusarium fasciculatum*, serine hydroxymethyltransferase, and a probable fusarubin cluster—esterase. From these 28 proteins, 13 (marked with * in Table 2) were also detected in Fov EVs previously [30].

Proteins detected in CD EVs that did not have significant differences in abundance compared to the CD cell lysate include an isotrichodermin c-15 hydroxylase-like protein, lipases, oxidation/reduction proteins, a LysM domain-containing protein, an SSCRP, a PR1-like protein, perilipin MPL1, a polyketide synthase, an NPP1 domain-containing protein, an AltA1 domain-containing protein, heat shock proteins, proteins similar to allergens Asp f 4 and 7, protein YOP1 and more than 20 proteins involved in cell wall modifications. Some proteins with potential roles in EV biogenesis were Rab GTPases (X0MUK8, X0N260, X0LGB4, X0LGK5), SEC factors (X0LKV6, X0LK74, X0N181), and SNARE proteins (X0MGA8).

3.4.2 | EV proteins from SDB cultures

From the 658 proteins detected, 19 were significantly more abundant in SDB EVs compared to the SDB cell lysate (Table 3). One of the most abundant EV proteins was an WSC domain-containing sequence with 98.9% identity to a protein related to cornifin B from *F. oxysporum*. Another protein (X0MBV9) shared 31.7% identity with IgE-binding allergen rAsp f 9 from *A. fumigatus*. Four proteins have putative roles in oxidation and reduction. Other proteins had roles in metabolism: a serine-rich protein, phosphoenolpyruvate carboxykinase, cystathionine gamma-lyase, and pyrABCN.

SDB EV proteins with no significant differences in abundance compared to the SDB cell lysate include an enniatin synthase-like protein, an allergen Asp f 2-like, NIS1, bikaverin cluster - o-methyltransferase, bikaverin cluster - transcription factor enhancer, bikaverin cluster—efflux pump, four MAP kinases, lipases, SnodProt1, tyrosinase, a concanavalin A-like protein, a SSCRP, GMP synthases, a PR1-like protein, and YOP1. Several proteins involved in cell wall remodeling were also detected. Proteins potentially involved in EV biogenesis included Rab GTPases (X0N260, X0LGB4, X0LGK5), SEC factors (X0LKV6, X0MRC2), and COPI coating-proteins (X0LJ42, X0LQL6, X0M7Y0). The full list is available in Table S2.

3.4.3 | EV proteins common to CD and SDB cultures

Ten significantly overrepresented EV proteins compared to the cell lysates were common between CD and SDB samples (ID highlighted in bold, Tables 2 and 3). The most abundant protein in CD and SDB EVs was a 21 kDa uncharacterized sequence (X0MGX0) without BLAST matches, that has a signal peptide and is not a predicted as effector by the EffectorP 2.0 tool [35]. The remaining proteins were involved in oxidoreduction, cell wall, cellular metabolism, or were uncharacterized.

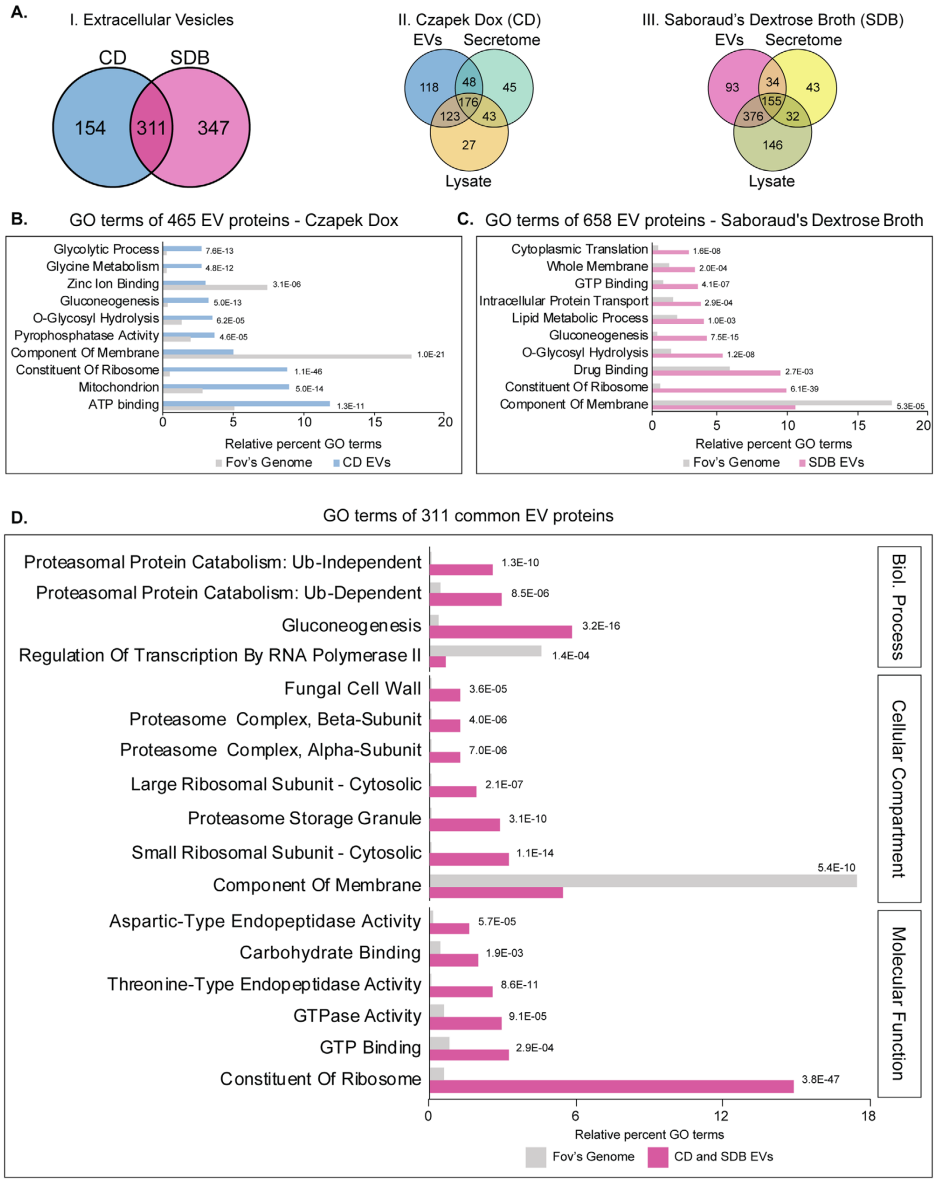

FIGURE 3 EV proteome in Fov changes in response to the growth medium. (A.I) Proteomic analyses detected 465 and 658 proteins in CD and SDB EVs, respectively; 311 were common to both EVs. (A.II and III.) Venn diagrams of proteins identified in CD and SDB samples, respectively. Proteins in Fov EVs were loaded onto Blast2GO to determine which gene ontology (GO) terms were upregulated, using Fisher's Exact Test. (B) More CD EV proteins were involved in O-glycosyl hydrolysis and ATP binding. (C) SDB EV proteins were overrepresented in lipid metabolism and drug binding, compared to Fov's genome. (D) Common EV proteins were overrepresented in protein catabolism, the fungal cell wall, and in carbohydrate binding

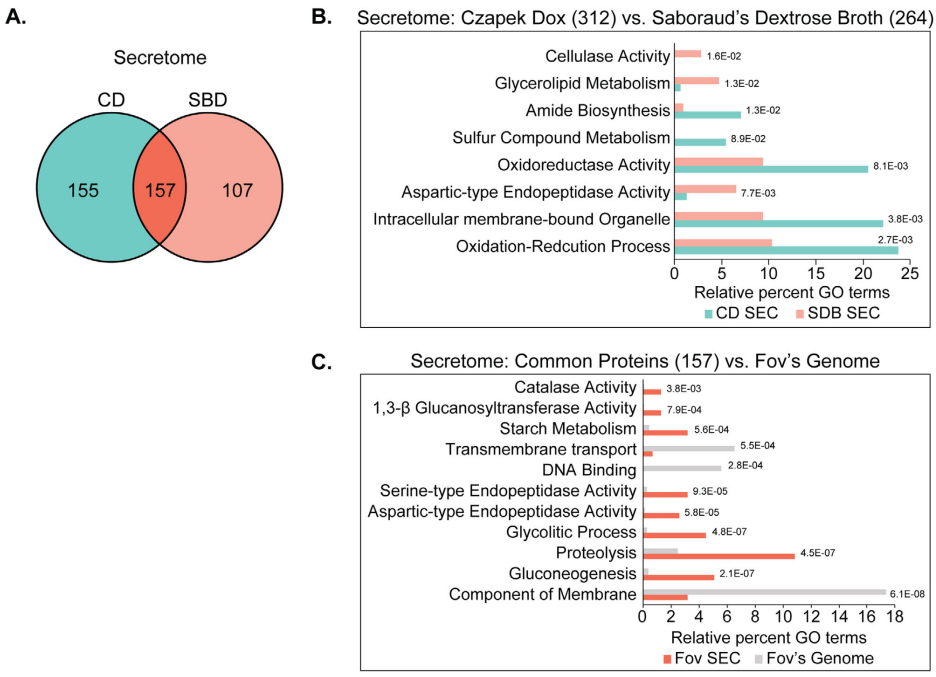

FIGURE 4 Analysis of secreted proteins from Fov cultures. (A) Proteomic analyses detected 312 and 264 proteins in CD and SDB secretomes, respectively; 157 were common to both secretomes. Proteins in Fov secretomes were loaded onto Blast2GO to identify upregulated gene ontology (GO) terms. (B) CD proteins were involved in oxidoreduction and amide biosynthesis; more SDB proteins had endopeptidase and cellulase activity. (C) Compared to Fov's Uniprot genome, the common secretome proteins were overrepresented in gluconeogenesis, proteolysis and endopeptidase activity

3.5 | Fov EVs are enriched with potential protein markers of fungal EVs

A *C. albicans* study has provided a list of 48 potential protein markers for fungal EVs [18]. From these 48 proteins, 16 homologues were detected in CD EVs and 15 in SDB EVs (Table S4). Eleven were common between the two types of Fov EVs. These are YOP1, Ras-like protein Rab-11B, three 1,3-β-glucanosyltransferases, lysophospholipase, a mitochondrial outer membrane porin, one ATPase, and three uncharacterized proteins with similarity to *C. albicans* MSB2, MIR1, and MP65.

3.6 | Fov secretomes contain proteins with various functions and without signal peptides

Proteins with significant differences in abundance compared to EVs are reported next.

3.6.1 | CD secretome

From 312 detected proteins, 30 varied significantly in abundance compared to CD EVs. The most abundant protein in the CD secretome was a probable isonitrile hydratase. This secretome also contained proteins involved in redox homeostasis and metabolism of carbohydrates. Signal peptides were annotated in 13 out of 30 secretome-enriched proteins (Table S3).

3.6.2 | SDB secretome

From 264 detected proteins, 28 showed significant differences in abundance compared to SDB EVs. Probable β-exoglucanase precursors were the most abundant proteins is the SDB secretome. Other proteins detected had functions in cell wall organization, oxidation-reduction, or had activity as hydrolases. Signal peptides were annotated in 23 out of 28 secretome-enriched proteins (Table S3).

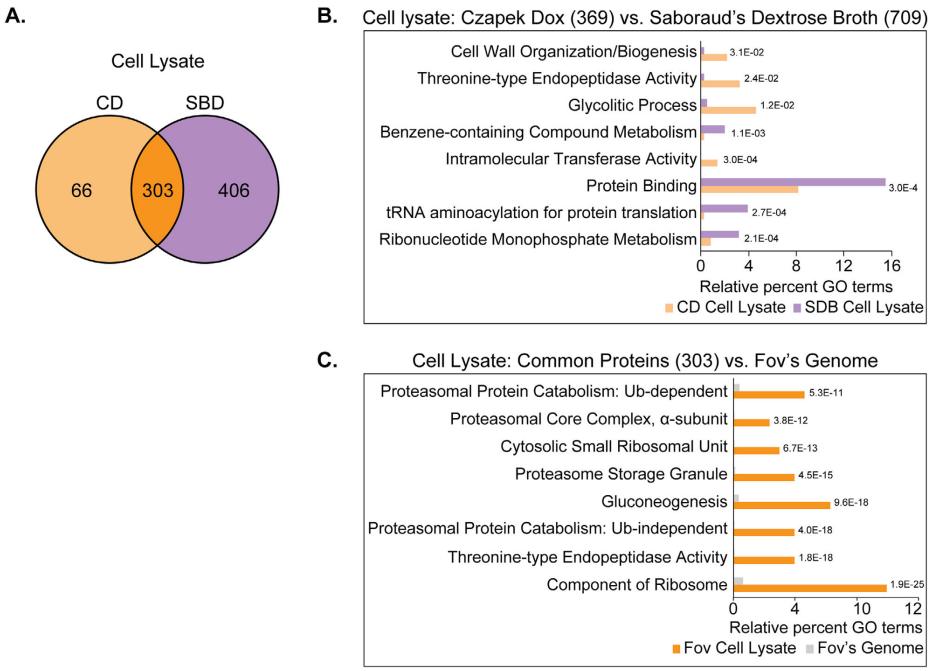

FIGURE 5 Analysis of cell lysate proteins from Fov cultures. (A) Proteomic analyses detected 369 and 709 proteins in CD and SDB cell lysates, respectively; 303 were common to both cell lysates. Proteins detected in Fov cell lysates were loaded onto Blast2GO to determine which gene ontology (GO) terms were upregulated. (B) CD proteins were involved in cell wall organization and in glycolytic processes; more SDB proteins function in ribonucleotide metabolism and protein binding. (C) Compared to Fov's Uniprot genome, the common cell lysate proteins were overrepresented as components of ribosomes and were involved in protein catabolism and gluconeogenesis

4 | DISCUSSION

We report the use of size-exclusion chromatography (SEC) for the isolation of EVs from filamentous fungi. EVs from *Fusarium oxysporum* f. sp. *vasinfectum* (Fov) were characterized morphologically by transmission-electron microscopy (TEM) and nanoparticle-tracking analysis (NTA) and were similar to EVs reported previously for Fov, *S. cerevisiae*, and *C. albicans* [9, 18, 30]. The EVs purified from Fov grown in the two different culture media had similar morphologies and were produced at comparable levels, but the gene ontology (GO) analysis revealed changes in protein cargo. Furthermore, proteins linked to virulence were identified in EV samples, suggesting a role for EVs in host-pathogen interactions.

To improve the isolation of Fov EVs we adopted a SEC-based isolation protocol. This new procedure yielded almost 3 times more EVs per isolation run when the fungus was grown in CD medium (1.4×10^{11} av. particles/isolation, n = 3) and more than double the EVs per liter when cultured in SDB medium (1.1×10^{11} av. particles/isolation; n = 3) compared to the yield of EVs from the UC isolation method on cultures in ½ PDB medium (5.0×10^{10} av. particles/isolation; n = 3) [30]. NTA data from individual biological replicates show that the difference in EV production between SDB or CD media is not statistically significant (*p*-value 0.8). Still, the fluctuation in particle number between the growth media may be influenced by their formulation, since CD is defined and SDB is an animal tissue lysate.

The increase in EV yield allowed the proteomic analysis of independent biological replicates without the need for pooling. Ultimately, a simple and efficient SEC purification of larger culture volumes will facilitate other "omic" analyses of EVs that can be performed on individual fungal cultures, improving the robustness and throughput of fungal EV studies.

Changes in EV yield between UC and SEC might be explained by differences in Fov EV density compared to yeast or mammalian EVs, which could limit their isolation by UC. Other researchers have reported damage, aggregation, and size variation of EVs that have been isolated by UC, as well as changes to EV functionality due to loss of integrity [36]. SEC offers benefits for EV isolation, since it does not require specialized equipment, does not submit EVs to high centrifugal forces, and

TABLE 2 CD EVs transport proteins with roles in virulence and cell wall remodeling

Uniprot ID	Protein name—CD EVs	Log_2FC	Gene ontology
X0MGX0	Uncharacterized protein FMAN_04916	8.89	
X0L0F5; X0L0A0	Related to isoamyl alcohol oxidase	7.18	F: oxidoreductase activity
X0LMZ6*	AltA-1 domain-containing protein	6.61	
X0M896*	WSC domain-containing protein	6.61	
X0MFG7*	Related to oxidoreductase	6.33	F: oxidoreductase activity
X0M2L7	Ser-Thr GPI-anchored family protein	4.98	
X0NMW4*	Carrier protein	4.76	C: integral component of membrane
X0MKD2	Uncharacterized protein FMAN_05603	4.68	
X0MN84	Related to aspartic-type signal peptidase	4.65	F: aspartic-type endopeptidase activity
X0LU36*	Plasma membrane ATPase	4.41	F: proton-exporting ATPase activity,
X0L9W5	Uncharacterized protein FPRN_08004	4.18	F: protein binding
X0MFV4	Outer mitochondrial membrane protein porin	4.13	F: voltage-gated anion channel activity
X0LTM1	WSC domain-containing protein	4.05	
X0MLZ4*	Woronin body major protein	3.81	F: translation elongation factor activity
X0M2C0	Related to extracellular matrix protein precursor	3.56	
X0M696	Uncharacterized protein FFUJ_13328	3.55	
X0MIG3*	Chitinase	3.43	F: chitin binding
X0KPE5*	Fusarubin cluster-esterase	3.14	
X0LPJ1	Related to CRH1-family of glycosidases	3.13	F: hydrolase activity, hydrolyzing O-glycosyl compounds
X0N9D4*	40s ribosomal protein s2	3.11	F: structural constituent of ribosome
X0L1L3	Related to berberine bridge enzyme	3.09	F: oxidoreductase activity
X0M106*	Related to tyrosinase precursor	3.05	F: oxidoreductase activity
X0KR93	Probable subtilisin-like serine protease	2.93	C: cell wall
X0LES6	AB hydrolase-1 domain-containing protein	2.82	
X0LXP8; X0LXC7	Serine hydroxymethyltransferase	2.70	P: glycine biosynthetic process
X0MAR8*	CFEM domain-containing protein	2.25	
X0L1P7*	Probable isoamyl alcohol oxidase	2.14	F: oxidoreductase activity
X0MFP7*	Related to beta-glucan glucosidase	1.96	F: hydrolase activity, hydrolyzing O-glycosyl compounds

The average LFQ intensity of three biological replicates was transformed to Log_2 base (Log_2FC) to compare changes in protein abundance between EVs and the CD cell lysate. $Log_2(FC)$ above 1 shows significant enrichment. Twenty-eight EV proteins were upregulated compared to the cell lysate. Some of these proteins have roles in virulence, cell wall remodeling, and cellular metabolism. For Gene ontology P: biological process, F: molecular function, C: cellular compartment.
ID in bold: protein common to CD and SDB EVs. *Protein also detected by Bleackley et al. [30]

allows direct proteomic analysis [19, 37]. The present isolation protocol produced EVs that are well separated from soluble protein, shown by micro BCA and NTA, and that are morphologically similar to those isolated by UC [30]. Although the fluorescence in the EV signal was consistent in all biological replicates, we cannot rule out the apparent unspecific interaction of FM5-95 with soluble protein around fraction 30.

The number of proteins detected in Fov EVs (465 for CD, 658 for SDB) in this study is higher than the numbers reported for other filamentous fungi like *A. infectoria* (20), *T. reesei* (188), or *A. fumigatus* (60) [26, 28, 38]. This variation can be attributed to the mass spectrometry instruments employed, the databases used to match peptides, the stringency of the statistical analysis of mass spectrometry data, and the EV isolation and sample preparation. In a previous study on Fov EVs isolated by UC 481 proteins were detected [30], which is similar to the 465 reported in the CD EVs in this study. The differences in the protein cargo of the CD and SDB EVs, as well as their function, might be explained by differences in the nutrient content of each growth medium. CD is a defined medium as opposed to SDB, which is a nutrient-rich tissue lysate. Hence, the CD medium may lead to activation of metabolic routes not required in the SDB medium. Prior to EV isolation, the biomass from the SDB cultures was higher than the biomass from the CD cultures (590 mg for CD, 2080 mg for SDB, n = 3), while the OD_{600} was more than twice higher for SDB (0.98, n = 3) than for CD (0.40, n = 3). Although these changes may be explained by differences in nutrient availability across media, it was surprising to find that

TABLE 3 SDB EVs transport proteins with roles in oxidoreduction and cellular metabolism

Uniprot ID	Protein name—SDB EVs	Log_2FC	Gene ontology
X0MGX0	Uncharacterized protein FMAN_04916	6.82	
X0M2L7	Ser-Thr GPI-anchored family protein	5.30	
X0M0D0	Protein pyrABCN	4.95	P: 'de novo' pyrimidine nucleobase biosynthetic process
X0M896*	WSC domain-containing protein	4.68	
X0N5Q5	Serine-rich protein	4.33	P: carbohydrate metabolic process
X0M106*	Related to tyrosinase precursor	4.16	F: oxidoreductase activity
X0MBV9	GH16 domain-containing protein	3.98	F: hydrolase activity, hydrolyzing O-glycosyl compounds
X0L1P7*	Probable isoamyl alcohol oxidase	3.98	F: oxidoreductase activity
X0MFG7*	Related to oxidoreductase	3.90	F: oxidoreductase activity
X0M2C0	Related to extracellular matrix protein precursor	3.86	
X0LTM1	Uncharacterized protein FMAN_16062	3.74	
X0MPK4	Phosphoenolpyruvate carboxykinase	3.28	P: gluconeogenesis
X0M4Y1	Cystathionine gamma-lyase	3.05	P: glycine metabolic process
X0LKV6	SEC14 cytosolic factor	2.85	P: Golgi vesicle transport
X0KPE5*	Fusarubin cluster-esterase	2.64	
X0MJP9; X0NMG2	3-isopropylmalate dehydrogenase	2.63	F: 3-isopropylmalate dehydrogenase activity
X0MAR8*	Cell wall protein	2.61	
X0M4T8	Uncharacterized protein FFUJ_01422	2.42	
X0LL20	Alcohol dehydrogenase 1	1.91	F: oxidoreductase activity

The average LFQ intensity of three biological replicates was transformed to Log_2 base (Log_2FC) to compare changes in protein abundance between EVs and the SDB cell lysate. $Log_2(FC)$ above 1 shows significant enrichment. Nineteen proteins were upregulated compared to the cell lysate. Proteins were involved in oxidation/reduction processes as well as basic metabolism. For Gene ontology P: biological process, F: molecular function, C: cellular compartment.
ID in bold: protein common to CD and SDB EVs. *Protein also detected by Bleackley et al. [30]

EV production was actually lower in SDB (6×10^{10} particles/mL, n = 3) than in CD (7.6×10^{10} particles/mL, n = 3). These data show that EV production in Fov may not necessarily correlate with available biomass or cell density.

The EV proteome from the human fungal pathogen *Histoplasma capsulatum* has also been reported to change with the growth medium [39]. Similarly, proteins [40] and metabolites [41] loaded in EVs from human cells also changed in response to differences in growth media.

This study supports the fact that fungal EVs are not an artifact. The number of exclusive proteins in Fov CD and SDB EVs was 118 and 93 (10%–20% of EV proteome), respectively. If EV samples were composed of cellular debris, the similarity of EVs and cell lysate would have to be greater. In addition, the differences between EVs and secretome/cell lysate were further confirmed by gene ontology and PCA analysis, and by research showing that the production of fungal EVs is an actively controlled process [42] that is involved in host-pathogen interactions [7, 43]. The discovery of putative EV markers in *Candida albicans* [18] supports that EVs may be distinct vesicles and not cellular debris, and while confirmation of these markers is still required, fungal EVs are morphologically similar to EVs from other organisms and isolated with protocols adapted from work on mammalian EVs that are widely accepted and undisputed.

F. oxysporum relies on secretion of cell wall-degrading enzymes, effectors and other virulence factors as part of its infection process [44]. To investigate the involvement of EVs in fungal virulence, we performed a detailed analysis of the EV proteome from Fov.

Proteins detected in both CD and SDB EVs suggest a role for EVs in toxin production. Both types of EVs were enriched with a polyketide synthase (X0LBU9) and a fusarubin cluster—esterase (X0KPE5), which may be involved in the production of pigments [45]. Polyketide synthases have been recognized as important machinery in the production of toxins from fungal pathogens of maize [46], banana [47], tobacco [48] and wheat [49], while the fusarubin cluster—esterase contributes to the production of the toxic pigment fusarubin, and has been detected in other pathogenic Fusarium species [50]. One enniatin synthase (X0KNM9) detected only in SDB EVs is involved in the production of enniatins and beauvericin, which are cyclic mycotoxins. The deleterious effect of these mycotoxins has been reported for Fusarium strains, including *F. oxysporum* and *F. graminearum*, on several crops [41, 51]. The polyketide synthase, Fusarubin cluster—esterase, and enniatin synthase were also reported in Fov EVs by Bleackley and colleagues [30]. One protein exclusive to CD EVs was similar to isotrichodermin c-15 hydroxylase (X0KPU2). In some Fusarium species, this hydrolase is part of the cluster involved in the production

of mycotoxins [52]. Similarly, tyrosinase (X0N0B4, exclusive to SDB EVs) is implicated in synthesis of pigments like melanin, which is known to contribute to virulence of human and fungal plant pathogens [53]. Based on this evidence, it's possible to think that fungal EVs work as "mini-factories" for the production and delivery of toxins, as supported by work with *Aspergillus parasiticus* and its production of aflatoxin [54]. Experimental confirmation of this hypothesis for Fov EVs is still required.

The Fov EV proteome analysis also revealed the presence of a plethora of proteins linked to fungal virulence. In Fov, chitinases and glucanases were abundant in EVs from both growth media, which may work in cell wall alterations that allow EV release, or to modify the cell wall of the host [55]. Oxidoreduction proteins, such as catalase-peroxidase (X0KGJ5), were also present in Fov EVs. These proteins might be transported by EVs to resist oxidative stress from the host and to increase fungal virulence [56,57]. Fov EVs were loaded with various proteases, which are also important for fungal colonization [58]. EV protease types included aspartic (X0MN84) and subtilisin-like (X0KR93). Other assorted proteins suggest a role for EVs in infection, such as the MAP kinase FMK1 from *F. oxysporum*. This kinase has an essential role in root penetration and pathogenicity [59], and a protein with 100% sequence identity was detected in SDB EVs, supporting the transport of proteins involved in pathogenesis. Finally, SDB EVs were enriched with five different sequences of GMP synthase, which is involved in the production of nucleotides and is required for virulence in *C. neoformans* [60], *C. albicans* and *A. fumigatus* [61]. Its presence in EVs may also be linked to virulence in Fov. Proteins that may work as effectors were also detected in Fov EVs. Some of these include small secreted cysteine-rich proteins (SSCRPs), which are effectors with a role in pathogenesis in Fusarium spp. The SSCRP FocCP1 was required for penetration and full virulence of *F. oxysporum* f. sp. *cubense* [62], and SSCRP's may also be involved in virulence of different species of Trichoderma [63]. Further potential effectors detected in Fov EVs were a probable Perilipin MPL1 (X0M659) that in *Metarhizium anisopliae* regulates virulence [64], and NIS1 (X0LCI2) from *Colletotrichum orbiculare* that causes cell death in *Nicotiana benthamiana* [65]. Other proteins in Fov EVs contained sequence domains that have been found in fungal effectors. These domains include LysM [66], NPP1 [67], and AltA-1 [68]. Our results support the recent discovery of potential effectors in EVs from the wheat pathogen *Zymoseptoria tritici* [29]. The presence of effectors with and without signal peptides inside fungal EVs could offer answers to unknown infection mechanisms where fungi rely on unconventional secretion to colonize the host. It is still required to confirm the presence of such effectors in EVs experimentally.

The secretomes from Fov grown in CD and SDB media also showed differences in protein enrichment compared to EVs. The majority of highly produced secreted proteins, common to CD and SDB secretomes, have roles in cell wall modifications. The CD secretome was overrepresented with GO terms of proteins involved in oxidoreduction, while the SDB secretome contained more proteins with functions as endopeptidases. Less proteins were detected in all CD samples except for the secretome. It is possible that the limited nutrient conditions from the CD medium activated stress responses in the cell and hence higher secretion of proteins, as opposed to SDB medium that permitted a higher production of biomass.

Some proteins identified in this study could have potential roles in EV formation such as Rab GTPases, SEC factors, SNARE proteins and COPI-coating proteins, although none of the previously reported proteins involved in EV biogenesis [69] were detected in this study.

One interesting observation was the detection of 59 ribosomal proteins in EV samples. Twelve ribosomal proteins were exclusive to SDB EVs, while none were exclusive to CD EVs. In mammalian systems, free ribosomal proteins occur after stress in the biosynthesis of ribosomes, which can be caused by nutrient starvation [70]. Although other studies have detected ribosomal proteins in mammalian EVs [6, 30, 71], their EV-relevance is virtually unknown, and the topic may pose an exciting new area of EV research.

The investigation of mammalian EVs is facilitated by techniques dependent on protein biomarkers for EVs. These marker proteins are either absent from fungi, as is the case with tetraspanins, or the homologs are not found in EVs as occurs with ESCRT proteins [4]. Proteins common to CD and SDB EVs that were exclusive to EVs or upregulated compared to the cell lysate, and that satisfy the recommendations for EV markers [72] include YOP1 (X0MQ72), 1,3-beta-glucanosyltransferase (X0MJ85), a cornifin B-like protein (X0M896), and a putative secreted lipase without signal peptide (X0KPE5). We have recently identified potential marker proteins for EVs from the human fungal pathogen *C. albicans*. [18], and in order to determine if any of these potential markers could act as pan-fungal markers, we searched for them in the Fov EV protein datasets. Of the 48 potential markers identified in *C. albicans*, 11 were detected in both CD and SDB EVs. One of the main candidates is Sur7 [18], and the presence of this protein was recently confirmed in EVs from *C. neoformans* and *Z. tritici* [29, 73], but its homologue was not detected in Fov EVs. This may be explained by the lack of homology between the *C. albicans* and Fov versions of Sur7, which only share 32% identity. However, these results support our previous discoveries and move the field closer to having broad-use fungal EV markers.

In summary, this study shows that SEC is an efficient, affordable and simple method for the isolation of EVs from filamentous fungi. We have characterized the proteome of EVs from Fov grown in two media and discovered that EV production remains similar but EVs undergo changes in protein cargo. Pathogenesis-related proteins, as well as cell wall remodeling enzymes, were detected in both EV types suggesting that EVs may work as an unconventional secretion mechanism, modulating the immune response from the host.

ACKNOWLEDGMENTS

We thank Dr. Peter Lock from the La Trobe Institute for Molecular Science Bioimaging Platform for transmission electron microscope training. We also thank Dr. Rohan Lowe for his support in the statistical analysis. This project was funded by the Australian Research Council [DP160100309] and [DP200103393]. DGC is funded by La Trobe University LTUPRS and LTUFFRS, and a Consejo Nacional de Ciencia y Tecnologia (CONACYT) Foreign scholarship.

CONFLICT OF INTEREST

The authors declare no conflict of interest.

DATA AVAILABILITY STATEMENT

The mass spectrometry data that support the findings of this study are openly available in the ProteomeXchange Consortium via the PRIDE partner repository with the dataset identifier PXD023907 and 10.6019/PXD023907. The source code for this study is available at github.com/csdaw/fovev.

ORCID

Donovan Garcia-Ceron https://orcid.org/0000-0003-4718-4233

REFERENCES

1. Willms, E., Cabañas, C., Mäger, I., Wood, M. J. A., & Vader, P. (2018). Extracellular vesicle heterogeneity: Subpopulations, isolation techniques, and diverse functions in cancer progression. *Frontiers in Immunology*, *9*, 738.
2. Raposo, G., & Stoorvogel, W. (2013). Extracellular vesicles: Exosomes, microvesicles, and friends. *The Journal of cell biology*, *200*, 373.
3. Bellingham, S. A., Guo, B. B., Coleman, B. M., & Hill, A. F. (2012). Exosomes: Vehicles for the transfer of toxic proteins associated with neurodegenerative diseases? *Frontiers in Physiology*, *3*, 124.
4. Bleackley, M. R., Dawson, C. S., & Anderson, M. A. (2019). Fungal extracellular vesicles with a focus on proteomic analysis. *Proteomics*, *19*, 1800232.
5. Ikeda, M. A. K., de Almeida, J. R. F., Jannuzzi, G. P., Cronemberger-Andrade, A., Torrecilhas, A. C. T., Moretti, N. S., da Cunha, J. P. C., de Almeida, S. R., & Ferreira, K. S. (2018). Extracellular vesicles from *Sporothrix brasiliensis* are an important virulence factor that induce an increase in fungal burden in experimental sporotrichosis. *Frontiers in microbiology*, *9*, 2286.
6. Alves, L. R., Peres da Silva, R., Sanchez, D. A., Zamith-Miranda, D., Rodrigues, M. L., Goldenberg, S., Puccia, R., & Nosanchuk, J. D. (2019). Extracellular vesicle-mediated RNA release in *Histoplasma capsulatum*. *mSphere*, *4*, e00176.
7. Bielska, E., Sisquella, M. A., Aldeieg, M., Birch, C., O'Donoghue, E. J., & May, R. C. (2018). Pathogen-derived extracellular vesicles mediate virulence in the fatal human pathogen *Cryptococcus gattii*. *Nature Communications*, *9*, 1556.
8. Rodrigues, M. L., Nimrichter, L., Oliveira, D. L., Frases, S., Miranda, K., Zaragoza, O., Alvarez, M., Nakouzi, A., Feldmesser, M., & Casadevall, A. (2007). Vesicular polysaccharide export in *Cryptococcus neoformans* is a eukaryotic solution to the problem of fungal trans-cell wall transport. *Eukaryotic cell*, *6*, 48.
9. Zhao, K., Bleackley, M., Chisanga, D., Gangoda, L., Fonseka, P., Liem, M., Kalra, H., Al Saffar, H., Keerthikumar, S., Ang, C.-S., Adda, C. G., Jiang, L., Yap, K., Poon, I. K., Lock, P., Bulone, V., Anderson, M., & Mathivanan, S. (2019). Extracellular vesicles secreted by *Saccharomyces cerevisiae* are involved in cell wall remodelling. *Communications Biology*, *2*, 305.
10. Zarnowski, R., Sanchez, H., Covelli, A. S., Dominguez, E., Jaromin, A., Bernhardt, J., Mitchell, K. F., Heiss, C., Azadi, P., Mitchell, A., & Andes, D. R. (2018*). Candida albicans* biofilm-"induced vesicles confer drug resistance through matrix biogenesis. *PLoS biology*, *16*, e2006872.
11. Dean, R., Van Kan, J. A. L., Pretorius, Z. A., Hammond-Kosak, K. E., Di Pietro, A., Spanu, P. D., Rudd, J. J., Dickman, M., Kahmann, R., Ellis, J., & Foster, G. D. (2012). The top 10 fungal pathogens in molecular plant pathology. *Molecular Plant Pathology*, *13*, 414.
12. DeIulio, G. A., Guo, L., Zhang, Y., Goldberg, J. M., Kistler, H. C., & Ma, L.-J. (2018). Kinome expansion in the *Fusarium oxysporum* species complex driven by accessory chromosomes. *mSphere*, *3*, e00231.
13. Edel-Hermann, V., & Lecomte, C. (2018). Current status of *Fusarium oxysporum* formae speciales and races. *Phytopathology*, *109*, 512.
14. Ragazzi, A. (1992). Different strains of *Fusarium oxysporum* f.sp. *vasinfectum* from cotton in Angola: Biological aspects and pathogenicity. *Journal of Plant Diseases and Protection*, *99*, 499–504.
15. Zhu, Y., Lujan, P. A., Wedegaertner, T., Nichols, R., Abdelraheem, A., Zhang, J. F., & Sanogo, S. (2019). First report of *Fusarium oxysporum* f. sp. *vasinfectum* race 4 causing Fusarium wilt of cotton in New Mexico, U.S.A. *Plant Disease*, *104*, 588.
16. Zhang, H., & Lyden, D. (2019). Asymmetric-flow field-flow fractionation technology for exomere and small extracellular vesicle separation and characterization. *Nature Protocols*, *14*, 1027.
17. Konoshenko, M. Y., Lekchnov, E. A., Vlassov, A. V., & Laktionov, P. P. (2018). Isolation of extracellular vesicles: General methodologies and latest trends. *BioMed Research International*, *2018*, 1.
18. Dawson, C. S., Garcia-Ceron, D., Rajapaksha, H., Faou, P., Bleackley, M. R., & Anderson, M. A. (2020). Protein markers for *Candida albicans* EVs include claudin-like Sur7 family proteins. *Journal of Extracellular Vesicles*, *9*, 1750810.
19. Böing, A. N., van der Pol, E., Grootemaat, A. E., Coumans, F. A. W., Sturk, A., & Nieuwland, R. (2014). Single-step isolation of extracellular vesicles by size-exclusion chromatography. *Journal of Extracellular Vesicles*, *3*, 23430. https://doi.org/10.3402/jev.v3.23430.
20. Monguió-Tortajada, M., Gálvez-Montón, C., Bayes-Genis, A., Roura, S., & Borràs, F. E. (2019). Extracellular vesicle isolation methods: Rising impact of size-exclusion chromatography. *Cellular and Molecular Life Sciences*, *76*, 2369.
21. Brennan, K., Martin, K., FitzGerald, S. P., O'Sullivan, J., Wu, Y., Blanco, A., Richardson, C., & Mc Gee, M. M. (2020). A comparison of methods for the isolation and separation of extracellular vesicles from protein and lipid particles in human serum. *Scientific Reports*, *10*, 1039.
22. Takov, K., Yellon, D. M., & Davidson, S. M. (2019). Comparison of small extracellular vesicles isolated from plasma by ultracentrifugation or size-exclusion chromatography: Yield, purity and functional potential. *Journal of Extracellular Vesicles*, *8*, 1560809.
23. Lozano-Ramos, I., Bancu, I., Oliveira-Tercero, A., Armengol, M. P., Menezes-Neto, A., Del Portillo, H. A., Lauzurica-Valdemoros, R., & Borras, F. E. (2015). Size-exclusion chromatography-based enrichment of extracellular vesicles from urine samples. *Journal of Extracellular Vesicles*, *4*, 27369.
24. Benedikter, B. J., Bouwman, F. G., Vajen, T., Heinzmann, A. C. A., Grauls, G., Mariman, E. C., Wouters, E. F. M., Savelkoul, P. H., Lopez-Iglesias, C., Koenen, R. R., Rohde, G. G. U., & Stassen, F. R. M. (2017). Ultrafiltration combined with size exclusion chromatography efficiently isolates extracellular vesicles from cell culture media for compositional and functional studies. *Scientific Reports*, *7*, 15297.
25. Monguió-Tortajada, M., Roura, S., Gálvez-Montón, C., Pujal, J. M., Aran, G., Sanjurjo, L., Franquesa, M., Sarrias, M. R., Bayes-Genis, A., & Borràs, F. E. (2017). Nanosized UCMSC-derived extracellular vesicles but not conditioned medium exclusively inhibit the inflammatory response of stimulated T cells: Implications for nanomedicine. *Theranostics*, *7*, 270.
26. Souza, J. A. M., Baltazar, L. d. M., Carregal, V. M., Gouveia-Eufrasio, L., de Oliveira, A. G., Dias, W. G., Campos Rocha, M., Rocha de Miranda, K., Malavazi, I.,Santos, D. D. A., Frézard, F. J. G., de Souza, D. d. G., Teixeira, M. M., & Soriani, F. M. (2019). Characterization of Aspergillus fumigatus extracellular vesicles and their effects on macrophages and neutrophils functions. *Frontiers in Microbiology*, *10*, 2008.
27. Brauer, V. S., Pessoni, A. M., Bitencourt, T. A., de Paula, R. G., de Oliveira Rocha, L., Goldman, G. H., & Almeida, F. (2020). Extracellular vesicles from *Aspergillus flavus* induce M1 polarization in vitro. *mSphere*, *5*, e00190.
28. Silva, B. M. A., Prados-Rosales, R., Espadas-Moreno, J., Wolf, J. M., Luque-Garcia, J. L., Gonçalves, T., & Casadevall, A. (2014).

Characterization of *Alternaria infectoria* extracellular vesicles. *Medical mycology*, *52*, 202.
29. Hill, E. H., & Solomon, P. S. (2020). Extracellular vesicles from the apoplastic fungal wheat pathogen *Zymoseptoria tritici*. *Fungal Biology and Biotechnology*, *7*, 13.
30. Bleackley, M., Samuel, M., Garcia-Ceron, D., Mckenna, J., Lowe, R., Pathan, M., Zhao, K., Ang, C., Mathivanan, S., & Anderson, M. (2019). Extracellular vesicles from the cotton pathogen *Fusarium oxysporum* f. sp. *vasinfectum* induce a phytotoxic response in plants. *Frontiers in Plant Science*, *10*, 1610.
31. Zhang, X., Smits, A. H., van Tilburg, G. B. A., Ovaa, H., Huber, W., & Vermeulen, M. (2018). Proteome-wide identification of ubiquitin interactions using UbIA-MS. *Nature Protocols*, *13*, 530.
32. Götz, S., García-Gómez, J. M., Terol, J., Williams, T. D., Nagaraj, S. H., Nueda, M. J., Robles, M., Talón, M., Dopazo, J., & Conesa, A. (2008). High-throughput functional annotation and data mining with the Blast2GO suite. *Nucleic Acids Res*, *36*, 3420.
33. Metsalu, T., & Vilo, J. (2015). ClustVis: A web tool for visualizing clustering of multivariate data using principal component analysis and heatmap. *Nucleic Acids Research*, *43*, W566.
34. Perez-Riverol, Y., Csordas, A., Bai, J., Bernal-Llinares, M., Hewapathirana, S., Kundu, D. J., Inuganti, A., Griss, J., Mayer, G., Eisenacher, M., Pérez, E., Uszkoreit, J., Pfeuffer, J., Sachsenberg, T., Yilmaz, S., Tiwary, S., Cox, J., Audain, E., Walzer, M., … Vizcaíno, J. A.. (2019). The PRIDE database and related tools and resources in 2019: Improving support for quantification data. *Nucleic Acids Res*, *47*, D442.
35. Sperschneider, J., Gardiner, D. M., Dodds, P. N., Tini, F., Covarelli, L., Singh, K. B., Manners, J. M., & Taylor, J. M. (2016). Effector P: Predicting fungal effector proteins from secretomes using machine learning. *The New phytologist*, *210*, 743.
36. Linares, R., Tan, S., Gounou, C., Arraud, N., & Brisson, A. R. (2015). High-speed centrifugation induces aggregation of extracellular vesicles. *Journal of Extracellular Vesicles*, *4*, 29509.
37. Lane, R. E., Korbie, D., Trau, M., & Hill, M. M. (2019). Optimizing size exclusion chromatography for extracellular vesicle enrichment and proteomic analysis from clinically relevant samples. *Proteomics*, *19*, 1800156.
38. de Paula, R. G., Antoniêto, A. C. C., Nogueira, K. M. V., Ribeiro, L. F. C., Rocha, M. C., Malavazi, I., Almeida, F., & Silva, R. N. (2019). Extracellular vesicles carry cellulases in the industrial fungus *Trichoderma reesei*. *Biotechnology for Biofuels*, *12*, 146.
39. Cleare, L. G., Zamith, D., Heyman, H. M., Couvillion, S. P., Nimrichter, L., Rodrigues, M. L., Nakayasu, E. S., & Nosanchuk, J. D. (2020). Media matters! Alterations in the loading and release of *Histoplasma capsulatum* extracellular vesicles in response to different nutritional milieus. *Cellular Microbiology*, *22*, e13217.
40. Rody W. J., Jr., Chamberlain, C. A., Emory-Carter, A. K., McHugh, K. P., Wallet, S. M., Spicer, V., Krokhin, O., & Holliday, L. S. (2019). The proteome of extracellular vesicles released by clastic cells differs based on their substrate. *PLOS ONE*, *14*, e0219602.
41. Stępień, L., & Waśkiewicz, A. (2013). Sequence divergence of the enniatin synthase gene in relation to production of beauvericin and enniatins in Fusarium species. *Toxins*, *5*, 537.
42. Coelho, C., & Casadevall, A. (2019). Answers to naysayers regarding microbial extracellular vesicles. *Biochemical Society Transactions*, *47*, 1005.
43. Baltazar, L. M., Zamith-Miranda, D., Burnet, M. C., Choi, H., Nimrichter, L., Nakayasu, E. S., & Nosanchuk, J. D. (2018). Concentration-dependent protein loading of extracellular vesicles released by *Histoplasma capsulatum* after antibody treatment and its modulatory action upon macrophages. *Scientific Reports*, *8*, 8065.
44. Roncero, M. I., Di Pietro, A., Ruiz-Roldán, M. C., Huertas-González, M. D., Garcia-Maceira, F. I., Méglecz, E., Jiménez, A., Caracuel, Z., Sancho-Zapatero, R., Hera, C., Gómez-Gómez, E., Ruiz-Rubio, M., González-Verdejo, C. I., & Páez, M. J. (2000). Role of cell wall-degrading enzymes in pathogenicity of *Fusarium oxysporum*. *Revista Iberoamericana de Micología*, *17*, S47–S53.
45. Coleman, J. J. (2016). The *Fusarium solani* species complex: Ubiquitous pathogens of agricultural importance. *Molecular Plant Pathology*, *17*, 146.
46. Yang, G., Rose, M. S., Turgeon, B. G., & Yoder, O. C. (1996). A polyketide synthase is required for fungal virulence and production of the polyketide T-toxin. *Plant Cell*, *8*, 2139–2150.
47. Noar, R. D., Thomas, E., Xie, D.-Y., Carter, M. E., Ma, D., & Daub, M. E. (2019). A polyketide synthase gene cluster associated with the sexual reproductive cycle of the banana pathogen, *Pseudocercospora fijiensis*. *PLOS ONE*, *14*, e0220319.
48. Choquer, M., Dekkers, K. L., Chen, H. Q., Cao, L., Ueng, P. P., Daub, M. E., & Chung, K. R. (2005). The CTB1 gene encoding a fungal polyketide synthase is required for cercosporin biosynthesis and fungal virulence of *Cercospora nicotianae*. *Molecular plant-microbe interactions: MPMI*, *18*, 468.
49. Gardiner, D. M., Kazan, K., & Manners, J. M. (2009). Nutrient profiling reveals potent inducers of trichothecene biosynthesis in *Fusarium graminearum*. *Fungal Genetics and Biology*, *46*, 604.
50. Edwards, J., Auer, D., de Alwis, S.-K., Summerell, B., Aoki, T., Proctor, R. H., Busman, M., & O'Donnell, K. (2016). *Fusarium agapanthi* sp. nov., a novel bikaverin and fusarubin-producing leaf and stem spot pathogen of *Agapanthus praecox* (African lily) from Australia and Italy. *Mycologia*, *108*, 981.
51. Nicholson, P., Simpson, D. R., Wilson, A. H., Chandler, E., & Thomsett, M. (2004). Detection and differentiation of trichothecene and enniatin-producing Fusarium species on small-grain cereals. *European Journal of Plant Pathology*, *110*, 503.
52. Alexander, N. J., Hohn, T. M., & McCormick, S. P. (1998). The TRI11 gene of *Fusarium sporotrichioides* encodes a cytochrome P-450 monooxygenase required for C-15 hydroxylation in trichothecene biosynthesis. *Applied and Environmental Microbiology*, *64*, 221.
53. Eisenman, H. C., & Casadevall, A. (2012). Synthesis and assembly of fungal melanin. *Applied Microbiology and Biotechnology*, *93*, 931.
54. Chanda, A., Roze, L. V., Kang, S., Artymovich, K. A., Hicks, G. R., Raikhel, N. V., Calvo, A. M., & Linz, J. E. (2009). A key role for vesicles in fungal secondary metabolism. *Proceedings of the National Academy of Sciences*, *106*, 19533.
55. Rodrigues, M. L., Godinho, R. M. C., Zamith-Miranda, D., & Nimrichter, L. (2015). Traveling into outer space: Unanswered questions about fungal extracellular vesicles. *PLOS Pathogens*, *11*, e1005240.
56. Pongpom, P., Cooper, C. R., Jr, & Vanittanakom, N. (2005). Isolation and characterization of a catalase-peroxidase gene from the pathogenic fungus, *Penicillium marneffei*. *Medical Mycology*, *43*, 403.
57. Trotter, E. W., & Grant, C. M. (2002). Thioredoxins are required for protection against a reductive stress in the yeast *Saccharomyces cerevisiae*. *Molecular microbiology*, *46*, 869.
58. Kennan, R. M., Wong, W., Dhungyel, O. P., Han, X., Wong, D., Parker, D., Rosado, C. J., Law, R. H., McGowan, S., Reeve, S. B., Levina, V., Powers, G. A., Pike, R. N., Bottomley, S. P., Smith, A. I., Marsh, I., Whittington, R. J., Whisstock, J. C., Porter, C. J., & Rood, J. I. (2010). The subtilisin-like protease AprV2 is required for virulence and uses a novel disulphide-tethered exosite to bind substrates. *PLoS Pathogens*, *6*, e1001210.
59. Di Pietro, A., Garcia-MacEira, F. I., Meglecz, E., & Roncero, M. I. (2001). A MAP kinase of the vascular wilt fungus *Fusarium oxysporum* is essential for root penetration and pathogenesis. *Molecular microbiology*, *39*, 1140.
60. Chitty, J. L., Tatzenko, T. L., Williams, S. J., Koh, Y. Q. A. E., Corfield, E. C., Butler, M. S., Robertson, A. A. B., Cooper, M. A., Kappler, U., Kobe, B., & Fraser, J. A. (2017). GMP synthase is required for virulence factor production and infection by *Cryptococcus neoformans*. *Journal of Biological Chemistry*, *292*(7), 3049–3059.
61. Rodriguez-Suarez, R., Xu, D., Veillette, K., Davison, J., Sillaots, S., Kauffman, S., Hu, W., Bowman, J., Martel, N., Trosok, S., Wang, H., Zhang, L.,

Huang, L. Y., Li, Y., Rahkhoodaee, F., Ransom, T., Gauvin, D., Douglas, C., Youngman, P., … Roemer, T. (2007). Mechanism-of-action determination of GMP synthase inhibitors and target validation in *Candida albicans* and *Aspergillus fumigatus*. *Chemistry & Biology*, *14*, 1163–1175.
62. Liu, S., Wu, B., Yang, J., Bi, F., Dong, T., Yang, Q., Hu, C., Xiang, D., Chen, H., Huang, H., Shao, C., Chen, Y., Yi, G., Li, C., & Guo, X. (2019). A ceratoplatanin family protein FocCP1 is essential for the penetration and virulence of *Fusarium oxysporum* f. sp. cubense tropical race 4. *Int J Mol Sci*, *20*, 3785.
63. Xu, Y., Zhang, J., Shao, J., Feng, H., Zhang, R., & Shen, Q. (2020). Extracellular proteins of *Trichoderma guizhouense* elicit an immune response in maize (Zea mays) plants. *Plant and Soil*, *449*, 133.
64. Wang, C., & St. Leger, R. J. (2007). The *Metarhizium anisopliae* perilipin homolog MPL1 regulates lipid metabolism, appressorial turgor pressure, and virulence. *Journal of Biological Chemistry*, *282*, 21110.
65. Yoshino, K., Irieda, H., Sugimoto, F., Yoshioka, H., Okuno, T., & Takano, Y. (2012). Cell death of *Nicotiana benthamiana* is induced by secreted protein NIS1 of *Colletotrichum orbiculare* and is suppressed by a homologue of CgDN3. *Molecular plant-microbe interactions: MPMI*, *25*, 625.
66. Muraosa, Y., Toyotome, T., Yahiro, M., & Kamei, K. (2019). Characterisation of novel-cell-wall LysM-domain proteins LdpA and LdpB from the human pathogenic fungus *Aspergillus fumigatus*. *Scientific Reports*, *9*, 3345.
67. Gijzen, M., & Nürnberger, T. (2006). Nep1-like proteins from plant pathogens: Recruitment and diversification of the NPP1 domain across taxa. *Phytochemistry*, *67*, 1800.
68. Guyon, K., Balagué, C., Roby, D., & Raffaele, S. (2014). Secretome analysis reveals effector candidates associated with broad host range necrotrophy in the fungal plant pathogen *Sclerotinia sclerotiorum*. *BMC Genomics*, *15*, 336.
69. Rizzo, J., Rodrigues, M. L., & Janbon, G. (2020). Extracellular vesicles in fungi: Past, present, and future perspectives. *Frontiers in Cellular and Infection Microbiology*, *10*, 346.
70. Zhou, X., Liao, W. J., Liao, J. M., Liao, P., & Lu, H. (2015). Ribosomal proteins: Functions beyond the ribosome. *Journal of Molecular Cell Biology*, *7*, 92.
71. Dozio, V., & Sanchez, J. C. (2017). Characterisation of extracellular vesicle-subsets derived from brain endothelial cells and analysis of their protein cargo modulation after TNF exposure. *Journal of Extracellular Vesicles*, *6*, 1302705.
72. Théry, C., Witwer, K. W., Aikawa, E., Alcaraz, M. J., Anderson, J. D., Andriantsitohaina, R., Antoniou, A., Arab, T., Archer, F., Atkin-Smith, G. K., Ayre, D. C., Bach, J. M., Bachurski, D., Baharvand, H., Balaj, L., Baldacchino, S., Bauer, N. N., Baxter, A. A., Bebawy, M., … Zuba-Surma, E. K.. (2018). Minimal information for studies of extracellular vesicles 2018 (MISEV2018): A position statement of the International Society for Extracellular Vesicles and update of the MISEV2014 guidelines. *Journal of Extracellular Vesicles*, *7*, 1535750.
73. Rizzo, J., Wong, S. S. W., Gazi, A. D.,Moyrand, F., Chaze, T., Commere, P.-H., Matondo, M., Novault, S., Pehau-Arnaudet, G., Reis, F., Vos, M., Alves, L. R., May, R. C., Nimrichter, L. H., Rodrigues, M. L., Aimanianda, V., & Janbon, G. (2020). New insights into Cryptococcus extracellular vesicles suggest a new structural model and an antifungal vaccine strategy. *bioRxiv*, 2020.08.17.253716.

SUPPORTING INFORMATION

Additional supporting information may be found online https://doi.org/10.1002/pmic.202000240 in the Supporting Information section at the end of the article.

How to cite this article: Garcia-Ceron, D., Dawson, C. S., Faou, P., Bleackley, M. R., & Anderson, M. A., (2021). Size-exclusion chromatography allows the isolation of EVs from the filamentous fungal plant pathogen *Fusarium oxysporum* f. sp. *vasinfectum* (Fov). *Proteomics*, e2000240. https://doi.org/10.1002/pmic.202000240

3. Chapter Three

As mentioned in section 1.2, *Fusarium graminearum* (*Fgr*) is a devastating pathogen of cereal crops, with worldwide presence that threatens food security. Using the new method to purify EVs developed for *F. oxysporum*, this thesis continued with an investigation on the EVs from *Fgr* and their potential role in virulence.

Fgr was grown on Czapek Dox medium for the separation of EVs, but this medium did not allow efficient isolation of EVs due to the blockage of the centrifugal filter units used to concentrate the culture supernatant. Hence, a different culture medium was tested, based on yeast-nitrogen base (YNB), and supplemented with amino acids. These new culture conditions allowed the recovery of EVs from *Fgr* using the size-exclusion chromatography method. The study presented in Section 3.1 presents the proteomic analysis of *Fgr* EVs with a focus on protein effectors, which are important for fungal pathogenesis.

3.1 Extracellular vesicles from *Fusarium graminearum* contain protein effectors expressed during infection of corn

The findings from this study have been published in a peer-reviewed journal, Journal of Fungi, November 2021.

Garcia-Ceron D., Lowe R. G. T., McKenna J. A., Brain L. M., Dawson C. S., Clark B., Berkowitz O., Faou P., Whelan J., Bleackley M. R., Anderson M. A. Extracellular Vesicles from *Fusarium graminearum* Contain Protein Effectors Expressed during Infection of Corn. Journal of Fungi. 2021; 7(11):977. https://doi.org/10.3390/jof7110977

Statement of Contribution

Donovan Garcia-Ceron:

- Designed and completed experiments for fungal culture, EV isolation, proteomics, gene ontology, and protein effector analysis
- Analyzed and interpreted data
- Prepared figures and wrote the manuscript
- Provided revisions during the peer-review of the manuscript

Other authors have made the following contributions:

- Bleackley MR and Anderson MA conceived the project, contributed to the experimental design, and edited the manuscript; Lowe GTR, Clark B, and McKenna JA performed the corn infection experiments; Lowe GTR and Brain LM performed the statistical analysis of the corn transcriptome; Berkowitz O, and Whelan J performed the RNA sequencing; Dawson CS performed part of the statistical analysis; Faou P processed the mass spectrometry samples.

Journal of *Fungi*

MDPI

Article

Extracellular Vesicles from *Fusarium graminearum* Contain Protein Effectors Expressed during Infection of Corn

Donovan Garcia-Ceron [1], Rohan G. T. Lowe [2], James A. McKenna [1], Linda M. Brain [1], Charlotte S. Dawson [1,3], Bethany Clark [4], Oliver Berkowitz [5], Pierre Faou [2], James Whelan [5], Mark R. Bleackley [1] and Marilyn A. Anderson [1,*]

[1] Department of Biochemistry and Genetics, La Trobe Institute for Molecular Science, La Trobe University, Bundoora 3086, Australia; d.garcia-ceron@latrobe.edu.au (D.G.-C.); j.mckenna@latrobe.edu.au (J.A.M.); 18686311@students.latrobe.edu.au (L.M.B.); csd51@cam.ac.uk (C.S.D.); m.bleackley@latrobe.edu.au (M.R.B.)
[2] La Trobe Comprehensive Proteomics Platform, La Trobe Institute for Molecular Science, La Trobe University, Bundoora 3086, Australia; r.lowe@latrobe.edu.au (R.G.T.L.); p.faou@latrobe.edu.au (P.F.)
[3] Cambridge Centre for Proteomics, MRC Toxicology Unit, University of Cambridge, Cambridge CB2 1TN, UK
[4] Centre for Crop and Disease Management, School of Molecular and Life Sciences, Curtin University, Bentley 6102, Australia; bethany.clark@curtin.edu.au
[5] Department of Animal, Plant and Soil Science, La Trobe Institute for Agriculture and Food, La Trobe University, Bundoora 3086, Australia; o.berkowitz@latrobe.edu.au (O.B.); j.whelan@latrobe.edu.au (J.W.)
* Correspondence: m.anderson@latrobe.edu.au

check for updates

Citation: Garcia-Ceron, D.; Lowe, R.G.T.; McKenna, J.A.; Brain, L.M.; Dawson, C.S.; Clark, B.; Berkowitz, O.; Faou, P.; Whelan, J.; Bleackley, M.R.; et al. Extracellular Vesicles from *Fusarium graminearum* Contain Protein Effectors Expressed during Infection of Corn. *J. Fungi* **2021**, *7*, 977. https://doi.org/10.3390/jof7110977

Academic Editors: Nuria Ferrol and Concepción Azcón Aguilar

Received: 13 October 2021
Accepted: 15 November 2021
Published: 17 November 2021

Publisher's Note: MDPI stays neutral with regard to jurisdictional claims in published maps and institutional affiliations.

Abstract: *Fusarium graminearum* (*Fgr*) is a devastating filamentous fungal pathogen that causes diseases in cereals, while producing mycotoxins that are toxic for humans and animals, and render grains unusable. Low efficiency in managing *Fgr* poses a constant need for identifying novel control mechanisms. Evidence that fungal extracellular vesicles (EVs) from pathogenic yeast have a role in human disease led us to question whether this is also true for fungal plant pathogens. We separated EVs from *Fgr* and performed a proteomic analysis to determine if EVs carry proteins with potential roles in pathogenesis. We revealed that protein effectors, which are crucial for fungal virulence, were detected in EV preparations and some of them did not contain predicted secretion signals. Furthermore, a transcriptomic analysis of corn (*Zea mays*) plants infected by *Fgr* revealed that the genes of some of the effectors were highly expressed in vivo, suggesting that the *Fgr* EVs are a mechanism for the unconventional secretion of effectors and virulence factors. Our results expand the knowledge on fungal EVs in plant pathogenesis and cross-kingdom communication, and may contribute to the discovery of new antifungals.

Keywords: EVs; fungal extracellular vesicles; fungi; *Fusarium graminearum*; protein effectors; unconventional secretion; virulence factors

1. Introduction

The filamentous fungus *Fusarium graminearum* (*Fgr*) is a devastating agricultural pathogen that infects cereals such as wheat, barley, and corn, where in the latter causes a disease known as Fusarium stalk rot that is characterized by low grain yield and premature plant death [1]. It also leads to losses in grain quality due to the accumulation of mycotoxins, which are toxic for humans and animals [2,3]. There is low efficiency in managing Fusarium stalk rot, partly because the interaction between *Fgr* and the corn plant is not well understood [1]. For these reasons, it is important to explore the infection process of *Fgr* to identify new targets for disease control.

Extracellular vesicles (EVs) are cell-derived particles delimited by lipid membranes that vary in size from 30 to 1000 nm in diameter. They are produced by cells from all three domains of life [4] and have different biological functions and cargo, composed mostly of protein, nucleic acids, and carbohydrates. EVs have been identified in more than 20 yeasts

and filamentous fungal species, although EVs from human pathogens such as *Candida albicans* [5], and *Cryptococcus neoformans* [6] are the best characterized.

EVs contribute to virulence of fungal pathogens during infection of their hosts [7,8], which led us to the question of whether EVs from filamentous plant pathogens also have an essential role during infection. EVs from the cotton pathogen *Fusarium oxysporum* f. sp. *vasinfectum* caused a hypersensitive response in cotton leaves [9], indicating that EVs do indeed function in fungal–plant interactions, although the molecules involved in these interactions have not been defined.

One key component of plant-fungal interactions is the secretion of protein effectors by the fungus. Fungal effectors suppress the plant immune response and support fungal survival, and while most known effectors are released from cells via the secretion of signals [10], leaderless effectors have been reported [11,12]. The mechanisms of this unconventional secretion have not been defined, but vesicular transport may have a pivotal role [13,14]. Hence, the study of fungal EVs as potential transporters of virulence factors may lead to the discovery of a new class of effectors previously unrecognized by conventional approaches.

In this study we performed a proteome analysis of EVs, secretome, and whole-cell lysate from *Fgr* and used bioinformatic tools to identify molecules in EV samples that may enhance fungal virulence, such as protein effectors. We also analyzed the *Fgr* transcriptome during the infection of corn to determine if EVs may carry proteins with transcripts expressed during infection. In addition, we optimized the growth medium to improve the yield of EVs from *Fgr* cultures.

The *Fgr* EV preparations contained proteins with annotated roles in pathogenesis together with proteins previously reported as effectors, as well as candidate effectors without conventional secretion signals. Some of the effector candidates were enriched compared to the *Fgr* secretome, suggesting that EVs have a role in the unconventional secretion of virulence factors. Furthermore, we discovered that expression of the genes encoding these potential effectors is increased when *Fgr* infects corn plants.

2. Materials and Methods

2.1. Fungal Cultures

Fusarium graminearum (*Fgr*) strain PH-1 was a gift from Dr. Kim Hammond-Kosack (Rothamsted Research, Harpenden, Herts., UK). The culture used for EV collection was prepared by incubating 500 mL of growth medium with 10^4 spores/mL in a 2-L flask. The medium contained yeast–nitrogen base (YNB) with ammonium sulfate, without amino acids and carbohydrates (6.7 g/L, US Biological Life Sciences, Salem, MA, USA), with added -Leu dropout supplement (0.69 g/L, Takara, Kusatsu, Shiga, Japan), L-leucine (0.076 g/L, Sigma, St. Louis, MO, USA), and L-glutamic acid (0.5 g/L, Sigma). The components were dissolved in ultrapure water, filter-sterilized using a 0.22-µm Steritop (Merck, Kenilworth, NJ, USA) and maintained at 4 °C until use. This growth medium was named "YNB+". The cultures were incubated for 5 days at 25 °C with 100 rpm agitation. Mycelia were removed with Miracloth and discarded. The culture fluid was filtered using 0.45-µm membrane filters (HAWP, Merck) and concentrated to about 500 µL using 100-kDa MWCO centrifugal filter units (Merck).

2.2. Separation of Extracellular Vesicles (EVs)

EVs were separated by size-exclusion chromatography (SEC) as described previously [15]. Briefly, the concentrated supernatant was mixed with the fluorescent lipophilic dye FM5-95 (Thermo Fisher, Waltham, MA, USA) at a concentration of 1.75 µM (5 µL, 0.1 mg/mL), on a rotary incubator for 15 m at room temperature with protection from light. The sample was loaded onto a 20 mL plastic column (Takara) containing 10 mL of Sepharose CL 2B (Sigma) equilibrated with Dulbecco's phosphate buffered saline (DPBS, Thermo Fisher). Forty-five fractions (approx. 300 µL each) were eluted with DPBS and collected in black microtiter plates with black bottom (Bunzl, London, UK). The fluorescence of the

fractions was measured immediately in a SpectraMax M2 plate reader (Molecular Devices, San Jose, CA, USA). Adjacent fractions with consistent positive relative fluorescence units (RFU) above the baseline were pooled and named "EV sample". The protein concentration of the EV sample was determined with a Qubit4 (Thermo Fisher). The protein content of the unpooled fractions was quantified by microBCA (Thermo Fisher). All samples were frozen in liquid nitrogen and preserved at −80 °C until further use.

2.3. Heat-Treatment of Fgr Cultures

Two controls were made to confirm that the separated particles were not an artifact. First, *Fgr* was grown as described above for 5 d at 25 °C. The mycelia were separated and rinsed with 20 mL of sterile DPBS, before they were heated to 90 °C for 18 h. An aliquot of the heat-treated mycelia was plated on half-strength potato dextrose broth (½ PDB) agar to confirm complete cell death. The remaining mycelia were returned to fresh YNB+ and incubated for 5 d at 25 °C with shaking. After incubation, the mycelia were removed and discarded. The culture supernatant was 0.45-µm-filtered and analyzed by nanoparticle tracking analysis (NTA) as described below. It was compared to a 0.45-µm filtrate from a culture that had not been heat-treated, and to uncultured YNB+. A second control was prepared by processing an *Fgr* culture for SEC isolation as described before but mixing the concentrated supernatant with 5 µL of DPBS, instead of FM5–95.

2.4. Preparation of Secretomes and Whole-Cell Lysates (WCL)

Secretomes (secreted soluble proteins and unenriched EVs) were obtained by concentrating 50 mL of the 0.45-µm-filtered culture supernatant to 1 mL using 3-kDa MWCO centrifugal units. WCL were prepared by grinding 80 mg of mycelia in 1 mL of DPBS with 70 mg of glass beads (710–1180 µm, Sigma) on a TissueLyser (Qiagen, Venlo, Limburg, Netherlands), with 30 s cycles shaking at a frequency of 30/s, incubating in an ice bath between cycles. The lysate was centrifuged at 21,130× *g* for 5 min at 4 °C and the supernatant retained for further analysis. The protein concentration of the lysate and secretome was determined immediately after collection with a Qubit4. Samples were stored at −80 °C.

2.5. Nanoparticle Tracking Analysis (NTA)

The size and concentration of the particles in the SEC fractions was measured using the scatter mode in a ZetaView instrument (Particle Metrix, software 8.05.12 SP1) with a 405-nm laser, which had been calibrated with a solution of 100-nm beads (Thermo Fisher). The concentration of particles in the samples was adjusted to 30–200 particles per frame, using DPBS in a total volume of 1 mL. Samples were diluted and immediately injected into the instrument's loading chamber. Eleven chamber positions were measured for data acquisition with a camera sensitivity of 80, shutter speed of 100, brightness between 30 and 255, area between 5 and 1000, and minimum trace length of 15. All samples were analyzed at least in duplicate at a temperature of 25 °C.

2.6. Transmission-Electron Microscopy (TEM)

Samples were prepared as described in [16]. Five µl of sample were adjusted to a protein concentration of 1 µg/µL using a Qubit4. Imaging was performed on a Jeol JEM-2100 electron microscope operating at 200 kV. Images were processed with Gatan Digital Micrograph, version 2.32.888.0.

2.7. Mass Spectrometry (MS)

EV samples, secretome, and cell lysates were prepared from the same culture, and the samples from three biological replicates were analyzed by LC-MS/MS, as described previously [16]. One µg of peptides was injected into an Ultimate 3000 RSLnano UPLC instrument (Thermo Fisher) coupled to a Q-Exactive HF Orbitrap mass spectrometer (Thermo Fisher). A peptide search was performed using MaxQuant 1.6.3.3, with the label-free quantitation (LFQ) function and matched against the *Fgr* proteome from Uniprot (UP000070720,

downloaded 09–10–19). The MaxQuant list was processed in R Studio running R 3.6.0 to remove contaminating proteins, proteins with only one matching peptide, or proteins present in only one biological replicate. LFQ intensities were quantile-normalized and missing LFQ values were imputed with the "candidaev" R package [16]. Proteins with a Benjamini–Hochberg-adjusted *p*-value below 0.05 and with a $\log_2$-(fold change) (Log_2-FC) above 1 were considered significantly enriched.

2.8. Computational Prediction of Effector Proteins in EV Samples

Proteins with predicted transmembrane domains as well as housekeeping and ribosomal proteins were removed from this analysis. The remaining sequences (356) were submitted to EffectorP 2.0 [17] to predict effector-like properties, ApoplastP to predict apoplastic location [18]; SignalP-5.0, PrediSi, and Phobius to predict signal peptides (SP) [19–21]; SecretomeP to predict unconventional secretion (mammalian settings) [22]; PredGPI to predict GPI anchoring [23]; and WolfPSORT and Deep Loc-1.0, to predict subcellular location [24,25]. The percentage of cysteine for each protein was calculated manually.

2.9. Gene Ontology (GO) Analysis

The reference genome for *Fgr* in a Uniprot (UP000070720, assembly GCA_900044135.1) was loaded into Blast2GO to annotate proteins with GO terms, using the default settings [26]. The resulting list was used as a reference to perform GO analyses on the EV, secretome and cell lysate proteins, using Fisher's exact test. The "reduce to most specific" function was applied to all analyses.

2.10. Maize Leaf Sheath Infection Assay

Zea mays cultivar PH17AW, provided by Corteva Agriscience, was employed in this assay. *Fgr* was grown on synthetic nutrient-poor agar (KH_2PO_4 0.1% (*w*/*v*), KNO_3 0.1% (*w*/*v*), $MgSO_4 \cdot 7H_2O$ 0.1% (*w*/*v*), glucose 0.02% (*w*/*v*), sucrose 0.02% (*w*/*v*), Bacto agar 1.5% (*w*/*v*)) at 25 °C with a 16:8 h light-dark cycle, under fluorescent lighting (Grolux, Sylvania, Newhaven, Sussex, UK) for about 3 weeks. Macroconidia were filtered through sterile facial tissue to remove hyphae. Corn plants were infected following protocols with modifications [27,28]. Briefly, a 6-mm disc of filter paper (Whatman Grade AA, GE) was soaked in a solution containing 10^6 conidia/mL and placed over a 1-mm × 2-mm wound in the corn leaf sheath. Four 8-week-old plants were grown in a greenhouse for each treatment (12 infected plants in total), with six wounds per sheath, and a total of 40 lesions per plant. Wounds were covered in plastic sealing wrap immediately after infection, and the paper disc and sealing wrap were removed after 3 days. Plants were randomized and each plant was considered a biological replicate. Infected tissue was harvested at 3, 5, and 7 days post-inoculation (d.p.i.). Fresh sheath tissue surrounding the lesion was discarded, and a 6-mm disc, collected from the center of the lesion, was frozen immediately after collection using liquid nitrogen, lyophilized, and stored at −80 °C.

2.11. RNA Extraction from Infected Corn Tissue and Fgr Mycelium

Total RNA was separated from infected corn tissue and from culture-derived mycelia using TRIzol reagent (Thermo Fisher) and treated with Turbo DNA-free DNase (Thermo Fisher). The RNA sample was purified by precipitation and quality was monitored by agarose gel electrophoresis and UV-Vis spectroscopy. The liquid *Fgr* culture for RNA extraction was prepared by inoculating 50 mL of ½ PDB into a 250 mL flask with 5×10^5 conidia/mL, followed by incubation in the dark at 25 °C with 90 rpm of agitation for 48 h. The mycelia were collected by filtration through Miracloth and were washed with ultrapure water before being frozen in liquid nitrogen, lyophilized, and stored at −80 °C. Each 50-mL culture was considered a biological replicate and four biological replicates were prepared. This sample was named "in vitro" for the transcriptome analysis.

2.12. Transcriptome Analysis

Libraries were prepared with an Illumina TruSeq Stranded mRNA kit (San Diego, CA, USA), collecting 75-bp single-ended sequence reads in an Illumina NextSeq sequencer using a NextSeq 500/550 high-output V2 kit. Two runs produced 50 to 70 million reads per biological replicate, with four biological replicates being sequenced per treatment. Data quality was assessed with FastQC (Babraham Bioinformatics, Cambridge, Cambridgeshire, UK) and trimmed with TrimGalore (github.com/FelixKrueger/TrimGalore, version 0.4.1 downloaded on 15 July 2017). Sequence reads were mapped to the *Fgr* PH-1 genome (GCA_000240135.3) using Tophat 2.1.0 [29], and gene expression values were calculated using Cufflinks [29]. The average gene expression per sample was expressed as fragments per kilobase of transcript per million of mapped reads (FPKM), and significant differential gene expression was identified using Cuffdiff [29]. The average transcript expressions of the four biological replicates of all samples (in-vitro, 3, 5, and 7 d.p.i.) were compared and transcripts with an adjusted *p*-value below 0.05 were considered to have significant changes in expression.

3. Results

3.1. Culture Optimization to Improve the Yield of EVs from Fgr

In our initial experiments we grew *Fgr* in ½ PDB broth and attempted to separate EVs using ultracentrifugation (UC) as we described for *Fusarium oxysporum* (*Fov*) [9]. However, the EV yield from *Fgr* was very low and the sample quality was poor. We then grew *Fgr* on Czapek Dox medium and used size-exclusion chromatography (SEC) rather than UC to isolate EVs because this procedure improved the yield and quality of the EVs from *Fov* [15]. However, when *Fgr* was grown in Czapek Dox medium the culture fluid partially obstructed the 100-kDa filters and could not be concentrated to the level required for SEC. Although the separation of EVs from ½ PDB and Czapek Dox was achieved, EVs from *Fgr* had the best quality and yield when using the "YNB+" medium, which uses amino acids rather than sucrose as the carbon source.

The elution of the EVs from the SEC column was monitored by fluorescence from the lipid-bound FM5–95 dye (Figure 1A). Fractions 7–15 were thus pooled and named "EV sample". The fluorescence signal aligned with particle number from the NTA analysis (Figure 1B), which revealed an average particle concentration of 4.3×10^{10} particles/mL of pooled fractions (2.2×10^{11} particles/L of culture), and an average particle size of about 120 nm (n = 2, Figure 1C). Most of the soluble protein eluted after the EV sample, in fractions 17 to 35 (Figure 1A). The heat-treated *Fgr* cultures and sterile YNB+ medium did not significantly increase the particle number of the EV samples (Figure S1).

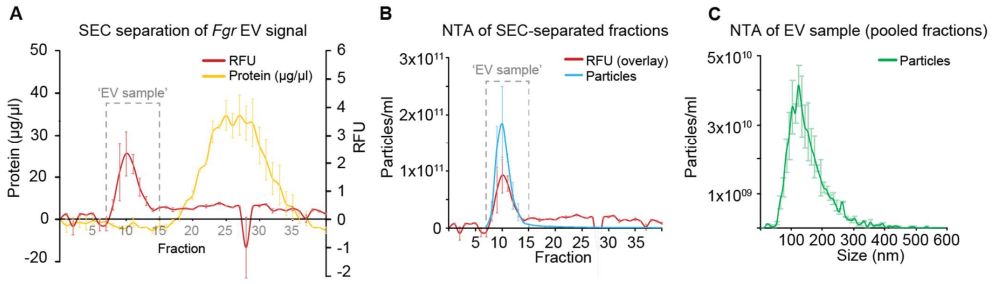

Figure 1. Separation of EVs from *Fusarium graminearum* by size-exclusion chromatography (SEC). (**A**) Particles labeled with the fluorescent dye FM5–95 eluted between fractions 7–15 (red line), while soluble protein eluted between fractions 17 to 35 (yellow line) (n = 2). (**B**) The particle number within each fraction was determined by NTA (blue line, n = 2), and matched the RFU pattern from (**A**). (**C**) The pooled EV sample (fractions 7–15) was analyzed by NTA and had an average of 4.3×10^{10} particles/mL of fraction, corresponding to 2.2×10^{11} particles/L of culture, and an average particle size of about 120 nm (green line, n = 2). Error bars are SEM.

TEM of the EV sample revealed particles partially dehydrated by the uranyl acetate treatment [30], that had the typical cup-like morphology (Figure 2) similar to EVs from other organisms, such as *S. cerevisiae* and *C. albicans* [16–44].

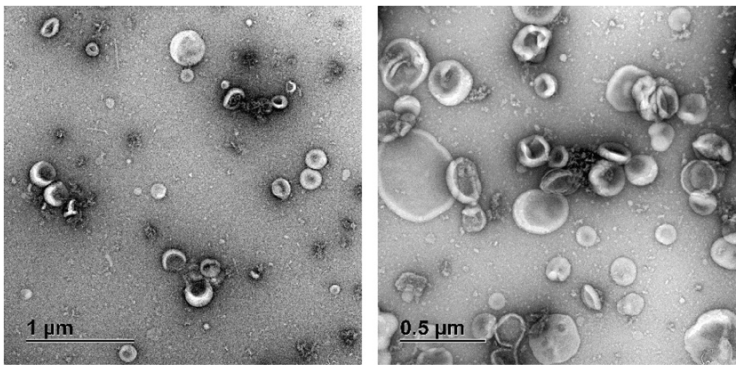

Figure 2. Transmission-electron microscopy (TEM) of EV samples from *Fusarium graminearum*. Five µL of the EV sample were adjusted to 1 µg/µL of protein and were placed on copper grids before treatment with uranyl acetate. TEM revealed spherical structures with apparent sizes ranging from around 50 to 500 nm.

3.2. Fgr EV Samples Contain Putative Fungal EV Protein Markers and Proteins with Potential Roles in Toxin Synthesis, Cell Wall Modifications, and Virulence

The proteomic analysis of the EV samples returned 647 validated proteins (Figure 3A), and 130 of these were enriched in EVs compared to the whole-cell lysate (Table 1, Figure 3B). The five most-abundant proteins in the EV preparations were a subtilisin-like serine protease 6, a polyol transporter, a peptide hydrolase, an AB hydrolase-1 domain-containing protein, and a carboxylic ester hydrolase. From the EV-enriched proteins, 55 were annotated membrane proteins, 28 were involved in transport, 17 were annotated peptidases and nine were involved in carbohydrate hydrolysis. Nine were GTPases and 10 were associated with redox homeostasis. The complete list is available in Table S1.

Table 1. Most abundant proteins detected in *Fusarium graminearum* (*Fgr*) EV samples compared to the whole-cell lysate. LFQ-based proteomics revealed 647 proteins in the *Fgr* EV samples. Proteins with a *p*-value below 0.05 and with a $\log_2$-fold change above 1.0 were considered significantly enriched. The 20 most-abundant proteins are presented. Homologs to uncharacterized proteins were identified with BLAST and the E-value of the best match is reported. Gene ontology (GO) terms were obtained with Blast2GO; P: biological process, C: cellular component, F: molecular function.

Uniprot ID	Protein Name	$\log_2$FC	GO Terms
I1S3S6 [1]	Putative subtilisin-like serine protease (E-value: 0.0)	7.17	C: cell wall
I1RJE2	Polyol transporter 5	5.99	P: transmembrane transport
A0A1C3YMP0 [1]	Peptide hydrolase	5.76	F: aminopeptidase activity
I1RQZ5 [1]	AB hydrolase-1 domain-containing protein	5.39	
A0A098DKT1 [1]	Carboxylic ester hydrolase	5.14	F: hydrolase activity
I1RY25	Niemann–Pick type C-related protein 1 (E-value: 0.0)	5.07	C: integral component of membrane
I1RUM2 [1]	Extracellular protein (E-value: 4.5×10^{-164})	4.96	
A0A1C3YIM6 [1]	Peptidase_M14 domain-containing protein	4.79	F: metallocarboxypeptidase activity
I1S050	Casein kinase I isoform gamma 2	4.70	F: protein serine/threonine kinase
A0A1C3YJM7 [1]	Amine oxidase	4.67	P: oxidation-reduction process
I1S2H9	Magnesium and cobalt transporter	4.49	C: integral component of membrane
I1RP91	Siderophore iron transporter 1	4.31	P: transmembrane transport

Table 1. *Cont.*

Uniprot ID	Protein Name	log_2FC	GO Terms
A0A1C3YNA9 [1]	Putative serine carboxypeptidase	4.30	F: serine-type carboxypeptidase
A0A098DS79 [1]	Gamma-glutamyltransferase (E-value: 0.0)	4.28	F: glutathione hydrolase activity
V6R949	K(+)/H(+) antiporter 1	4.28	F: solute:proton antiporter activity
A0A098E0Z5	H(+)/Cl(−) exchange transporter 5	4.27	F: voltage-gated Cl channel activity
I1RJ42 [1]	Alpha-amylase (E-value: 0.0)	4.26	F: alpha-amylase activity
I1RDK3	Flotillin-like protein 1	4.20	
I1RMG9 [1]	Iron transport multicopper oxidase FET3 precursor	4.11	F: oxidoreductase activity
I1RF73 [1]	Beta-fructofuranosidase (E-value: 0.0)	4.07	P: carbohydrate metabolic process

[1] Protein also detected in the secretome.

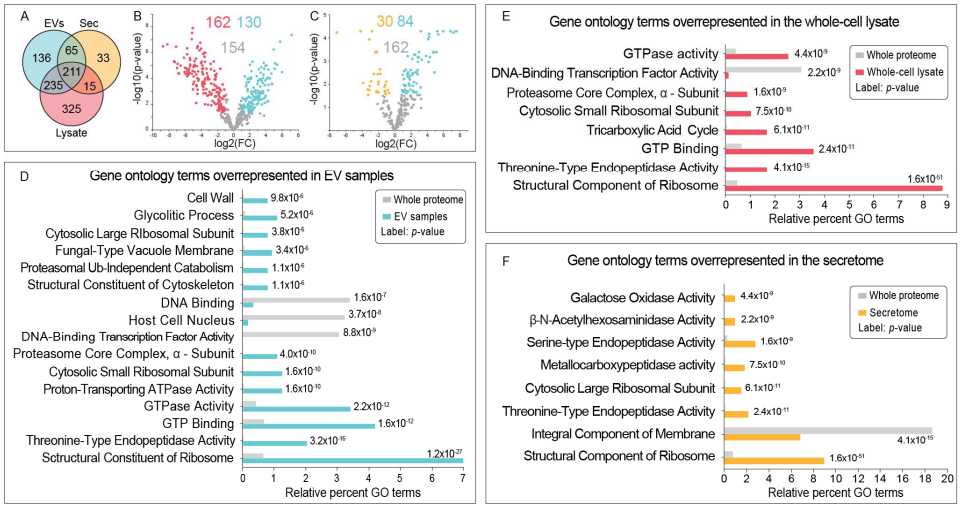

Figure 3. Proteomic analysis revealed potential roles for proteins in the *Fusarium graminearum* (*Fgr*) EV samples. (**A**) Label-free quantitative proteomics detected 647 proteins in the EV samples, 786 in the whole-cell lysate, and 324 in the secretome (Sec). (**B**) Proteins with a *p*-value below 0.05 and a log_2 fold-change above 1.0 were considered significantly enriched; 130 proteins were enriched in the EV samples (blue) compared with the whole-cell lysate (red); (**C**) 84 proteins in the EV samples (blue) were enriched compared with the secretome (yellow). All gene ontology (GO) comparisons were performed against the complete *Fgr* proteome from Uniprot. GO analysis revealed that proteins in the EV samples (**D**) were overrepresented in cell wall functions and GTPase activity. The cell lysate had more proteins with roles in cellular metabolism or ribosome structure/function (**E**), and the secretome proteins were overrepresented with hydrolase activities (**F**).

Gene ontology revealed that GTP-related functions, cell wall and glycolytic processes were overrepresented in the EV proteome, compared to the whole *Fgr* proteome (Figure 3D).

From the 47 putative protein markers reported for *Candida albicans* [16], 16 were detected in *Fgr* EVs. These are similar to *C. albicans* proteins, CDC42, FET34, MTS1, orf19.1054, PHR1, RAC1, RHO3, SEC4, SUR7, VAC8, YCK2, YKT6, PHM7, PMA1, SEC61 and YOP1. Three of these were exclusive to EVs (similar to CDC42, RHO3, and YKT6), and eight were enriched in EVs compared to the whole-cell lysate (similar to FET34, PHR1, RAC1, SUR7, YCK2, PHM7, SEC61, and YOP1).

Compared to the whole-cell lysate, 201 proteins were exclusively detected in EVs (Table 2). Some had annotated roles in toxin synthesis such as zearalenone biosynthesis protein 1-like. Other proteins had roles in cell wall modification, such as chitinase 1-like, endo-1,5-alpha-L-arabinanase B-like, glucanase, and mannosidase, and further proteins had roles in virulence, such as effector NIS1-like, and superoxide dismutase.

Table 2. Proteins in the *Fusarium graminearum* (*Fgr*) EV samples and not in the whole-cell lysate have putative roles in toxin synthesis, carbohydrate metabolism, hydrolysis, and vesicle transport. LFQ-based proteomics revealed 647 proteins present in the *Fgr* EV samples. From these, 201 proteins were exclusive to EVs compared with the cell lysate. Several proteins had annotated roles in metabolite biosynthesis, carbohydrate metabolism, hydrolysis, and vesicle transport. Gene ontology (GO) terms were obtained with Blast2GO; P: biological process, C: cellular component, F: molecular function.

Uniprot ID	Protein Name	GO Terms
	Host-pathogen interactions	
A0A1C3YLT0	Allergen Asp f 9-like	F: hydrolase; P: cell wall organization
I1RF56	Rubrofusarin-specific efflux pump aurT	P: transmembrane transport
I1RFS2	Secreted effector NIS1-like	
I1RGY5	Allergen Asp f 9-like	F: hydrolase; P: cell wall organization
I1RIM4 [1]	Allergen Asp f 34-like	
	Transport	
A0A1C3YHZ2	GTP-binding protein RHO3-like	F: GTPase activity; F: GTP binding
A0A1C3YJH3	Multidrug resistance protein FNX1	P: transmembrane transport
A0A1C3YK53	VPS74	F: phosphatidylinositol-4-phosphate binding
I1RAS9 [1]	VPS10-like	P: protein transport
I1RFK0	GTP-binding protein RHY1	F: GTPase activity; F: GTP binding
I1RG99	VPS35	P: endosome to Golgi transport
I1RN81	CDC42Sp-like	F: GTPase activity; F: GTP binding
I1RQD6	SEC17 homolog	P: vesicle-mediated transport
I1S278	Syntaxin PEP12	P: vesicle-mediated transport
I1SAM5	v-SNARE protein VTI1	P: vesicle-mediated transport
	Hydrolysis	
A0A098DV80 [1]	Podosporapepsin-like	F: aspartic-type endopeptidase activity
A0A0E0RMK7 [1]	N-acetyl-beta-glucosaminidase 1-like	P: carbohydrate metabolic process
A0A1C3YMS8 [1]	Mannanase B	P: carbohydrate metabolic process
I1REC8 [1]	Probable secreted lipase ARB_02369	F: hydrolase activity
I1RF87 [1]	Chitinase 1-like	P: carbohydrate metabolic process
I1RHG0 [1]	Chitinase 1-like	P: carbohydrate metabolic process
I1RHW3	Ribonuclease Trv	F: RNA binding
I1RJF8 [1]	Oryzapsin B-like	F: aspartic-type endopeptidase activity
I1RLG1 [1]	Aspartic proteinase yapsin-6-like	F: aspartic-type endopeptidase activity
I1RMU2 [1]	Laminarinase eglC-like	P: carbohydrate metabolic process
I1RR60 [1]	Subtilisin protease 6-like	C: cell wall
I1RRY4 [1]	Endo-1,3(4)-beta-glucanase-like	P: carbohydrate metabolic process
I1RXM5 [1]	Lipase 4-like	F: hydrolase activity
I1S2W9 [1]	Carboxypeptidase MCPB-like	F: metallocarboxypeptidase activity
I1S3J9 [1]	Secreted lipase ARB07186/07185-like	
I1S3S2 [1]	Endo-1,5-alpha-L-arabinanase B-like	P: xylan catabolic process
V6R5G9	Exo-1,3-beta-glucanase-like	P: carbohydrate metabolic process
V6R5Q6 [1]	Man(9)-alpha-mannosidase 1b-like	F: mannosyl hydrolysis; C: membrane
	Biosynthesis	
A0A098DAH0	Yanuthone D synthesis protein D	
A0A098DV37	Pestheic acid biosynthesis cluster protein K-like	P: oxidation-reduction process
A0A098DVT4	Sesquiterpene synthase BOT2	C: membrane; F: lyase activity
A0A1C3YLJ5	Anditomin synthesis protein L-like	C: integral component of membrane
A0A1C3YLR9	Leucinostatins biosynthesis cluster protein R-like	F: phospholipase D activity
A0A1C3YMY7	Aspirochlorine biosynthesis protein Q-like	
I1R9G1 [1]	Solanapyrone biosynthesis protein 5-like	F: oxidoreductase; F: FAD binding
I1RII9 [1]	Citrinin synthesis protein MPL7-like	F: oxidoreductase activity
I1RS87	Dothistromin biosynthesis protein epoA-like	F: cis-stilbene-oxide hydrolase activity
I1RT88	Pestheic acid biosynthesis cluster protein L-like	F: oxidoreductase activity
I1RUE8 [1]	Zearalenone biosynthesis protein 1-like	F: oxidoreductase; F: FAD binding
I1RXR7 [1]	Terrein biosynthesis cluster protein terF-like	
I1S011	Himeic acid A biosynthesis cluster protein E-like	C: integral component of membrane
I1S1K2	Tropolone synthesis protein G	
I1S6B9 [1]	Prenyl xanthone synthesis protein C-like	F: oxidoreductase activity

[1] Protein also detected in the secretome.

Proteins of interest that were present in EVs but more abundant in the whole-cell lysate also had potential roles in toxin production, such as core trichothecene cluster protein 8, sirodesmin biosynthesis protein J-like, patulin synthesis protein E-like, aflatoxin biosynthesis protein-like, AF-toxin biosynthesis protein 10-1-like, and penitrem biosynthesis cluster protein S-like. This group of EV proteins also included cell wall-modifying enzymes such as class 3 chitin synthase and chitinase 1-like, and proteins with roles in virulence such as allergen Alt A 7-like, effector SnodProt 1-like, and allergen Fusp4.0101-like.

3.3. The Secretome from Fgr Contains Proteins with Potential Roles in Carbohydrate Metabolism, Oxidoreduction and Pathogenesis

Thirty of the 324 proteins detected in the secretome were more abundant in the secretome compared to the EVs (Figure 3C). The five most abundant were a putative endoglucanase, mannitol 2-dehydrogenase, a putative small-secreted cysteine-rich protein (SSCRP), prenyl xanthone synthesis protein C-like, and galactose oxidase. Most of the proteins in the secretomes had annotated roles in metabolism of carbohydrates, hydrolysis, or oxidoreduction (Table S3). The GO analysis revealed that, compared with the complete *Fgr* proteome, more proteins in the secretomes had peptidase functions (Figure 3F). The GO analysis of the whole-cell lysate is also presented (Figure 3E).

3.4. EV Samples from Fgr Contain Candidate Protein Effectors

The detection of proteins with roles in fungal virulence in the EV preparations led us to investigate if EVs also transport protein effectors. A computational analysis of proteins in *Fgr* EV samples (Figure S4) revealed 9 effector candidates that have been reported before [31,32], and three proteins that are similar to the known effectors SnodProt1 [33,34], NIS1 [35], and extracellular lipase [36] (Table 3). Our analysis also revealed hydrophobin 3 (FGSG_09066), a previously unreported effector candidate from *Fgr* (Table 4). All these putative effectors had a predicted signal peptide (SP).

Table 3. Effector candidates detected in the EV samples from *Fusarium graminearum* (*Fgr*) that have been reported previously. The EV proteome from *Fgr* had 12 effector candidates that have been reported previously, although only seven were identified by EffectorP 2.0. All proteins had a predicted signal peptide (Uniprot). The "Enrichment" column indicates the sample in which a protein was most abundant (Sec up: enriched in secretome; EV up: enriched in EV samples; Not sig: no statistical difference). Effectors with characterized function.

Uniprot ID	Protein Name (Gene Symbol)	Length (a.a.)	Enrichment	EffectorP2	Effector Function
I1RFS2	Effector NIS1-like (FGSG_02560)	140	Sec up	non-effector	cell death [35]
I1S341	SnodProt1-like (FGSG_11205)	140	Not sig	unlikely effector	required for virulence [33,34]
I1RPD9	Extracellular lipase (FGSG_05906) [1]	349	EV up	effector	inhibits innate immunity [36]
I1RUM2	Hypothetical protein FGSG_07921	221	Not sig	effector	unknown [32]
I1RIV3	Hypothetical protein FGSG_03748	253	EV up	effector	unknown [32]
I1RIE9	Hypothetical protein FGSG_03581	198	Not sig	effector	unknown [31]
I1REI8	Hypothetical protein FGSG_02077	184	EV up	non-effector	unknown [31]
I1RAQ3	Hypothetical protein FGSG_00588	160	Not sig	unlikely effector	unknown [31]
I1RW93	Hypothetical protein FGSG_08554	207	EV up	non-effector	unknown [31]
I1RK25	AltA1 domain-containing protein FGSG_04213	166	Sec up	effector	unknown [31]
I1S0H8	Hypothetical protein FGSG_10206	162	Not sig	effector	unknown [31]
I1S1J8	Hypothetical protein FGSG_10603	158	Not sig	effector	unknown [31]

[1] Confirmed effector characterized in *F. graminearum* [36].

Table 4. Prediction of new effector candidates in EV samples from *Fusarium graminearum* (*Fgr*). The computational prediction returned sequences with effector potential with and without predicted signal peptide (SP). Uniprot ID and gene symbol are shown in parenthesis. "Enrichment" indicates if the protein was most abundant in EVs, or secretome, or cell lysate. The EffectorP2.0 result was included to monitor the prediction of candidate effectors with unconventional characteristics (size > 300 a.a., Cys < 2%, no SP). The consensus of PrediSi, Uniprot, SignalP 5.0, and Phobius was used to determine the potential presence of signal peptide. SecretomeP 2.0 was used to predict leader-less secretion under the mammalian settings, where a score > 0.5 indicates possible secretion. PredGPI was used to predict GPI anchoring. ApoplastP 1.0, WolfPSORT and DeepLoc 1.0 were used to predict the cellular location of the candidates.

Effector Candidate	Enrichment	Length (a.a.)	Effector P 2.0	Cys %	Signal Peptide [1]	Secretome P 2.0	PredGPI	Apoplast P 1.0	Location Prediction
Hydrophobin 3 (I1RXJ5, FGSG_09066)	EV exclusive	82	effector	9.8	yes	NA	unlikely	yes	extracellular/ mitochondria
Superoxide dismutase [Cu-Zn] (A0A098DGQ1, FGSG_08721)	cell lysate	228	effector	2.2	no	0.706	-	no	cytoplasm/ nucleus
Chitinase (I1RIF9, FGSG_03591)	no difference	417	non effector	0.5	no	0.505	-	yes	cytoplasm
LysM domain-containing protein (I1RIC3, FGSG_03554)	no difference	403	non effector	0.2	no	0.747	-	no	cytoplasm/ nucleus
Glucoamylase (A0A1C3YK33, FGSG_06278)	no difference	667	non effector	1.2	no	0.518	-	yes	extracellular
Glucan endo-1,3-beta-glucosidase eglC-like (I1RMU2, FGSG_05292)	no difference	409	non effector	1.2	no	0.703	-	yes	extracellular/ cell membrane

Five effector candidates without a predicted SP were also identified: superoxide dismutase [Cu-Zn], chitinase, LysM domain-containing protein, glucoamylase, and glucan endo 1,3-beta-glucosidase eglC-like (Table 4). The *Fgr* superoxide dismutase and chitinase sequences were aligned with characterized sequences from other fungi to determine if the catalytic residues were conserved (Figures S2 and S3, respectively). The complete protein list generated in this analysis is presented in Table S2.

3.5. Candidate Protein Effectors Detected in EV Samples Are Expressed In Vivo

We then asked whether any of these potential effectors are produced during an infection. To determine this, corn plants were inoculated with *Fgr* and tissue samples were taken at 3, 5, and 7 d.p.i. for transcriptome analysis (Figure 4A). The infected corn tissue and *Fgr* mycelium, grown in vitro, returned 14,790 transcripts expressed in the infected corn tissue at one or multiple timepoints. For better interpretation, the genes encoding these transcripts were divided into relatively high (Figure 4B), medium (Figure 4C), and low expression (Figure 4D). Superoxide dismutase [Cu-Zn] transcripts were highly expressed with FKPM values around 5000, while transcripts for secreted effector NIS1-like, hydrophobin 3, and SnodProt1-like had medium expression with FKPM values between 3000 and 500. Transcripts of the uncharacterized effector candidates (Table 3) had relatively low expression (Figure 4D). The statistical analysis of gene expression for individual replicates is presented in Tables S4 and S5, respectively.

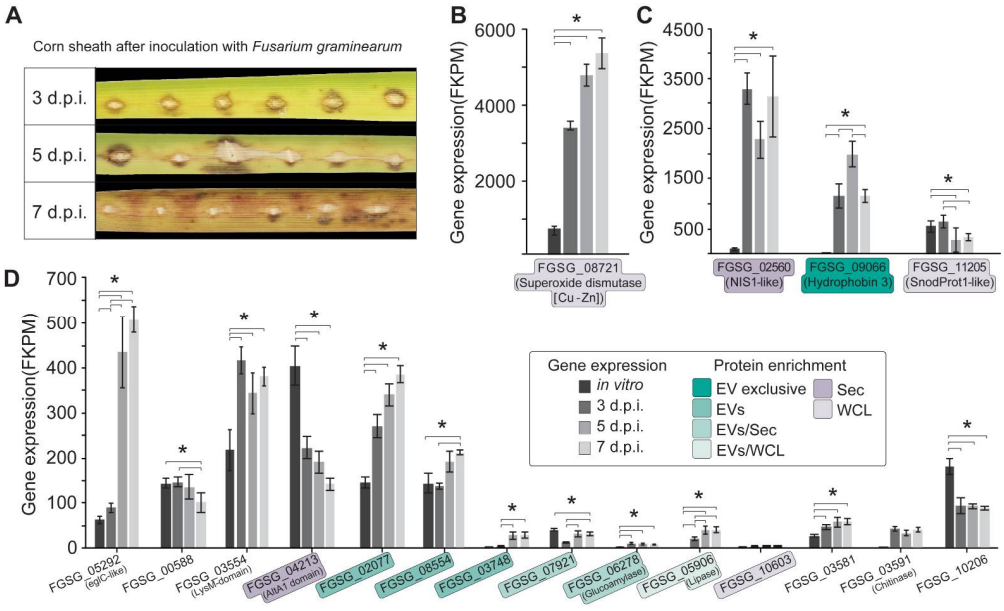

Figure 4. *Fusarium graminearum* (*Fgr*) genes encoding candidate effector proteins detected in extracellular vesicles (EVs) are expressed during corn infection. (**A**) Corn (*Zea mays*) plants were infected with *Fgr* and infected tissue was collected at 3, 5, and 7 days post inoculation (d.p.i.). Mycelia from *Fgr*, grown in vitro, were also collected. Corn tissue and mycelia were analyzed by RNAseq to identify fungal genes expressed during infection and in vitro culture. Gene expression was expressed as fragments per kilobase of transcript per million of mapped reads (FPKM). The gene annotation from the Broad Institute (FGSG_) was employed. Genes from the candidate effectors were significantly expressed in vivo (n = 4). The transcripts were separated by their relative level of gene expression in high (**B**), medium (**C**), and low (**D**). Annotated proteins are labelled, and the rest are hypothetical proteins. (*) significant changes in expression across time points (adjusted *p*-value < 0.05). Error bars are SEM. The protein corresponding to each transcript was retrieved from the EV proteome and its relative abundance is reported in green or purple. Unhighlighted transcripts had no significant differences in protein abundance between EVs, secretome, or cell lysate.

4. Discussion

The discovery that extracellular vesicles (EVs) from yeast pathogens have a role in the progression of fungal diseases in humans [38,39] led us to examine whether EVs also contribute to the virulence of filamentous fungal pathogens of plants. In this study we isolated EVs from *Fusarium graminearum* (*Fgr*) and searched their proteome for potential virulence factors or effectors that are either transported in EVs through unconventional secretion or are stabilized by EVs in the extracellular environment.

A challenge in the study of EVs from filamentous pathogens has been the preparation of sufficient quantities of EVs of a quality suitable for biochemical analysis. This quality varies between fungal species and the growth medium used for culture [15,40]. We discovered that the culture supernatant from *Fgr* grown in Czapek Dox was viscous and could not be concentrated sufficiently for the separation of EVs by size-exclusion chromatography (SEC). This is likely due to the production of extracellular polysaccharides [41]. Furthermore, we discovered that the use of half-strength potato dextrose broth (½ PDB), which is an undefined medium, produced inconsistencies in the growth of *Fgr* as well as low yields of EVs, impeding further biochemical analyses and compromising experimental reproducibility. To address these issues, we grew *Fgr* in YNB+ medium, which contained

amino acids rather than carbohydrates as a carbon source [42]. This solved the viscosity problem and allowed the separation of EVs by SEC.

Fgr EVs have been separated before by ultracentrifugation (UC) [43], requiring pooled EVs from several cultures to obtain sufficient material. The authors reported around 4.1×10^{10} particles/mL per pooled separation, although the total culture volume required was not reported [45] impeding a direct comparison with our procedure. Our initial EV separations using UC also produced low yields of EVs and poor particle quality. By using SEC and the YNB+ medium, we obtained an average of 2.2×10^{11} particles/L of culture (n = 2), with size and morphology consistent with other fungal EVs [9,15,44].

The cargo of EVs from plant pathogens suggests a role for EVs in fungal virulence. For example, *Fusarium oxysporum* EVs contain biosynthetic proteins for secondary metabolites involved in virulence, cell wall-degrading enzymes, and proteases [9,15]. *Fgr* EV samples contained proteins similar to those that produce the toxic secondary metabolites dothistromin, aspirochlorines, solanapyrone, citrinin, and zearalenone [45–49]. The latter is one of the main mycotoxins produced by *Fgr*. The presence of biosynthetic enzymes indicates that EVs may transport phytotoxic secondary metabolites. Additionally, zearalenone, citrinin, and dothistromin have low water solubility [50–52], explaining why vesicular transport may facilitate delivery. Interestingly, *Aspergillus parasiticus* employs vesicles to synthesize and release aflatoxin B1 [53].

The characterization of fungal secretomes followed by the prediction of protein effectors is an effective way to identify components of the plant-pathogen interaction [54]. Of the 647 proteins detected in the *Fgr* EV samples in this study, 18 have potential effector properties. Twelve of these have been reported as candidate effectors before [31–35], and six new effector candidates are proposed in this study.

The 12 previously reported candidate effectors had a predicted signal peptide (SP). Indeed, the bioinformatics programs used to identify them selected proteins with conventional effector features, such as SP, high Cys content, and size < 300 a.a. [10]. From these 12 candidates, NIS1, SnodProt1, and extracellular lipase are well characterized effectors in other fungi [33,35,36], while the rest are uncharacterized [31,32].

Our corn infection data revealed that the transcripts from NIS1-like were among the most abundant and had significant differences in expression between the in vitro and in planta samples, implying a role in virulence. Three other genes produced transcripts that increased in abundance as the infection progressed and thus merit further study to evaluate their potential roles in infection. They were FGSG_05295 (eglC-like endoglucanase) and, interestingly, two genes encoding proteins that are enriched in EVs (FGSG_02077 and FGSG_08544).

A promising new effector candidate for *Fgr* is the 82 amino acid-long hydrophobin 3 (FgHyd3) [55]. This protein was detected only in EV samples, had a predicted SP, Cys content of almost 10%, and is predicted to reside in the plant apoplast. In our corn infection study, expression from the encoding gene was almost 400-fold higher in planta than in vitro, suggesting a role in pathogenesis. FgHyd3 is also expressed during the infection of barley by *Fgr* [55]. Germlings from *Fgr* mutants lacking FgHyd3 bind poorly to hydrophobic surfaces, such as plant leaves, and are not as infectious [55]. Other fungal hydrophobins have effector activity [56,57], hence it is possible that FgHyd3 also has effector activity, but this needs to be confirmed experimentally. The observation that FgHyd3 was exclusive to the EV samples suggests that EVs function as an unconventional secretion mechanism for some classes of protein effectors, that EVs could transport FgHyd3 to other areas of the plant, or that EVs shield it from early recognition by the plant's defenses. Since most of the EV proteomes published to date contain numerous proteins with SP [9,58], we hypothesize that EVs might physically encounter and bind secreted proteins and transport them through the cell wall. Secreted hydrophobic proteins, such as the hydrophobins, may interact with the membrane of EVs and hence be more mobile in the extracellular environment.

The second new effector candidate for *Fgr* is a superoxide dismutase [Cu-Zn] previously named SOD1 (FGSG_08721) [59]. The *Fgr* SOD1 does not have a predicted SP, was

enriched in the whole-cell lysate, has 2.2% Cys content and had high expression in our corn infection assay. This supports Yao's and colleagues observations that SOD1 is highly expressed in *Fgr*-infected wheat coleoptiles, and although they reported it as a cytosolic protein [59], SOD1 from other organisms has been detected extracellularly [60,61]. It is unclear if this occurs exclusively via EVs [60,62]. However, SOD1 secretion has been attributed to EVs [63] and has been detected in the EV proteome from numerous fungi [15,16,44,64–66]. SOD1 from *Fgr* and in homologs from *B. cinerea*, *M. oryzae*, *Fusarium* spp., *Verticillium* spp., and the human SOD1 contain a diacidic Asp-Glu motif implicated in unconventional secretion [64]. Hence, we believe that SOD1 may be secreted unconventionally via EVs in *Fgr*, although experimental confirmation is still required.

The remaining group of proposed effectors are carbohydrate-active enzymes (CAZy). One chitinase (FGSG_03591) has similarity to chitinases from other fungal pathogens [67,68]. This *Fgr* chitinase does not have a predicted SP although it is annotated as secreted (Uniprot), has >300 a.a., and has a low Cys content. The gene encoding this chitinase was expressed at relatively low levels during our corn infection assay, and did not change as the infection progressed, indicating that its involvement in virulence may differ from other chitinases that are highly expressed in vivo [69].

Another candidate effector was an eglC-like endoglucanase (FGSG_05292), which in *A. niger* is involved in the degradation of plant cell walls [70]. The role of the eglC-like has not been elucidated in *Fgr*, although our infected corn transcriptome data revealed almost a five-fold increase in gene expression between 3 and 5 d.p.i. Such increase is a characteristic of some effectors [71].

One further effector candidate is a LysM domain-containing protein (FGSG_03554). LysM proteins interact with chitin and support fungal survival [72]. The last candidate effector is a glucoamylase (FGSG_06278) with 57% identity to BcGs1 from *B. cinerea*. BcGs1 causes necrosis, accumulation of ROS, and cell death in different hosts [73]. The *Fgr* glucoamylase and BcGs1 have no predicted SP although they are potentially secreted (WolfPSORT, DeepLoc 1.0), suggesting that they are unconventionally secreted. The transcript expression of this protein during corn infection was low compared with other effector candidates, hence it is possible that the abundance of this glucoamylase does not need to be as high as other candidate effectors, since the expression of fungal effector genes is known to be differentially regulated [74,75].

The variety of CAZy enzymes detected in EV samples from *Fgr* suggests roles on host pathogenesis and EV release. For instance, the endo-1,5-alpha-L-arabinanase B-like is a virulence factor in *B. cinerea* during infection of Arabidopsis [76], and a similar arabinanase B was detected in *Fgr* EV samples (FGSG_11468). The substrate for this arabinanase is yet to be defined. Conversely, the presence of chitinase and glucanase in EV preparations suggests that these enzymes loosen the fungal cell wall and facilitate EV release [77].

The leaderless candidate effectors identified in this study and the ones reported previously [11,12] have characteristics that would prevent their identification by bioinformatic tools, such as lack of SP or low Cys content. This is not a limitation of these tools, but rather an unintended bias towards proteins that fit conventional effector criteria. Our results support evidence that a different class of protein effectors exists that are transported via unconventional secretion mechanisms [78,79], and in the case of *Fgr* this is likely to occur via EVs. The purification of these candidate effectors, their inplanta study, and the generation of knockout fungal strains can confirm this notion.

Yang and colleagues identified 154 secretome proteins from *Fgr* that have potential roles in the pathogenesis of wheat and barley [80]. We detected 21 of these proteins in our secretome data, with the majority having annotated functions as glycosidases, proteases, and esterases.

EVs from *Fgr* contained some of putative EV protein markers that have been reported for *C. albicans*. Among these, the eisosomal SUR7 has similarity to the mammalian tetraspanins, making it one ideal candidate to be a true fungal EV marker [16]. SUR7 has been detected in EVs from *Zymoseptoria tritici* [81], *S. cerevisiae* [46] and *A. fumigatus* [64].

Similarly, *C. neoformans* EVs contain proteins with SUR7 domains [6] suggesting that SUR7 is a conserved protein marker of fungal EVs.

In summary, we demonstrate that the filamentous fungal pathogen *Fusarium graminearum* produces extracellular vesicles, and their cargo includes proteins associated with virulence that are expressed during the infection of corn. Evidence from other fungal EV studies [5,7,9] suggests that EVs from *Fgr* could support the infection of corn, although future efforts must be directed at determining the specific role of these EVs.

These results contribute to the elucidation of the mechanism of action of EVs from plant pathogens, which is mostly unknown, and indicate that EVs are a mechanism for unconventional secretion that could protect and transport secreted proteins with conventional secretion signals. Our study has revealed effector candidates that might be involved in pathogenesis and are of interest for future research.

Supplementary Materials: The following are available online at https://www.mdpi.com/article/10.3390/jof7110977/s1, Figure S1. Controls for the separation of EVs from *Fusarium graminearum* (*Fgr*) by SEC. Figure S2. The superoxide dismutase [Cu-Zn] (SOD1) from F. *graminearum* (*Fgr*) contains a diacidic amino acid motif implicated in unconventional secretion. Figure S3. Sequence alignment of the chitinase GH18 domain. Figure S4. Computational prediction of effector candidates detected in EV samples from *Fusarium graminearum* (*Fgr*). Table S1. List of proteins detected in EVs from *Fusarium graminearum* (*Fgr*). Table S2. List of proteins employed in the computational effector prediction analysis. Table S3. Proteins identified in the secretome from *Fusarium graminearum* (*Fgr*). Table S4. List of transcripts identified in corn (*Zea mays*) infected by *Fusarium graminearum* (*Fgr*). Table S5. Gene expression values per biological replicate.

Author Contributions: D.G.-C. designed the experiments, collected the data, and wrote the manuscript. R.G.T.L. performed the corn infection experiments and transcriptome analysis. J.A.M. and B.C. performed the corn infection experiments and collected data. C.S.D. performed the statistical analysis of mass spectrometry data. L.M.B. performed the analysis of the transcriptome data. O.B. and J.W. performed the RNA sequencing. P.F. processed the mass spectrometry samples. M.A.A. and M.R.B. conceived the project, designed the experiments, and edited the manuscript. All authors read the manuscript and accepted co-authorship. All authors have read and agreed to the published version of the manuscript.

Funding: This research was funded by the Australian Research Council under grant DP160100309 and DP200103393. D.G.-C. is funded by La Trobe University LTUPRS and LTUFFRS, and a Consejo Nacional de Ciencia y Tecnologia (CONACYT) Foreign Scholarship.

Institutional Review Board Statement: Not applicable.

Informed Consent Statement: Not applicable.

Data Availability Statement: Proteomics data have been deposited on the ProteomeXchange consortium via the PRIDE repositorium [38] (ID: PXD028657). The archives include RAW files, MaxQuant search parameters and .txt output file, and the *Fgr* reference genome FASTA file. The source code used in this study was adapted from a previous study [17] and is available at github.com/csdawson/*Fgr*ev. The transcriptomics data have been deposited on the sequence read archive database under identifier PRJNA529541.

Acknowledgments: We would like to thank Peter Solomon for his crucial advice on fungal growth in vitro. We thank the La Trobe Bioimaging platform, the La Trobe Comprehensive Proteomics Platform, and the La Trobe Genomics Platform for access to research infrastructure and expertise.

Conflicts of Interest: The authors declare no conflict of interest.

References

1. Oghenekaro, A.; Oviedo-Ludena, M.; Serajazari, M.; Wang, X.; Henriquez, M.; Wenner, N.; Kuldau, G.; Navabi, A.; Kutcher, H.; Fernando, W. Population Genetic Structure and Chemotype Diversity of *Fusarium graminearum* Populations from Wheat in Canada and North Eastern United States. *Toxins* **2021**, *13*, 180. [CrossRef]
2. Chen, Y.; Kistler, H.C.; Ma, Z. *Fusarium graminearum* Trichothecene Mycotoxins: Biosynthesis, Regulation, and Management. *Annu. Rev. Phytopathol.* **2019**, *57*, 15–39. [CrossRef]

3. Munkvold, G.P.; Proctor, R.H.; Moretti, A. Mycotoxin Production in Fusarium According to Contemporary Species Concepts. *Annu. Rev. Phytopathol.* **2021**, *59*, 373–402. [CrossRef]
4. de Castilla, P.E.M.; Tong, L.; Huang, C.; Sofias, A.M.; Pastorin, G.; Chen, X.; Storm, G.; Schiffelers, R.M.; Wang, J.-W. Extracellular vesicles as a drug delivery system: A systematic review of preclinical studies. *Adv. Drug Deliv. Rev.* **2021**, *175*, 113801. [CrossRef] [PubMed]
5. Vargas, G.; Honorato, L.; Guimarães, A.J.; Rodrigues, M.L.; Reis, F.C.G.; Vale, A.M.; Ray, A.; Nosanchuk, J.D.; Nimrichter, L. Protective effect of fungal extracellular vesicles against murine candidiasis. *Cell. Microbiol.* **2020**, *22*, e13238. [CrossRef] [PubMed]
6. Rizzo, J.; Wong, S.S.W.; Gazi, A.D.; Moyrand, F.; Chaze, T.; Commere, P.; Novault, S.; Matondo, M.; Péhau-Arnaudet, G.; Reis, F.C.G.; et al. *Cryptococcus extracellular* vesicles properties and their use as vaccine platforms. *J. Extracell. Vesicles* **2021**, *10*, e12129. [CrossRef] [PubMed]
7. Bielska, E.; Sisquella, M.A.; Aldeieg, M.; Birch, C.; O'Donoghue, E.J.; May, R.C. Pathogen-derived extracellular vesicles mediate virulence in the fatal human pathogen *Cryptococcus gattii*. *Nat. Commun.* **2018**, *9*, 1556. [CrossRef]
8. Brauer, V.S.; Pessoni, A.M.; Bitencourt, T.A.; de Paula, R.G.; Rocha, L.D.O.; Goldman, G.H.; Almeida, F. Extracellular Vesicles from *Aspergillus flavus* Induce M1 Polarization In Vitro. *mSphere* **2020**, *5*, 00190-20. [CrossRef]
9. Bleackley, M.R.; Samuel, M.; Garcia-Ceron, D.; McKenna, J.A.; Lowe, R.; Pathan, M.; Zhao, K.; Ang, C.-S.; Mathivanan, S.; Anderson, M.A. Extracellular Vesicles from the Cotton Pathogen *Fusarium oxysporum* f. sp. *vasinfectum* Induce a Phytotoxic Response in Plants. *Front. Plant Sci.* **2020**, *10*, 1610. [CrossRef]
10. Lo Presti, L.; Lanver, D.; Schweizer, G.; Tanaka, S.; Liang, L.; Tollot, M.; Zuccaro, A.; Reissmann, S.; Kahmann, R. Fungal Effectors and Plant Susceptibility. *Annu. Rev. Plant Biol.* **2015**, *66*, 513–545. [CrossRef]
11. Liu, T.; Song, T.; Zhang, X.; Yuan, H.; Su, L.; Li, W.; Xu, J.; Liu, S.; Chen, L.; Chen, T.; et al. Unconventionally secreted effectors of two filamentous pathogens target plant salicylate biosynthesis. *Nat. Commun.* **2014**, *5*, 4686. [CrossRef] [PubMed]
12. Ridout, C.; Skamnioti, P.; Porritt, O.; Sacristan, S.; Jones, J.; Brown, J.K. Multiple Avirulence Paralogues in Cereal Powdery Mildew Fungi May Contribute to Parasite Fitness and Defeat of Plant Resistance. *Plant Cell* **2006**, *18*, 2402–2414. [CrossRef]
13. Micali, C.O.; Neumann, U.; Grunewald, D.; Panstruga, R.; O'Connell, R. Biogenesis of a specialized plant-fungal interface during host cell internalization of *Golovinomyces orontii* haustoria. *Cell. Microbiol.* **2010**, *13*, 210–226. [CrossRef] [PubMed]
14. Reindl, M.; Hänsch, S.; Weidtkamp-Peters, S.; Schipper, K. A Potential Lock-Type Mechanism for Unconventional Secretion in Fungi. *Int. J. Mol. Sci.* **2019**, *20*, 460. [CrossRef]
15. Garcia-Ceron, D.; Dawson, C.S.; Faou, P.; Bleackley, M.R.; Anderson, M.A. Size-exclusion chromatography allows the isolation of EVs from the filamentous fungal plant pathogen *Fusarium oxysporum* f. sp. vasinfectum (Fov). *Proteomics* **2021**, *21*, 2000240. [CrossRef] [PubMed]
16. Dawson, C.S.; Garcia-Ceron, D.; Rajapaksha, H.; Faou, P.; Bleackley, M.R.; Anderson, M.A. Protein markers for *Candida albicans* EVs include claudin-like Sur7 family proteins. *J. Extracell. Vesicles* **2020**, *9*, 1750810. [CrossRef]
17. Sperschneider, J.; Dodds, P.N.; Gardiner, D.M.; Singh, K.B.; Taylor, J.M. Improved prediction of fungal effector proteins from secretomes with EffectorP 2.0. *Mol. Plant Pathol.* **2018**, *19*, 2094–2110. [CrossRef]
18. Sperschneider, J.; Dodds, P.N.; Singh, K.B.; Taylor, J.M. ApoplastP: Prediction of effectors and plant proteins in the apoplast using machine learning. *New Phytol.* **2018**, *217*, 1764–1778. [CrossRef] [PubMed]
19. Hiller, K.; Grote, A.; Scheer, M.; Münch, R.; Jahn, D. PrediSi: Prediction of signal peptides and their cleavage positions. *Nucleic Acids Res.* **2004**, *32*, W375–W379. [CrossRef]
20. Armenteros, J.J.A.; Tsirigos, K.D.; Sønderby, C.K.; Petersen, T.N.; Winther, O.; Brunak, S.; Von Heijne, G.; Nielsen, H. SignalP 5.0 improves signal peptide predictions using deep neural networks. *Nat. Biotechnol.* **2019**, *37*, 420–423. [CrossRef]
21. Käll, L.; Krogh, A.; Sonnhammer, E.L. A Combined Transmembrane Topology and Signal Peptide Prediction Method. *J. Mol. Biol.* **2004**, *338*, 1027–1036. [CrossRef] [PubMed]
22. Bendtsen, J.D.; Kiemer, L.; Fausbøll, A.; Brunak, S. Non-classical protein secretion in bacteria. *BMC Microbiol.* **2005**, *5*, 58. [CrossRef]
23. Pierleoni, A.; Martelli, P.L.; Casadio, R. PredGPI: A GPI-anchor predictor. *BMC Bioinform.* **2008**, *9*, 392. [CrossRef] [PubMed]
24. Horton, P.; Park, K.-J.; Obayashi, T.; Fujita, N.; Harada, H.; Adams-Collier, C.J.; Nakai, K. WoLF PSORT: Protein localization predictor. *Nucleic Acids Res.* **2007**, *35*, W585–W587. [CrossRef]
25. Armenteros, J.J.A.; Sønderby, C.K.; Sønderby, S.K.; Nielsen, H.; Winther, O. DeepLoc: Prediction of protein subcellular localization using deep learning. *Bioinformatics* **2017**, *33*, 3387–3395. [CrossRef]
26. Götz, S.; Garcia-Gomez, J.M.; Terol, J.; Williams, T.D.; Nagaraj, S.H.; Nueda, M.J.; Robles, M.; Talón, M.; Dopazo, J.; Conesa, A. High-throughput functional annotation and data mining with the Blast2GO suite. *Nucleic Acids Res.* **2008**, *36*, 3420–3435. [CrossRef] [PubMed]
27. Gao, J.; Chen, Z.; Luo, M.; Peng, H.; Lin, H.; Qin, C.; Yuan, G.; Shen, Y.; Ding, H.; Zhao, M.; et al. Genome expression profile analysis of the maize sheath in response to inoculation to *R. solani*. *Mol. Biol. Rep.* **2014**, *41*, 2471–2483. [CrossRef]
28. Altier, J.; Dahlbacka, I.; Herrmann, R.; Hunter-Cervera, J.; McCutchen, B.; Presnail, J.; Rice, J.; Schepers, E.; Simmons, C.; Torok, T.; et al. Antifungal Polypeptides. European Patent EP1763536B1, 8 September 2010.
29. Trapnell, C.; Williams, B.A.; Pertea, G.; Mortazavi, A.; Kwan, G.; Van Baren, M.J.; Salzberg, S.L.; Wold, B.J.; Pachter, L. Transcript assembly and quantification by RNA-Seq reveals unannotated transcripts and isoform switching during cell differentiation. *Nat. Biotechnol.* **2010**, *28*, 511–515. [CrossRef]

30. Raposo, G.; Stoorvogel, W. Extracellular vesicles: Exosomes, microvesicles, and friends. *J. Cell Biol.* **2013**, *200*, 373–383. [CrossRef]
31. Lu, S.; Edwards, M.C. Genome-Wide Analysis of Small Secreted Cysteine-Rich Proteins Identifies Candidate Effector Proteins Potentially Involved in *Fusarium graminearum*—Wheat Interactions. *Phytopathology* **2016**, *106*, 166–176. [CrossRef]
32. Brown, N.A.; Evans, J.; Mead, A.; Hammond-Kosack, K.E. A spatial temporal analysis of the *Fusarium graminearum* transcriptome during symptomless and symptomatic wheat infection. *Mol. Plant Pathol.* **2017**, *18*, 1295–1312. [CrossRef]
33. Jeong, J.S.; Mitchell, T.K.; Dean, R.A. The *Magnaporthe grisea* snodprot1 homolog, MSP1, is required for virulence. *FEMS Microbiol. Lett.* **2007**, *273*, 157–165. [CrossRef] [PubMed]
34. Zhang, Y.; Gao, Y.; Liang, Y.; Dong, Y.; Yang, X.; Yuan, J.; Qiu, D. The *Verticillium dahliae* SnodProt1-Like Protein VdCP1 Contributes to Virulence and Triggers the Plant Immune System. *Front. Plant Sci.* **2017**, *8*, 1880. [CrossRef] [PubMed]
35. Yoshino, K.; Irieda, H.; Sugimoto, F.; Yoshioka, H.; Okuno, T.; Takano, Y. Cell Death of *Nicotiana benthamiana* Is Induced by Secreted Protein NIS1 of *Colletotrichum orbiculare* and Is Suppressed by a Homologue of CgDN3. *Mol. Plant-Microbe Interact.* **2012**, *25*, 625–636. [CrossRef] [PubMed]
36. Blümke, A.; Falter, C.; Herrfurth, C.; Sode, B.; Bode, R.; Schäfer, W.; Feussner, I.; Voigt, C. Secreted Fungal Effector Lipase Releases Free Fatty Acids to Inhibit Innate Immunity-Related Callose Formation during Wheat Head Infection. *Plant Physiol.* **2014**, *165*, 346–358. [CrossRef]
37. Perez-Riverol, Y.; Csordas, A.; Bai, J.; Bernal-Llinares, M.; Hewapathirana, S.; Kundu, D.J.; Inuganti, A.; Griss, J.; Mayer, G.; Eisenacher, M.; et al. The PRIDE database and related tools and resources in 2019: Improving support for quantification data. *Nucleic Acids Res.* **2019**, *47*, D442–D450. [CrossRef]
38. Piffer, A.C.; Kuczera, D.; Rodrigues, M.L.; Nimrichter, L. The paradoxical and still obscure properties of fungal extracellular vesicles. *Mol. Immunol.* **2021**, *135*, 137–146. [CrossRef]
39. Garcia-Ceron, D.; Bleackley, M.R.; Anderson, M.A. Fungal Extracellular Vesicles in Pathophysiology. In *New Frontiers: Extracellular Vesicles*; Subcellular Biochemistry, 2021/03/30 ed.; Mathivanan, S., Fonseka, P., Nedeva, C., Atukorala, I., Eds.; Springer: Cham, Switzerland, 2021; Volume 97, pp. 151–177.
40. Cleare, L.G.; Zamith, D.; Heyman, H.M.; Couvillion, S.P.; Nimrichter, L.; Rodrigues, M.L.; Nakayasu, E.S.; Nosanchuk, J.D. Media matters! Alterations in the loading and release of *Histoplasma capsulatum* extracellular vesicles in response to different nutritional milieus. *Cell. Microbiol.* **2020**, *22*, e13217. [CrossRef]
41. Takegawa, K.; Satoh, K.; Ramli, N.; Jikibara, T.; Iwahara, S. Production and characterization of extracellular uronic acid-containing glycoproteins from *Fusarium oxysporum*. *J. Ferment. Bioeng.* **1997**, *83*, 197–200. [CrossRef]
42. Giese, H.; Sondergaard, T.E.; Sørensen, J.L. The AreA transcription factor in *Fusarium graminearum* regulates the use of some nonpreferred nitrogen sources and secondary metabolite production. *Fungal Biol.* **2013**, *117*, 814–821. [CrossRef]
43. Koch, A.; Schlemmer, T.; Lischka, R. Elucidating the role of extracellular vesicles in the Barley-*Fusarium* interaction. *Trillium Exctracell. Vesicles* **2020**, *2*, 28–35. [CrossRef]
44. Zhao, K.; Bleackley, M.; Chisanga, D.; Gangoda, L.; Fonseka, P.; Liem, M.; Kalra, H.; Al Saffar, H.; Keerthikumar, S.; Ang, C.-S.; et al. Extracellular vesicles secreted by *Saccharomyces cerevisiae* are involved in cell wall remodelling. *Commun. Biol.* **2019**, *2*, 305. [CrossRef]
45. Liu, J.; Applegate, T. Zearalenone (ZEN) in Livestock and Poultry: Dose, Toxicokinetics, Toxicity and Estrogenicity. *Toxins* **2020**, *12*, 377. [CrossRef]
46. Čulig, B.; Bevardi, M.; Bošnir, J.; Serdar, S.; Lasić, D.; Racz, A.; Galić, A.; Kuharić, Ž. Presence of Citrinin in Grains and Its Possible Health Effects. *Afr. J. Tradit. Complement. Altern. Med.* **2017**, *14*, 22–30. [CrossRef]
47. Kasahara, K.; Miyamoto, T.; Fujimoto, T.; Oguri, H.; Tokiwano, T.; Oikawa, H.; Ebizuka, Y.; Fujii, I. Solanapyrone Synthase, a Possible Diels-Alderase and Iterative Type I Polyketide Synthase Encoded in a Biosynthetic Gene Cluster from *Alternaria solani*. *ChemBioChem* **2010**, *11*, 1245–1252. [CrossRef]
48. Klausmeyer, P.; McCloud, T.G.; Tucker, K.D.; Cardellina, J.H.; Shoemaker, R.H. Aspirochlorine Class Compounds from Aspergillus flavus Inhibit Azole-Resistant *Candida albicans*. *J. Nat. Prod.* **2005**, *68*, 1300–1302. [CrossRef] [PubMed]
49. Bradshaw, R.E.; Bhatnagar, D.; Ganley, R.J.; Gillman, C.J.; Monahan, B.J.; Seconi, J.M. *Dothistroma pini*, a Forest Pathogen, Contains Homologs of Aflatoxin Biosynthetic Pathway Genes. *Appl. Environ. Microbiol.* **2002**, *68*, 2885–2892. [CrossRef] [PubMed]
50. Hidy, P.; Baldwin, R.; Greasham, R.; Keith, C.; Mcmullen, J. Zearalenone and Some Derivatives: Production and Biological Activities. In *Advances in Applied Microbiology*; Perlman, D., Ed.; Academic Press: Cambridge, MA, USA, 1977; Volume 22, pp. 59–82.
51. Harvey, A.M. Mode of Action of Dothistromin. Ph.D. Thesis, Massey University, Palmerston North, New Zealand, 1974.
52. Doughari, J.H. The Occurrence, Properties and Significance of Citrinin Mycotoxin. *J. Plant Pathol. Microbiol.* **2015**, *6*, 2.
53. Chanda, A.; Roze, L.V.; Kang, S.; Artymovich, K.A.; Hicks, G.R.; Raikhel, N.V.; Calvo, A.M.; Linz, J.E. A key role for vesicles in fungal secondary metabolism. *Proc. Natl. Acad. Sci. USA* **2009**, *106*, 19533–19538. [CrossRef] [PubMed]
54. Sonah, H.; Deshmukh, R.; Bélanger, R.R. Computational Prediction of Effector Proteins in Fungi: Opportunities and Challenges. *Front. Plant Sci.* **2016**, *7*, 126. [CrossRef]
55. Quarantin, A.; Hadeler, B.; Kröger, C.; Schäfer, W.; Favaron, F.; Sella, L.; Martínez-Rocha, A.L. Different Hydrophobins of *Fusarium graminearum* Are Involved in Hyphal Growth, Attachment, Water-Air Interface Penetration and Plant Infection. *Front. Microbiol.* **2019**, *10*, 751. [CrossRef]

56. Casarrubia, S.; Daghino, S.; Kohler, A.; Morin, E.; Khouja, H.-R.; Daguerre, Y.; Veneault-Fourrey, C.; Martin, F.M.; Perotto, S.; Martino, E. The Hydrophobin-Like OmSSP1 May Be an Effector in the Ericoid Mycorrhizal Symbiosis. *Front. Plant Sci.* **2018**, *9*, 546. [CrossRef]
57. Guzmán-Guzmán, P.; Alemán-Duarte, M.I.; Delaye, L.; Herrera-Estrella, A.; Olmedo-Monfil, V. Identification of effector-like proteins in *Trichoderma* spp. and role of a hydrophobin in the plant-fungus interaction and mycoparasitism. *BMC Genet.* **2017**, *18*, 16. [CrossRef] [PubMed]
58. Wolf, J.M.; Espadas, J.; Luque-Garcia, J.; Reynolds, T.; Casadevall, A. Lipid Biosynthetic Genes Affect *Candida albicans* Extracellular Vesicle Morphology, Cargo, and Immunostimulatory Properties. *Eukaryot. Cell* **2015**, *14*, 745–754. [CrossRef] [PubMed]
59. Yao, S.-H.; Guo, Y.; Wang, Y.-Z.; Zhang, D.; Xu, L.; Tang, W.-H. A cytoplasmic Cu-Zn superoxide dismutase SOD1 contributes to hyphal growth and virulence of *Fusarium graminearum*. *Fungal Genet. Biol.* **2016**, *91*, 32–42. [CrossRef]
60. Mondola, P.; Ruggiero, G.; Serù, R.; Damiano, S.; Grimaldi, S.; Garbi, C.; Monda, M.; Greco, D.; Santillo, M. The Cu, Zn superoxide dismutase in neuroblastoma SK-N-BE cells is exported by a microvesicles dependent pathway. *Mol. Brain Res.* **2003**, *110*, 45–51. [CrossRef]
61. Tian, L.; Li, J.; Huang, C.; Zhang, D.; Xu, Y.; Yang, X.; Song, J.; Wang, D.; Qiu, N.; Short, D.P.G.; et al. Cu/Zn superoxide dismutase (VdSOD1) mediates reactive oxygen species detoxification and modulates virulence in *Verticillium dahliae*. *Mol. Plant Pathol.* **2021**, *22*, 1092–1108. [CrossRef]
62. Cruz-Garcia, D.; Brouwers, N.; Duran, J.M.; Mora, G.; Curwin, A.J.; Malhotra, V. A diacidic motif determines unconventional secretion of wild-type and ALS-linked mutant SOD1. *J. Cell Biol.* **2017**, *216*, 2691–2700. [CrossRef]
63. Basso, M.; Pozzi, S.; Tortarolo, M.; Fiordaliso, F.; Bisighini, C.; Pasetto, L.; Spaltro, G.; Lidonnici, D.; Gensano, F.; Battaglia, E.; et al. Mutant Copper-Zinc Superoxide Dismutase (SOD1) Induces Protein Secretion Pathway Alterations and Exosome Release in Astrocytes. *J. Biol. Chem.* **2013**, *288*, 15699–15711. [CrossRef]
64. Rizzo, J.; Chaze, T.; Miranda, K.; Roberson, R.W.; Gorgette, O.; Nimrichter, L.; Matondo, M.; Latgé, J.-P.; Beauvais, A.; Rodrigues, M.L. Characterization of Extracellular Vesicles Produced by *Aspergillus fumigatus* Protoplasts. *mSphere* **2020**, *5*, 00476-20. [CrossRef]
65. Wolf, J.M.; Espadas-Moreno, J.; Luque-Garcia, J.L.; Casadevall, A. Interaction of *Cryptococcus neoformans* Extracellular Vesicles with the Cell Wall. *Eukaryot. Cell* **2014**, *13*, 1484–1493. [CrossRef] [PubMed]
66. Fang, Y.; Wang, Z.; Zhang, S.; Peng, Q.; Liu, X. Characterization and proteome analysis of the extracellular vesicles of *Phytophthora capsici*. *J. Proteom.* **2021**, *238*, 104137. [CrossRef]
67. Romero, D.; Thon, M.; de Vicente, A. Effectors with chitinase activity (EWCAs), a family of conserved, secreted fungal chitinases that suppress chitin-triggered immunity. *Plant Cell* **2021**, *33*, 1319–1340. [CrossRef]
68. Burg, H.A.V.D.; Harrison, S.J.; Joosten, M.H.A.J.; Vervoort, J.; de Wit, P.J.G.M. *Cladosporium fulvum* Avr4 Protects Fungal Cell Walls Against Hydrolysis by Plant Chitinases Accumulating During Infection. *Mol. Plant-Microbe Interact.* **2006**, *19*, 1420–1430. [CrossRef] [PubMed]
69. Fiorin, G.L.; Sanchéz-Vallet, A.; Thomazella, D.P.D.T.; Prado, P.F.V.D.; Nascimento, L.C.D.; Figueira, A.; Thomma, B.P.; Pereira, G.A.G.; Teixeira, P.J.P.L. Suppression of Plant Immunity by Fungal Chitinase-like Effectors. *Curr. Biol.* **2018**, *28*, 3023–3030.e5. [CrossRef]
70. Hasper, A.A.; Dekkers, E.; van Mil, M.; van de Vondervoort, P.J.I.; de Graaff, L.H. EglC, a New Endoglucanase from *Aspergillus niger* with Major Activity towards Xyloglucan. *Appl. Environ. Microbiol.* **2002**, *68*, 1556–1560. [CrossRef]
71. Rouxel, T.; Grandaubert, J.; James, K.H.; Claire, H.; Angela, P.V.D.W.; Arnaud, C.; Victoria, D.; Véronique, A.; Pascal, B.; Salim, B.; et al. Effector diversification within compartments of the *Leptosphaeria maculans* genome affected by Repeat-Induced Point mutations. *Nat. Commun.* **2011**, *2*, 202. [CrossRef]
72. Bolton, M.D.; van Esse, H.P.; Vossen, J.H.; de Jonge, R.; Stergiopoulos, I.; Stulemeijer, I.J.E.; Berg, G.C.M.V.D.; Borrás-Hidalgo, O.; Dekker, H.L.; de Koster, C.G.; et al. The novel *Cladosporium fulvumlysin* motif effector Ecp6 is a virulence factor with orthologues in other fungal species. *Mol. Microbiol.* **2008**, *69*, 119–136. [CrossRef]
73. Zhang, Y.; Zhang, Y.; Qiu, D.; Zeng, H.; Guo, L.; Yang, X. BcGs1, a glycoprotein from *Botrytis cinerea*, elicits defence response and improves disease resistance in host plants. *Biochem. Biophys. Res. Commun.* **2015**, *457*, 627–634. [CrossRef]
74. Soyer, J.L.; El Ghalid, M.; Glaser, N.; Ollivier, B.; Linglin, J.; Grandaubert, J.; Balesdent, M.-H.; Connolly, L.R.; Freitag, M.; Rouxel, T.; et al. Epigenetic Control of Effector Gene Expression in the Plant Pathogenic Fungus *Leptosphaeria maculans*. *PLoS Genet.* **2014**, *10*, e1004227. [CrossRef]
75. Phan, H.T.; Rybak, K.; Furuki, E.; Breen, S.; Solomon, P.; Oliver, R.P.; Tan, K. Differential effector gene expression underpins epistasis in a plant fungal disease. *Plant J.* **2016**, *87*, 343–354. [CrossRef]
76. Nafisi, M.; Stranne, M.; Zhang, L.; van Kan, J.; Sakuragi, Y. The Endo-Arabinanase BcAra1 Is a Novel Host-Specific Virulence Factor of the Necrotic Fungal Phytopathogen *Botrytis cinerea*. *Mol. Plant-Microbe Interact.* **2014**, *27*, 781–792. [CrossRef]
77. Brown, L.; Wolf, J.M.; Prados-Rosales, R.; Casadevall, A. Through the wall: Extracellular vesicles in Gram-positive bacteria, mycobacteria and fungi. *Nat. Rev. Microbiol.* **2015**, *13*, 620–630. [CrossRef] [PubMed]
78. Krombach, S.; Reissmann, S.; Kreibich, S.; Bochen, F.; Kahmann, R. Virulence function of the *Ustilago maydissterol* carrier protein 2. *New Phytol.* **2018**, *220*, 553–566. [CrossRef] [PubMed]
79. Giraldo, M.C.; Dagdas, Y.F.; Gupta, Y.K.; Mentlak, T.A.; Yi, M.; Martinez-Rocha, A.L.; Saitoh, H.; Terauchi, R.; Talbot, N.J.; Valent, B. Two distinct secretion systems facilitate tissue invasion by the rice blast fungus *Magnaporthe oryzae*. *Nat. Commun.* **2013**, *4*, 1996. [CrossRef]

80. Yang, F.; Jensen, J.D.; Svensson, B.; Jørgensen, H.J.L.; Collinge, D.B.; Finnie, C. Secretomics identifies *Fusarium graminearum* proteins involved in the interaction with barley and wheat. *Mol. Plant Pathol.* **2011**, *13*, 445–453. [CrossRef] [PubMed]
81. Hill, E.H.; Solomon, P.S. Extracellular vesicles from the apoplastic fungal wheat pathogen *Zymoseptoria tritici*. *Fungal Biol. Biotechnol.* **2020**, *7*, 13. [CrossRef] [PubMed]

4. Chapter Four

As described in Chapter 1, research into fungal EVs is a relatively new field compared to the study of mammalian EVs. The latter has been enhanced by the availability of EV-specific markers used for the development of advanced EV isolation and characterization techniques, as well as *in vivo* analyses. When this thesis began no markers were available to specifically tag fungal EVs. This has hindered the development of new methods such as improved purifications of fungal EVs using density gradients, or experiments to monitor EV interactions with the host. Hence, many of the procedures used to study fungal EVs are based on elemental techniques developed for mammalian EVs. The article presented in this chapter describes the first set of EV-specific markers for a fungal species. The electron microscopy methods developed in chapters 2 and 3 were employed to confirm that the EVs that had been isolated from *Candida albicans* had the typical appearance of fungal EVs, which were also similar to mammalian EVs. This study revealed that the protein Sur7 had similarity to the mammalian tetraspanins, hence other collaborators are now examining the application of Sur7 as a marker for *C. albicans* EVs. This work was extended to determine whether Sur7 can also be used as a marker of EVs from *Fusarium graminearum,* and whether an antibody can be generated to detect Sur7, which is described in section 4.2, potentially unlocking new characterization techniques for *Fgr* EVs.

4.1 Protein markers for EVs from *Candida albicans* and *Fusarium graminearum* include the claudin-like Sur7

Part of the work from this chapter was a study on identifying potential protein markers for EVs produced by the human fungal pathogen *Candida albicans* and the plant pathogen *Fusarium graminearum.* The findings from the study on *C. albicans* have been published in a peer-reviewed journal: Journal of Extracellular Vesicles, March 2020.

Dawson CS, Garcia-Ceron D, Rajapaksha H, Faou P, Bleackley MR, Anderson MA. Protein markers for *Candida albicans* EVs include claudin-like Sur7 family proteins. Journal of Extracellular Vesicles. 2020 Apr 16;9(1):1750810. doi: 10.1080/20013078.2020.1750810.

Statement of Contribution

Donovan Garcia-Ceron:

- Developed the transmission-electron microscopy methods used in this article
- Acquired the micrographs of *C. albicans* EVs
- Wrote the corresponding method

JOURNAL OF EXTRACELLULAR VESICLES
2020, VOL. 9, 1750810
https://doi.org/10.1080/20013078.2020.1750810

Taylor & Francis
Taylor & Francis Group

RESEARCH ARTICLE

OPEN ACCESS Check for updates

Protein markers for *Candida albicans* EVs include claudin-like Sur7 family proteins

Charlotte S Dawson [a,b], Donovan Garcia-Ceron [a], Harinda Rajapaksha [c], Pierre Faou [c], Mark R Bleackley [a§] and Marilyn A Anderson [a§]

[a]Department of Biochemistry and Genetics, La Trobe Institute for Molecular Science. La Trobe University, Australia; [b]Department of Biochemistry, Cambridge Centre for Proteomics, Milner Therapeutics Institute, Jeffrey Cheah Biomedical Centre, University of Cambridge, Cambridge, UK; [c]La Trobe Comprehensive Proteomics Platform, La Trobe Institute for Molecular Science. La Trobe University, Australia

ABSTRACT

Background: Fungal extracellular vesicles (EVs) have been implicated in host-pathogen and pathogen-pathogen communication in some fungal diseases. In depth research into fungal EVs has been hindered by the lack of specific protein markers such as those found in mammalian EVs that have enabled sophisticated isolation and analysis techniques. Despite their role in fungal EV biogenesis, ESCRT proteins such as Vps23 (Tsg101) and Bro1 (ALIX) are not present as fungal EV cargo. Furthermore, tetraspanin homologs are yet to be identified in many fungi including the model yeast S. cerevisiae.
Objective: We performed de novo identification of EV protein markers for the major human fungal pathogen Candida albicans with adherence to MISEV2018 guidelines.
Materials and methods: EVs were isolated by differential ultracentrifugation from DAY286, ATCC90028 and ATCC10231 yeast cells, as well as DAY286 biofilms. Whole cell lysates (WCL) were also obtained from the EV-releasing cells. Label-free quantitative proteomics was performed to determine the set of proteins consistently enriched in EVs compared to WCL.
Results: 47 proteins were consistently enriched in C. albicans EVs. We refined these to 22 putative C. albicans EV protein markers including the claudin-like Sur7 family (Pfam: PF06687) proteins Sur7 and Evp1 (orf19.6741). A complementary set of 62 EV depleted proteins was selected as potential negative markers.
Conclusions: The marker proteins for C. albicans EVs identified in this study will be useful tools for studies on EV biogenesis and cargo loading in C. albicans and potentially other fungal species and will also assist in elucidating the role of EVs in C. albicans pathogenesis. Many of the proteins identified as putative markers are fungal specific proteins indicating that the pathways of EV biogenesis and cargo loading may be specific to fungi, and that assumptions made based on studies in mammalian cells could be misleading.

Abbreviations: A1 – ATCC10231; A9 – ATCC90028; DAY B – DAY286 biofilm; DAY Y – DAY286 yeast; EV – extracellular vesicle; Evp1 – extracellular vesicle protein 1 (orf19.6741); GO – gene ontology; Log_2 (FC) – log_2(fold change); MCC – membrane compartment of Can1; MDS – multidimensional scaling; MISEV – minimal information for studies of EVs; sEVs – small EVs; SP – signal peptide; TEMs – tetraspanin enriched microdomains; TM – transmembrane; VDM – vesicle-depleted medium; WCL – whole cell lysate

ARTICLE HISTORY
Received 18 July 2019
Revised 24 March 2020
Accepted 27 March 2020

KEYWORDS
Candida albicans; extracellular vesicles; proteomics; markers; pathogen; fungi

Introduction

Fungal infections are ubiquitous and are estimated to affect over 20% of the world's population [1]. These infections range from non-life-threatening mycoses of the skin and nails, to deadly systemic infections. They represent a significant burden on healthcare systems, with the direct medical cost of fungal disease in the USA in 2017 estimated to be 7.2 billion USD [2]. The fungi responsible for most fungal infections worldwide are the various species of *Candida* [3]. *Candida* is primarily associated with relatively harmless superficial infections [4], but infections of the bloodstream or internal organs are associated with mortality rates as high as 75% [4,5]. Over 12,000 people were hospitalised for invasive candidiasis in the US in 2017 alone, at a cost of almost 1.2 billion USD [2]. The species responsible for the majority of *Candida* infections is *Candida albicans* [6]. *C. albicans* infections are most often treated with two classes of antifungals, the azoles

CONTACT Marilyn A Anderson m.anderson@latrobe.edu.au La Trobe Institute for Molecular Science, La Trobe University, 3086 Bundoora, Victoria, Australia
[†]These authors contributed equally to this work
Supplemental data for this article can be accessed here.

which target biosynthesis of the fungal-specific sterol ergosterol, and the echinocandins, which target biosynthesis of the major cell wall polysaccharide 1,3-β-glucan [7]. Resistance to these and other antifungals has begun to emerge [8–11] making the development of new antifungals with novel mechanisms of action paramount. Understanding the interface between the host and pathogen will help to identify new targets for controlling *C. albicans* infections.

Extracellular vesicles (EVs) are key factors in the progression of many diseases ranging from cancer [12] to neurodegenerative diseases [13] and bacterial infections [14]. EVs are defined as "particles naturally released from the cell that are delimited by a lipid bilayer and cannot replicate" [15]. Packaging of cargo into EVs is a method for the coordinated release of biological molecules via a non-classic method of secretion. This facilitates intercellular communication both within an organism [16] and between organisms [17].

Recently, EVs have been proposed to function in the pathogenesis of fungal disease, particularly in yeast infections including those from the genera *Cryptococcus* [18–20], *Paracoccidioides* [21,22] and *Candida* [23–25]. The cargo of fungal EVs comprises proteins [26], nucleic acids [27], lipids [23,24,28,29] and carbohydrates [22,28]. Fungal EVs activate innate immune cells in vitro [18,23,24,30] and are responsible for the hypervirulence of a *Cryptococcus gattii* strain that caused disease in immunocompetent individuals [20]. Given the potential roles for EVs in host-pathogen interactions, there is significant motivation to better understand the biology of fungal EVs.

C. albicans EVs are typical of fungal EVs. They contain proteins, lipids, nucleic acids and carbohydrates [23,24,27,31,32]. Activation of murine macrophages and dendritic cells by EVs from *C. albicans* indicates a potential role for EVs in modulating the innate immune response to the fungus [23,24]. Formation of biofilms is a critical component of *C. albicans* pathogenesis [33] and the biofilm matrix provides a protective layer for the fungus against antifungal drugs [34]. The cargo of EVs produced by *C. albicans* biofilms includes key proteins and carbohydrates for biofilm biogenesis, making EVs crucial contributors to the establishment of biofilms [32]. Furthermore, "add-back" of EVs from wildtype biofilms restored the loss of azole resistance in biofilms formed by strains with deletions in genes encoding important enzymes for matrix generation [32]. That is, EVs also function in antifungal drug resistance.

The tools and techniques for the study of fungal EVs have been adapted from those established for mammalian systems, where EVs are most intensively studied. Many of the cutting-edge experimental techniques for isolation, tracking and analysis of mammalian EVs are dependent on protein markers [35]. They include identifying fractions containing EVs after density gradient centrifugation [36] or size exclusion chromatography [37], purification of EVs via immunoaffinity capture [38], and imaging of EV release and uptake [39]. Unfortunately, proteomic analyses of fungal EVs have revealed that the markers that have been so useful for the isolation and study of mammalian EVs are not present in fungal EVs [26]. Thus, there are differences in the protein cargo and possibly the biogenesis of EVs from fungi and mammalian cells, and *de novo* identification of fungal EV markers is essential. Inconsistencies between published data sets on the protein content of fungal EVs [26] means that a robust proteomic analysis of EVs from a particular species is required to provide an adequate data set for EV marker identification. In this study, we have addressed this problem by performing in-depth proteomic analyses on multiple *C. albicans* strains to define a set of broadly applicable *C. albicans* EV markers.

Label-free quantitative proteomics was employed to generate an overview of the differences in EV and whole cell lysate (WCL) proteomes for a selection of different *C. albicans* strains and morphologies; DAY286 yeast, DAY286 biofilm, ATCC90028 yeast and ATCC10231 yeast. By comparing the EV versus WCL data across all strains and morphologies we identified 47 putative EV markers which are enriched in *C. albicans* EVs regardless of source, cell strain, or morphology. These candidate protein markers include GTPases, enzymes crucial for cell wall synthesis, and plasma membrane proteins resembling mammalian tetraspanins or claudins. The "minimal information for studies of EVs" (MISEV) 2018 position statement indicates that, in addition to demonstrating the enrichment of EV marker proteins in EV preparations, a deficiency of non-EV proteins should also be shown [15]. With this in mind, we identified 62 proteins that were depleted in *C. albicans* EVs compared to the WCL from the four data sets. Validation of these putative EV markers *in vitro* will allow future *C. albicans* EV research to align better with the recommendations set out in MISEV2018. Furthermore, robust *C. albicans* EV markers will allow adaptation of mammalian EV analysis techniques for use in the study of EVs in *C. albicans* pathogenesis and will provide potential new targets for the development of novel antifungals.

Materials and methods

C. albicans *strains and maintenance*

C. albicans strains used in this study were DAY286 [40], ATCC90028 and ATCC10231. All strains were

maintained on YPD Agar plates (1% yeast extract, 2% peptone, 2% dextrose, 2% agar). Liquid starter cultures were grown overnight in YPD medium (1% yeast extract, 2% peptone, 2% dextrose) at 30°C and 300 rpm.

Yeast culture conditions

For isolation of EVs from yeast form *C. albicans* (DAY286, ATCC90028, ATCC10231), YPD starter cultures were used to inoculate 150 or 300 mL YPD at an OD_{600} = 0.2 in a baffled flask. Cultures were incubated at 30°C overnight (approximately 20 h). The culture OD_{600} was measured immediately prior to EV isolation.

Biofilm culture conditions

Biofilms (DAY286) were generated based on the method described in [41] with modifications. Briefly, 500 mL pre-warmed ½ strength RPMI (250 mL RPMI 1640 (Sigma), 0.165 M MOPS (Sigma) and 250 mL 3.6% dextrose) was inoculated using a liquid starter culture to 1.0×10^6 cells/mL. Five 25 × 25 cm non-treated bioassay dishes (Thermo Fisher Scientific) were each filled with 100 mL of inoculated ½ RPMI and incubated statically for 4 h at 37°C to allow for adhesion of cells to the dish. Following cell adhesion, the culture medium (and any non-adherent cells) was decanted and replaced with 200 mL pre-warmed full strength RPMI. Biofilms were formed by incubating the dishes for 54 h at 37°C with agitation at 28 rpm in an Incu-Shaker Mini (Benchmark Scientific).

EV isolation

EVs were isolated according to the method described in [28] with minor modifications. In brief, yeast cells or biofilm fragments were separated from the culture supernatants by centrifugation at 4000 x g for 15 min in an Heraeus Multifuge X3 R (75,003,607 rotor, k_{adj} = 11,778.7, Thermo Scientific), then 15,000 x g for 30 min in an Avanti J-E centrifuge (JLA 16.250 rotor, k_{adj} = 2790.4, Beckman Coulter). Supernatants were 0.45 µm filtered (Millipore) then ultracentrifuged at 100,000 x g for 1 h in a Beckman Coulter Optima L-100XP using 70 mL polycarbonate bottle assemblies (45Ti rotor, k_{adj} = 312.6, Beckman Coulter) to pellet EVs, which were resuspended in phosphate buffered saline (137 mM NaCl, 2.7 mM KCl, 10 mM Na_2HPO_4, 1.8 mM KH_2PO_4) (PBS) and transferred to 1.5 mL polypropylene tubes (Beckman Coulter). EVs were ultracentrifuged again at 120,000 x g for 1 h using a Beckman TL-100 ultracentrifuge (TLA55 rotor, k_{adj} = 102.3, Beckman Coulter) then resuspended in 100 µL PBS. An aliquot of yeast cells (250 µL) was reserved for preparation of yeast whole cell lysate. Similarly, 250 µL of biofilm scrapings were resuspended in PBS for preparation of biofilm lysate.

Preparation of whole cell lysate and protein quantification

C. albicans cells were washed three times with PBS prior to the addition of approximately 400 µL of acid washed glass beads (Sigma). Cells were lysed using a TissueLyser (Qiagen) at 30 bps for 3 × 1 min bursts with 1 min incubations on ice between bursts. Debris and beads were pelleted by centrifugation for 5 min at 23,000 x g at 4°C. The supernatant was retained as the respective lysate sample. Protein concentration of EVs and whole cell lysates (WCL) was determined using a Qubit™ 4 fluorimeter (Life Technologies) and the Qubit™ protein assay kit according to the manufacturer's instructions.

Nanoparticle tracking analysis

The particle size and concentration of EV samples was determined using a NanoSight NS300 equipped with a 405 nm (blue) laser (Malvern Instruments). Immediately prior to injection, EVs were diluted between 1:250 and 1:6000 in 0.22 µm (Millipore) filtered PBS to bring the particle concentration within the manufacturer's recommended range (10^8–10^9 particles/mL). NTA software version 3.2 was used to record data in 60 s reads in triplicate. Instrument settings included: a syringe infusion rate of 70, temperature held at 25°C, a camera level of 11, and a detection threshold of 6. The particle concentrations and particle size parameters were recorded. Dilution factor correction and averaging of data across biological replicates was performed using the R package *tidyNano* [42].

Transmission electron microscopy

Carbon-coated 400-mesh copper grids (ProSciTech) were glow discharged for 1 min in a K950X turbo evaporator coupled to a K350 glow discharge unit (Quorum Technologies Ltd). EVs (5 µL) were deposited onto the grid and incubated for 1 min. Grids were then washed once with ultrapure water and negatively stained three times with 2% (v/v) uranyl acetate (Agar Scientific). Excess solution was blotted off and the grids were dried overnight. AJEM 2100 electron microscope (JEOL Ltd) operated at 200 kV was used for imaging.

Sample preparation for mass spectrometry

A total of 14 EV and WCL samples from four different *C. albicans* strains were used for proteomics and NTA analyses; DAY286 yeast (n = 3), ATCC90028 yeast (n = 3), ATCC10231 yeast (n = 3), and DAY286 biofilm (n = 5). Details of each independent culture from which the EV and WCL samples were isolated are provided in Supplementary Table 1. Preparation of EV and WCL proteomics samples and MS data acquisition was performed in three separate batches; DAY286 yeast, DAY286 biofilm, and then both ATCC strains.

EVs or WCLs (15 µg protein) were boiled in LDS sample buffer (Life Technologies) and TCEP (tris(2-carboxyethyl)phosphine) (Thermo Fisher Scientific), then separated by short-range SDS-PAGE [43]. The gel was fixed in 50% (v/v) methanol, 7% (v/v) acetic acid for 30 min, and the samples were excised. The proteins were reduced (2 mM TCEP, 1 h) and alkylated (40 mM iodoacetamide, 30 min in the dark) before digestion with 1 µg trypsin (Promega) for 18 h at 37°C. Peptides were then extracted from the gel pieces with 85% (v/v) ACN, 0.5% (v/v) TFA, lyophilised and resuspended in 20 µL of 5% (v/v) ACN, 0.5% (v/v) TFA.

Mass spectrometry (ESI-LC-MS/MS) of EVs and WCL proteins

Two injections of 6 µL were used for each biological replicate and the samples were randomised prior to injection. Peptides were analysed as described previously [44] with modifications. Using a nanoflow UPLC instrument (UltiMate^{TM} 3000 RSLCnano, Thermo Fisher Scientific), the reconstituted peptides were loaded onto a precolumn (C18 PepMap 300 µm ID x 2 cm trapping column, Thermo Fisher Scientific) and washed (water with 0.1% formic acid, 2% ACN) prior to separation using a 90 min linear ACN gradient on an analytical column (BEH C18, 1.7 µm, 130 Å and 75 µm ID x 25 cm, Waters).

The nanoflow UPLC was coupled on-line to a Q Exactive HF mass spectrometer (Thermo Fisher Scientific) with a nanoelectrospray ion source (Nanospray Flex, Thermo Fisher Scientific). The separation of peptides was performed at 45°C, 250 nL/min using a linear ACN gradient of buffer A(water with 0.1% formic acid, 2% ACN) and buffer B (water with 0.1% formic acid, 80% ACN). The gradient started from 2% buffer B to 13% in 6 min, to 33% buffer B over 70 min, followed by 50% at 80 min. The gradient was then increased from 50% buffer B to 95% for 5 min and stayed 95% for 1 min. The column was then equilibrated for 4 min with buffer A.

Data were collected in data-dependent acquisition mode using an MS scan range of m/z 350–1500 and resolution of 60,000. HCD MS/MS spectra were collected for the 15 most intense ions per MS scan at 30,000 resolution with a normalised collision energy of 28% and an isolation window of 1.4 m/z. Dynamic exclusion parameters were set as follows: exclude isotope on, duration 30 s and peptide match preferred. Other Orbitrap instrument parameters included an MS maximum injection time of 30 ms with AGC target 3 x 10^6, for a maximum injection time of 110 ms with an AGT target of 1×10^5.

Database search and protein identification

Tandem MS data collected for EVs and WCLs were processed in MaxQuant version 1.6.0.16 [45]. Andromeda was used to search the data against the UniProt *C. albicans* reference proteome (UP000000559; downloaded 16/06/2018; 6035 entries) and the common contaminants and decoys list [46]. The raw data from both injections of each biological replicate was combined into one sample using the "set experiment" option in MaxQuant. Trypsin was selected as the digestion enzyme and up to 2 missed cleavages were allowed. Carbamidomethylation of cysteine was set as a fixed modification and oxidation of methionine and N-terminal acetylation were set as variable modifications. Peptide mass tolerances were 20 ppm (first search) and 4.5 ppm (main search), and false discovery rate (FDR) cut offs were 0.01 for both proteins and peptides. Minimum and maximum peptide lengths were set to 8 and 25 respectively and match between runs was not selected.

Label-free quantification (LFQ) of protein abundances was performed using the MaxLFQ algorithm [47]. Fast LFQ was selected and normalisation was skipped. The proteinGroups.txt MaxQuant output was used for further analyses. Metadata for identified proteins (localisation, topology, function) were obtained from the UniProt *C. albicans* reference proteome as well as the *C. albicans* SC5314 Assembly 22 chromosomal feature file available from the Candida Genome Database (candidagenome.org/download/chromosomal_feature_files) [48,49].

Protein filtering and proteomic analysis

All proteomics statistical and data analyses were performed using R version 3.6.0 [50], Statistical tests, multiple comparison corrections and important individual R and Bioconductor packages are referenced where they have been used. The DAY286 yeast, DAY286 biofilm and ATCC proteinGroups.txt MaxQuant output files were initially processed and analysed separately. The analysis

Table 1. Candidate positive protein markers for *C. albicans* EVs. This list of proteins consists of those that were found to be exclusive to EVs or significantly enriched in EVs across the four *C. albicans* strains examined in this study. Proteins are grouped according to their subcellular localisation as annotated in the Candida Genome Database (candidagenome.org) [48,49] unless otherwise indicated. The log2 ratio of the abundance (mean MaxQuant LFQ intensity) of each protein in EVs compared to whole cell lysate (WCL) for each strain is listed. "ex" indicates where a protein was only quantified in the EV fraction and not the WCL for that strain. The "TM" column indicates the number of transmembrane domains for each protein as annotated in UniProt. "SP" indicates whether a protein is annotated as having a signal peptide according to UniProt. "VDM" shows whether a protein has been detected previously in vesicle-depleted culture media (i.e. the proteins may also be in the soluble secretome) [31]. Underlined proteins are those identified as the best candidates for positive EV markers according to the criteria depicted in Supplementary Figure S1.

		log_2(fold change) EV vs WCL						
Name	Function	DAY Y	A9	A1	DAY B	TM	SP	VDM
Plasma membrane								
ARF3	Arf family GTPase[a]	ex	1.69	ex	3.45			
CDC42	Rho family GTPase	ex	ex	ex	ex			
CDR1;CDR2	Multidrug transporter of ABC superfamily	ex	ex	ex	11.19	12;12		
CHS3	Major chitin synthase of yeast and hyphae	ex	4.12	ex	ex	5		
ENA21	Predicted P-type ATPase sodium pump[a]	ex	ex	ex	ex	9		
FAA4	Long-chain fatty acid-CoA ligase[a]	2.89	2.24	2.28	1.45			
FET34	Multicopper feroxidase	ex	ex	ex	6.18	1	Y	
GAP4	High-affinity S-adenosylmethionine permease	ex	ex	ex	4.28	12		
GSC1	1,3-beta-glucan synthase	2.57	3.45	5.97	8.01	15		
HGT1	High-affinity MFS glucose transporter	ex	ex	ex	ex	12		
HGT6	Putative high-affinity MFS glucose transporter	4.04	4.78	6.53	5.68	11		
HGT7	Putative MFS glucose transporter	ex	5.95	ex	ex	11		
MTS1	Sphingolipid C9-methyltransferase	2.20	1.86	1.41	2.13	2		
NCE102	Non-classical protein export protein	3.34	2.20	ex	5.32	4		
EVP1[d]	*S. cerevisiae* ortholog is Pun1, plasma membrane protein[a]	ex	ex	ex	ex	3		Y
PHM7	Putative ion transporter	ex	ex	ex	ex	11		
PMA1	Plasma membrane ATPase	5.65	4.38	5.60	6.46	8		
RAC1	G-protein of RAC subfamily	ex	ex	ex	3.92			
RHO1	Rho family GTPase	2.81	3.68	3.74	4.03			
RHO3	Rho family GTPase	ex	ex	ex	ex			
SSO2	Plasma membrane t-SNARE[a]	ex	1.88	3.57	ex	1		
SUR7	Protein required for normal cell wall, plasma membrane[c]	ex	ex	ex	7.04	4		
YCK2	*S. cerevisiae* ortholog is Yck2, casein kinase	ex	4.42	ex	ex			
Cell wall, cell surface								
BGL2	1,3-beta-glucanosyltransferase	7.26	9.44	11.08	ex		Y	Y
CRH11	GPI-anchored cell wall transglycosylase	ex	ex	ex	ex		Y	Y
ECM33	GPI-anchored cell wall protein	4.39	5.28	8.31	7.03		Y	Y
GPD2	Glycerol-3-phosphate dehydrogenase	ex	3.48	2.39	1.30			
MP65	Cell surface mannoprotein	ex	ex	ex	ex		Y	Y
MSB2	Mucin family adhesin-like protein	ex	ex	ex	ex	1	Y	Y
PGA4	1,3-beta-glucanosyltransferase	ex	ex	ex	ex		Y	Y
PGA52	GPI-anchored cell surface protein of unknown function	ex	ex	ex	ex		Y	Y
PHR1	Cell surface glycosidase	ex	ex	ex	5.65		Y	
PHR2	Glycosidase	ex	3.51	6.44	ex		Y	Y
PLB4.5	Phospholipase B	ex	ex	ex	ex		Y	Y
SAP9	Secreted aspartyl protease	ex	ex	ex	ex	1	Y	Y
YWP1	Secreted yeast cell wall protein	2.37	3.51	6.17	ex		Y	Y
Endoplasmic reticulum								
ERO1	ER oxidoreductin	ex	ex	2.32	1.68		Y	Y
orf19.1054	*S. cerevisiae* ortholog is Pom33, transmembrane nucleoporin[b]	5.66	ex	ex	2.51	4		
orf19.2168.3	*S. cerevisiae* ortholog is Yop1, reticulon-interacting protein[a]	4.77	1.98	2.29	1.81	4		
orf19.3799	*S. cerevisiae* ortholog is Rtn1, reticulon protein[b]	2.24	1.40	3.00	1.29	2		
SEC61	ER protein-translocation complex subunit	2.53	2.16	2.10	1.46	8		
Endosome, Golgi, transport vesicle								
SEC4	Rab family GTPase[a]	1.88	1.20	1.86	2.90			
YKT6	Palmitoyltransferase, putative vacuolar SNARE complex protein[a]	ex	4.01	5.46	3.20			
YPT31	Rab family GTPase[a]	ex	1.57	1.33	3.33			
Vacuole								
VAC8	Protein involved in vacuolar inheritance[a]	2.79	ex	ex	3.83			
Mitochondrion								
MIR1	Putative mitochondrial phosphate transporter[a]	3.68	4.38	4.24	1.60			
POR1	Mitochondrial outer membrane porin[a]	3.44	2.51	3.69	1.38			

[a]Protein localisation was inferred from sequence similarity with *S. cerevisiae* homolog as annotated in the Candida Genome Database [48,49].
[b]Protein localisation was obtained from the GO Cellular Component annotation in the *C. albicans* UniProt reference proteome UP000000559 [58].
[c]Presence of transmembrane domains and absence of a signal peptide was predicted using TOPCONS2 [59].
[d]The name Evp1 for the protein encoded by orf19.6741 was proposed in the present study.

methodology and some modified functions were derived from the Bioconductor package *DEP* [51].

First, reversed and contaminant proteins as well as proteins identified by less than 2 unique peptides were

removed. The resulting proteins were filtered for those quantified (LFQ intensity > 0) in a minimum of 2/3 yeast or 4/5 biofilm EV or WCL biological replicates (Supplementary Data S1). LFQ intensities were $\log_2$ transformed, then normalised using the cyclic loess normalisation method available in the Bioconductor package *limma* [52]. Proteins were then separated into two groups: those exclusive to EVs or WCL, and those quantified in both samples. Missing LFQ values in the latter group were imputed using the bpca method from the Bioconductor package *pcaMethods* [53], while exclusive proteins were left untouched. Finally, differential abundance analyses of proteins in EV versus WCL or EV vs EV were performed using the empirical Bayes method available in *limma* [52,54]. The resulting p-values were adjusted using the Benjamini-Hochberg approach [55] and the significance threshold was set at an adjusted p-value of 0.01 and a $\log_2$(fold change) of 1. Results of the differential abundance analyses are available in Supplementary Data S2 and Supplementary Data S6.

Functional enrichment analysis and clustering

The online tool FungiFun2 version 2.2.8 (sbi.hki-jena.de/fungifun) was used for all GO term enrichment analyses [56]. The hypergeometric distribution significance test was used and resulting p-values were adjusted using the Benjamini-Hochberg procedure. Enriched GO terms were those with an adjusted p-value less than 0.01. Full results from the functional enrichment analyses are presented in Supplementary Data S3 and S7. Multidimensional scaling (MDS) plots were constructed using the plotMDS function from *limma* [52]. To construct the heatmap in (Figure 5), unsupervised clustering of $\log_2$(FC) for the proteins common to EVs from all strains was performed using Gower's formula via the daisy function from the R package *cluster* [57].

Protein localisation and attribute prediction

Location information of proteins was obtained from the Candida Genome Database (candidagenome.org) or the *C. albicans* UniProt reference proteome (UP000000559; downloaded 16/06/2018; 6035 entries) [48,49,58]. When this information was not available, the subcellular location of a *C. albicans* protein was inferred from the *S. cerevisiae* homolog as annotated in the Candida Genome Database [48,49]. Signal peptide and transmembrane domain annotations for each protein were obtained from UniProt or were predicted using TOPCONS2 (topcons.cbr.su.se) [58,59]. Prediction of protein palmitoylation sites was performed using CSS-PALM 4.0 (csspalm.biocuckoo.org) [60].

C. albicans *EV marker definition*

Lists of proteins significantly enriched and exclusive to EVs from each strain were compared using the R package *VennDiagram* [61]. Proteins common to all the three strains and both morphologies were selected as potential EV positive protein markers. This was repeated for significantly enriched and exclusive proteins in WCL to define potential EV negative protein markers. Initial candidate EV marker proteins were refined using the following criteria to obtain a shortlist of the best potential markers. Ideal positive EV markers were proteins that satisfied MISEV2018 marker categories 1 and 2 [15] and had less than five transmembrane domains, no recognisable signal peptide, and were not detected in vesicle-depleted media [31]. Ideal negative EV marker proteins were selected based on prior tagging with fluorescent proteins in literature, prior detection via Western blot, and adherence to MISEV2018 marker categories 3 or 4 [15].

Data availability

The proteomics data have been deposited in the ProteomeXchange Consortium database via the PRIDE partner repository [62,63] with the data set identifiers PXD014367 (DAY286 yeast), PXD014388 (ATCC90028 and ATCC10231) and PXD014389 (DAY286 biofilm). These data include "RAW" files, peak list files, MaxQuant search parameters, MaxQuant search engine txt output and the UniProt *C. albicans* reference proteome FASTA file. The proteinGroups.txt files and source code used in this study is freely available in an online research compendium available at github.com/csdaw/candidaev. It was constructed using the R package *rrtools* [64] and is structured as an R package which can be used to reproduce the results as submitted. The compendium has also been permanently archived at zenodo (https://www.doi.org/10.5281/zenodo.3747549).

Results

EV size distribution is dependent on the C. albicans source strain

EVs were isolated from different strains using a modified version of the differential ultracentrifugation method defined by [28] (Supplementary Figure S1). The strains included the clinical isolate strains ATCC90028 (isolated from blood) and ATCC10231 (isolated from a patient with bronchomycosis). Areference strain commonly used in experiments with *C. albicans* mutants, DAY286,

was also assessed in both yeast and biofilm morphology. Characterisation was performed in accordance with the MISEV2018 recommendations wherein the EV preparation and the EV source are imaged and described quantitatively [15]. Information on each EV preparation used for proteomics experiments and the EV source culture is provided in Supplementary Table S1.

The final protein yield of the EV samples ranged from 18.0 to 71.6 µg with concentrations of 0.192 to 0.716 µg/µL (Supplementary Table S1). EVs from DAY286 yeast and ATCC90028 had a higher protein content than those from ATCC10231 cultures and DAY286 biofilms.

TEM visualisation revealed cup-shaped particles typically 200 nm or less in diameter as well as some non-vesicular co-isolated components (Figure 1(A)). Nanoparticle tracking analysis (NTA) of the EV preparations agreed with the TEM imaging, revealing that the mode size of *C. albicans* EVs isolated at 100,000 x g was less than 200 nm for all samples (Supplementary Table S1). The EVs examined in this study are primarily "small EVs" (sEVs) as defined in MISEV2018 [15], hence the proteomics results are relevant for sEVs and not necessarily larger EVs.

The distribution of EV particle size differed slightly for each strain (Figure 1(B), Supplementary Figure S2). The yeast form strains had a broader range of EV sizes, with particles up to 500 nm being detected. Conversely, the biofilm EVs showed a tight, symmetrical distribution centred around 100 nm. Interestingly, EVs from both ATCC strains had a significantly larger mode diameter than EVs from either morphology of DAY286 (Supplementary Figure S3A) which was reflected by a lack of detected particles for ATCC strain EVs below 100 nm (Figure 1(B)). The total particle concentration of EVs from ATCC90028, DAY286 yeast and DAY286 biofilm was not significantly different (Supplementary Figure S3B), and typically ranged from 1 to 3 × 10^{12} particles/mL; although one exceptional biofilm EV preparation had 8 × 10^{12} particles/mL that skewed the biofilm average (Supplementary Table S1). Conversely, the particle concentration of ATCC10231 EVs was lower than all the other EV samples (2 to 5 × 10^{11} particles/mL), but this difference was only significant compared to the biofilm EV preparations (Supplementary Figure S3B). Comparing the ratio of particles per µg of protein for each EV sample revealed that DAY286 biofilm EVs had a significantly higher ratio of particles per µg of protein than the other *C. albicans* EVs.

C. albicans *strains show similar numbers of differentially abundant EV proteins*

MaxQuant and the Andromeda search engine were used to identify proteins in EVs and WCL for each

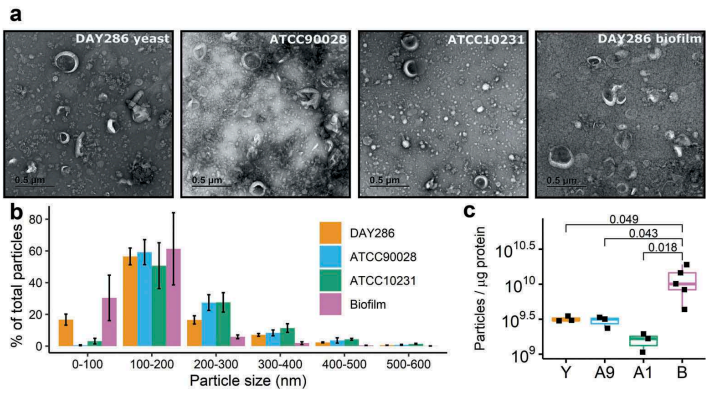

Figure 1. Characterisation and quantification of EVs from different *C. albicans* strains. *(a)* Representative TEM images of EVs isolated from different *C. albicans* strains. Scale bar indicates 0.5 µm. *(B)* Size distribution of DAY286 yeast (n = 3), ATCC90028 yeast (n = 3), ATCC10231 yeast (n = 3), and DAY286 biofilm (n = 5) EVs as measured by nanoparticle tracking analysis. Bar plots show the percentage of the total number of EVs that can be assigned to each size range. The size of the bars indicates the mean percentage across each biological replicate and the error bars indicate the standard error of the mean. NTA traces for the individual biological replicates are presented in Supplementary Figure S2. *(C)* Comparison of the ratio of particle concentration to protein concentration of the EV fraction, (particles/mL) ÷ (µg protein/mL), across the four EV sources. Each dot represents one biological replicate. Sample means were compared using One-way ANOVA followed by Tukey's HSD *post-hoc* test. Adjusted p-values indicating significant differences are shown. The particle and protein concentrations for each biological replicate are provided in Supplementary Table S1.

strain (Figure 2(A)). Raw MS/MS spectra were used to query the *C. albicans* (SC5314) reference proteome in the UniProt database. Initially, proteins identified by less than two unique peptides were removed. Proteins with two or more unique peptides were filtered to ensure that they were detected in at least 2/3 replicates of EV or WCL for the yeast strains and 4/5 replicates of EV or WCL for the biofilm strain. EV proteins remaining post-filtering ranged from 690 in DAY286 yeast EVs to 1202 proteins in ATCC90028 yeast EVs. Similarly, WCL proteins numbered from 760 for DAY286 yeast WCL to 1229 for ATCC90028. There was at least a 50% overlap between the proteins quantified in EVs and those in WCL for each strain. The biofilm samples had the highest degree of overlap at 77.1% whilst for ATCC10231 54.8% of proteins were common to EVs and WCL (Figure 2(A)). For all strains, the number of proteins exclusive to EVs was less than WCL exclusive proteins. Of the proteins quantified in EVs from DAY286 biofilms or yeast cells, 44% were common (Supplementary Figure S4A).

Differential abundance analysis was performed on the common EV and WCL proteins from each strain to identify enriched proteins (Figure 2(B)). The full results including $\log_2$(FC) values and p-values are available in Supplementary Data S2. Following imputation of missing values, the mean normalised $\log_2$ LFQ intensities for each protein were compared using the empirical Bayes method implemented in *limma* [52,54]. The resulting t-statistics were adjusted using the Benjamini-Hochberg method [55] and an adjusted p-value cut-off of 0.01, along with a $\log_2$(FC) cut-off of 1, was used to identify significantly enriched EV and WCL proteins for each strain (Figure 2(B)). a similar number of proteins were significantly enriched in EVs compared to WCL across all datasets. The number of EV-enriched proteins ranged from 101 to 121 whereas the number of WCL-enriched proteins ranged from

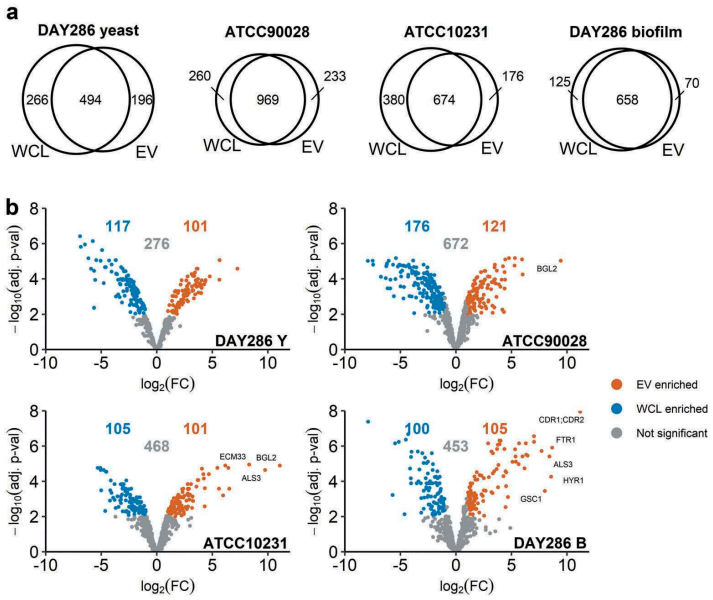

Figure 2. Differential abundance analysis of proteins identified in *C. albicans* EVs and whole cell lysates (WCL). *(a)* Venn diagrams comparing the EV and WCL proteomes from four *C. albicans* strains; DAY286 yeast (n = 3), ATCC90028 yeast (n = 3), ATCC10231 yeast (n = 3), and DAY286 biofilm (n = 5). Whole cell lysates were prepared from the EV source cells. Proteins were quantified (MaxQuant LFQ intensity) in a minimum of 2/3 (yeast) and 4/5 (biofilm) biological replicates of EV or WCL. *(B)* Volcano plots depicting significantly enriched EV or WCL proteins. Differential abundance analysis was performed by comparing the mean normalised LFQ intensities of proteins identified in both EV and WCL (i.e. proteins in the Venn overlap) using the package *limma* [47,52]. Significantly enriched proteins were identified using a Benjamini-Hochberg adjusted p-value cut-off of 0.01 and $\log_2$(FC) cut-off of 1. Counts of significant and non-significant proteins are indicated on each graph. Proteins with a $\log_2$(FC) greater than 8 are labelled. Data tables underlying the Venn diagrams and volcano plots are provided in Supplementary Data S2.

100 to 176. The differential abundance analysis was repeated to compare the enrichment of proteins common to DAY286 yeast and biofilm EVs (Supplementary Figure S4B, Supplementary Data S6). From the 433 shared proteins, 129 were significantly enriched in biofilm EVs versus 136 proteins which were significantly more abundant in DAY286 yeast EVs.

Cell wall and pathogenesis proteins are overrepresented in EVs

We performed functional enrichment analyses on proteins significantly enriched or exclusive to *C. albicans* EVs from each strain (Figure 2(A,B)) to explore whether there were common biological roles for the cargo, and to provide insight on potential functions of *C. albicans* EVs (Figure 3). This was implemented using the online resource FungiFun2 which is a web-tool specific for analysis of fungal genes and proteins [56]. In agreement with previous reports [24,31], fungal-type or yeast-type cell wall organisation were significantly enriched biological processes that were identified for all four types of EVs. Furthermore, *C. albicans* EV proteins from all isolations were commonly associated with the *C. albicans* cell wall, the plasma membrane, or generally to the cell surface. Proteins involved in ER localisation and protein glycosylation were overrepresented in the three yeast EV data sets (Supplementary Data S3) and may relate to the production of glycoproteins that are directed to the fungal cell wall. Enrichment of ER, cell wall and plasma membrane proteins suggest that the EVs contain a mix of EV subtypes derived from potentially different vesicle biogenesis pathways.

EVs from the two clinical isolates ATCC90028 and ATCC10231 as well as the DAY286 biofilms were enriched for proteins that function in pathogenesis, consistent with the notion that EVs are crucial to the interaction between the fungus and the host. For example, proteins with aspartic protease activity and adhesion functions which were enriched in ATCC10213 and biofilm EVs are linked to *C. albicans* virulence [65,66]. All EV data sets were enriched with proteins with 1,3 beta-glucanosyltransferase activity. However, the biofilm EVs were also enriched with proteins with exo-1,3-beta-glucosidase activity indicating that the role for EVs in cell wall dynamics may change between morphologies.

Consequently, we performed functional analyses on the differentially abundant proteins found in DAY286 biofilm and yeast EVs to explore how EV function may change depending on source cell morphology (Supplementary Figure S5). Compared to biofilm EVs, DAY286 yeast EVs were enriched in ribosomal and mitochondrial proteins and proteins that function in post-translational modification. EVs from *C. albicans* biofilms have been shown to function in extracellular matrix biogenesis [32], which was reflected here by an enrichment of cell surface and cell wall proteins that function in carbohydrate metabolism. Furthermore, biofilm EVs were enriched in oxidative and heat stress response proteins, which is reflective of the different growth conditions compared to DAY286 yeast EVs.

WCL proteomes have a higher degree of similarity than the EV proteomes from four C. albicans strains

EV proteins from each isolation were compared to identify proteins that are packaged into *C. albicans* EVs, regardless of cell morphology or strain. Of the 1487 proteins quantified in EVs across the four data sets, 396 (26.7%) were common to all (Figure 4(A)). Conversely, more WCL proteins; 556 out of 1389 proteins (40.0%) were common to the four proteomes (Figure 4(B)).

The relationship between the *C. albicans* proteomes presented in this study was explored further via multi-dimensional scaling plots (Figure 4(C,D)). Dimension 1, which represents the leading factor explaining the $\log_2$(FC) between the four data sets, separates the samples based on source strain; DAY286 versus both ATCC strains. The second dimension shows a batch effect associated with each LC-MS/MS experiment. The two ATCC strains cluster closely together, away from both DAY286 yeast and biofilm. Likewise, the two ATCC sample sets were run on the MS and analysed together, whereas the other two strains were run separately and analysed separately. Finally, dimension 3 separates the samples according to the primary condition of interest; EVs versus WCL (Figure 4(D)).

Immunogenic cell surface and cell wall organisation proteins are universally EV enriched

The 396 proteins common to EVs from all sources (Figure 4(A)) were assessed by unsupervised hierarchical clustering to group proteins based on their $\log_2$ (FC) across the four data sets, with the results plotted in a heatmap (Figure 5). The proteins were grouped into eight clusters, C1 to C8. C1, C2 and C3 contained proteins that were highly enriched or exclusive to EVs with an abundance of proteins that were exclusive to one or more EV isolations. C4 also contained EV enriched proteins which were largely not EV exclusive. C5 and C6 contained proteins with varied relative abundance in EVs versus WCL, with C7 containing highly WCL enriched proteins. Finally, C8 included

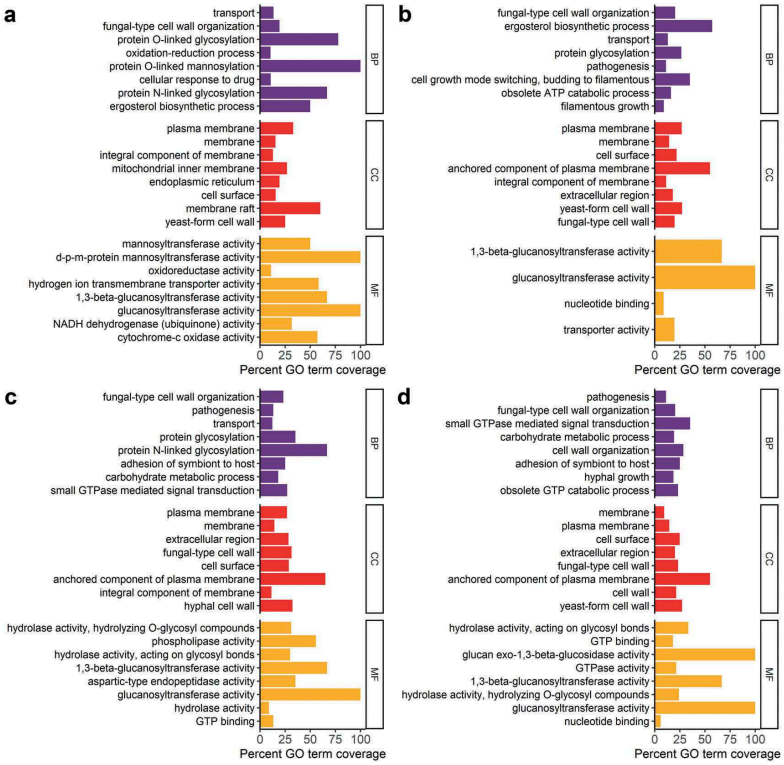

Figure 3. Functional enrichment analyses of the significantly enriched and exclusive *C. albicans* EV proteins. The online tool FungiFun2 (elbe.hki-jena.de/fungifun) was used to identify enriched biological process (BP), cellular component (CC), and molecular function (MF) GO terms [56] based on EV enriched or exclusive proteins from *(a)* DAY286 yeast, *(B)* ATCC90028, *(C)* ATCC10231, and *(D)* DAY286 biofilm. The top 8 (where present) significantly enriched terms for each GO domain are shown (Hypergeometric distribution, Benjamini-Hochberg adjusted p-value < 0.01). They are presented top to bottom in order of increasing Benjamini-Hochberg adjusted p-value. Full lists of enriched GO terms can be found in Supplementary Data S3.

proteins that were exclusive to EVs across all four data sets. These could not be included in the cluster analysis because they did not have any valid $\log_2$(FC) values and were appended to the heat map manually. Supplementary Data S5 contains the names and functions of all the proteins represented in the heatmap in order of appearance from top to bottom.

GO enrichment analyses of the proteins in each of these clusters were performed to provide further insight into the functional roles of *C. albicans* EV proteins with similar $\log_2$(FC) patterns. The 13 proteins in C8 are cell surface/wall (Crh11, Mp65, Msb2, Pga4, Pga52, Plb4.5, Sap9) or plasma membrane-localised proteins (Cdc42, Ena21, Hgt1, orf19.6741, Phm7, Rho3) involved in cell wall organisation, establishment of cell polarity and pathogenesis. Many of the cell surface/wall proteins, such as Mp65 and Bgl2, are immunogenic and are released extracellularly by soluble secretion as well as in vesicles *in vitro* [31,67,68]. C1, C2 and C3 also contain primarily plasma membrane-associated proteins, many of which function in cell wall biosynthesis and organisation, morphogenesis and pathogenesis. Of note is the enrichment of proteins from the eisosome; a fungal plasma membrane domain also known as the membrane compartment containing Can1 (MCC). Several

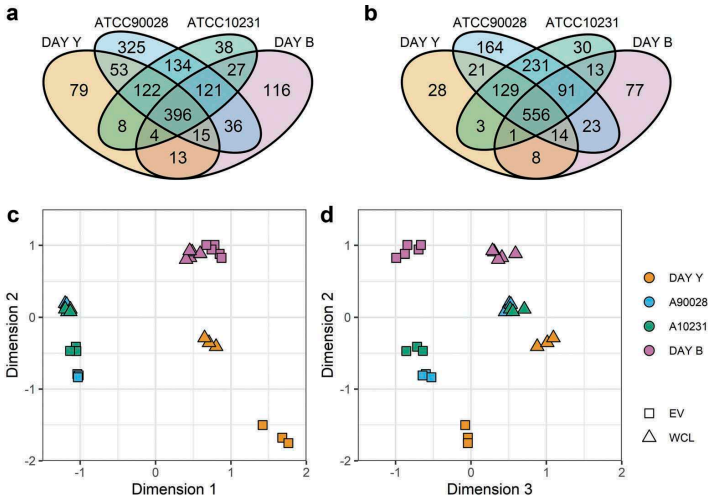

Figure 4. **Combined comparison of *C. albicans* proteomes**. *(a)* Venn diagram comparing four *C. albicans* EV proteomes. Lists of EV proteins present in the Venn diagrams in Figure 2A were compared to identify proteins common to all four EV datasets. *(B)* Venn diagram comparing four *C. albicans* WCL proteomes. Lists of WCL proteins present in the Venn diagrams in Figure 2A were compared to identify proteins common to all four WCL datasets. The data tables underlying Figuress 4A and 4B are provided in Supplementary Data S4. *(C)* Multidimensional scaling (MDS) plot of each LC-MS/MS biological replicate sample with the first 2 dimensions shown. Pairwise distance between samples approximately indicates the log2(FC) between samples. The plotMDS function from *limma* was used to generate the MDS plots [52]. *(D)* MDS plot of each LC-MS/MS biological replicate sample with the second and third dimensions shown.

MCC/eisosome proteins are EV enriched or exclusive across all *C. albicans* strains including the transmembrane proteins Sur7, Nce102, orf19.6741. The cytosolic eisosome proteins Lsp1 and Pil1 were also detected in EVs but were not enriched. C1 also contains the multidrug transporter Cdr1 (and Cdr2, which cannot be distinguished from Cdr1 based on the peptides identified in this study) that is associated with azole resistance [69]. The locations and functions of C4 proteins are more varied but importantly include GTPases and secretory pathway proteins. Small GTPases are associated with intracellular vesicular trafficking and regulate a variety of membrane fusion events [70,71]. C5, C6 and C7 proteins are mostly cytosolic or ribosomal proteins with functions in glycolysis and translation.

Putative C. albicans EV positive markers include trans-plasma membrane domain Sur7 family proteins

Potential protein markers for *C. albicans* EVs were selected firstly on the criteria that they were EV exclusive or significantly enriched in EVs. That is, the proteins had a $\log_2$(FC) greater than 1 and adjusted p-value of less than 0.01 across all four datasets (Figure 6(A)). The 47 candidate positive EV markers that were identified are listed in Table 1. These proteins are mostly located on the plasma membrane and cell surface, with ER, endosome and vacuole proteins also represented. Of note were two mitochondrial proteins, which were unexpectedly enriched across all strains.

The 47 candidate proteins were filtered according to specific criteria (Supplementary Figure S1) to obtain a list of the best potential markers for future use. Proteins with signal peptides that had previously been detected in a proteomic analysis of *C. albicans* vesicle-depleted culture medium (VDM) [31], and proteins with more than 5 predicted transmembrane domains were not considered the best marker candidates. This was because proteins with signal peptides that have been detected in VDM are likely secreted canonically as well as in EVs, hence they would not be EV-specific markers. Furthermore, though marker candidates with numerous transmembrane domains such as GSC1 are likely to be secreted specifically in EVs, they may prove difficult to work with in subsequent applications. Following this refinement, 22 proteins were identified as ideal *C. albicans* EV positive markers (Figure 7). These

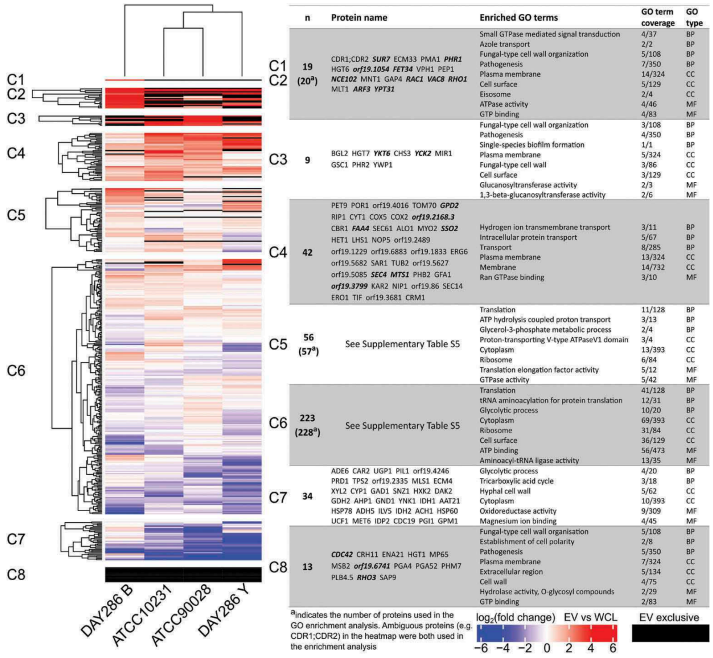

Figure 5. Identification of commonly enriched EV proteins across different *C. albicans* strains. Heatmap of proteins identified in all four EV samples (n = 396, Venn overlap in Figure 4A). Each column represents a *C. albicans* strain and each row represents a protein. The colours indicate the $\log_2$(FC) of the protein for that particular strain; red is EV enriched, blue is EV depleted, and black is EV exclusive. Unsupervised clustering of rows and columns was performed using Gower's formula via the daisy function from the R package *cluster* [57]. Proteins which were exclusive to EVs in all four data sets and therefore had no valid $\log_2$(FC) values were separated prior to clustering, in the group designated "Cluster 8". Functional enrichment analyses were performed on the heatmap protein clusters using the online tool FungiFun2 [56]. a selection of significantly enriched GO terms, biological process (BP), cellular component (CC), and molecular function (MF), are presented in the table inset. Full lists of enriched GO terms and proteins in each cluster are available in Supplementary Data S3 and S5 respectively. Proteins in bold italics are the 22 putative *C. albicans* EV marker proteins presented in Figure 7.

included trans-plasma membrane proteins such as the Sur7 family proteins orf19.6741 and Sur7 (Pfam: PF06687) and the MARVEL family protein Nce102 (Pfam: PF01284). Anumber of GTPases, which associate with the plasma membrane (Arf3, Cdc42, Rac1, Rho1, Rho3) and secretory pathway (Sec4, Ypt31), respectively, were also determined to be ideal marker candidates. The 22 proteins were only present in clusters C1-C4 and C8 of the heatmap in Figure 5 which included only proteins that were consistently enriched across all four proteomics experiments. Metadata regarding these proteins including their localisation and associated GO terms are provided in Supplementary Data S8.

The process for defining candidate EV positive markers was repeated to identify potential EV negative markers. Specifically, the lists of exclusive and significantly enriched WCL proteins from each strain were compared (Figure 6 (B)). Sixty-two proteins were selected as potential negative EV markers (Supplementary Table S2). These candidates were refined to a short-list of seven proteins which have been fluorescently tagged or detected by Western blot in previous literature. The 7 proteins are located in the mitochondria (Lpd1, Sod2), vacuole (Apr1, Cpy1, Lap41), cell wall (Gpm1) and actin cortical patches (Abp1).

Discussion

EVs are increasingly being identified as crucial components of cell-cell communication. Most EV studies have

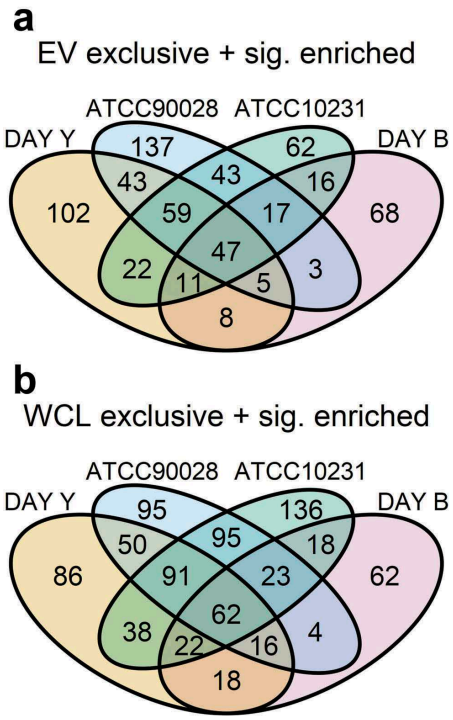

Figure 6. Identification of common significantly enriched or exclusive *C. albicans* EV and WCL proteins. Proteins identified as significantly enriched or exclusive to EVs in Figure 2 were compared to select those which were common to all four datasets. (A) 47 proteins were identified as potential positive EV protein markers and (B) 62 proteins as potential negative EV protein markers. The data tables underlying Figure 6 are provided in Supplementary Data S4. Details of the 47 positive EV protein marker candidates and 62 negative candidates can be found in Table 1 and Supplementary Table S2, respectively.

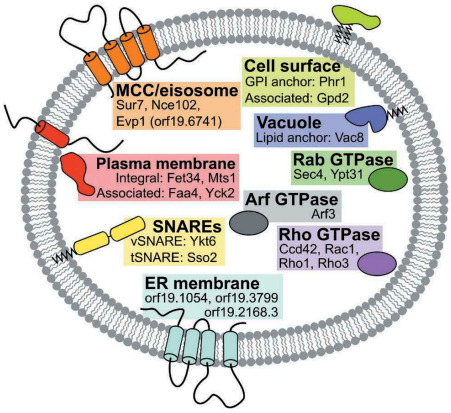

Figure 7. Twenty-two best potential *C. albicans* positive EV protein markers. The most promising EV marker proteins are underlined in Table 1. They are enriched or exclusive to EVs isolated from all the *C. albicans* strains investigated in this study. The proteins fit within the EV biomarker categories 1 and 2 from MISEV2018 which includes transmembrane, GPI-anchored, and cytosolic proteins that are EV enriched [15].

been performed in mammalian systems and a reliable set of EV-specific marker proteins has been identified [15]. These markers have been invaluable for tracking EVs during isolation and have also been exploited for immunoaffinity purification and monitoring of EV release and distribution *in vivo* with fluorescently tagged markers [72–74]. More recently EVs have been identified in a range of yeast and filamentous fungi and their importance in fungal biology has been acknowledged particularly in the interaction between the fungal pathogens and their hosts [75]. However, research on fungal EVs has been limited to the basic techniques developed early in the investigation of mammalian EVs because of the absence of suitable marker proteins to assist in purification and tracking in biological systems. Many of the mammalian EV marker proteins either have no homologs in fungi, or the homologs are not found in fungal EVs [26]. This has led to the need for *de novo* identification of fungal EV protein markers based on the recommendations outlined in MISEV2018 [15]. These markers will enable researchers to adapt cutting edge techniques from mammalian EV research to the study of fungal EVs.

We have defined a suite of 22 proteins that are putative markers of *C. albicans* EVs (Figure 7). These positive markers are complemented by seven negative markers that are depleted or absent from EVs versus cell lysates. Both sets of markers were identified from analysis of robust proteomic data sets generated from multiple, independent isolations of EVs from three *C. albicans* strains grown in the yeast form and one strain grown as a biofilm. This represents a step change in the quality of proteomic data published for *C. albicans* EVs as three out of four previous studies analysed EVs from a single isolation [26]. Thus, we are highly confident that the proteins we have identified as putative EV markers are present in *C. albicans* EVs. These markers will need to be validated in future studies using techniques including Western blotting, immunogold labelling on TEM and/or Nano-FACS. The validation studies will depend on generation of

antibodies to EV marker proteins, particularly the extracellular loops of membrane proteins, as no commercial antibodies to specific *C. albicans* proteins are available. One putative marker, Hgt1, has already been independently confirmed to be packaged into *C. albicans* EVs using immunogold labelling and electron microscopy [76]. The immunogold TEM images from Kenno et al. [76] show the plasma membrane protein Hgt1 present in the membrane of small EVs released from the *C. albicans* strain SN152. This result not only confirms Hgt1 as *C. albicans* EV cargo, but also demonstrates that the markers presented here may be applicable to EVs isolated from *C. albicans* strains other than those assessed in this study.

Generally, the EVs isolated in this study had morphologies and size distributions consistent with published data [23,24,31,32]. The main difference was in the number of proteins identified in EVs. Initial investigations into the proteome of *C. albicans* yeast EVs repeatedly found fewer than 100 proteins [23,24,31]. We identified 690–1202 proteins in EVs, which is consistent with the most recent *C. albicans* EV report which identified 862 and 729 proteins in yeast and biofilm EVs, respectively [32]. In addition to the improved quality of our data due to analysis of multiple biological replicates for EVs from each strain, this work also represents the first comparative label-free quantitative analyses of proteins in *C. albicans* EVs and their parent planktonic cells. This is particularly important because our meta-analysis of previously published EV proteomes revealed only 12 proteins that were common to all available data sets [26]. Ten of these were also detected in all four EV proteomes in this study (Supplementary Data S1) but there was no consistent significant difference in abundance between EVs and WCL for seven of the proteins (Eft2, Eno1, Hsp70, Pdc11, Pgk1, Tal1 and Tdh3) (Supplementary Data S2). Furthermore, one protein (Gpm1) was consistently EV depleted compared to WCL. Two out of ten proteins were confirmed as enriched in all EVs tested; the cell surface glycosidase Phr2 and the aspartyl protease Sap9.

Phr2 and Sap9 were among 47 proteins that were either unique or significantly enriched in EVs across the four EV proteomes analysed in this study. To identify putative markers for *C. albicans* EVs, we refined these 47 proteins to eliminate those with unfavourable characteristics for downstream applications or where there was published data indicating that they are not secreted exclusively within EVs [31]. This left us with 22 potential markers that could be grouped into two broad categories, transmembrane/GPI-anchored proteins and lumenal/cytosolic proteins, which align with MISEV2018 biomarker categories 1 and 2.

The cytosolic/lumenal group of marker proteins consists mainly of GTPases, which are associated with different internal membranes. Rho-type GTPases (Rho1, Rho3, Rac1 and Cdc42) are of particular interest because they are from the same protein family as the mammalian EV marker RhoA, which is involved in microvesicle biogenesis alongside Rac1 [77,78]. The primary role of *C. albicans* Rho GTPases is in polarised growth and morphogenesis [79–81], but we show they may also have a role in vesicle release from the fungal plasma membrane. This is supported by the enrichment of Arf3 in all four EV data sets (Table 1). Arf3 is the *C. albicans* homolog of human ARF6, a key regulator of selective cargo recruitment and microvesicle shedding [82].

Potential functional roles of *C. albicans* EVs may also be related to other activities of Rho GTPases. EVs from *S. cerevisiae* are enriched for the cell wall 1,3-β-glucan synthase Fks1 and can provide a protective effect against the 1,3-β-glucan synthase inhibitor caspofungin [83]. Rho1 is the essential regulatory GTPase that forms a complex with the 1,3-β-glucan synthase in *C. albicans*, Gsc1 [84]. This 1,3- β-glucan synthase in *C. albicans* is also enriched in EVs, supporting a conserved role for EVs in cell wall maintenance between *S. cerevisiae* and *C. albicans*.

The four non-plasma membrane associated cytosolic/luminal markers are predicted to associate with secretory compartments (Ykt6, Sec4, Ypt31), and the vacuole (Vac8). These proteins all have roles in intracellular vesicle transport in yeast [85–87], particularly the v-SNARE Ykt6 which is involved in vesicle fusion to the ER, Golgi and vacuole [88,89]. In *Drosophila* and human cells, Ykt6 is required for sorting of Wnt proteins into exosomes for secretion [90,91]. Interestingly, another SNARE protein similar to human syntaxin-2 was enriched in all the EV proteomes (Supplementary Data S2). This t-SNARE, Sso2, is an integral membrane protein involved in the fusion of secretory vesicles with the plasma membrane [92]. Enrichment of these proteins may reflect an endocytic origin of some *C. albicans* EVs, similar to exosomes produced via fusion of multivesicular bodies with the plasma membrane in mammalian cells [73]. This is supported by the abundance of the Rab GTPases Sec4 and Ypt31 which function in the vesicular exocytic pathway of *C. albicans* and *S. cerevisiae* [87,93].

The transmembrane/GPI-anchored proteins could be grouped into four subcellular locations; the membrane compartment of Can1 (MCC)/eisosome, the cell surface, the plasma membrane and the ER membrane. Of these the MCC/eisosome proteins, Sur7 and orf19.6741 were the most intriguing.

Sur7 is a four TM domain protein present in the plasma membrane in stable, sphingolipid and ergosterol enriched microdomains known as the MCC [94]. orf19.6741 is a non-essential, chlamydospore induced gene which encodes a predicted 3 TM domain protein homologous to the *S. cerevisiae* MCC/eisosome protein Pun1 [95,96]. Based on the detection of the orf19.6741 protein exclusively in all EV samples with particularly high abundance, we designate this protein as 'EV associated Protein 1′ or Evp1. Sur7 and Evp1 are both part of the fungal-specific Sur7 family (Pfam: PF06687). This family describes a group of fungal specific transmembrane proteins which localise to the plasma membrane and have a conserved cysteine motif similar to mammalian claudins [97,98]. Alongside their similarities to claudins, Sur7 and Evp1 have predicted topologies reminiscent of mammalian tetraspanins, which are key markers for mammalian EVs (Figure 8) [15]. Tetraspanin family (Pfam: PF00335) proteins have four transmembrane alpha helices and two extracellular loops, one short and one long which contains four or more conserved cysteine residues. Similarly, Sur7 and Evp1 have 4 or 3 predicted transmembrane domains, with two extracellular loops of different lengths. The long extracellular loops of Sur7 and Evp1 have at least two cysteine residues in a conserved motif.

We hypothesize that Sur7 and Evp1 will be ideal *C. albicans* EV markers after validation because of their potential topological similarity to tetraspanin EV markers, specifically CD9, CD81 and CD63. The utility of tetraspanins as EV markers is characterised by their abundant and broad expression in different cell types, their stability as part of tetraspanin-enriched microdomains (TEMs) in EV membranes, and the plethora of monoclonal antibodies that are available for them. Antibodies raised against tetraspanins typically bind to epitopes in the large extracellular loop [99–102], which protrudes from the EV surface. This interaction has been exploited to isolate EVs from complex biological fluids such as plasma, serum and urine

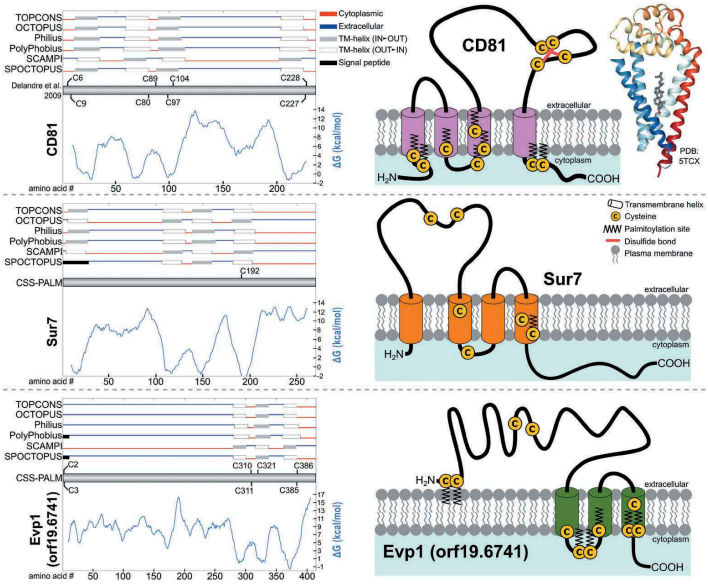

Figure 8. Predicted topology and palmitoylation sites of *C. albicans* MCC/eisosome proteins Sur7 and Evp1 (orf19.6741) compared to the human tetraspanin CD81. TOPCONS2 (topcons.cbr.su.se) [59] was used to analyse the amino acid sequences of human CD81 and *C. albicans* Sur7 and Evp1 to predict their topology and the location of transmembrane (TM) domains. The hydrophobicity plots (light blue chart) and topology diagrams (red and blue lines) are shown on the left side of the figure. Additionally, cysteine residues of Sur7 and Evp1 predicted to be palmitoylated using CSS-PALM 4.0 (csspalm.biocuckoo.org) have been annotated [60]. For CD81, palmitoylation sites experimentally determined in previous literature are shown [119]. The right side of the figure shows a cartoon representation of the TOPCONS2 consensus topology prediction for the three proteins as well as the crystal structure of CD81 (PDB: 5TCX) [120].

[72,103,104]. Unfortunately, commercial antibodies for Sur7 are not available and Evp1 has largely been investigated at the transcript level [96,105]. However, if these Sur7 and Evp1 are validated as *C. albicans* EV membrane proteins, then raising antibodies against their extracellular loops would be vital for future *in vivo* research. Alternatively, the genetic manipulability of *C. albicans* means that the expression of fusion proteins is relatively simple and rapid [106], as demonstrated for Sur7 [98]. Isolation of EVs from *C. albicans* strains with GFP-tagged Sur7 or Evp1 will enable monitoring of EVs via fluorescence or the use anti-GFP antibodies for EV marker detection via Western blot. Furthermore, if the predicted topology of Evp1 is correct, expression of Evp1 with a small N-terminal tag may permit immunocapture of *C. albicans* EVs.

Of the 22 putative *C. albicans* EV markers, the MCC/eisosome proteins Sur7 and Evp1 are certainly the most promising candidates. Interestingly, other MCC/eisosome proteins including Nce102, Pil1 and Lsp1 were detected in all four EV proteomes and Fmp45 was quantified in both DAY286 data sets. MCC/eisosomes are important for cell wall synthesis and organisation as well as the recruitment of proteins to the plasma membrane [107]. We speculate that these fungal-specific microdomains also have a role in EV biogenesis from *C. albicans*, and potentially other fungi, based on the role of TEMs in sorting specific cargo into mammalian EVs [108].

To supplement the positive EV markers, we selected 62 proteins that were significantly less abundant in, or were absent from *C. albicans* EVs as potential negative markers. They included ribosome associated proteins such as Tif11 and Tma19, which are potential MISEV2018 category 3 markers. Proteins of this category are part of non-EV co-isolated structures (such as ribosomes) and their depletion in EV isolations is a measure of purity [15]. The 62 candidates were refined to seven proteins that had been interrogated using antibodies or fluorescent constructs as reported in previous literature [109–114]; making them prime targets for initial validation. All seven were from intracellular compartments such as the mitochondria (Lpd1, Sod2), the vacuole (Apr1, Cpy1, Lap41), the cell wall (Gpm1) and actin cortical patches (Apb1) and can be roughly assigned to MISEV2018 marker category 4.

We have focused on the identification of EV marker proteins; however, the biological activities of these proteins provide insight into the function of *C. albicans* EVs. Functional enrichment analysis of the EV proteins indicated a likely role in pathogenesis (Figure 3). Several of the most enriched proteins in all four data sets are antigenic virulence factors involved in morphogenesis such as Bgl2, Mp65 and Phr1 [68,115,116]. Furthermore, hyphal-specific virulence proteins including Xog1, Sap5, Hyr1 and Ece1 are highly abundant in biofilm EVs but absent from the biofilm cell lysates or EVs from yeast-form cells of the same strain (Supplementary Data S2). Also, of note was the enrichment of Cdr1/Cdr2 in EVs from all strains (Table 1). These drug efflux pump proteins are important in the development of resistance to azole antifungals [69]. Their presence in *C. albicans* EVs indicates that EVs may function in azole resistance through transportation of efflux pumps from resistant to non-resistant *C. albicans* cells. This differs from previous studies where *C. albicans* EVs contribute to azole resistance through delivery of matrix components and glucan modification enzymes to promote biofilm growth [32].

Conclusion

In summary, the most promising putative markers for *C. albicans* EVs are the plasma membrane proteins Sur7 and Evp1, which have potential to be the fungal equivalents of the tetraspanin markers used for mammalian EV research. Complementary negative EV markers include the cell surface protein Gpm1, the actin binding protein Apb1, and the intracellular proteins Apr1, Cpy1, Lap41, Sod2 and Lpd1. We are confident that these positive and negative EV marker proteins will be valuable in future investigations on *C. albicans* EVs but antibody-based validation is required. Following *in vitro* validation, these markers will enable the use of a plethora of EV analysis methods, which have not yet been applied to fungal EVs due to the absence of protein markers. Examples include EV immunocapture, *in vitro* tracking of vesicle release and fusion, and *in vivo* monitoring of *C. albicans* EVs over the course of an infection, for example, in mice [73,117,118]. Gaining access to these techniques will allow researchers to answer important questions regarding *C. albicans* EV biology. Specifically, are EVs involved in *C. albicans* pathogenesis *in vivo*, what is their role during infection, and what are the EV biogenesis pathways in *C. albicans*? At this point, it is unclear whether the markers identified in this study will be applicable to other fungal species. Our previous analysis determined that the likelihood of cross-species fungal EV markers is low [26]. Therefore, the process of defining EV enriched markers should be repeated for other pathogenic fungi including *C. neoformans, C. gattii* and *P. brasiliensis*, all of which are known to release EVs.

Acknowledgments

The authors would like to thank Dr Peter Lock from the La Trobe Institute for Molecular Science BioImaging Platform for his help with the TEM imaging.

Disclosure statement

The authors have no conflict of interest.

Funding

This work was supported by a grant awarded to MAA; Australian Research Council [DP160100309].

ORCID

Charlotte S Dawson http://orcid.org/0000-0002-7151-5971
Donovan Garcia-Ceron http://orcid.org/0000-0003-4718-4233
Harinda Rajapaksha http://orcid.org/0000-0001-7521-0991
Pierre Faou http://orcid.org/0000-0002-3755-7502
Mark R Bleackley http://orcid.org/0000-0002-9717-7560
Marilyn A Anderson http://orcid.org/0000-0002-8257-5128

References

[1] Havlickova B, Czaika VA, Friedrich M. Epidemiological trends in skin mycoses worldwide. Mycoses. 2008;51 (s4):2–15.
[2] Benedict K, Jackson BR, Chiller T, et al. Estimation of direct healthcare costs of fungal diseases in the USA. Clin Infect Dis. 2018;68(11):1791–1797.
[3] Pfaller MA, Diekema DJ. Epidemiology of invasive candidiasis: a persistent public health problem. Clin Microbiol Rev. 2007;20(1):133–163.
[4] Brown GD, Denning DW, Gow NAR, et al. Hidden killers: human fungal infections. Sci Transl Med. 2012;4(165):165rv13.
[5] Kullberg BJ, Arendrup MC. Invasive Candidiasis. N Engl J Med. 2015;373(15):1445–1456.
[6] Guinea J. Global trends in the distribution of candida species causing candidemia. Clin Microbiol Infect. 2014;20(Suppl. 6):5–10.
[7] Pappas PG, Kauffman CA, Andes DR, et al. Clinical practice guideline for the management of candidiasis: 2016 update by the infectious diseases society of America. Clin Infect Dis. 2016;62(4):e1–e50.
[8] Whaley SG, Berkow EL, Rybak JM, et al. Azole antifungal resistance in candida albicans and emerging non-albicans Candida species. Front Microbiol. 2017;7:2173.
[9] Perlin DS. Mechanisms of echinocandin antifungal drug resistance. Ann N Y Acad Sci. 2015;1354(1):1–11.
[10] Perlin DS, Rautemaa-Richardson R, Alastruey-Izquierdo a. The global problem of antifungal resistance: prevalence, mechanisms, and management. Lancet Infect Dis. 2017;17(12):e383–e392.
[11] Fisher MC, Hawkins NJ, Sanglard D, et al. Worldwide emergence of resistance to antifungal drugs challenges human health and food security. Science. 2018;360 (6390):739–742.
[12] Xu R, Rai a, Chen M, et al. Extracellular vesicles in cancer - implications for future improvements in cancer care. Nat Rev Clin Oncol. 2018;15(10):617–638.
[13] Quek C, Hill AF. The role of extracellular vesicles in neurodegenerative diseases. Biochem Biophys Res Commun. 2017;483(4):1178–1186.
[14] Pathirana RD, Kaparakis-Liaskos M. Bacterial membrane vesicles: biogenesis, immune regulation and pathogenesis. Cell Microbiol. 2016;18(11):1518–1524.
[15] Théry C, Witwer KW, Aikawa E, et al. Minimal information for studies of extracellular vesicles 2018 (MISEV2018): a position statement of the international society for extracellular vesicles and update of the MISEV2014 guidelines. J Extracell Vesicles. 2018;7 (1):1535750.
[16] Maas SLN, Breakefield XO, Weaver AM. Extracellular vesicles: unique intercellular delivery vehicles. Trends Cell Biol. 2017;27(3):172–188.
[17] Schorey JS, Cheng Y, Singh PP, et al. Exosomes and other extracellular vesicles in host-pathogen interactions. EMBO Rep. 2015;16(1):24–43.
[18] Oliveira DL, Freire-de-Lima CG, Nosanchuk JD, et al. Extracellular vesicles from cryptococcus neoformans modulate macrophage functions. Infect Immun. 2010;78(4):1601–1609.
[19] Rodrigues ML, Nakayasu ES, Oliveira DL, et al. Extracellular vesicles produced by cryptococcus neoformans contain protein components associated with virulence. Eukaryot Cell. 2008;7(1):58–67.
[20] Bielska E, Sisquella MA, Aldeieg M, et al. Pathogen-derived extracellular vesicles mediate virulence in the fatal human pathogen cryptococcus gattii. Nat Commun. 2018;9(1):1556.
[21] Vallejo MC, Matsuo AL, Ganiko L, et al. The pathogenic fungus paracoccidioides brasiliensis exports extracellular vesicles containing highly immunogenic α-galactosyl epitopes. Eukaryot Cell. 2011;10 (3):343–351.
[22] da Silva RP, Heiss C, Black I, et al. Extracellular vesicles from paracoccidioides pathogenic species transport polysaccharide and expose ligands for DC-SIGN receptors. Sci. Rep. 2015;5(1):14213.
[23] Wolf JM, Espadas J, Luque-Garcia J, et al. Lipid biosynthetic genes affect candida albicans extracellular vesicle morphology, cargo, and immunostimulatory properties. Eukaryot Cell. 2015;14(8):745–754.
[24] Vargas G, Rocha JDB, Oliveira DL, et al. Compositional and immunobiological analyses of extracellular vesicles released by Candida albicans. Cell Microbiol. 2015;17(3):389–407.
[25] Joffe LS, Nimrichter L, Rodrigues ML, et al. Potential roles of fungal extracellular vesicles during infection. mSphere. 2016;1(4):e00099–16.
[26] Bleackley MR, Dawson CS, Anderson MA. Fungal extracellular vesicles with a focus on proteomic analysis. PROTEOMICS. 2019;19(8):1800232.
[27] da Silva RP, Puccia R, Rodrigues ML, et al. Extracellular vesicle-mediated export of fungal RNA. Sci. Rep. 2015;5(1):7763.
[28] Rodrigues ML, Nimrichter L, Oliveira DL, et al. Vesicular polysaccharide export in cryptococcus neoformans is a eukaryotic solution to the problem of fungal trans-cell wall transport. Eukaryot Cell. 2007;6 (1):48–59.
[29] Oliveira DL, Nimrichter L, Miranda K, et al. Cryptococcus neoformans cryoultramicrotomy and

vesicle fractionation reveals an intimate association between membrane lipids and glucuronoxylomannan. Fungal Genet Biol. 2009;46(12):956–963.
[30] da Silva TA, Roque-Barreira MC, Casadevall a, et al. Extracellular vesicles from paracoccidioides brasiliensis induced M1 polarization in vitro. Sci Rep. 2016;6(1):35867.
[31] Gil-Bona a, Llama-Palacios a, Parra CM, et al. Proteomics unravels extracellular vesicles as carriers of classical cytoplasmic proteins in Candida albicans. J Proteome Res. 2015;14(1):142–153.
[32] Zarnowski R, Sanchez H, Covelli AS, et al. Candida Albicans biofilm–induced vesicles confer drug resistance through matrix biogenesis. PLoS Biol. 2018;16(10):e2006872.
[33] Nobile CJ, Johnson AD. Candida albicans biofilms and human disease. Annu Rev Microbiol. 2015;69(1):71–92.
[34] Taff HT, Nett JE, Zarnowski R, et al. A candida biofilm-induced pathway for matrix glucan delivery: implications for drug resistance. PLoS Pathog. 2012;8(8):e1002848.
[35] Lötvall J, Hill AF, Hochberg F, et al. Minimal experimental requirements for definition of extracellular vesicles and their functions: a position statement from the international society for extracellular vesicles. J Extracell Vesicles. 2014;3(1):26913.
[36] Greening DW, Xu R, Ji H, et al. a Protocol for Exosome Isolation and Characterization: evaluation of Ultracentrifugation, Density-Gradient Separation, and Immunoaffinity Capture Methods. In *Proteomic Profiling: methods and Protocols*. In: Posch a, editor. Methods in molecular biology. New York: Springer New York; 2015. p.179–209. DOI:10.1007/978-1-4939-2550-6_15
[37] Gámez-Valero a, Monguió-Tortajada M, Carreras-Planella L, et al. Size-exclusion chromatography-based isolation minimally alters extracellular vesicles' characteristics compared to precipitating agents. Sci. Rep. 2016;6(1):33641.
[38] Oksvold MP, Neurauter a, Pedersen KW. Magnetic bead-based isolation of exosomes. in *rna interference: challenges and therapeutic opportunities*. In: Sioud M, editor. Methods in Molecular Biology. New York: Springer New York; 2015. p.465–481. DOI:10.1007/978-1-4939-1538-5_27
[39] Suetsugu a, Honma K, Saji S, et al. Imaging exosome transfer from breast cancer cells to stroma at metastatic sites in orthotopic nude-mouse models. Adv Drug Deliv Rev. 2013;65(3):383–390.
[40] Davis DA, Bruno VM, Loza L, et al. Candida albicans Mds3p, a conserved regulator of ph responses and virulence identified through insertional mutagenesis. Genetics. 2002;162(4):1573–1581.
[41] Ramage G, Saville SP, Wickes BL, et al. Inhibition of candida albicans biofilm formation by farnesol, a quorum-sensing molecule. Appl Environ Microbiol. 2002;68(11):5459–5463.
[42] Nguyen SL, Greenberg JW, Wang H, et al. Quantifying murine placental extracellular vesicles across gestation and in preterm birth data with tidynano: a computational framework for analyzing and visualizing nanoparticle data in R. Plos One. 2019;14(6):e0218270.
[43] Greening DW, Nguyen HPT, Elgass K, et al. Human endometrial exosomes contain hormone-specific cargo modulating trophoblast adhesive capacity: insights into endometrial-embryo interactions. Biol Reprod. 2016;94(2). DOI:10.1095/biolreprod.115.134890
[44] Fingerhut LCHW, Strugnell JM, Faou P, et al. Shotgun proteomics analysis of saliva and salivary gland tissue from the common octopus octopus vulgaris. J Proteome Res. 2018;17(11):3866–3876.
[45] Tyanova S, Temu T, Cox J. The maxquant computational platform for mass spectrometry-based shotgun proteomics. Nat Protoc. 2016;11(12):2301–2319.
[46] Cox J, Neuhauser N, Michalski a, et al. Andromeda: a peptide search engine integrated into the maxquant environment. J Proteome Res. 2011;10(4):1794–1805.
[47] Cox J, Hein MY, Luber CA, et al. Accurate proteome-wide label-free quantification by delayed normalization and maximal peptide ratio extraction, termed MaxLFQ. Mol Cell Proteomics. 2014;13(9):2513–2526.
[48] Arnaud MB, Costanzo MC, Skrzypek MS, et al. The Candida Genome Database (CGD), a community resource for candida albicans gene and protein information. Nucleic Acids Res. 2005;33(suppl_1):D358–D363.
[49] Skrzypek MS, Binkley J, Binkley G, et al. The Candida Genome Database (CGD): incorporation of assembly 22, systematic identifiers and visualization of high throughput sequencing data. Nucleic Acids Res. 2017;D45(D1):D592–D596.
[50] R Core Team. R: a language and environmental for statistical computing. R Foundation for Statistical Computing; 2018. Vienna, Austria https://www.R-project.org
[51] Zhang X, Smits AH, van Tilburg GB, et al. Proteome-wide identification of ubiquitin interactions using UbIA-MS. Nat Protoc. 2018;13(3):530–550.
[52] Ritchie ME, Phipson B, Wu D, et al. Limma powers differential expression analyses for rna-sequencing and microarray studies. Nucleic Acids Res. 2015;43(7):e47–e47.
[53] Stacklies W, Redestig H, Scholz M, et al. PcaMethods—a bioconductor package providing PCA methods for incomplete data. Bioinformatics. 2007;23(9):1164–1167.
[54] Phipson B, Lee S, Majewski IJ, et al. Robust hyperparameter estimation protects against hypervariable genes and improves power to detect differential expression. Ann Appl Stat. 2016;10(2):946–963.
[55] Benjamini Y, Hochberg Y. Controlling the false discovery rate: a practical and powerful approach to multiple testing. J R Stat Soc Ser B Methodol. 1995;57(1):289–300.
[56] Priebe S, Kreisel C, Horn F, et al. FungiFun2: a comprehensive online resource for systematic analysis of gene lists from fungal species. Bioinformatics. 2015;31(3):445–446.
[57] Maechler M, Rousseeuw P, Struwf a, et al. Cluster: cluster analysis basics and extensions. R Package Version 208. 2019.
[58] The UniProt Consortium. UniProt: a worldwide hub of protein knowledge. Nucleic Acids Res. 2019;47(D1):D506–D515. .

[59] Tsirigos KD, Peters C, Shu N, et al. The TOPCONS web server for consensus prediction of membrane protein topology and signal peptides. Nucleic Acids Res. 2015;43(W1):W401–W407.
[60] Ren J, Wen L, Gao X, et al. CSS-Palm 2.0: an updated software for palmitoylation sites prediction. Protein Eng Des Sel. 2008;21(11):639–644.
[61] Chen H, Boutros PC. VennDiagram: a package for the generation of highly-customizable venn and euler diagrams in R. BMC Bioinformatics. 2011;12(1):35.
[62] Deutsch EW, Csordas a, Sun Z, et al. The proteomexchange consortium in 2017: supporting the cultural change in proteomics public data deposition. Nucleic Acids Res. 2017;45(D1):D1100–D1106.
[63] Perez-Riverol Y, Csordas a, Bai J, et al. The PRIDE database and related tools and resources in 2019: improving support for quantification data. Nucleic Acids Res. 2019;47(D1):D442–D450.
[64] Marwick B, Boettiger C, Mullen L. Packaging data analytical work reproducibly using R (and Friends). Am Stat. 2018;72(1):80–88.
[65] Dutton LC, Jenkinson HF, Lamont RJ, et al. Role of Candida albicans secreted aspartyl protease Sap9 in interkingdom biofilm formation. Pathog Dis. 2016;74 (3):ftw005.
[66] Hoyer LL, Green CB, Oh S-H, et al. Discovering the secrets of the candida albicans agglutinin-like sequence (ALS) gene family — a sticky pursuit. Med Mycol. 2008;46(1):1–15.
[67] Gomez MJ, Maras B, Barca a, et al. Biochemical and immunological characterization of MP65, a Major mannoprotein antigen of the opportunistic human pathogencandida albicans. Infect Immun. 2000;68 (2):694–701.
[68] Pitarch a, Jiménez a, Nombela C, et al. Decoding serological response to candida cell wall immunome into novel diagnostic, prognostic, and therapeutic candidates for systemic candidiasis by proteomic and bioinformatic analyses. Mol Cell Proteomics. 2006;5 (1):79–96.
[69] Holmes AR, Lin Y-H, Niimi K, et al. ABC transporter cdr1p contributes more than cdr2p does to fluconazole efflux in fluconazole-resistant candida albicans clinical isolates. Antimicrob Agents Chemother. 2008;52 (11):3851–3862.
[70] Hessvik NP, Llorente a. Current knowledge on exosome biogenesis and release. Cell Mol Life Sci. 2018;75 (2):193–208.
[71] Bobrie a, Colombo M, Raposo G, et al. Exosome secretion: molecular mechanisms and roles in immune responses. Traffic. 2011;12(12):1659–1668.
[72] Fang S, Tian H, Li X, et al. Clinical application of a microfluidic chip for immunocapture and quantification of circulating exosomes to assist breast cancer diagnosis and molecular classification. Plos One. 2017;12(4):e0175050.
[73] Verweij FJ, Bebelman MP, Jimenez CR, et al. Quantifying exosome secretion from single cells reveals a modulatory role for GPCR signaling. J Cell Biol. 2018;217(3):1129–1142.
[74] Takahashi Y, Nishikawa M, Shinotsuka H, et al. Visualization and in vivo tracking of the exosomes of murine melanoma B16-BL6 cells in mice after intravenous injection. J Biotechnol. 2013;165(2):77–84.
[75] Zamith-Miranda D, Nimrichter L, Rodrigues ML, et al. Fungal extracellular vesicles: modulating host–pathogen interactions by both the fungus and the host. Microbes Infect. 2018;20(9):501–504.
[76] Kenno S, Speth C, Rambach G, et al. Candida albicans factor H binding molecule Hgt1p – a low glucose-induced transmembrane protein is trafficked to the cell wall and impairs phagocytosis and killing by human neutrophils. Front Microbiol. 2019;9. DOI:10.3389/fmicb.2018.03319.
[77] Li B, Antonyak MA, Zhang J, et al. RhoA triggers a specific signaling pathway that generates transforming microvesicles in cancer cells. Oncogene. 2012;31 (45):4740–4749.
[78] Sedgwick AE, Clancy JW, Olivia Balmert M, et al. Invadopodia mediate non-overlapping modes of tumor cell invasion. Sci. Rep. 2015;5(1):14748.
[79] Bassilana M, Arkowitz RA. Rac1 and Cdc42 have different roles in candida albicans development. Eukaryot Cell. 2006;5(2):321–329.
[80] Corvest V, Bogliolo S, Follette P, et al. Spatiotemporal regulation of Rho1 and Cdc42 activity during candida albicans filamentous growth. Mol Microbiol. 2013;89 (4):626–648.
[81] Dünkler a, Wendland J. Candida albicans rho-type gtpase-encoding genes required for polarized cell growth and cell separation. Eukaryot Cell. 2007;6 (5):844–854.
[82] Tricarico C, Clancy J, Biology D-SC. Biogenesis of Shed Microvesicles. Small GTPases. 2017;8(4):220–232.
[83] Zhao K, Bleackley M, Chisanga D, et al. Extracellular vesicles secreted by saccharomyces cerevisiae are involved in cell wall remodelling. Commun Biol. 2019;2(1):1–13.
[84] Kondoh O, Tachibana Y, Ohya Y, et al. Cloning of the RHO1 gene from candida albicans and its regulation of beta-1,3-glucan synthesis. J Bacteriol. 1997;179 (24):7734–7741.
[85] Barelle CJ, Richard ML, Gaillardin C, et al. Candida albicans VAC8 is required for vacuolar inheritance and normal hyphal branching. Eukaryot Cell. 2006;5 (2):359–367.
[86] Lupashin VV, Pokrovskaya ID, McNew JA, et al. Characterization of a novel yeast snare protein implicated in golgi retrograde traffic. Mol Biol Cell. 1997;8 (12):2659–2676.
[87] Jedd G, Mulholland J, Segev N. Two new ypt gtpases are required for exit from the yeast trans-golgi compartment. J Cell Biol. 1997;137(3):563–580.
[88] McNew JA, Søgaard M, Lampen NM, et al. Ykt6p, a prenylated SNARE essential for endoplasmic reticulum-golgi transport. J Biol Chem. 1997;272 (28):17776–17783.
[89] Kweon Y, Rothe a, Conibear E, et al. Ykt6p is a multifunctional yeast r-snare that is required for multiple membrane transport pathways to the vacuole. Mol Biol Cell. 2003;14(5):1868–1881.
[90] Gross JC, Chaudhary V, Bartscherer K, et al. Active wnt proteins are secreted on exosomes. Nat Cell Biol. 2012;14(10):1036–1045.

[91] Linnemannstöns K, Karuna P, Witte L, et al. Ykt6 membrane-to-cytosol cycling regulates exosomal Wnt secretion. bioRxiv. 2018:485565. DOI:10.1101/485565.
[92] Bernardo SM, Rane HS, Chavez-Dozal a, et al. Secretion and filamentation are mediated by the candida albicans T-SNAREs Sso2p and Sec9p. FEMS Yeast Res. 2014;14(5):762–775.
[93] Bishop a, Lane R, Beniston R, et al. Hyphal growth in candida albicans requires the phosphorylation of Sec2 by the Cdc28-Ccn1/Hgc1 Kinase. Embo J. 2010;29 (17):2930–2942.
[94] Douglas LM, Wang HX, Li L, et al. Membrane compartment occupied by can1 (MCC) and eisosome subdomains of the fungal plasma membrane. Membranes (Basel). 2011;1(4):394–411.
[95] Noble SM, French S, Kohn LA, et al. Systematic screens of a candida albicans homozygous deletion library decouple morphogenetic switching and pathogenicity. Nat Genet. 2010;42(7):590–598.
[96] Palige K, Linde J, Martin R, et al. Global transcriptome sequencing identifies chlamydospore specific markers in candida albicans and candida dubliniensis. Plos One. 2013;8(4):e61940.
[97] Young ME, Karpova TS, Brügger B, et al. The Sur7p family defines novel cortical domains in saccharomyces cerevisiae, affects sphingolipid metabolism, and is involved in sporulation. Mol Cell Biol. 2002;22 (3):927–934.
[98] Alvarez FJ, Douglas LM, Rosebrock a, et al. The Sur7 protein regulates plasma membrane organization and prevents intracellular cell wall growth in candida albicans. Mol Biol Cell. 2008;19(12):5214–5225.
[99] Grove J, Hu K, Farquhar MJ, et al. A new panel of epitope mapped monoclonal antibodies recognising the prototypical tetraspanin CD81. Wellcome Open Res. 2017;2:82.
[100] Cook GA, Longhurst CM, Grgurevich S, et al. Identification of CD9 extracellular domains important in regulation of CHO cell adhesion to fibronectin and fibronectin pericellular matrix assembly. Blood. 2002;100(13):4502–4511.
[101] Kim T-K, Park CS, Jeoung MH, et al. Generation of a human antibody that inhibits tspan8-mediated invasion of metastatic colorectal cancer cells. Biochem Biophys Res Commun. 2015;468(4):774–780.
[102] Saint-Pol J, Billard M, Dornier E, et al. New insights into the tetraspanin tspan5 using novel monoclonal antibodies. J Biol Chem. 2017;292(23):9551–9566.
[103] Sina AAI, Vaidyanathan R, Dey S, et al. Label free profiling of clinically relevant exosomes. Sci. Rep. 2016;6(1):30460.
[104] Hildonen S, Skarpen E, Halvorsen TG, et al. Mass spectrometry analysis of urinary extraexosomal proteins. Sci. Rep. 2016;6(1):36331.
[105] García-Sánchez S, Mavor AL, Russell CL, et al. Global roles of Ssn6 in Tup1- and Nrg1-dependent gene regulation in the fungal pathogen, candida albicans. Mol Biol Cell. 2005;16(6):2913–2925.
[106] Gola S, Martin R, Walther a, et al. New modules for PCR-based gene targeting in candida albicans: rapid and efficient gene targeting using 100 Bp of flanking homology region. Yeast. 2003;20(16):1339–1347.
[107] Foderaro JE, Douglas LM, Konopka JB. MCC/eisosomes regulate cell wall synthesis and stress responses in fungi. J Fungi. 2017;3(4):61.
[108] Perez-Hernandez D, Gutiérrez-Vázquez C, Jorge I, et al. The intracellular interactome of tetraspanin-enriched microdomains reveals their function as sorting machineries toward exosomes. J Biol Chem. 2013;288(17):11649–11661.
[109] Kim S-Y, Kim J. Roles of dihydrolipoamide dehydrogenase lpd1 in candida albicans filamentation. Fungal Genet Biol. 2010;47(9):782–788.
[110] Broxton CN, Culotta VC. An adaptation to low copper in candida albicans involving SOD enzymes and the alternative oxidase. Plos One. 2016;11(12):e0168400.
[111] Bauerova V, Pichova I, Nitrogen Source H-HO. Growth stage of candida albicans influence expression level of vacuolar aspartic protease aprlp and carboxypeptidase cpylp. Can J Microbiol. 2012;58(5):678–681.
[112] Yu Q, Jia C, Dong Y, et al. Candida albicans autophagy, no longer a bystander: its role in tolerance to er stress-related antifungal drugs. Fungal Genetics and Biology. 2017;2:238–249.
[113] Lopez CM, Wallich R, Riesbeck K, et al. Candida albicans uses the surface protein gpm1 to attach to human endothelial cells and to keratinocytes via the adhesive protein vitronectin. Plos One. 2014;9(3):e90796.
[114] Rida PCG, Nishikawa a, Won GY, et al. Yeast-to-hyphal transition triggers formin-dependent golgi localization to the growing tip in candida albicans. Mol Biol Cell. 2006;17(10):4364–4378.
[115] Sandini S, Stringaro a, Arancia S, et al. The MP65 gene is required for cell wall integrity, adherence to epithelial cells and biofilm formation in candida albicans. BMC Microbiol. 2011;11(1):106.
[116] Saporito-Irwin SM, Birse CE, Sypherd PS, et al. PHR1, a PH-regulated gene of candida albicans, is required for morphogenesis. Mol Cell Biol. 1995;15(2):601–613.
[117] Kowal J, Arras G, Colombo M, et al. Proteomic Comparison defines novel markers to characterize heterogeneous populations of extracellular vesicle subtypes. Proc Natl Acad Sci. 2016;113(8):E968–E977.
[118] Hikita T, Miyata M, Watanabe R, et al. Rapid quantification of exosomes by fusing luciferase to exosome marker proteins. Sci Rep. 2018;8(1):14035.
[119] Delandre C, Penabaz TR, Passarelli AL, et al. Mutation of juxtamembrane cysteines in the tetraspanin CD81 affects palmitoylation and alters interaction with other proteins at the cell surface. Exp Cell Res. 2009;315 (11):1953–1963.
[120] Zimmerman B, Kelly B, McMillan BJ, et al. Crystal structure of a full-length human tetraspanin reveals a cholesterol-binding pocket. Cell. 2016;167(4):1041–1051.e11.

4.2 Identification of protein markers in EVs from *Fusarium graminearum*

The study presented in Section 4.1 produced a list of 47 putative protein markers for EVs from *Candida albicans*, with 22 of them being the best candidates for further validation. The *Fusarium graminearum* (*Fgr*) EV proteome was thus scanned to determine whether any of these proteins are conserved in *Fgr*, and to assess the potential of these proteins for the generation of antibodies. Thirteen of the 22 *C. albicans* candidates were detected in EVs from *Fgr*. This section presents the predicted topology of the potential *Fgr* markers, the search for antigenic epitopes that are likely to be exposed on the surface of the EVs, the generation of a polyclonal antibody directed to the membrane protein Sur7 and the detection of Sur7 in samples of *Fgr* EVs.

4.2.1 Introduction

The study of mammalian EVs has progressed rapidly due to the availability of EV protein markers such as Rab-5b, TSG101, annexin2, integrin beta 1, flotillin-1, cavolin-1, and the tetraspanins CD9, CD81, and CD63 [61]. These markers have helped in the development of isolation procedures, characterization of subsets of EVs, and the study of EV function *in vivo*. When this thesis started there were no reported markers for fungal EVs and hence isolation procedures were based on those developed for mammalian EVs based on size and/or density and there were few studies on EV function. The article presented in section 4.1 described 47 putative protein markers for EVs from *Candida albicans* and revealed that the markers for mammalian EVs were not suitable for fungal EVs [17]. Twenty-two of the potential fungal EV markers were either enriched or were exclusive to EVs from *C. albicans*, making them the ideal candidates for EV markers. They included proteins from the cell surface, cytosol, GTPases, SNAREs, and most importantly components of the "membrane compartment of Can1" (MCC)/eisosome (Sur7, Nce101, and Evp1), which have similar topology to the mammalian tetraspanins [17]. The MCC/eisosome are stable complexes of proteins and lipids that have a key role in the architecture and organization of the plasma membrane in yeast and have been linked to sites of endocytosis [62]. Some of the proteins in the MCC/eisosome such as Sur7 and Evp1, have transmembrane domains and extracellular loops making them potential targets for antibody recognition. Here, the work on *C. albicans* EV markers was expanded to determine whether the EV

proteome from *Fusarium graminearum* (*Fgr*), described in section 3.1, has any of the putative EV markers identified in *C. albicans.* A polyclonal antibody was generated to detect *Fgr* Sur7, which was successfully identified in EV samples via Western blot.

4.2.2 Materials and methods

4.2.2.1 Identification of Fusarium graminearum *(Fgr) orthologs of protein markers*

The list of the 22 best candidate protein markers from *C. albicans* [17] was retrieved from the *Candida* genome database [63], and the *Fgr* proteome (assembly ASM24013v3) was scanned for the 22 sequences using NCBI's BLASTp [64], using default settings. The $\log_2$-fold change ($\log_2$FC) obtained in Section 3.1, which compares the protein abundance between the *Fgr* EVs and the whole-cell lysate, was retrieved to determine whether the putative markers were enriched in *Fgr* EVs.

4.2.2.3 Prediction of the membrane topology of the putative EV markers

Protein sequences were analyzed using TOPCONS2 [65] and Protter 1.0 [66] to predict their membrane topology and stretches of amino acids likely to be located in the extracellular environment, using default settings.

4.2.2.4 Prediction of antigenic epitopes in putative protein markers

Complete protein sequences were analyzed with Bepipred [67] using default settings to detect amino acid epitopes that are likely to be antigenic.

4.2.2.5 Generation of a polyclonal antibody directed to a putative EV marker

A putative protein marker that had a peptide with a predicted extracellular location and high probability of being antigenic was selected to generate a polyclonal antibody, in collaboration with the company Mimotopes Pty. Ltd. The sequence of the candidate peptide was modified to contain a cysteine residue at the beginning of the peptide to link to the carrier protein keyhole limpet hemocyanin (KLH). Five mg of synthetic peptide was mixed with 5 mg of KLH, and coupled using Sulfo-SMCC, in 1 mL of PBS (pH 7.4). The conjugated peptide was purified by HPLC, and the expected mass was confirmed by electrospray ionization mass spectrometry. The KLH-conjugated peptide was mixed with complete or incomplete Freund's adjuvant in a 1:1 ratio in saline solution and injected twice subcutaneously into two New Zealand white rabbits at different timepoints. Serum and blood were collected on day 42 and 64, respectively (Table 1).

Day	Immunization	Immunization composition
1	1st	Complete Freund's adjuvant + 500 μg of conjugated peptide
15	2nd	Complete Freund's adjuvant + 500 μg of conjugated peptide
29	3rd	Incomplete Freund's adjuvant + 250 μg of conjugated peptide
35	4th	Incomplete Freund's adjuvant + 250 μg of conjugated peptide
42	-	Serum collection
43	5th	Incomplete Freund's adjuvant + 250 μg of conjugated peptide
50	6th	Incomplete Freund's adjuvant + 250 μg of conjugated peptide
57	7th	Incomplete Freund's adjuvant + 250 μg of conjugated peptide
63	-	Blood collection

Table 1 Immunization schedule for the generation of polyclonal antibodies in rabbits.

Antibody production was monitored by ELISA. Blood from the two rabbits was recovered from the ear artery, and serum was collected after standing at room temperature overnight. The antibodies were affinity purified from the serum using synthetic peptide linked to SulfoLink coupling resin (Thermo Fisher). The antibodies were eluted using PBS and freeze-dried. The *Fgr* anti-Sur7 antibody (anti-*Fgr*Sur7) was made up to a final concentration of 1 mg/ml using ultrapure water. The sample was centrifuged briefly at 4000 x *g* and 1 µL aliquots of the supernatant were stored at -20°C.

4.2.2.6 SDS-PAGE and Western blot

The following samples were analyzed by SDS-PAGE: 25 µg of protein from EVs or whole-cell lysate (WCL), and 20 µg of the 24-amino acid synthetic *Fgr* Sur7 peptide. Each sample was mixed with 5 µl of NuPAGE LDS sample buffer (Thermo Fisher) and with 1 µl TCEP (Thermo Fisher), before being heated to 95°C for 5 min. Samples were loaded onto precast 4-12% Bis-Tris polyacrylamide gels (Thermo Fisher), using MES running buffer (Thermo Fisher) containing NuPAGE antioxidant (Thermo Fisher). Five µL of the size marker SeeBlue Plus2 (Thermo Fisher) were included for reference. Samples were resolved for 15 min running at 180 volts. The gel was then rinsed twice with distilled water and transferred onto a mini PVDF transfer pack (Bio-Rad) using a Trans-blot Turbo transfer system (Bio-Rad) at 25 volts for 7 min. The membrane was processed following the Amersham ECL Select Western blotting protocol (Cytiva) by blocking with 3% BSA containing 0.1% Tween 20 for 1 h at room temperature. For simplicity onwards, one

membrane "wash" represents two brief rinses, plus two 15-min washes, plus three 5-min washes in TBS buffer (8 g/L NaCl, 20 mL of 1 M Tris HCl/L, pH 7.6, 0.1%Tween). All washes and incubations were performed at room temperature in an orbital shaker. After blocking, the membrane was washed, and probed with anti-*Fgr*Sur7 antibody diluted 1:1000 in TBS for 1 h at RT. The membrane was then washed and probed with a goat anti-rabbit HRP-IgG secondary antibody (Pierce) diluted 1:50000 in TBS, followed by incubation for 1 h. The membrane was washed, and excess TBS was removed gently from the edges of the membrane using a paper towel. The membrane was then placed on clear plastic wrap and 10 ml of a 1:1 solution of detection reagents A and B was pipetted onto the membrane, followed by an incubation of 1 min without shaking. Immediately, the excess solution was removed, and the membrane was placed into the chamber of a G Box Chemi XX6 (Syngene) and images were acquired using the "chemi" blot function.

4.2.3 Results

4.2.3.1 EVs from Fusarium graminearum *(Fgr) contain proteins that are orthologs of putative* C. albicans *EV markers*

The study of *C. albicans* EVs yielded a list of 22 protein candidates as potential markers for fungal EVs (Section 4.1). Using BLASTp, 13 of the 22 proteins were detected in EVs from *Fgr* and had high identity to the putative markers from *C. albicans* EVs indicating that they are potential orthologs (Table 2). The enrichment of the putative protein markers in *Fgr* EVs was compared with the whole-cell lysate (WCL), revealing that three were exclusively in the *Fgr* EV samples, six were

enriched in EVs, and four had no difference between EVs and WCL ("Enrichment *Fgr* EVs" column, Table 2). The *Fgr* proteins Fet3 and sphingolipid C9-methyltransferase 2 have been reported to be true orthologs of Fet34 and Mts1 of *C. albicans*, respectively (Table 2).

***C. albicans* marker**	***Fgr* potential ortholog**	**E-value**	**Sequence identity**	**Query coverage**	***Fgr* gene name**	**Enrichment *Fgr* EVs**	**Source**
Cdc42	CDC42 homolog	3×10^{-112}	79.4%	98%	FGSG_05447	EV ex	BLAST
Rho3	RHO3-like	9×10^{-198}	66.8%	99%	FGSG_00170	EV ex	BLAST
Ykt6	YKT6-like	9×10^{-82}	55.0%	99%	FGSG_06394	EV ex	BLAST
Fet34	Cell surface ferroxidase Fet3	0.0	51.8%	92%	FGSG_05159	EV up	[68]
Phr1	1,3-beta-glucanosyltransferase	3×10^{-152}	48.8%	81%	FGSG_09980	EV up	BLAST
Rac1	Uncharacterized protein	2×10^{-88}	65.5%	75%	FGSG_08857	EV up	BLAST
Sur7	Sur7-like	3×10^{-20}	27.4%	71%	FGSG_08692	EV up	BLAST
Yck2	Kinase domain-containing protein	1×10^{-166}	65.2%	70%	FGSG_10066	EV up	BLAST
orf19.2168.3	Yop1	2×10^{-46}	46.4%	95%	FGSG_07419	EV up	BLAST
Mts1	Sphingolipid C9-methyltransferase 2	0.0	63.3%	96%	FGSG_05593	No diff	[69]
orf19.1054	Uncharacterized protein	2×10^{-25}	28.0%	84%	FGSG_04983	No diff	BLAST
Sec4	Similar to GTP-binding protein YPT2	1×10^{-90}	61.9%	97%	FGSG_06209	No diff	BLAST
Vac8	Vacuolar protein 8	0.0	67.2%	89%	FGSG_08997	No diff	BLAST

Table 2 Orthologs of potential *Candida albicans* protein markers that are found in *Fusarium graminearum* (*Fgr*) EVs. EV ex: EV exclusive; EV up: upregulated in EVs; No diff: no difference in protein abundance between EVs and the whole-cell lysate

Proteins that were not exclusive or enriched in *Fgr* EVs were removed from further analysis. Also, proteins without predicted transmembrane domains were not

analyzed further since they are unlikely to present domains on the EV surface for recognition by antibodies. Four of the remaining candidates had transmembrane domains, predicted extracellular domains, and were enriched in EVs, making them the best candidates for *Fgr* EV markers. They were Fet3, 1,3-beta-glucanosyltransferase, Sur7, and Yop1.

4.2.3.2 Potential **Fusarium graminearum** *EV markers with predicted extracellular domains*

Figure 2 illustrates the predicted topology of the four potential *Fgr* markers: 1,3-β-glucanosyltransferase, Fet3, Yop1, and Sur7 (Figure 2).

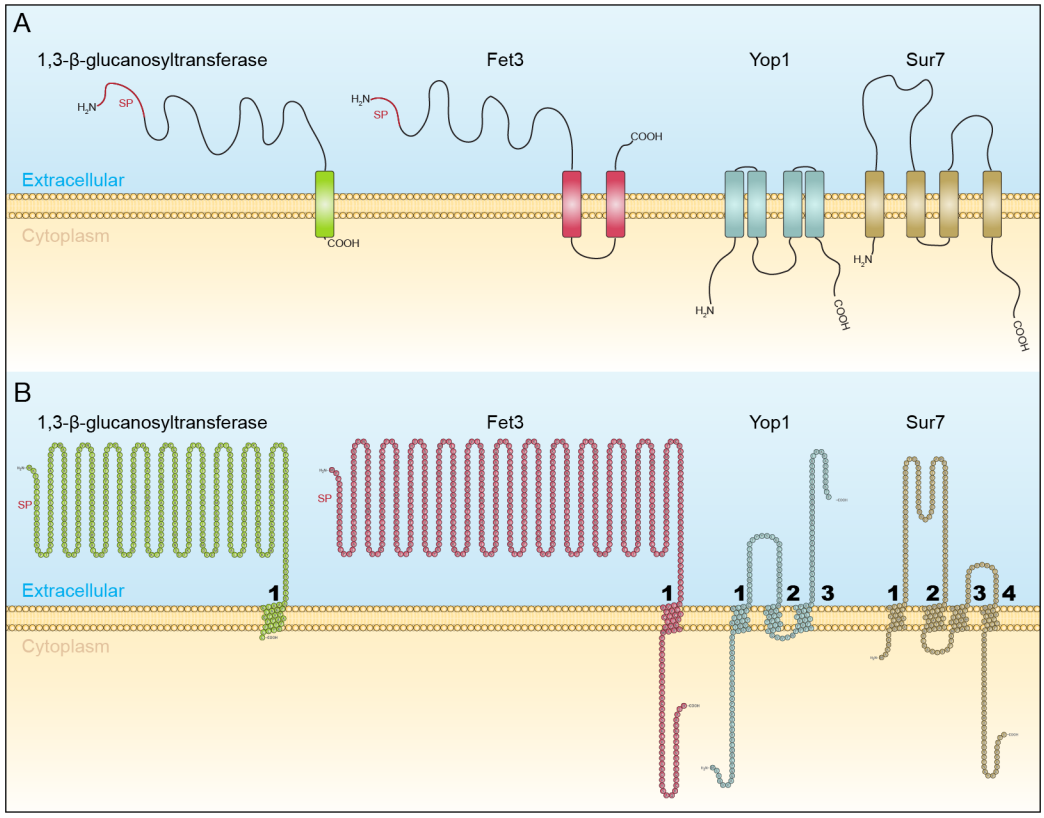

Figure 2 Membrane topology prediction of the potential protein markers for *Fusarium graminearum* extracellular vesicles (EVs). (A) TOPCONS2 [65] and (B) Protter 1.0 [66] were used to identify the intra-protein domains of 1,3-β-

glucanosyltransferase, Fet3, Yop1, and Sur7 presented on the outer surface the EV membrane. SP: signal peptide predicted by TOPCONS2.

For Yop1, Protter 1.0 projected one extracellular loop and three transmembrane domains, while TOPCONS2 predicted four transmembrane domains without a significant stretch of amino acids on the surface. This discrepancy led to the removal of Yop1 from the analysis because the potential lack of extracellularly exposed amino acids could compromise the detection of Yop1 by an antibody. The predicted topology of *Fgr* Sur7 was similar to *C. albicans* Sur7 [17], as well as the mammalian tetraspanins [70]. For this reason, *Fgr* Sur7 was chosen as the best candidate for generation of a polyclonal antibody that binds EVs. *Fgr* Sur7 had a global sequence similarity of 40.7%, and identity of 27.4% (EMBOSS needle) compared to *C. albicans* Sur7, and the predicted extracellular amino acids of both proteins were located in similar positions (highlighted in magenta, Figure 3).

Figure 3 Sequence alignment of Sur7 from *Candida albicans* and *Fusarium graminearum* (*Fgr*). The amino acid position of the predicted extracellular residues (highlighted in magenta) were taken from Protter and TOPCONS.

4.2.3.3 Sur7 from **Fusarium graminearum** *contains epitopes with potential antigenicity*

Five peptides with potential antigenic properties were identified in *Fgr* Sur7 (Table 3) using the bioinformatics software Bepipred [67]. The first four peptides were in the predicted extracellular domains of Sur7 (extra), while peptide five was predicted to be intracellular (intra) and was thus removed from the analysis. The probability of the peptides to have antigenic properties is also reported in Table 3.

Peptide three, minus the first three residues (NND) to improve linkage to the carrier protein KLH, was selected (CDGARAAPVIGKAWDSNPRNAPSS) to generate a polyclonal antibody for the recognition of Sur7 in *Fgr* EVs.

Prediction	Start	End	Peptide	Length (amino acids)	Epitope probability
1 - extra	32	36	STTPF	5	0.516
2 - extra	49	54	ITGARD	6	0.545
3 - extra	68	94	NNDCDGARAAPVIGKAWDSNPRNAPSS	27	0.587
4 - extra	96	104	VGGRAGDTT	9	0.571
5 - intra	213	245	DKSSSSGGYSGRSWRRRRSVRSTNGYEGRRVKD	33	0.638

Table 3 Prediction of potentially antigenic peptides in Sur7 from *Fusarium graminearum*. Extra: epitope is predicted to be extracellular; intra: epitope is predicted to be intracellular.

4.2.3.4 Detection of Fgr Sur7 in Fgr EVs

A Western blot analysis was performed to determine whether the polyclonal antibody could detect the *Fgr*Sur7 protein in EV samples. The anti-*Fgr*Sur7 antibody bound to a protein doublet of approximately 27 kDa in the EV sample

(lane 4, Figure 4), that was not detected in the whole-cell lysate (WCL, lane 3, Figure 4). In contrast, there was a strong signal in the sample containing the purified, 24 residue-long peptide without KLH (expected size around 2600 Da) synthesized by Mimotopes, around the 3000 Da mark (lane 2, Figure 4).

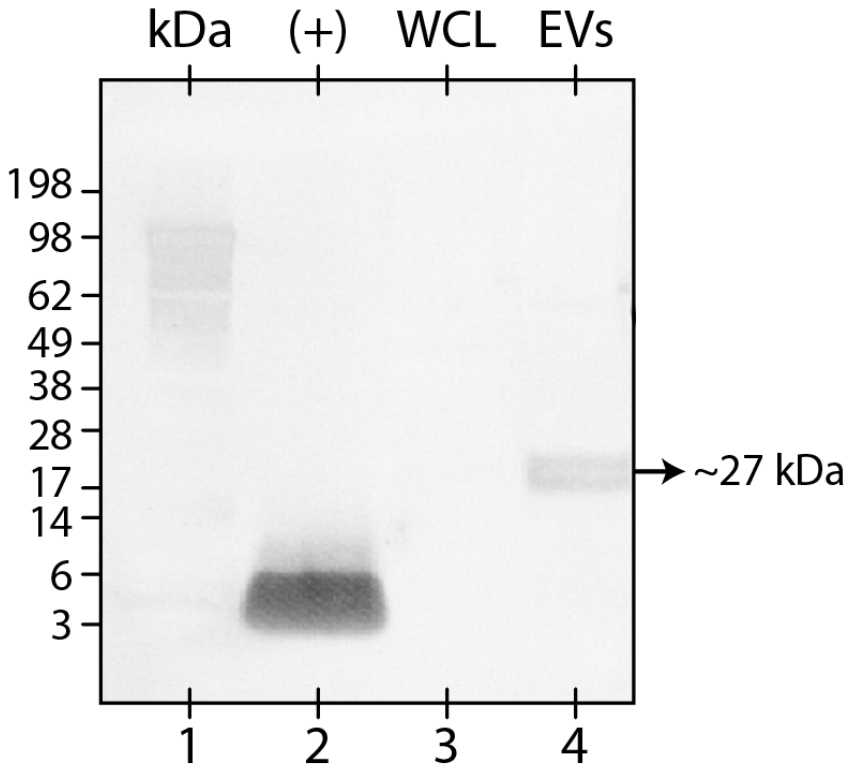

Figure 4 Western blot of Sur7 in extracellular vesicle (EV) samples from *Fusarium graminearum*. Proteins in samples of EVs, whole-cell lysate (WCL), and synthetic Sur7 epitope peptide without keyhole limpet hemocyanin (KLH) (+) were separated by SDS-PAGE and analyzed by Western blot. A doublet of approximately 27 kDa was detected in EV samples but not in the WCL.

4.2.4 Discussion

Finding new protein markers is crucial for the development of technologies to isolate and track fungal EVs in biological systems. Here we report that Sur7 is also enriched in EVs from *Fgr*, and we have generated an antibody to Sur7 for further study of its suitability as a fungal EV marker.

The putative protein marker of *C. albicans* EVs Sur7 [17] is a tetraspanin-like component of two plasma membrane complexes, the "membrane compartment of Can1" (MCC) and the eisosome (Figure 5). The MCC in *C. albicans* is formed in part by other tetraspanins-like proteins [17], while the eisosome is a collection of cytoplasmic proteins that localize to the plasma membrane (PM) next to the MCC, and together function in PM organization, sphingolipid homeostasis, and cell wall morphogenesis (Figure 5) [71].

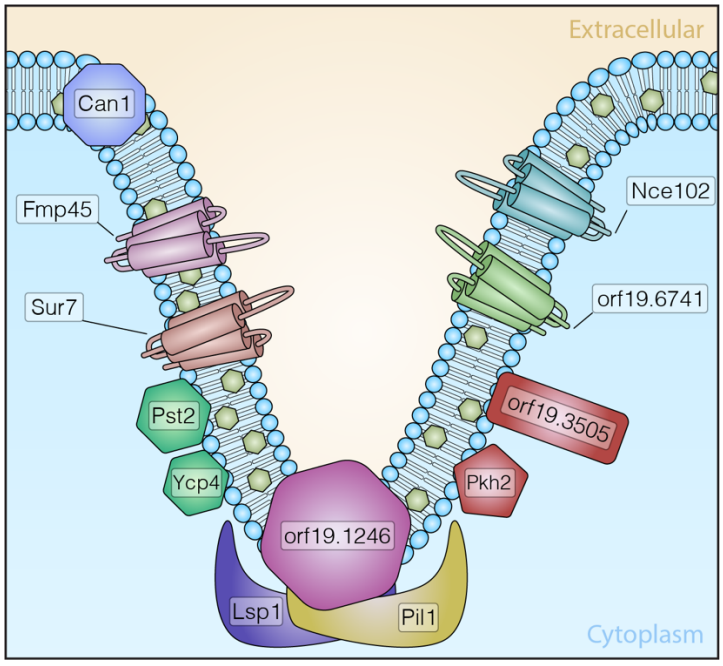

Figure 5 Model of the membrane compartment of Can1 (MCC)/eisosome complex in *Candida albicans*. The MCC is a transmembrane complex while the eisosome is formed by cytoplasmic proteins that co-localize with the MCC. Together, the MCC/eisosome form grooves on the plasma membrane that have roles in plasma membrane organization, sphingolipid homeostasis, and cell wall morphogenesis [71]. The putative extracellular vesicle (EV) protein marker Sur7 is relatively more abundant than some MCC/eisosomal proteins [71]. Figure adapted from [17,71]

The MCC/eisosome forms furrows on the cell surface that are surrounded by Sur7 [72], making Sur7 one of the most abundant proteins among the MCC/eisosomal components [73]. This may explain why Sur7 is also enriched in EVs from *Zymoseptoria tritici* [74], *S. cerevisiae* [60], and *Aspergillus fumigatus* [75]. However, although Sur7 has been detected in EVs from filamentous fungi, studies on the *A. fumigatus* and *A. nidulans* orthologs of Pil1 and Sur7 revealed that these proteins are not located in distinct MCC/eisosomal-like structures, hence MCC/eisosome function may be different in filamentous fungi [76]. Indeed, the *Fgr* EV proteome obtained in section 3.1 did not contain all the MCC/eisosome proteins known in *C. albicans*. Only proteins related to Sur7 and Pst2 were detected. This supports the hypothesis that the MCC/eisosomal proteins may differ between yeast and filamentous fungi.

In *S. cerevisiae* the protein Pil1 (also present in *C. albicans*, Figure 5), is essential for eisosome formation and Sur7 localization [77]. *S. cerevisiae pil1Δ* strains cannot localize Sur7 to the plasma membrane [77], hence if we assume that Sur7 is a true EV marker, it could be speculated that Pil1 may have an effect in the production of fungal EVs. Therefore, it would be interesting to study the production of EVs from fungi deficient in the production of Pil1.

The Sur7 proteins from *Fgr* and *C. albicans* have similar predicted topology, having four transmembrane domains with a long extracellular loop between the first two TM sections (obtained with TMHMM, Figure 6).

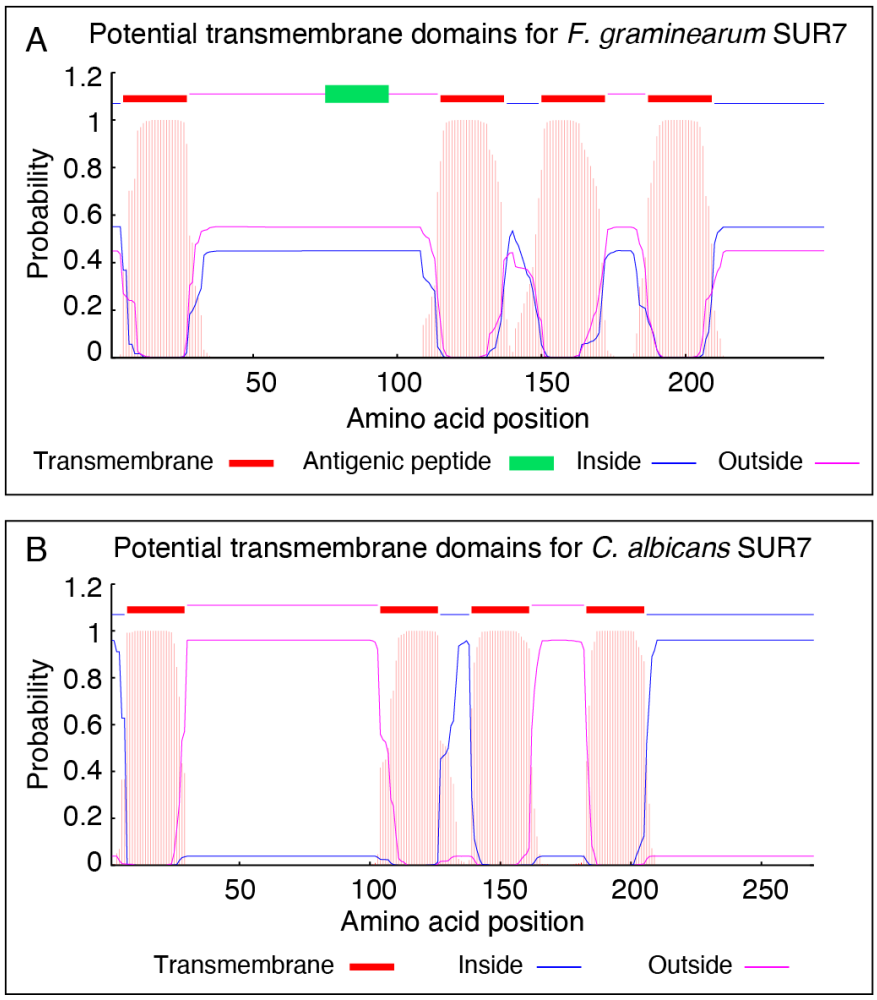

Figure 6 Predicted membrane topology of Sur7 from *Fusarium graminearum* (*Fgr*). The amino acid sequence from *Fgr* Sur7 (Uniprot ID: I1RWL7) was processed with Bepipred 2.0 [67] to predict epitopes with antigenic potential. A peptide comprised of 24 amino acids (highlighted in green) had antigenic potential and was used to produce the polyclonal antibody. The software TMHMM was used to compare the position of the transmembrane domains in Sur7 from (A) *Fgr* and (B) *Candida albicans*. Both proteins have four predicted transmembrane domains. The blue and magenta lines indicate the probability of amino acids to be located inside or outside the plasma membrane, respectively.

A multiple sequence alignment of potential orthologs of Sur7 from other fungi revealed that the epitope used to generate the anti-*Fgr*Sur7 antibody (Figure 7A,

highlighted in magenta) is conserved in the major pathogens *F. oxysporum* (*Fox*), *F. oxysporum* f. sp. *cubense* (*Foc*), *F. oxysporum* f. sp. *vasinfectum* (*Fov*), *F. oxysporum* f. sp. *lycopersici* (*Fol*), and partially conserved in the plant pathogens *Botrytis cinerea* and *Verticillium dahliae* (Figure 7A). This indicates that the anti-*Fgr*Sur7 antibody could bind to Sur7 in other plant pathogens, particularly other *Fusarium* species. Conversely, there was little identity between the *Fgr*Sur7 epitope and the putative Sur7 sequences from the human pathogens *Histoplasma capsulatum*, *Paracoccidioides brasiliensis*, and *Aspergillus fumigatus*, suggesting that the *Fgr* antibody may not be a useful EV marker for these organisms.

Our laboratory has also generated polyclonal antibodies against the *C. albicans* Sur7 using different antigenic peptides (highlighted in magenta in Figure 7B), resulting in two antibodies that can detect Sur7 in EV samples from *C. albicans* (Dr. James McKenna, unpublished). These peptides were located in similar positions in the *C. albicans* Sur7 sequence compared with *Fgr*Sur7. A second sequence alignment revealed similarity between *C. albicans* Sur7 and the listed human pathogens, including the peptides used to generate the *C. albicans* anti-Sur7 antibodies (Figure 7B). Thus, it is possible that the *C. albicans* anti-Sur7 antibodies could be used to track Sur7 in other human fungal pathogens.

Figure 7 Multiple sequence alignment of the longest extracellular domain of Sur7. The *Candida albicans* Sur7 sequence (Uniprot ID: Q5A4M8) was used to find potential orthologs in (A) *Fusarium oxysporum* (*Fox*), *Fusarium oxysporum* f. sp. *cubense* (*Foc*), *Fusarium oxysporum* f. sp. *vasinfectum* (*Fov*), *Fusarium oxysporum* f. sp. *lycopersici* (*Fol*), *Fusarium graminearum* (*Fgr*), *Verticillium dahliae, Botrytis cinerea*, (B) *Histoplasma capsulatum*, *Paracoccidioides brasiliensis*, and *Aspergillus fumigatus*. Clustal Omega was employed to align the sequences of the first extracellular domain. The peptides used to generate the *C. albicans* (Dr. James McKenna, unpublished) and *Fgr* anti-Sur7 antibodies were located in this region and are highlighted in magenta.

BLAST did not find a significant match for Sur7 in *Cryptococcus neoformans* when the *C. albicans* or *Fgr* sequences were used as the query. EVs from *C. neoformans*, which are the best characterized to date, contain the proteins THS1, THS2 and THS3 that have Sur7 domains [78], although these proteins have little similarity to *C. albicans* Sur7. This is likely explained due to the evolutionary distance between *C. neoformans*, which is a basidiomycete, and the rest of the human pathogens mentioned above, which are ascomycetes. This also suggests that the plasma membrane reorganization function of *C. albicans* Sur7 may have evolved differently in *C. neoformans*.

Taken together, these sequence alignments imply that the anti-*Fgr*Sur7 antibody may be useful to detect EVs from other plant pathogens, while a *C. albicans* Sur7

antibody may be a suitable marker for EVs from some human pathogens. The cross-reactivity of the anti-Sur7 antibodies must be further tested for example by using EVs from other organisms that have Sur7, EVs from fungi that do not have Sur7, or by treating EVs with proteinase K to remove the extracellular domain of Sur7. Confirming the presence of *Fgr*Sur7 on the surface of extracellular vesicles could be accomplished using immunogold electron microscopy [79] (Figure 8).

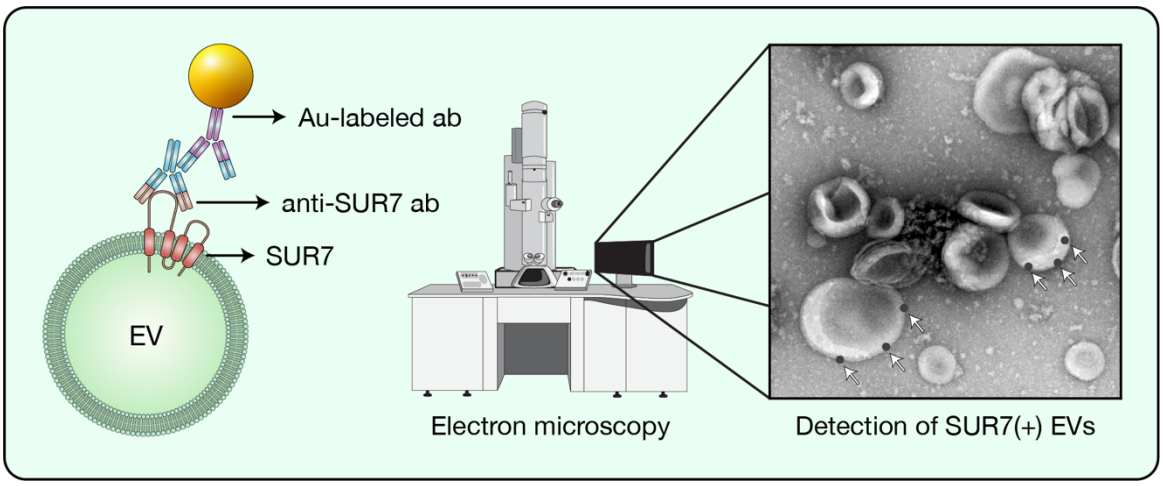

Figure 8 Potential identification of extracellular vesicles (EVs) using gold-labeled antibodies (ab).

The Western blot analysis revealed a protein of approximately 27 kDa that bound the anti-*Fgr*Sur7 antibody which corresponds to the predicted mass of *Fgr* Sur7 of 27,041 Da (Uniprot: I1RWL7). The presence of the doublet indicates that some post-translation processing of Sur7 has occurred such as glycosylation. Sur7 was not detected in the whole-cell lysate (WCL) on the Western blot, but this protein was detected in only one out of three biological replicates of the WCL in the proteomic analysis (section 3.1), and thus is likely to be less abundant in WCL than it is in EVs.

New EV proteomes from other fungi should be screened for the presence of Sur7 to determine if this potential fungal EV marker is conserved in other fungal species. The results presented in this chapter support the hypothesis that Sur7 is a protein marker for fungal EVs and advance the research field towards improved isolation and characterization techniques. For instance, Sur7 could be immobilized on beads that would capture EVs in solution, as has been done with mammalian EVs [80], or Sur7-GFP constructs could be generated and used to visualize EVs *in vivo* [81], providing more direct evidence of the involvement of EVs in modulating host-pathogen interactions.

Finally, other putative markers that were exclusive to *Fgr* EVs and thus have promising potential are Cdc42, Rho3, and Ykt6-like. Similarly, Yop1 is a promising candidate and more information on its protein structure will be helpful for the future development of antibodies to track fungal EVs.

5. Chapter Five

5.1 Concluding remarks

Extracellular vesicles (EVs) are small particles (30-1000 nm) released from cells from all kingdoms studied to date [10], and have important roles in pathologies [82], cellular communication, and transport of macromolecules [49]. For yeast, EVs influence host-pathogen interactions, modulate the immune response of the host and transport molecules that support the fungal infection [83,84]. However, when the work for this thesis began there were three important gaps in the study of fungal EVs. First, little was known about EVs from filamentous fungi that infect plants and their potential roles in virulence, despite the enormous importance that these pathogens have on global food security. Second, conventional isolation methods had generally been adapted from procedures used for mammalian cells and are associated with poor yields and low sample quality while being time-consuming and expensive. Thirdly, there were no markers to assist in the identification and tracking of EVs from filamentous fungi, placing a limitation on the number and type of techniques used to study EVs. These topics have been addressed in this thesis and the associated future directions are discussed next.

5.2 Size-exclusion chromatography (SEC) is a scalable method to separate EVs

Although finding a better technique to isolate EVs from filamentous fungi was not an original aim for this thesis, it quickly became evident that the ultracentrifugation (UC) protocol that had been used in the laboratory for

preparation of EVs from *S. cerevisiae* and *C. albicans* was not suitable for filamentous fungi because it was slow and irreproducible, and the sample quality was relatively poor. The first improvement was the development of the SEC isolation method which gave a 6-fold increase in particle yield for *Fusarium oxysporum* f. sp. *vasinfectum* (*Fov*) compared to UC and halved the preparation time. Further refinement was required for *Fusarium graminearum* (*Fgr*) because it produced polysaccharides that blocked the filters in the concentration step required before SEC. This was solved using a fully defined medium that used amino acids in place of sugars as the carbon source. These modifications have created the potential to produce fungal EVs at scale (Figure 9). The culture medium could be concentrated by tangential-flow filtration (TFF) coupled to SEC as described before for EVs from human cells [85]. TFF units are reusable, therefore would be less expensive in the long term and would reduce laboratory waste.

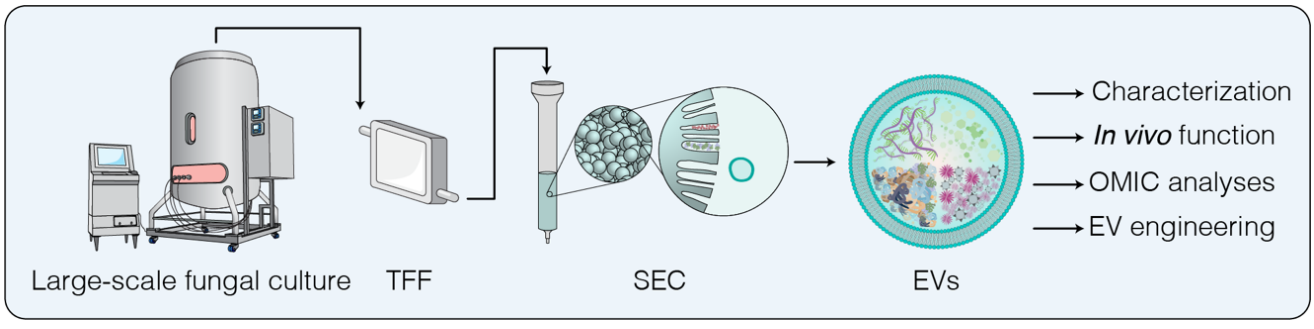

Figure 9 Potential large-scale fungal extracellular vesicle (EV) purification. Coupling of tangential-flow filtration (TFF) with size-exclusion chromatography (SEC) has been proposed as a potential pipeline for upscaled production of EVs [85]. This thesis demonstrates that a similar isolation process could be adapted for work with fungal EVs.

In addition, obtaining larger amounts of EVs would lead to more reproducible and biologically relevant results for future fungal EV studies. For instance, the characterization of EVs derived from only one fungal culture would avoid the normal biological changes that occur by chance in every fungal cultivation *in vitro*, such as slight fluctuations in biomass production, EV yield, or production of soluble protein. A greater EV yield permits multiple analyses to be performed in parallel on a single sample, facilitating linkages between different classes of biomolecular cargoes. Performing different omic analyses on one sample of EVs will ensure that any assessments across experiments are truly comparable, and that error is minimized. This approach would not replace the need to analyze an appropriate number of biological replicates.

Due to the immunogenic proteins present in EVs, particularly yeast EVs, they have been proposed as potential vaccine platforms against pathogenic fungi [78,86]. For instance, mice immunized with EVs from a *C. neoformans* strain deficient in the production of capsular polysaccharides were able to survive a wild-type *C. neoformans* challenge compared to unimmunized mice, and produced antibodies against EV proteins [78]. Similarly, mice and *Galleria mellonella* larvae exposed to EVs from *C. albicans* lived longer than unimmunized controls after being challenged with *C. albicans* cells [86]. In both studies, there was an increased production of cytokines and antibodies in response to the EVs. It is possible that similar results can be obtained for other important human pathogens such as *A.*

fumigatus [75,87,88]. Finally, the content of fungal EVs could be engineered to expose molecules, such as proteins or polysaccharides, that induce a desired immune response, similar to the generalized modules of membrane antigens (GMMA) system that has been described for bacterial outer membrane vesicles [89]. If these technologies reach a commercial level, EV production most certainly needs a scalable process such as the one hypothesized above (Figure 9).

The ability to produce fungal EVs inexpensively at large scale also makes them a promising vehicle for the delivery of different drugs for humans. To achieve this, the immune effect of different fungal EVs in humans must be studied to determine their safety and efficacy in delivering EV cargo. Furthermore gene silencing tools such as small interfering RNA (siRNA) and short hairpin RNA (shRNA) [90,91] may be loaded into fungal EVs and administered intravenously, as has been established for mammalian EVs [92]. If a particular type of fungal EVs are found to be non-immunogenic and biocompatible with human cells, fungal EVs may be significantly easier to produce than EVs from mammalian cells, while also being less expensive.

Regarding plant-fungal interactions, the discovery of proteins with roles in virulence led to a further examination of the *Fgr* EV proteome, revealing that protein effectors may be transported via unconventional secretion. These results are discussed next.

5.3 EVs are likely to transport protein effectors

The proteomics conducted in this thesis revealed that fungal EVs carry hundreds of proteins with a wide range of functions. For instance, EVs from *Fusarium spp.* carry cell wall remodeling enzymes that may assist the EV release from the fungal cell [60,93]. EVs also transport virulence factors and redox proteins that may alter the defense response of the host cells [84]. These findings contribute to our understanding of fungal EV functions (Figure 10).

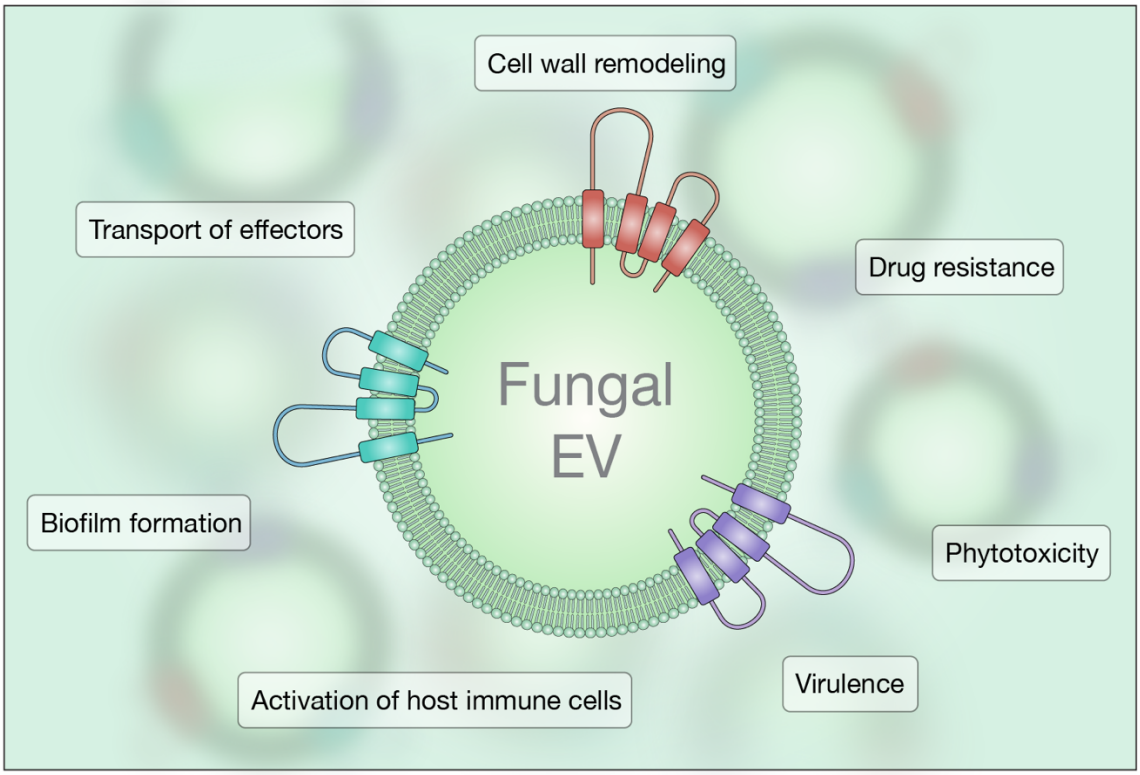

Figure 10 Functions of fungal extracellular vesicles (EVs). Fungal EVs carry cell wall synthases and degrading enzymes to potentially facilitate EV release from the fungal cell [60], are involved in drug resistance and biofilm formation [9], transport phytotoxic compounds [50,83], activate the host immune cells [94], and as presented in this thesis, may transport protein effectors [95].

Furthermore, EVs from *Fgr* potentially transport protein effectors, which are important in plant-fungal interactions. They are generally peptides (<300 a. a.)

produced from precursors with a signal peptide (SP) and hence are secreted conventionally, are disulphide rich and may interact with products of the plant *R* genes [96]. Some effectors have been described for filamentous fungal pathogens that do not have SP and are secreted unconventionally through a variety of mechanisms [97-99]. This thesis revealed that the EVs produced by *Fgr* may carry virulence factors and effectors. Among these candidates, there are proteins with SP, such as hydrophobin 3, and others without a SP, such as superoxide dismutase 1.

Hydrophobin 3 fits the criteria of a typical, SP-led effector. Why this protein was only detected in EVs remains unclear, although there are potential explanations. Some EVs may bud off directly from the plasma membrane transporting components of the cytoplasm in the process. Both secretory vesicles and medium EVs have sites in the plasma membrane that direct their fusion and excision, respectively [100,101]. If both sites are in close proximity to one another, a secretory vesicle of smaller size (approx. 100-200 nm [102]) may be engulfed by the medium EVs (150-1000 nm) as the EV contents are being recruited. Alternatively, hydrophobic proteins released from secretory vesicles at the plasma membrane may bind to the lipid surrounding the EVs which subsequently transport them through the fungal cell wall (Figure 11).

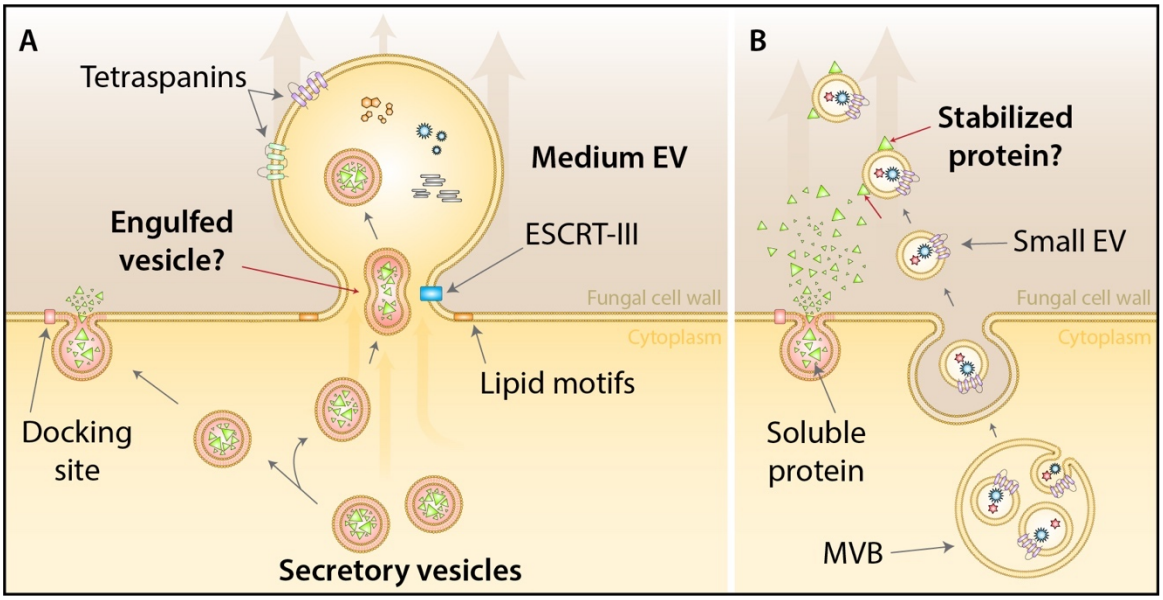

Figure 11 Potential explanations for the presence of proteins with predicted signal peptides in or on extracellular vesicles (EVs). If the docking site of secretory vesicles and the lipid motifs that direct the excision of medium EVs are in proximity, it is possible that (A) secretory vesicles that are smaller than medium EVs are engulfed inside the EV lumen, or that (B) free soluble protein might encounter the surface of EVs and be carried and stabilized. MVB: multivesicular body; ESCRT-III: endosomal sorting complexes required for transport III.

The study in section 3.1 generated a list of potential effectors that may be transported by EVs. The function of these candidate effectors needs to be confirmed, and several approaches could be used to do this. One approach would be to produce the candidate effector recombinantly at small scale using systems such as PichiaPink [103]. After ensuring the purified effector candidate is folded, it could be infiltrated into wheat leaves to examine whether it induces a hypersensitive response as described for other fungal effectors [104,105]. If recombinant expression fails, the protein could be expressed transiently in *Nicotiana benthamiana* to determine whether it is toxic to plant tissues [106]. The potential role of the protein in *Fgr* virulence could also be examined by producing

Fgr strains deficient in the production of the candidate effector through the use of a genome editing technique, such as CRISPR-Cas9 [107]. If the KO strain is viable, virulence could be monitored by comparing the virulence of the KO strain with the wild type *Fgr* in wheat head infection assays [108] or wheat leaf infiltrations [105]. The variety of proteins in EVs from *Fgr* would make it difficult to study the role of only one candidate effector. However, there could be differences in the plant's response when exposed to wild-type EVs compared to EVs from *Fgr* strains lacking a particular protein effector. These infiltration experiments would have to be adapted for the study of EVs, as it was done for *F. oxysporum* infecting cotton [83].

5.4 The protein Sur7 is a potential marker for fungal EVs

The results presented in Chapter 4 support Sur7 as a true protein marker for fungal EVs. Indeed, Sur7 has recently been detected in EVs from *Zymoseptoria tritici* [74], *Aspergillus fumigatus* [75], *S. cerevisiae* [60], and as Sur7 domains in *Cryptococcus neoformans* [78].

Further research is required to verify that Sur7 is a true marker of fungal EVs. For instance, the cross-reactivity and/or non-specific interaction of the anti-*Fgr*Sur7 antibody must be tested using EVs from different sources, such as human, bacterial, and fungal cells. This will determine if the current polyclonal anti-

*Fgr*Sur7 antibody has the necessary specificity to track EVs in complex biological samples.

The Sur7 orthologs that are distributed in yeast and filamentous fungi share similar topologies that include four transmembrane domains and two extracellular loops of approximately 85 and 19 amino amino acids, respectively (Figure 12). The orientation of the *V. dahliae* Sur7-like protein needs to be confirmed. As presented in this thesis, antibodies have been raised against the largest extracellular loop for *C. albicans* (Dr. James McKenna, unpublished) and *Fgr*. This loop is highly conserved in Sur7 from other *Fusarium* species, and moderately conserved in Sur7 proteins from *V. dahliae* and *B. cinerea*. This is not the same for different families of human pathogenic fungi such as *H. capsulatum*, *A. fumigatus*, and *P. brasiliensis*, which all share more similarity to *C. albicans* Sur7. Hence, the anti-*Fgr*Sur7 antibody is likely to be specific for EVs from *Fusarium* species.

One important development for the study of fungal EVs and their potential role in the plant-pathogen interactions would be the visual confirmation of EVs at the plant-fungal interface, where they deliver virulence factors that enhance the infection [109]. This could be achieved by obtaining thin sections of plant material that was infected by *Fgr* and labeling the fungal EVs with the anti-*Fgr* Sur7 antibody followed by a secondary antibody coupled to gold nanoparticles. Similar approaches have been used to image mammalian EVs [79].

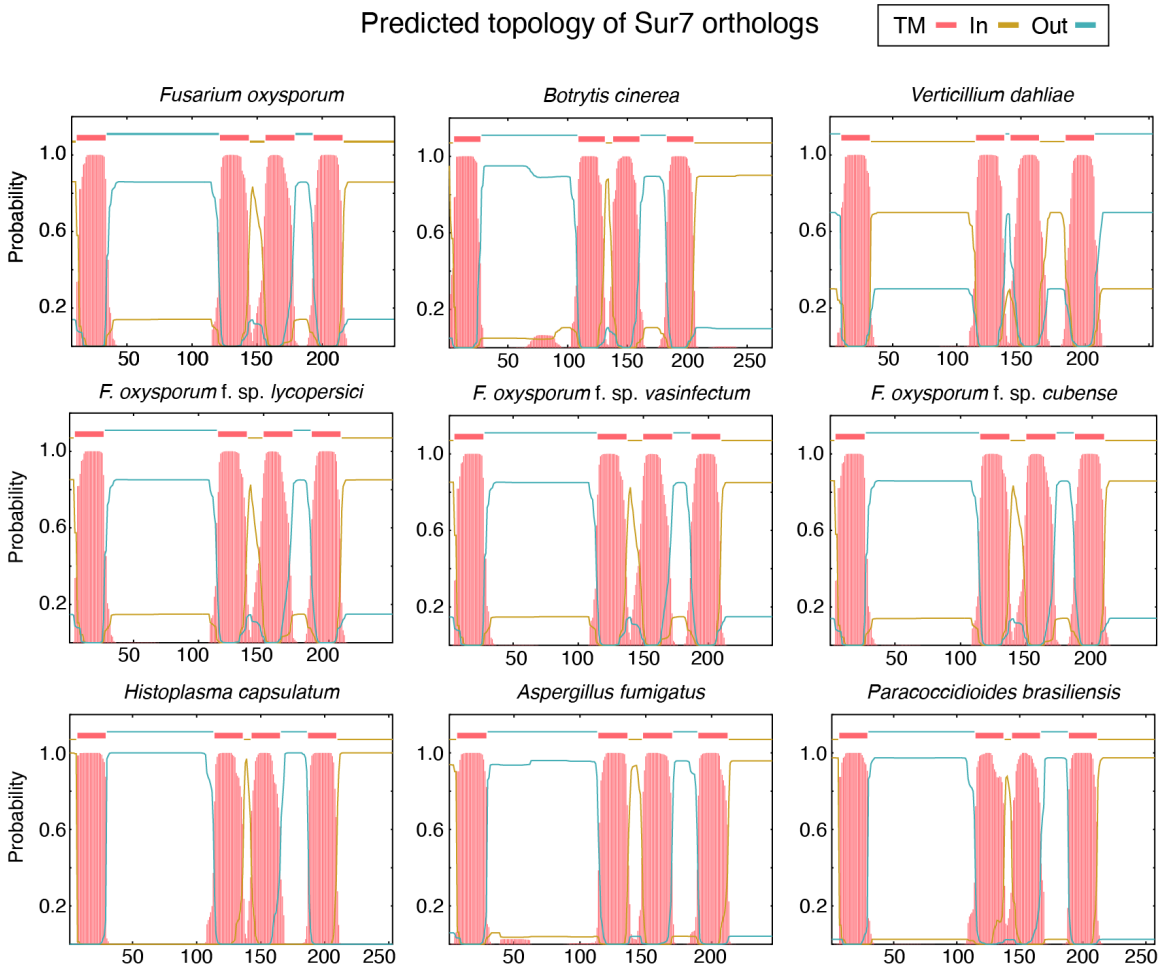

Figure 12 Predicted topology of Sur7 orthologs in other fungal pathogens. The *Candida albicans* Sur7 (Uniprot: Q5A4M8) sequence was used to find potential Sur7 orthologs in other fungi, using BLASTp. TMHMM was employed to predict the topology of the putative orthologs in *Fusarium oxysporum* (KAH7227783.1), *Botrytis cinerea* (XP_024549305.1), *Verticillium dahliae* (XP_009651730.1), *Fusarium oxysporum* f. sp. *lycopersici* (XP_018236958.1), *Fusarium oxysporum* f. sp. *vasinfectum* (EXM34724.1), *Fusarium oxysporum* f. sp. *cubense* (N4TZG3), *Histoplasma capsulatum* (KAG5297300.1), *Aspergillus fumigatus* (KAF4269045.1), and *Paracoccidioides brasiliensis* (XP_010760610.1), revealing that the amino acid positions (X axis) of the four transmembrane domains (TM, highlighted in red) and two extracellular domains ("out", highlighted in blue) are conserved. The intracellular domains ("in") are highlighted in yellow.

It is likely that fungi produce subtypes of EVs depending on the biosynthetic routes activated during different growing conditions. Indeed, isolation procedures have been developed to separate different classes of mammalian EVs cells [110]. In the future, the subpopulations of EVs produced by *Fgr* and *C. albicans* should be

investigated to determine if the anti *Fgr* Sur7 antibodies react with all EVs from *Fgr* or just with a particular population. Not all protein markers are ubiquitous to all subtypes of mammalian EVs [111], hence other protein markers for fungal EVs will be needed in the case Sur7 is present only in a subset of EVs. In the future, having several protein markers of fungal EVs will allow, for instance, the purification of fungal EVs by immunocapture [112], detection of EVs by flow cytometry [113], and the detection of EVs in biological systems using microscope techniques [114].

Finally, because of the importance of Sur7 in the normal physiology of *C. albicans* [115], it would be interesting to determine the role of this protein in the production, morphology, cargo, and functional role of both *C. albicans* and *Fgr* EVs. This could be achieved by using cutting-edge genome editing technologies such as CRISPR-Cas9 to delete Sur 7 and examine the impact of a Sur 7 knockout on EV production. This technology has been used to produce gene deletions in *Fgr* [107]. Similarly, *C. albicans Sur7*Δ strains are available [116].

5.5 Future applications of fungal EVs

The discoveries presented in this thesis have opened opportunities for new developments in fungal EV research. Fungal EVs are likely to transport cargo to

the plant and modulate host defense mechanisms, suggesting that fungal EVs could be exploited to protect crops from fungal pathogens.

The most obvious way to achieve crop protection would be by characterizing the biogenesis of fungal EVs and finding chemicals that alter their production. This might be a complicated task, since it is possible that several processes regulate the production of EVs, with several mechanisms contributing to the production of different classes of EVs and their cargo. However, since fungal EVs transport molecules are likely associated with virulence, a chemical that blocks production of EVs or the activity of one or more components of the EV cargo will attenuate damage from a fungal pathogen.

In the future, EVs could also be employed in the diagnosis of fungal diseases. For instance, a PCR could be performed to detect EV-associated fungal RNA in plant samples, potentially simplifying the diagnosis. This could also be employed to identify fungal infections in humans, detecting the EV nucleic acids in blood samples by PCR instead of which may be more rapid than current diagnostic procedures. Other EV components in human bodily fluids could be revealed by ELISA or diagnostic magnetic resonance [117].

In summary, this thesis has broadened the understanding of extracellular vesicles from filamentous fungi that infect plants. It provides a scalable method that yields

EVs of suitable quality and in appropriate amounts for biochemical analysis. Also, this thesis provides evidence that EVs from *Fusarium* contain virulence factors and candidate effectors that may influence host-pathogen interactions. Finally, a solid candidate for a protein marker was identified, potentially unlocking improved techniques for the study of fungal EVs.

6. Bibliography

1. Dean, R.; Van Kan, J.A.L.; Pretorius, Z.A.; Hammond-Kosak, K.E.; Di Pietro, A.; Spanu, P.D.; Rudd, J.J.; Dickman, M.; Kahmann, R.; Ellis, J.; et al. The Top 10 fungal pathogens in molecular plant pathology. *Molecular Plant Pathology* **2012**, *13*, 414-430, doi:10.1111/j.1364-3703.2011.00783.x.
2. Zhu, Y.; Abdelraheem, A.; Lujan, P.A.; Idowu, J.; Sullivan, P.; Nichols, R.L.; Wedegaertner, T.; Zhang, J. Detection and characterization of Fusarium wilt (*Fusarium oxysporum* f. sp. *vasinfectum*) race 4 causing Fusarium wilt of cotton seedlings in New Mexico, USA. *Plant Disease* **2021**, doi:10.1094/PDIS-10-20-2174-RE.
3. Oghenekaro, A.O.; Oviedo-Ludena, M.A.; Serajazari, M.; Wang, X.; Henriquez, M.A.; Wenner, N.G.; Kuldau, G.A.; Navabi, A.; Kutcher, H.R.; Fernando, W.G.D. Population genetic structure and chemotype diversity of *Fusarium Graminearum* populations from wheat in canada and north eastern united states. *Toxins* **2021**, *13*, 180, doi:10.3390/toxins13030180.
4. McMullen, M.; Jones, R.; Gallenberg, D. Scab of wheat and barley: A re-emerging disease of devastating impact. *Plant Disease* **1997**, *81*, 1340-1348, doi:10.1094/PDIS.1997.81.12.1340.
5. Crespo-Sempere, A.; Estiarte, N.; Marín, S.; Sanchis, V.; Ramos, A.J. Targeting *Fusarium graminearum* control via polyamine enzyme inhibitors and polyamine analogs. *Food Microbiology* **2015**, *49*, 95-103, doi:10.1016/j.fm.2015.01.020.
6. Sanogo, S.; Zhang, J. Resistance sources, resistance screening techniques and disease management for Fusarium wilt in cotton. *Euphytica* **2016**, *207*, 255-271, doi:http://dx.doi.org/10.1007/s10681-015-1532-y.
7. Rodrigues, M.L.; Nimrichter, L.; Oliveira, D.L.; Frases, S.; Miranda, K.; Zaragoza, O.; Alvarez, M.; Nakouzi, A.; Feldmesser, M.; Casadevall, A. Vesicular polysaccharide export in *Cryptococcus neoformans* is a eukaryotic solution to the problem of fungal trans-cell wall transport. *Eukaryotic cell* **2007**, *6*, 48-59, doi:10.1128/EC.00318-06.
8. Baltazar, L.M.; Zamith-Miranda, D.; Burnet, M.C.; Choi, H.; Nimrichter, L.; Nakayasu, E.S.; Nosanchuk, J.D. Concentration-dependent protein loading of extracellular vesicles released by *Histoplasma capsulatum* after antibody treatment and its modulatory action upon macrophages. *Scientific Reports* **2018**, *8*, 8065, doi:10.1038/s41598-018-25665-5.
9. Zarnowski, R.; Sanchez, H.; Covelli, A.S.; Dominguez, E.; Jaromin, A.; Bernhardt, J.; Mitchell, K.F.; Heiss, C.; Azadi, P.; Mitchell, A.; et al. *Candida albicans* biofilm-induced vesicles confer drug resistance through matrix biogenesis. *PLoS biology* **2018**, *16*, e2006872-e2006872, doi:10.1371/journal.pbio.2006872.
10. Raposo, G.; Stoorvogel, W. Extracellular vesicles: exosomes, microvesicles, and friends. *The Journal of Cell Biology* **2013**, *200*, 373-383, doi:10.1083/jcb.201211138.
11. Varderidou-Minasian, S.; Lorenowicz, M.J. Mesenchymal stromal/stem cell-derived extracellular vesicles in tissue repair: challenges and opportunities. *Theranostics* **2020**, *10*, 5979-5997, doi:10.7150/thno.40122.
12. Kabani, M. Extracellular vesicles-encapsulated yeast prions and what they can tell us about the physical nature of propagons. *International Journal of Molecular Sciences* **2021**, *22*, 90.

13. Marimpietri, D.; Airoldi, I.; Faini, A.C.; Malavasi, F.; Morandi, F. The role of extracellular vesicles in the progression of human neuroblastoma. *International Journal of Molecular Sciences* **2021**, *22*, 3964.
14. Femminò, S.; Penna, C.; Margarita, S.; Comità, S.; Brizzi, M.F.; Pagliaro, P. Extracellular vesicles and cardiovascular system: biomarkers and cardioprotective effectors. *Vascular Pharmacology* **2020**, *135*, 106790, doi:https://doi.org/10.1016/j.vph.2020.106790.
15. Herrmann, I.K.; Wood, M.J.A.; Fuhrmann, G. Extracellular vesicles as a next-generation drug delivery platform. *Nature Nanotechnology* **2021**, *16*, 748-759, doi:10.1038/s41565-021-00931-2.
16. Nagelkerke, A.; Ojansivu, M.; van der Koog, L.; Whittaker, T.E.; Cunnane, E.M.; Silva, A.M.; Dekker, N.; Stevens, M.M. Extracellular vesicles for tissue repair and regeneration: Evidence, challenges and opportunities. *Advanced Drug Delivery Reviews* **2021**, *175*, 113775, doi:https://doi.org/10.1016/j.addr.2021.04.013.
17. Dawson, C.S.; Garcia-Ceron, D.; Rajapaksha, H.; Faou, P.; Bleackley, M.R.; Anderson, M.A. Protein markers for *Candida albicans* EVs include claudin-like Sur7 family proteins. *Journal of Extracellular Vesicles* **2020**, *9*, 1750810, doi:10.1080/20013078.2020.1750810.
18. Snyder, W.C.; Hansen, H.N. The species concept in *Fusarium*. *American Journal of Botany* **1940**, *27*, 64-67, doi:https://doi.org/10.1002/j.1537-2197.1940.tb14217.x.
19. McFadden, H.G.; Wilson, I.W.; Chapple, R.M.; Dowd, C. Fusarium wilt (*Fusarium oxysporum* f. sp. *vasinfectum*) genes expressed during infection of cotton (*Gossypium hirsutum*) dagger. *Molecular Plant Pathology* **2006**, *7*, 87-101, doi:10.1111/j.1364-3703.2006.00327.x.
20. Maas, S.; Allen, S.; Weir, D. Cotton Symptoms Guide - The guide to symptoms of diseases and disorders in Australian Cotton; 2012.
21. Smith, S.N.; Snyder, W.C. Persistence of *Fusarium oxysporum* f. sp. *vasinfectum* in fields in the absence of cotton. *Phytopathology* **1974**, *65*, 190-196.
22. Liu, N.; Ma, X.; Sun, Y.; Hou, Y.; Zhang, X.; Li, F. Necrotizing activity of *Verticillium dahliae* and *Fusarium oxysporum* f. sp. *vasinfectum* endopolygalacturonases in cotton. *Plant Disease* **2017**, *101*, 1128-1138, doi:10.1094/PDIS-05-16-0657-RE.
23. Meiting, L.; Shaosheng, Z. Induction of extracellular cell wall-degrading enzymes from *Fusarium oxysporum* f.sp. *cubense* and their effect on degradation of banana tissue. *Chinese Agricultural Science Bulletin* **2010**.
24. Köller, W.; Allan, C.R.; Kolattukudy, P.E. Role of cutinase and cell wall degrading enzymes in infection of *Pisum sativum* by *Fusarium solani* f. sp. *pisi*. *Physiological Plant Pathology* **1982**, *20*, 47-60, doi:https://doi.org/10.1016/0048-4059(82)90023-6.
25. Di Pietro, A.; Garcia-MacEira, F.I.; Meglecz, E.; Roncero, M.I. A MAP kinase of the vascular wilt fungus *Fusarium oxysporum* is essential for root penetration and pathogenesis. *Molecular Microbiology* **2001**, *39*, 1140-1152.
26. Tonukari, N.J.; Scott-Craig, J.S.; Walton, J.D. The *Cochliobolus carbonum SNF1* gene is required for cell wall-degrading enzyme expression and virulence on maize. *Plant Cell* **2000**, *12*, 237-248.
27. Ospina-Giraldo, M.D.; Mullins, E.; Kang, S. Loss of function of the *Fusarium oxysporum* SNF1 gene reduces virulence on cabbage and *Arabidopsis*. *Current Genetics* **2003**, *44*, 49-57, doi:10.1007/s00294-003-0419-y.

28. Douaiher, M.-N.; Nowak, E.; Durand, R.; Halama, P.; Reignault, P. Correlative analysis of *Mycosphaerella graminicola* pathogenicity and cell wall-degrading enzymes produced in vitro: the importance of xylanase and polygalacturonase. *Plant Pathology* **2007**, *56*, 79-86, doi:https://doi.org/10.1111/j.1365-3059.2006.01460.x.
29. Gilchrist, L.; Dubin, H.J. Fusarium Head Blight. *Bread Wheat* **2002**, *30*.
30. Stack, R. Return of an Old Problem: Fusarium Head Blight of Small Grains. *Plant Health Progress* **2000**, *Plant Health Reviews*, doi:10.1094/PHP-2000-0622-01-RV.
31. Vogelgsang, S.; Beyer, M.; Pasquali, M.; Jenny, E.; Musa, T.; Bucheli, T.D.; Wettstein, F.E.; Forrer, H.-R. An eight-year survey of wheat shows distinctive effects of cropping factors on different Fusarium species and associated mycotoxins. *European Journal of Agronomy* **2019**, *105*, 62-77, doi:https://doi.org/10.1016/j.eja.2019.01.002.
32. Bushnell, W.R.; Hazen, B.E.; Pritsch, C. Histology and physiology of Fusarium head blight. **2003**, 44-83.
33. Wise, K.; Woloshuk, C.; Freije, A. Fusarium Head Blight (Head Scab). *Purdue Extension* **2015**.
34. Goswami, R.S.; Kistler, H.C. Heading for disaster: *Fusarium graminearum* on cereal crops. *Molecular Plant Pathology* **2004**, *5*, 515-525, doi:10.1111/j.1364-3703.2004.00252.x.
35. Majer-Baranyi, K.; Adányi, N.; Székács, A. Biosensors for deoxynivalenol and zearalenone determination in feed quality control. *Toxins* **2021**, *13*, doi:10.3390/toxins13070499.
36. Eskola, M.; Kos, G.; Elliott, C.T.; Hajšlová, J.; Mayar, S.; Krska, R. Worldwide contamination of food-crops with mycotoxins: validity of the widely cited 'FAO estimate' of 25%. *Critical Reviews in Food Science and Nutrition* **2020**, *60*, 2773-2789, doi:10.1080/10408398.2019.1658570.
37. Zhao, L.; Zhang, L.; Xu, Z.; Liu, X.; Chen, L.; Dai, J.; Karrow, N.A.; Sun, L. Occurrence of aflatoxin B1, deoxynivalenol and zearalenone in feeds in China during 2018–2020. *Journal of Animal Science and Biotechnology* **2021**, *12*, 74, doi:10.1186/s40104-021-00603-0.
38. Xu, J.R.; Staiger, C.J.; Hamer, J.E. Inactivation of the mitogen-activated protein kinase Mps1 from the rice blast fungus prevents penetration of host cells but allows activation of plant defense responses. *Proceedings of the National Academy of Science* **1998**, *95*, 12713-12718.
39. Hou, Z.; Xue, C.; Peng, Y.; Katan, T.; Kistler, H.C.; Xu, J.R. A mitogen-activated protein kinase gene (*MGV1*) in *Fusarium graminearum* is required for female fertility, heterokaryon formation, and plant infection. *Molecular Plant-Microbe Interactions* **2002**, *15*, 1119-1127, doi:10.1094/mpmi.2002.15.11.1119.
40. Jenczmionka, N.J.; Maier, F.J.; Lösch, A.P.; Schäfer, W. Mating, conidiation and pathogenicity of *Fusarium graminearum*, the main causal agent of the head-blight disease of wheat, are regulated by the MAP kinase *gpmk1*. *Current Genetics* **2003**, *43*, 87-95, doi:10.1007/s00294-003-0379-2.
41. Ruiz-Roldan, M.C.; Maier, F.J.; Schafer, W. PTK1, a mitogen-activated-protein kinase gene, is required for conidiation, appressorium formation, and pathogenicity of *Pyrenophora teres* on barley. *Molecular Plant-Microbe Interactions* **2001**, *14*, 116-125, doi:10.1094/mpmi.2001.14.2.116.
42. Mey, G.; Oeser, B.; Lebrun, M.H.; Tudzynski, P. The biotrophic, non-appressorium-forming grass pathogen *Claviceps purpurea* needs a Fus3/Pmk1 homologous mitogen-activated protein kinase for colonization of rye ovarian tissue. *Molecular Plant-Microbe Interactions* **2002**, *15*, 303-312, doi:10.1094/mpmi.2002.15.4.303.

43. Boenisch, M.J.; Schäfer, W. *Fusarium graminearum* forms mycotoxin producing infection structures on wheat. *BMC Plant Biology* **2011**, *11*, 110, doi:10.1186/1471-2229-11-110.
44. Menke, J.; Weber, J.; Broz, K.; Kistler, H.C. Cellular development associated with induced mycotoxin synthesis in the filamentous fungus *Fusarium graminearum*. *PLoS ONE* **2013**, *8*, e63077, doi:10.1371/journal.pone.0063077.
45. Kruger, W.M.; Pritsch, C.; Chao, S.; Muehlbauer, G.J. Functional and comparative bioinformatic analysis of expressed genes from wheat spikes infected with *Fusarium graminearum*. *Molecular Plant-Microbe Interactions* **2002**, *15*, 445-455, doi:10.1094/mpmi.2002.15.5.445.
46. Taylor, R.D.; Saparno, A.; Blackwell, B.; Anoop, V.; Gleddie, S.; Tinker, N.A.; Harris, L.J. Proteomic analyses of *Fusarium graminearum* grown under mycotoxin-inducing conditions. *Proteomics* **2008**, *8*, 2256-2265, doi:10.1002/pmic.200700610.
47. Ji, X.-L.; Yan, M.; Yang, Z.-D.; Li, A.-F.; Kong, L.-R. Shotgun analysis of the secretome of *Fusarium graminearum*. *Indian Journal of Microbiology* **2013**, *53*, 400-409, doi:10.1007/s12088-013-0392-1.
48. Paper, J.M.; Scott-Craig, J.S.; Adhikari, N.D.; Cuomo, C.A.; Walton, J.D. Comparative proteomics of extracellular proteins in vitro and in planta from the pathogenic fungus *Fusarium graminearum*. *Proteomics* **2007**, *7*, 3171-3183, doi:10.1002/pmic.200700184.
49. Rizzo, J.; Rodrigues, M.L.; Janbon, G. Extracellular vesicles in fungi: past, present, and future perspectives. *Frontiers in Cellular and Infection Microbiology* **2020**, *10*, doi:10.3389/fcimb.2020.00346.
50. Costa, J.H.; Bazioli, J.M.; Barbosa, L.D.; dos Santos, P.L.T.; Reis, F.C.G.; Klimeck, T.; Crnkovic C.M.; Berlinck, R.G.S.; Sussulini, A.; Rodrigues, M.L.; et al. Phytotoxic tryptoquialanines produced in vivo by *Penicillium digitatum* are exported in extracellular vesicles. *mBio* **2021**, *12*, e03393-03320, doi:10.1128/mBio.03393-20.
51. Rodrigues, M.L.; Nakayasu, E.S.; Oliveira, D.L.; Nimrichter, L.; Nosanchuk, J.D.; Almeida, I.C.; Casadevall, A. Extracellular vesicles produced by *Cryptococcus neoformans* contain protein components associated with virulence. *Eukaryotic Cell* **2008**, *7*, 58-67, doi:10.1128/EC.00370-07.
52. Abbas, M.; Jesel, L.; Auger, C.; Amoura, L.; Messas, N.; Manin, G.; Rumig, C.; Leon-Gonzalez, A.J.; Ribeiro, T.P.; Silva, G.C.; et al. Endothelial microparticles from acute coronary syndrome patients induce premature coronary artery endothelial cell aging and thrombogenicity: role of the Ang II/AT1 receptor/NADPH oxidase-mediated activation of MAPKs and PI3-kinase pathways. *Circulation* **2017**, *135*, 280-296, doi:10.1161/circulationaha.116.017513.
53. Raposo, G.; Nijman, H.W.; Stoorvogel, W.; Liejendekker, R.; Harding, C.V.; Melief, C.J.; Geuze, H.J. B lymphocytes secrete antigen-presenting vesicles. *The Journal of Experimental Medicine* **1996**, *183*, 1161-1172.
54. Mittelbrunn, M.; Gutiérrez-Vázquez, C.; Villarroya-Beltri, C.; González, S.; Sánchez-Cabo, F.; González, M.Á.; Bernad, A.; Sánchez-Madrid, F. Unidirectional transfer of microRNA-loaded exosomes from T cells to antigen-presenting cells. *Nature Communications* **2011**, *2*, 282, doi:10.1038/ncomms1285.
55. Athman, J.J.; Wang, Y.; McDonald, D.J.; Boom, W.H.; Harding, C.V.; Wearsch, P.A. Bacterial membrane vesicles mediate the release of mycobacterium tuberculosis lipoglycans and

lipoproteins from infected macrophages. *Journal of Immunology* **2015**, *195*, 1044-1053, doi:10.4049/jimmunol.1402894.

56. Albuquerque, P.C.; Nakayasu, E.S.; Rodrigues, M.L.; Frases, S.; Casadevall, A.; Zancope-Oliveira, R.M.; Almeida, I.C.; Nosanchuk, J.D. Vesicular transport in *Histoplasma capsulatum*: an effective mechanism for trans-cell wall transfer of proteins and lipids in ascomycetes. *Cellular Microbiology* **2008**, *10*, 1695-1710, doi:10.1111/j.1462-5822.2008.01160.x.
57. Gil-Bona, A.; Llama-Palacios, A.; Parra, C.M.; Vivanco, F.; Nombela, C.; Monteoliva, L.; Gil, C. Proteomics unravels extracellular vesicles as carriers of classical cytoplasmic proteins in *Candida albicans*. *Journal of Proteome Research* **2015**, *14*, 142-153, doi:10.1021/pr5007944.
58. Abdi, A.; Yu, L.; Goulding, D.; Rono, M.K.; Bejon, P.; Choudhary, J.; Rayner, J. Proteomic analysis of extracellular vesicles from a *Plasmodium falciparum* Kenyan clinical isolate defines a core parasite secretome. *Wellcome Open Research* **2017**, *2*, 50-50, doi:10.12688/wellcomeopenres.11910.2.
59. Cui, Y.; Gao, J.; He, Y.; Jiang, L. Plant extracellular vesicles. *Protoplasma* **2020**, *257*, 3-12, doi:10.1007/s00709-019-01435-6.
60. Zhao, K.; Bleackley, M.; Chisanga, D.; Gangoda, L.; Fonseka, P.; Liem, M.; Kalra, H.; Al Saffar, H.; Keerthikumar, S.; Ang, C.-S.; et al. Extracellular vesicles secreted by *Saccharomyces cerevisiae* are involved in cell wall remodelling. *Communications Biology* **2019**, *2*, 305, doi:10.1038/s42003-019-0538-8.
61. Yoshioka, Y.; Konishi, Y.; Kosaka, N.; Katsuda, T.; Kato, T.; Ochiya, T. Comparative marker analysis of extracellular vesicles in different human cancer types. *Journal of Extracellular Vesicles* **2013**, *2*, 20424, doi:10.3402/jev.v2i0.20424.
62. Wang, H.X.; Douglas, L.M.; Veselá, P.; Rachel, R.; Malinsky, J.; Konopka, J.B. Eisosomes promote the ability of Sur7 to regulate plasma membrane organization in *Candida albicans*. *Molecular Biology of the Cell* **2016**, *27*, 1663-1675, doi:10.1091/mbc.E16-01-0065.
63. Skrzypek, M.S.; Binkley, J.; Binkley, G.; Miyasato, S.R.; Simison, M.; Sherlock, G. The Candida Genome Database (CGD): incorporation of Assembly 22, systematic identifiers and visualization of high throughput sequencing data. *Nucleic Acids Research* **2017**, *45*, D592-D596, doi:10.1093/nar/gkw924.
64. Altschul, S.F.; Gish, W.; Miller, W.; Myers, E.W.; Lipman, D.J. Basic local alignment search tool. *Journal of Molecular Biology* **1990**, *215*, 403-410, doi:https://doi.org/10.1016/S0022-2836(05)80360-2.
65. Tsirigos, K.D.; Peters, C.; Shu, N.; Käll, L.; Elofsson, A. The TOPCONS web server for consensus prediction of membrane protein topology and signal peptides. *Nucleic Acids Research* **2015**, *43*, W401-407, doi:10.1093/nar/gkv485.
66. Omasits, U.; Ahrens, C.H.; Müller, S.; Wollscheid, B. Protter: interactive protein feature visualization and integration with experimental proteomic data. *Bioinformatics* **2014**, *30*, 884-886, doi:10.1093/bioinformatics/btt607.
67. Jespersen, M.C.; Peters, B.; Nielsen, M.; Marcatili, P. BepiPred-2.0: improving sequence-based B-cell epitope prediction using conformational epitopes. *Nucleic Acids Research* **2017**, *45*, W24-w29, doi:10.1093/nar/gkx346.

68. Greenshields, D.L.; Liu, G.; Feng, J.; Selvaraj, G.; Wei, Y. The siderophore biosynthetic gene *SID1*, but not the ferroxidase gene *FET3*, is required for full *Fusarium graminearum* virulence. *Molecular Plant Pathology* **2007**, *8*, 411-421, doi:10.1111/j.1364-3703.2007.00401.x.
69. Ramamoorthy, V.; Cahoon, E.B.; Thokala, M.; Kaur, J.; Li, J.; Shah, D.M. Sphingolipid C-9 methyltransferases are important for growth and virulence but not for sensitivity to antifungal plant defensins in *Fusarium graminearum*. *Eukaryotic Cell* **2009**, *8*, 217-229, doi:10.1128/ec.00255-08.
70. Zimmerman, B.; Kelly, B.; McMillan, B.J.; Seegar, T.C.M.; Dror, R.O.; Kruse, A.C.; Blacklow, S.C. Crystal structure of a full-length human tetraspanin reveals a cholesterol-binding pocket. *Cell* **2016**, *167*, 1041-1051.e1011, doi:https://doi.org/10.1016/j.cell.2016.09.056.
71. Douglas, L.M.; Konopka, J.B. Fungal membrane organization: the eisosome concept. *Annual Review of Microbiology* **2014**, *68*, 377-393, doi:10.1146/annurev-micro-091313-103507.
72. Straťalová, V.; Stahlschmidt, W.; Grossmann, G.; Blažíková, M.; Rachel, R.; Tanner, W.; Malinsky, J. Furrow-like invaginations of the yeast plasma membrane correspond to membrane compartment of Can1. *Journal of Cell Science* **2009**, *122*, 2887-2894, doi:10.1242/jcs.051227.
73. Ghaemmaghami, S.; Huh, W.-K.; Bower, K.; Howson, R.W.; Belle, A.; Dephoure, N.; O'Shea, E.K.; Weissman, J.S. Global analysis of protein expression in yeast. *Nature* **2003**, *425*, 737-741, doi:10.1038/nature02046.
74. Hill, E.H.; Solomon, P.S. Extracellular vesicles from the apoplastic fungal wheat pathogen *Zymoseptoria tritici*. *Fungal Biology and Biotechnology* **2020**, *7*, 13, doi:10.1186/s40694-020-00103-2.
75. Rizzo, J.; Chaze, T.; Miranda, K.; Roberson, R.W.; Gorgette, O.; Nimrichter, L.; Matondo, M.; Latgé, J.P.; Beauvais, A.; Rodrigues, M.L. Characterization of extracellular vesicles produced by *Aspergillus fumigatus* protoplasts. *mSphere* **2020**, *5*, doi:10.1128/mSphere.00476-20.
76. Vangelatos, I.; Roumelioti, K.; Gournas, C.; Suarez, T.; Scazzocchio, C.; Sophianopoulou, V. Eisosome organization in the filamentous ascomycete *Aspergillus nidulans*. *Eukaryotic Cell* **2010**, *9*, 1441-1454, doi:10.1128/EC.00087-10.
77. Walther, T.C.; Brickner, J.H.; Aguilar, P.S.; Bernales, S.; Pantoja, C.; Walter, P. Eisosomes mark static sites of endocytosis. *Nature* **2006**, *439*, 998-1003, doi:10.1038/nature04472.
78. Rizzo, J.; Wong, S.S.W.; Gazi, A.D.; Moyrand, F.; Chaze, T.; Commere, P.-H.; Novault, S.; Matondo, M.; Péhau-Arnaudet, G.; Reis, F.C.G.; et al. Cryptococcus extracellular vesicles properties and their use as vaccine platforms. *Journal of Extracellular Vesicles* **2021**, *10*, e12129, doi:https://doi.org/10.1002/jev2.12129.
79. Brisson, A.R.; Tan, S.; Linares, R.; Gounou, C.; Arraud, N. Extracellular vesicles from activated platelets: a semiquantitative cryo-electron microscopy and immuno-gold labeling study. *Platelets* **2017**, *28*, 263-271, doi:10.1080/09537104.2016.1268255.
80. Beekman, P.; Enciso-Martinez, A.; Rho, H.S.; Pujari, S.P.; Lenferink, A.; Zuilhof, H.; Terstappen, L.; Otto, C.; Le Gac, S. Immuno-capture of extracellular vesicles for individual multi-modal characterization using AFM, SEM and Raman spectroscopy. *Lab on a Chip* **2019**, *19*, 2526-2536, doi:10.1039/c9lc00081j.

81. Zhang, J.; Qiu, Y.; Xu, K. Characterization of GFP-AtPEN1 as a marker protein for extracellular vesicles isolated from *Nicotiana benthamiana* leaves. *Plant Signaling & Behavior* **2020**, *15*, 1791519, doi:10.1080/15592324.2020.1791519.
82. Garcia-Ceron, D.; Bleackley, M.R.; Anderson, M.A. Fungal Extracellular Vesicles in Pathophysiology. In *New Frontiers: Extracellular Vesicles. Subcellular Biochemistry*, 2021/03/30 ed.; Mathivanan S., F.P., Nedeva C., Atukorala I. (eds), Ed.; Springer, Cham.: 2021; Volume 97, pp. 151-177.
83. Bleackley, M.; Samuel, M.; Garcia-Ceron, D.; Mckenna, J.; Lowe, R.; Pathan, M.; Zhao, K.; Ang, C.; Mathivanan, S.; Anderson, M. Extracellular vesicles from the cotton pathogen *Fusarium oxysporum* f. sp. *vasinfectum* induce a phytotoxic response in plants. *Frontiers in Plant Science* **2019**, *10*, 1610, doi:10.3389/fpls.2019.01610.
84. Bielska, E.; Sisquella, M.A.; Aldeieg, M.; Birch, C.; O'Donoghue, E.J.; May, R.C. Pathogen-derived extracellular vesicles mediate virulence in the fatal human pathogen *Cryptococcus gattii*. *Nature Communications* **2018**, *9*, 1556, doi:10.1038/s41467-018-03991-6.
85. Corso, G.; Mäger, I.; Lee, Y.; Görgens, A.; Bultema, J.; Giebel, B.; Wood, M.J.A.; Nordin, J.Z.; Andaloussi, S.E.L. Reproducible and scalable purification of extracellular vesicles using combined bind-elute and size exclusion chromatography. *Scientific Reports* **2017**, *7*, 11561, doi:10.1038/s41598-017-10646-x.
86. Vargas, G.; Honorato, L.; Guimarães, A.J.; Rodrigues, M.L.; Reis, F.C.G.; Vale, A.M.; Ray, A.; Nosanchuk, J.D.; Nimrichter, L. Protective effect of fungal extracellular vesicles against murine candidiasis. *Cellular Microbiology* **2020**, e13238, doi:10.1111/cmi.13238.
87. Shopova, I.A.; Belyaev, I.; Dasari, P.; Jahreis, S.; Stroe, M.C.; Cseresnyés, Z.; Zimmermann, A.-K.; Medyukhina, A.; Svensson, C.-M.; Krüger, T.; et al. Human neutrophils produce antifungal extracellular vesicles against *Aspergillus fumigatus*. *mBio* **2020**, *11*, e00596-00520, doi:10.1128/mBio.00596-20.
88. Souza, J.A.M.; Baltazar, L.d.M.; Carregal, V.M.; Gouveia-Eufrasio, L.; de Oliveira, A.G.; Dias, W.G.; Campos Rocha, M.; Rocha de Miranda, K.; Malavazi, I.; Santos, D.d.A.; et al. Characterization of *Aspergillus fumigatus* extracellular vesicles and their effects on macrophages and neutrophils functions. *Frontiers in Microbiology* **2019**, *10*, doi:10.3389/fmicb.2019.02008.
89. Berlanda Scorza, F.; Colucci, A.M.; Maggiore, L.; Sanzone, S.; Rossi, O.; Ferlenghi, I.; Pesce, I.; Caboni, M.; Norais, N.; Di Cioccio, V.; et al. High yield production process for *Shigella* outer membrane particles. *PLoS ONE* **2012**, *7*, e35616, doi:10.1371/journal.pone.0035616.
90. Paddison, P.J.; Caudy, A.A.; Bernstein, E.; Hannon, G.J.; Conklin, D.S. Short hairpin RNAs (shRNAs) induce sequence-specific silencing in mammalian cells. *Genes & Development* **2002**, *16*, 948-958, doi:10.1101/gad.981002.
91. Xia, H.; Mao, Q.; Paulson, H.L.; Davidson, B.L. siRNA-mediated gene silencing in vitro and in vivo. *Nature Biotechnology* **2002**, *20*, 1006-1010, doi:10.1038/nbt739.
92. Wiklander, O.P.B.; Nordin, J.Z.; O'Loughlin, A.; Gustafsson, Y.; Corso, G.; Mäger, I.; Vader, P.; Lee, Y.; Sork, H.; Seow, Y.; et al. Extracellular vesicle in vivo biodistribution is determined by cell source, route of administration and targeting. *Journal of Extracellular Vesicles* **2015**, *4*, 26316, doi:10.3402/jev.v4.26316.

93. Brown, L.; Wolf, J.M.; Prados-Rosales, R.; Casadevall, A. Through the wall: extracellular vesicles in Gram-positive bacteria, mycobacteria and fungi. *Nature Reviews Microbiology* **2015**, *13*, 620-630, doi:10.1038/nrmicro3480.
94. Oliveira, D.L.; Freire-de-Lima, C.G.; Nosanchuk, J.D.; Casadevall, A.; Rodrigues, M.L.; Nimrichter, L. Extracellular vesicles from *Cryptococcus neoformans* modulate macrophage functions. *Infection and Immunity* **2010**, *78*, 1601-1609, doi:10.1128/iai.01171-09.
95. Garcia-Ceron, D.; Lowe, R.G.T.; McKenna, J.A.; Brain, L.M.; Dawson, C.S.; Clark, B.; Berkowitz, O.; Faou, P.; Whelan, J.; Bleackley, M.R.; et al. Extracellular vesicles from *Fusarium graminearum* contain protein effectors expressed during infection of corn. *Journal of Fungi* **2021**, *7*, doi:10.3390/jof7110977.
96. Jones, J.D.G.; Dangl, J.L. The plant immune system. *Nature* **2006**, *444*, 323-329, doi:10.1038/nature05286.
97. Stock, J.; Sarkari, P.; Kreibich, S.; Brefort, T.; Feldbrügge, M.; Schipper, K. Applying unconventional secretion of the endochitinase Cts1 to export heterologous proteins in *Ustilago maydis*. *Journal of Biotechnology* **2012**, *161*, 80-91, doi:doi.org/10.1016/j.jbiotec.2012.03.004.
98. Burggraaf, A.-M.; Punt, P.J.; Ram, A.F.J. The unconventional secretion of PepN is independent of a functional autophagy machinery in the filamentous fungus *Aspergillus niger*. *FEMS Microbiology Letters* **2016**, *363*, doi:10.1093/femsle/fnw152.
99. Liu, T.; Song, T.; Zhang, X.; Yuan, H.; Su, L.; Li, W.; Xu, J.; Liu, S.; Chen, L.; Chen, T.; et al. Unconventionally secreted effectors of two filamentous pathogens target plant salicylate biosynthesis. *Nature Communications* **2014**, *5*, 4686, doi:10.1038/ncomms5686.
100. Oheim, M.; Loerke, D.; Stühmer, W.; Chow, R.H. Multiple stimulation-dependent processes regulate the size of the releasable pool of vesicles. *European Biophysics Journal* **1999**, *28*, 91-101, doi:10.1007/s002490050188.
101. van Niel, G.; D'Angelo, G.; Raposo, G. Shedding light on the cell biology of extracellular vesicles. *Nature Reviews Molecular Cell Biology* **2018**, *19*, 213-228, doi:10.1038/nrm.2017.125.
102. Borges, R.; Jaén, R.; Freire, F.; Gómez, J.F.; Villafruela, C.; Yanes, E. Morphological and functional characterization of beige mouse adrenomedullary secretory vesicles. *Cell and Tissue Research* **2001**, *304*, 159-164, doi:10.1007/s004410000320.
103. Li, Z.; Miao, Y.; Yang, J.; Zhao, F.; Lin, Y.; Han, S. Efficient improvement of surface displayed lipase from *Rhizomucor miehei* in PichiaPink™ protease-deficient system. *Protein Expression and Purification* **2021**, *180*, 105804, doi:https://doi.org/10.1016/j.pep.2020.105804.
104. Liu, Z.; Friesen, T.L.; Ling, H.; Meinhardt, S.W.; Oliver, R.P.; Rasmussen, J.B.; Faris, J.D. The Tsn1–ToxA interaction in the wheat–*Stagonospora nodorum* pathosystem parallels that of the wheat–tan spot system. *Genome* **2006**, *49*, 1265-1273, doi:10.1139/g06-088.
105. Lu, S.; Faris, J.D.; Sherwood, R.; Friesen, T.L.; Edwards, M.C. A dimeric PR-1-type pathogenesis-related protein interacts with ToxA and potentially mediates ToxA-induced necrosis in sensitive wheat. *Molecular Plant Pathology* **2014**, *15*, 650-663, doi:https://doi.org/10.1111/mpp.12122.
106. Hao, G.; McCormick, S.; Usgaard, T.; Tiley, H.; Vaughan, M.M. Characterization of three *Fusarium graminearum* effectors and their roles during fusarium head blight. *Frontiers in Plant Science* **2020**, *11*, doi:10.3389/fpls.2020.579553.

107. Gardiner, D.M.; Kazan, K. Selection is required for efficient Cas9-mediated genome editing in *Fusarium graminearum*. *Fungal Biology* **2018**, *122*, 131-137, doi:doi.org/10.1016/j.funbio.2017.11.006.
108. Hou, Z.; Xue, C.; Peng, Y.; Katan, T.; Kistler, H.C.; Xu, J.-R. A Mitogen-activated protein kinase gene (MGV1) in *Fusarium graminearum* is required for female fertility, heterokaryon formation, and plant infection. *Molecular Plant-Microbe Interactions* **2002**, *15*, 1119-1127, doi:10.1094/mpmi.2002.15.11.1119.
109. Samuel, M.; Bleackley, M.; Anderson, M.; Mathivanan, S. Extracellular vesicles including exosomes in cross kingdom regulation: a viewpoint from plant-fungal interactions. *Frontiers in Plant Science* **2015**, *6*, 766-766, doi:10.3389/fpls.2015.00766.
110. Crescitelli, R.; Lässer, C.; Lötvall, J. Isolation and characterization of extracellular vesicle subpopulations from tissues. *Nature Protocols* **2021**, *16*, 1548-1580, doi:10.1038/s41596-020-00466-1.
111. Kowal, J.; Arras, G.; Colombo, M.; Jouve, M.; Morath, J.P.; Primdal-Bengtson, B.; Dingli, F.; Loew, D.; Tkach, M.; Théry, C. Proteomic comparison defines novel markers to characterize heterogeneous populations of extracellular vesicle subtypes. *Proceedings of the National Academy of Sciences* **2016**, *113*, E968, doi:10.1073/pnas.1521230113.
112. Beekman, P.; Enciso-Martinez, A.; Rho, H.S.; Pujari, S.P.; Lenferink, A.; Zuilhof, H.; Terstappen, L.W.M.M.; Otto, C.; Le Gac, S. Immuno-capture of extracellular vesicles for individual multi-modal characterization using AFM, SEM and Raman spectroscopy. *Lab on a Chip* **2019**, *19*, 2526-2536, doi:10.1039/C9LC00081J.
113. Salmond, N.; Khanna, K.; Owen, G.R.; Williams, K.C. Nanoscale flow cytometry for immunophenotyping and quantitating extracellular vesicles in blood plasma. *Nanoscale* **2021**, *13*, 2012-2025, doi:10.1039/d0nr05525e.
114. Lai, C.P.; Mardini, O.; Ericsson, M.; Prabhakar, S.; Maguire, C.A.; Chen, J.W.; Tannous, B.A.; Breakefield, X.O. Dynamic biodistribution of extracellular vesicles in vivo using a multimodal imaging reporter. *ACS Nano* **2014**, *8*, 483-494, doi:10.1021/nn404945r.
115. Douglas Lois, M.; Wang Hong, X.; Keppler-Ross, S.; Dean, N.; Konopka James, B.; Berman, J. Sur7 promotes plasma membrane organization and is needed for resistance to stressful conditions and to the invasive growth and virulence of *Candida albicans*. *mBio* **2011**, *3*, e00254-00211, doi:10.1128/mBio.00254-11.
116. Bernardo, S.M.; Lee, S.A. *Candida albicans* SUR7 contributes to secretion, biofilm formation, and macrophage killing. *BMC Microbiology* **2010**, *10*, 133, doi:10.1186/1471-2180-10-133.
117. van der Meel, R.; Krawczyk-Durka, M.; van Solinge, W.W.; Schiffelers, R.M. Toward routine detection of extracellular vesicles in clinical samples. *International Journal of Laboratory Hematology* **2014**, *36*, 244-253, doi:https://doi.org/10.1111/ijlh.12247.